

UNCLASSIFIED

AD NUMBER
AD871961
NEW LIMITATION CHANGE
TO Approved for public release, distribution unlimited
FROM Distribution authorized to U.S. Gov't. agencies and their contractors; Administrative/Operational Use; JUN 1970. Other requests shall be referred to Air Force Materials Lab., Wright-Patterson AFB, OH 45433.
AUTHORITY
AFML ltr 7 Dec 1972

THIS PAGE IS UNCLASSIFIED

AFML-TR-70-95
PART I

AD871961

AD No. —

DDC FILE COPY

ABLATIVE MATERIALS FOR HIGH HEAT LOADS
PART I
ENVIRONMENTAL SIMULATION AND MATERIALS CHARACTERIZATION

P.W. Juneau, Jr.
J. Metzger
L. Markowitz
F.P. Curtis

Document No. 70SD649

General Electric Company

TECHNICAL REPORT AFML-TR-70-95, PART I

JUNE 1970

AIR FORCE MATERIALS LABORATORY
AIR FORCE SYSTEMS COMMAND
WRIGHT-PATTERSON AIR FORCE BASE, OHIO

DDC
RECEIVED
JUL 24 1970
B

Part I

When Government drawings, specifications, or other data are used for any purpose other than in connection with a definitely related Government procurement operation, the United States Government thereby incurs no responsibility nor any obligation whatsoever; and the fact that the government may have formulated, furnished, or in any way supplied the said drawings, specifications, or other data, is not to be regarded by implication or otherwise as in any manner licensing the holder or any other person or corporation, or conveying any rights or permission to manufacture, use, or sell any patented invention that may in any way be related thereto.

This document is subject to special export controls and each transmittal to foreign governments or foreign nationals may be made only with prior approval of the Air Force Materials Laboratory, Wright-Patterson AFB, Ohio 45433.

Distribution of this report is limited because the U.S. Export Control Act is applicable.

ACCESSION FOR	
CPSTX	WHITE SECTION <input type="checkbox"/>
CDC	DIFF SECTION <input checked="" type="checkbox"/>
BRANV	ED <input type="checkbox"/>
SEC. FUNCTION	
BY	
DISTRIBUTION/AVAILABILITY CODES	
DIST.	AVAIL. AND/OR SPECIAL
2	

Copies of this report should not be returned unless return is required by security considerations, contractual obligations, or notice on a specific document.

AFML-TR-70-95
PART I

ABLATIVE MATERIALS FOR HIGH HEAT LOADS
PART I
ENVIRONMENTAL SIMULATION AND MATERIALS CHARACTERIZATION

P.W. Juneau, Jr.
J. Metzger
L. Markowitz
F.P. Curtis

TECHNICAL REPORT AFML-TR-70-95, PART I

JUNE 1970

This document is subject to special export controls and each transmittal to foreign governments or foreign nationals may be made only with prior approval of the Air Force Materials Laboratory (MANC), Wright-Patterson AFB, Ohio 45433.

This Document Contains
Missing Page/s That Are
Unavailable In The
Original Document

OR are
Blank pgs.
that have
Been Removed

**BEST
AVAILABLE COPY**

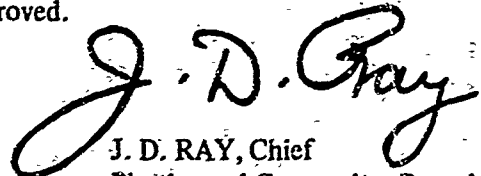
FOREWORD

This report was prepared by the Re-entry and Environmental Systems Division of the General Electric Company, Philadelphia, Pennsylvania, under USAF Contract F33615-69-C-1503. This contract was initiated under Project 7340, "Nonmetallic and Composite Materials", Task No. 734001, "Thermally Protective Plastics and Composites". The work was administered under the direction of the Nonmetallic Materials Division, Air Force Materials Laboratory (AFML). The AFML project engineer was Mr. R. Farmer (MANC).

This report covers work performed between 24 February 1969 and 30 March 1970.

The manuscript of this report was released by the authors 30 March 1970. The General Electric Company report number is 70SD649.

This technical report has been reviewed and is approved.



J. D. RAY, Chief
Plastics and Composites Branch
Nonmetallic Materials Division
Air Force Materials Laboratory

ABSTRACT

Ablative plastic composite materials were investigated and developed for long time heating environments. The desirable materials performance goals were high erosive resistance, insulative ability, spallation or other thermomechanical effects.

Carbon cloth reinforced phenolic resin and silica cloth reinforced phenolic resin heat shield materials gave acceptable thermochemical ablative surface patterns, erosive rates, and internal temperatures, but these heat shield materials are relatively heavy. Consequently, the multilayer concept was examined with the objective of determining if such constructions could perform comparably with appropriate weight savings. Low density quartz (LDQ) was an effective insulative layer, when bonded between the heat shield and metallic substrates. The LDQ consisted of phenolic impregnated silica strands, which alternated at right angles to yield a square wall, non-laced construction.

The environment to which the specimens were subjected was generated by a five megawatt arc heater which was operated stepwise for 300 seconds. Calibration of the heat transfer rates indicated nominal values of 25 and 440 Btu/ft²-sec, yielding an integrated heat transfer of 36550 Btu/ft². Other nominal conditions over the 230 and 70 second heating intervals were: 5000 and 5000 Btu/lb enthalpy, 25 and 400 Btu/ft²-sec heat flux, 0.4 and 2.5 lb/ft² shear stress. Specimen dimensions were 5-inches long by 1.75-inch wide by a variable thickness. There was a bonded aluminum structure, five thermocouples, and a 20 degree fiber angle for the simulated tapewrap specimen.

The ablative response to high heat loads was found to be dependent upon material composition and construction. Asymmetrical erosion, excessive erosion, or high internal temperatures was found for six of the candidate composites.

This Abstract is subject to export controls and each transmittal to foreign governments or foreign nationals may be made only with prior approval of the Air Force Materials Laboratory (MANC), Wright-Patterson Air Force Base, Ohio 45433.

TABLE OF CONTENTS

Section	Page
I INTRODUCTION	1
II TECHNICAL APPROACH	3
Reference Test Specimens (R1, R2 and R3)	3
Ablative Shield Test Specimens (A1, A2, A3 and A4)	3
Low Density Composite Test Specimens (C1, C2 and C3)	4
Test Specimen Instrumentation	5
Laboratory Characterization	9
Chronology of Ablation Test Program	11
Mechanical Redesigns	14
Specimens	14
Arc Heater Performance	15
Some Aspects of Testing	16
Data Evaluation	17
Thermal Calculations	23
III SUMMARY AND CONCLUSIONS	27
IV RECOMMENDATIONS	31

LIST OF ILLUSTRATIONS

Figure		Page
1	Short Time Heating	2
2	Long Time Heating	2
3	Quartz Layup Ready for Compaction	6
4	Heat Shield Prepregs in Position	6
5	Cured Blank	6
6	Machined Carbon Phenolic Specimens	7
7	Machined Silica Phenolic Specimens	7
8	X-ray Views of Two Types of Instrumented Specimens	8
9	Method for Estimating Thermocouple Position	10
10	Tandem Gerdien Arc Chamber (Schematic)	10
11	Nominal Shear and Heat Transfer Ablation Test Program	11
12	Arc and Channel Ablation Test Fixture	12
13	Equipment Installed at the Arc	13
14	Modification of Graphite Inserts for Bypass	15
15	Pressure Run 89-69, Specimen R2-1	33
16	Internal Temperature, Run 89-69, Specimen R2-1	34
17	Ablated Test Specimen R2-1 (Run 89-69)	35
18	Ablated Test Specimen R2-1 (Sectioned)	36
19	Pressure Run 95-69, Specimen R1-1	37
20	Surface Temperature, Run 95-69, Specimen R1-1	38
21	Internal Temperatures, Run 95-69, Specimen R1-1	39
22	Ablated Test Specimen R1-1 (Run 96-59)	40
23	Ablated Test Specimen R1-1 (Sectioned)	41
24	Run 96-69, Specimen R2-2	42
25	Surface Temperature, Run 96-69, Specimen R2-2	43
26	Internal Temperatures, Run 96-69, Specimen R2-2	44
27	Ablated Test Specimen R2-2 (Run 96-69)	45
28	Ablated Test Specimen R2-2 (Sectioned)	46
29	Pressures Run 97-69, Specimen R1-3	47
30	Surface Temperature, Run 97-69, Specimen R1-3	48
31	Internal Temperatures, Run 97-69, Specimen R1-3	49
32	Ablated Test Specimen R1-3 (Run 97-69)	50
33	Ablated Test Specimen R1-3 (Sectioned)	51
34	Ablated ATJ Graphite Test Specimen (Run 98-69)	52
35	Ablated Test Specimen R2-3 (Run 102-69)	53
36	Ablated Test Specimen R2-3 (Sectioned)	54
37	Ablative Recession Profiles, Specimens R1-1 and R1-3	55
38	Ablative Recession Profiles, Specimens R2-1, R2-2 and R2-3	56
39	Ablative Recession Profile, ATJ Graphite Specimen	57
40	Surface Temperature - Silica Phenolic C3-1; C3-2; R1-4	58
41	Surface Temperature - Silica Phenolic R1-1; R1-3	59
42	Ablative Profile - Silica Phenolic C3-2; R1-4	60
43	Surface Temperature - Carbon Phenolic C1-1; R2-4	61
44	Ablative Profile - Carbon Phenolic C1-1; R2-4	62

LIST OF ILLUSTRATIONS (Cont'd)

Part II

Figure		Page
45	Surface Temperature — Carbon Phenolic C2-1; C2-2; R3-6	63
46	Ablative Profile — Carbon Phenolic C2-2; R3-6	64
47	Silica Phenolic — Post Test R1-4	65
48	Silica Phenolic — Post Test R1-4 (Sectioned)	66
49	Surface Temperature — Silica Phenolic R1-4	67
50	Pressures — Silica Phenolic R1-4	68
51	Internal Temperatures — Silica Phenolic R1-4	69
52	Char Measurement — Silica Phenolic R1-4	70
53	Carbon Phenolic — Post Test R2-4	71
54	Carbon Phenolic — Post Test R2-4 (Sectioned)	72
55	Surface Temperature — Carbon Phenolic R2-4	73
56	Pressures — Carbon Phenolic R2-4	74
57	Internal Temperatures — Carbon Phenolic R2-4	75
58	Char Measurements — Carbon Phenolic R2-4	76
59	Carbon Phenolic — Post Test R3-6	77
60	Carbon Phenolic — Post Test R3-6 (Sectioned)	78
61	Pressures — Carbon Phenolic R3-6	79
62	Surface Temperatures — Carbon Phenolic R3-6	80
63	Internal Temperatures — Carbon Phenolic R3-6	81
64	Char Measurements — Carbon Phenolic R3-6	82
65	Carbon Phenolic — Post Test A1-2	83
66	Carbon Phenolic — Post Test A1-2 (Sectioned)	84
67	Pressures — Carbon Phenolic A1-2	85
68	Surface Temperatures — Carbon Phenolic A1-2	86
69	Internal Temperatures — Carbon Phenolic A1-2	87
70	Char Measurements — Carbon Phenolic A1-2	88
71	Silica Phenolic — Post Test A2-1	89
72	Silica Phenolic — Post Test A2-1 (Sectioned)	90
73	Pressures — Silica Phenolic A2-1	91
74	Surface Temperatures — Silica Phenolic A2-1	92
75	Internal Temperatures — Silica Phenolic A2-1	93
76	Char Measurements — Silica Phenolic A2-1	94
77	Carbon Polyimide Post Test A4-2A	95
78	Carbon Polyimide — Post Test A4-2A (Sectioned)	96
79	Pressures — Carbon Polyimide A4-2A	97
80	Surface Temperatures — Carbon Polyimide A4-2A	98
81	Internal Temperatures — Carbon Polyimide A4-2A	99
82	Char Measurements — Carbon Polyimide A4-2A	100
83	Carbon Phenolic — Post Test C1-1	101
84	Carbon Phenolic — Post Test C1-1 (Sectioned)	102
85	Pressures — Carbon Phenolic C1-1	103
86	Surface Temperature — Carbon Phenolic C1-1	104
87	Internal Temperatures — Carbon Phenolic C1-1	105
88	Char Measurements — Carbon Phenolic C1-1	106

LIST OF ILLUSTRATIONS (Cont'd)

Figure		Page
89	Post Test - Carbon Phenolic - Insulative Layer C2-1 (Sectioned)	107
90	Pressures - Carbon Phenolic - Insulative Layer C2-1	108
91	Surface Temperature - Carbon Phenolic - Insulative Layer C2-1	109
92	Internal Temperatures - Carbon Phenolic - Insulative Layer C2-1	110
93	Char Measurements - Carbon Phenolic - Insulative Layer C2-1	111
94	Post Test - Carbon Phenolic - Insulative Layer C2-2	112
95	Post Test - Carbon Phenolic - Insulative Layer C2-2 (Sectioned)	113
96	Pressures - Carbon Phenolic - Insulative Layer C2-2	114
97	Surface Temperature - Carbon Phenolic Insulative Layer C2-2	115
98	Internal Temperatures - Carbon Phenolic - Insulative Layer C2-2	116
99	Char Measurements - Carbon Phenolic - Insulative Layer C2-2	117
100	Post Test - Silica Phenolic - Insulative Layer C3-1	118
101	Pressures - Silica Phenolic - Insulative Layer C3-1	119
102	Surface Temperature - Silica Phenolic - Insulative Layer C3-1	120
103	Internal Temperatures - Silica Phenolic - Insulative Layer C3-1	121
104	Char Measurements - Silica Phenolic - Insulative Layer C3-1	122
105	Post Test - Silica Phenolic - Insulative Layer C3-2	123
106	Post Test - Silica Phenolic - Insulative Layer C3-2 (Sectioned)	124
107	Pressures - Silica Phenolic - Insulative Layer C3-2	125
108	Surface Temperature - SilicalPhenolic - Insulative Layer C3-2	126
109	Internal Temperatures - Silica Phenolic - Insulative Layer C3-2	127
110	Char Measurements - Silica Phenolic - Insulative Layer C3-2	127
111	Transverse Cross Sections, R1-4	129
112	Transverse Cross Sections, R2-4	130
113	Integrated Heats of Ablation	131
114	Cold Wall Heats of Ablation Carbon Fiber Specimens	132
115	Thermochemical Heats of Ablation	133

LIST OF TABLES

Table		Page
I	Cycle 1 Test Series	135
II	Description of Test Specimens	136
III	Materials Data	137
IV	Ablation Parameters	138
V	Specimen R2-1 Model Measurements	139
VI	Specimen R1-1 Model Measurements	140
VII	Specimen R2-2 Model Measurements	141
VIII	Specimen R1-3 Model Measurements	142
IX	ATJ Graphite Specimen Model Measurements	143
X	Specimen R2-3 Model Measurements	144
XI	Ablation Test Results (Uncorrected)	145
XII	Specimen R1-4 Model Measurements	147
XIII	Specimen R2-3 Model Measurements	148
XIV	Specimen R2-4 Model Measurements	149
XV	Specimen R3-6 Model Measurements	150
XVI	Specimen A1-2 Model Measurements	151
XVII	Specimen A2-1 Model Measurements	152
XVIII	Specimen A4-2A Model Measurements	153
XIX	Specimen C1-1 Model Measurements	154
XX	Specimen C2-1 Model Measurements	155
XXI	Specimen C2-2 Model Measurements	156
XXII	Specimen C2-3 Model Measurements	157
XXIII	Specimen C3-2 Model Measurements	158
XXIV	Ablation Test Results Reference Test Specimens	159
XXV	Ablation Test Results LDQ Composite Test Specimens	160
XXVI	Ablation Test Results Experimental Test Specimens	161
XXVII	Summary of Heat of Ablation Data	163

I. INTRODUCTION

The selection of ablation materials and concepts for application as heat shields of vehicles subjected to high integrated heat loads can be made only if the total environmental problem area imposed by these thermal conditions is thoroughly understood. The heat shield concepts must be selected on the basis of their ability to cope with the problem areas, while imposing minimum weight and volume penalties on the vehicle. Briefly, the heat shield must maintain an acceptable internal temperature, while it remains intact and maintains an aerodynamically stable shape.

The heat flux histories for the heat shields of two types of vehicles are compared in Figures 1 and 2. Figure 1 shows the history of a typical high speed re-entry vehicle subjected to short time heating, while Figure 2 shows the heat flux exposure of a hypothetical vehicle subjected to long term heating.

The structural integrity of the standard carbon phenolic tape wrapped heat shield under long term, high heat load conditions has been observed to be poor, especially under conditions of variable heat load. Organic resin bonded refractory fiber composites, upon exposure to high temperatures far in excess of normal environmental conditions such as those encountered during re-entry, undergo decomposition reactions that produce shape changes governed by the mode of decomposition of the resin. A resin that yields a large proportion of char, and that allows gaseous decomposition products to escape slowly and in controlled fashion, will form a more stable composite than a resin that breaks down rapidly into large volumes of gas, yielding little char. The characteristics of the fiber, in particular such properties as thermal conductivity, surface area, and oxidative stability, will also affect composite stability under these conditions. The processing steps that a composite undergoes, and the density, porosity, and degree of cure of the resin in the finished material, will influence the shape stability and integrity of the piece upon pyrolysis. The tendency of a laminate to crack, split, and warp upon exposure to an arc or some other high temperature environment is due to an interaction of the resin/fiber components during decomposition.

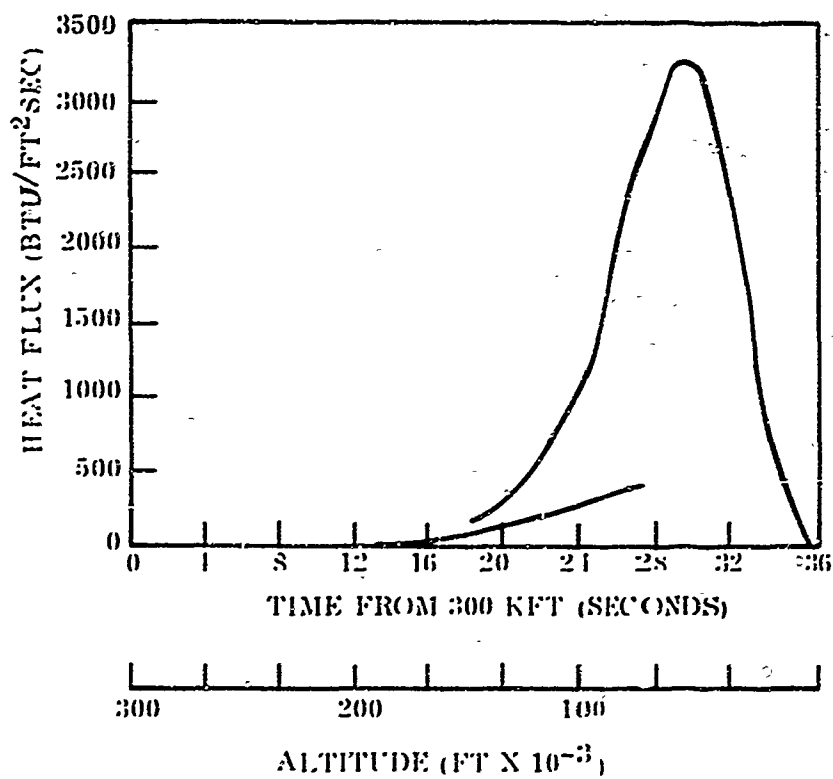


Figure 1. Short Time Heating

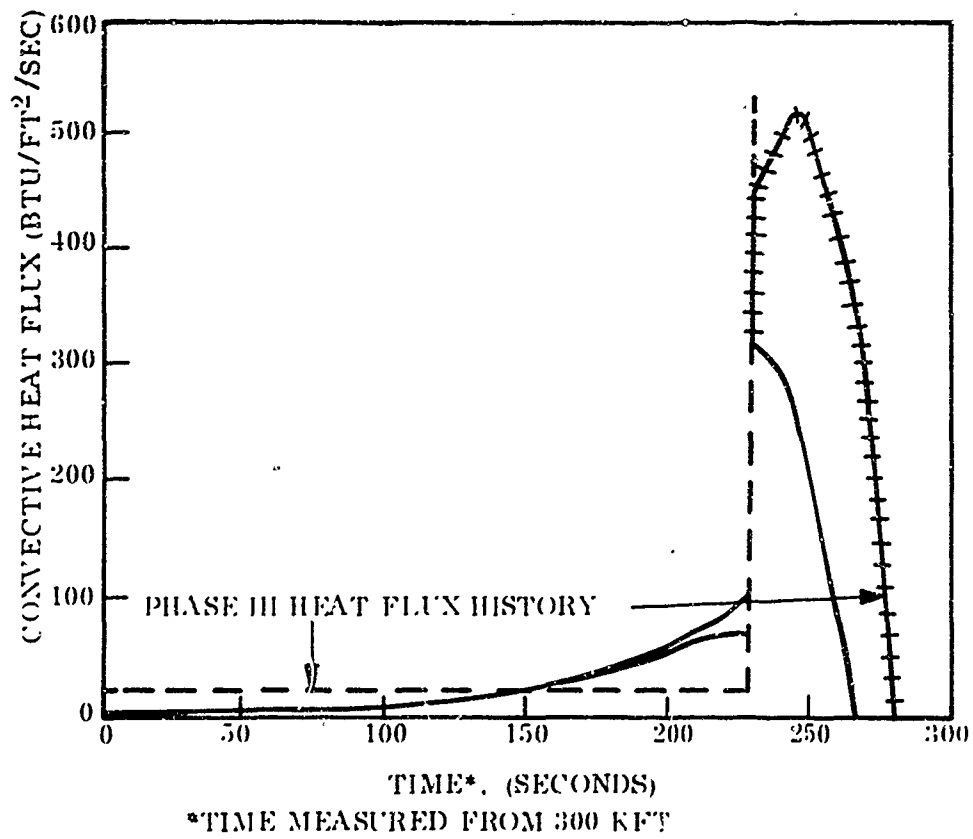


Figure 2. Long Time Heating

II. TECHNICAL APPROACH

Current practice utilizes a 20 degree tape wrapped heat shield fabricated from a bias prepreg tape. Three reference (control) laminates were prepared from two types of carbon cloth and one type of silica fabric impregnated with phenolic resin. In addition, seven developmental test specimens were prepared consisting of four ablative shield samples and three low density quartz (LDQ) samples sandwiched between an ablative shield and a 2024-T3 aluminum plate. (Tables I and II describe the test specimens.) Table III gives the properties of the pre-preg materials used in making the specimens. ATJ graphite was used in a calibration run, and its properties are also given.

REFERENCE TEST SPECIMENS (R1, R2 AND R3)

Two types of carbon fabric and one type of silica fabric in the form of a 45 degree bias tape and impregnated with phenolic resin were cut into strips 6 inches long. The 6 x 2 inch strips were stacked in an aluminum holding fixture which contained a 20 degree wedge at one end. This facilitated the maintenance of a 20 degree orientation of all the impregnated strips simulating a 20 degree tape wrapped ablative shield. The assembly was then vacuum bagged, and the impregnated fabric was subjected to B-stage consolidation at 15 psi and 180°F for one hour. The bagged assembly was then placed in an autoclave and exposed to the following cure schedule at 150 psi:

2 hours at 200°F

2 hours at 250°F

4 hours at 325°F

The cured material was then removed from the vacuum bag and post-cured for four hours at 400°F.

Test specimens, 5.00 x 1.75 x 0.50 were machined from the cured laminate and bonded to chromic acid etched 2024-T3 aluminum (0.0625 inch thick) with HT-435 epoxy-phenolic film adhesive. The assembly was clamped and the adhesive was cured for one hour at 350°F.

ABLATIVE SHIELD TEST SPECIMENS (A1, A2, A3 AND A4)

A. Phenolic Impregnated Carbon and Silica Fabric

VCX carbon fabric and reffrasil silica fabric were dried at 250°F for one hour. A 67 percent solution of DP2510 (solvated phenyl phenolic resin) in methyl ethyl ketone was used to impregnate the dried fabrics. Two coats of the resin solution were brushed onto the fabrics. The impregnated fabrics were allowed to air dry for 16 hours. An additional coating was then applied and the coated fabrics were dried six hours in air. Each fabric was then B-staged at 180°F for one hour in a circulating air oven. Two inch wide strips were then cut on a 45 degree bias from each fabric. In addition, samples for the determination of resin content, volatile content and flow were cut from each impregnated fabric. Carbon-phenolic and silica phenolic laminates and test specimens were then prepared.

B. Polyimide Impregnated Carbon and Silica Fabrics

CCA1-1641 carbon fabric and reffrasil silica fabric were dried at 250°F for one hour. A 50 percent solution of Skybond 700 (solvated polyimide resin) in methyl ethyl ketone was used to impregnate

the dried fabrics. Two coats of the resin solution were brushed onto the fabrics. The impregnated fabrics were allowed to dry 16 hours. An additional coating was then applied and the coated fabrics were dried for six hours. Each fabric was then B-staged at 250°F for 45 minutes. Two inch wide strips were then cut on a 45 degree bias from each fabric. In addition samples for the determination of resin content, volatile content and flow were cut from each impregnated fabric. Carbon-polyimide and silica polyimide laminates and test specimens were then prepared as previously described with the exception of the cure schedules. B-stage consolidation in the 20 degree holding fixture was accomplished at 250°F for one hour at 15 psi. The laminates were cured in the autoclave at 150 psi at 350°F for four hours. The cured laminates were then post-cured four hours each at 400°F, 450°F, 500°F and 600°F.

LOW DENSITY COMPOSITE TEST SPECIMENS (C1, C2 AND C3)

A. General

The process used in the fabrication of the C1 and C3 composites (Tables I and II) involved the simultaneous curing of the primary ablative shield with the LDQ component. Test specimen C2 was prepared by bonding cured constituents of the multilayered material.

B. Fabrication of C1 and C3 Low Density Composites

A loom was fabricated for weaving the resin impregnated LDQ component of the composite shield material. Nails, driven into a plywood panel, were spaced 0.25 inch between centers and formed a 6 x 6 inch square. A 2024-T3 aluminum panel, 6 x 6 x 0.063 inch, was degreased, scrubbed with Comet cleanser, dried and placed at the base of the loom.

Q-24 quartz thread, impregnated with HT-424 epoxy-phenolic resin was woven into a non-interlaced "egg-crate" construction on top of the aluminum panel. Twenty-two plies of the impregnated yarn were woven in alternating 90 degree, non-interlaced layers resulting in a total of 44 yarn layers.

A 6 x 6 inch piece of 181 glass cloth was impregnated with HT-424 resin and placed on top of the "egg-crate" construction. The LDQ "egg-crate" assembly was then vacuum-bagged and subjected to B-staging at 15 psi and 180°F for one hour.

The stacked carbon-phenolic and silica phenolic tape, similar to the pre-B-staged material described previously, was placed on top of the B-staged LDQ construction covered with the impregnated glass cloth. The entire unit was then vacuum-bagged and subjected to 15 psi and 180°F for one hour. The bagged assembly was then placed in an autoclave and exposed to the following cure schedule at 150 psi:

2 hours at 200°F

2 hours at 250°F

4 hours at 325°F

The cured multilayered material was then removed from the vacuum bag and post cured for four hours at 400°F. The composite was then machined into test specimens 5.00 x 1.75 x 0.75 inch (typical). The simultaneous curing process just described was employed to facilitate the anticipated

fabrication of a composite frustum. Because of this processing technique, a wavy interface between the ablative and LDQ layers resulted. It should be emphasized that this may not be a deleterious effect.

C Fabrication of C2 Low Density Composite

This technique involved the separate curing of the ablative and LDQ components followed by bonding with HT-435 (HT-424 without aluminum filler) film adhesive. This procedure resulted in a more reproducible LDQ thickness and a more uniform bond line between the ablative and LDQ components. In addition, the modified process included the use of 36 yarn layers, rather than 44 and the LDQ layer was bonded to 0.0625-inch thick 2024-T3, chromic acid etched aluminum with HT-435 film adhesive.

Since all of the test specimens were fabricated by means of the same basic process, Figures 3, 4, and 5 can be looked upon as typical intermediate processing steps. These figures illustrate the fabrication of the low density quartz fiber reinforced section, the lay-up of ablative material, and the cured blank. Figures 6 and 7 are top views of test specimens prepared from the cured blanks.

TEST SPECIMEN INSTRUMENTATION

Carbon phenolic and silica phenolic specimens were provided in the form of rectangular pieces machined to 1.75 x 5 x 0.5 inches. Fiber orientation was within the prescribed tolerances. Overall weights measures and material density were provided. A specimen test record sheet was used to maintain control over each specimen.

The specimens provided were accurately instrumented with four thermocouples and a tungsten reference wire. In the process, a new drilling technique was evolved and used with success. It was found that the small diameter drills used to provide thermocouple insertion holes tended to break when they encountered the fibrous components of the materials while running hot. Carbide tipped drills suffered the same failure as the steel drills. It was concluded that heating helped to weaken the drills. The first attempt to control the heating was to add water as a coolant, but that was not successful because fragments of the test material produced a slurry which, in turn, tended to interfere with the drilling operation. A workable system was evolved using compressed air as the coolant. Ordinary steel drills are used. Several are broken in preparing a specimen, but in each case, the broken section has protruded and was extracted from the hole. No specimen for test retained a drill fragment.

An area that has been subject to some concern is the accurate determination of the depth of the thermocouple junction. Supplemental to the technique currently used in the laboratory, x-ray films have been taken of the first group of specimens. The films have been examined to evaluate depths; however, measurements from x-ray films may contain inaccuracies averaging as much as five mils. Sources of error include parallax, specimen alignment, and film shrinkage. A technique developed to satisfy the geometric restrictions of our particular model configuration could provide accuracies to less than one mil. Figure 8, shows x-ray views of two of the specimens provided.

The technique used in the instrumentation laboratory can provide good accuracy. An optical comparator is employed to project images magnified ten times of the specimen (Calibration with a standardized length easily confirms the magnification factor). After the instrumentation holes are drilled, a drill of micrometrically measured length is then inserted in each hole. The projecting length is measured to obtain the depth of the hole, by difference. The angular position of the projecting length in the appropriate plane indicates the direction the drill has taken relative to the

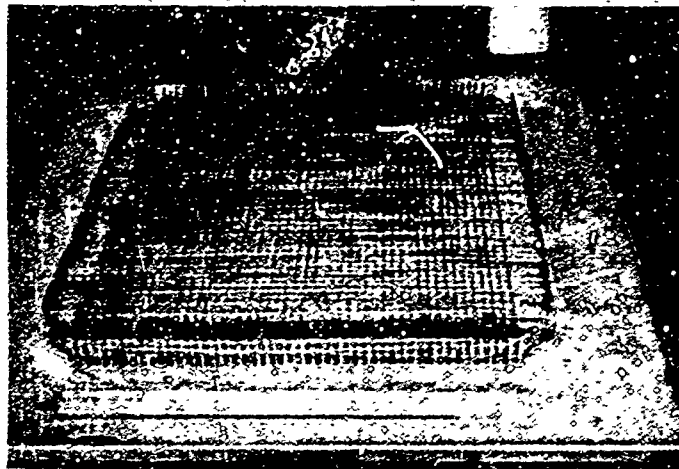


Figure 3. Quartz Layup Ready for Compaction

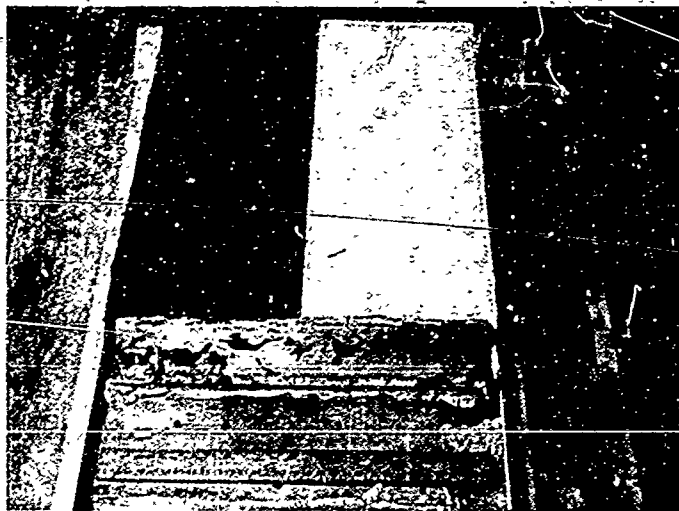


Figure 4. Heat Shield Prepregs in Position

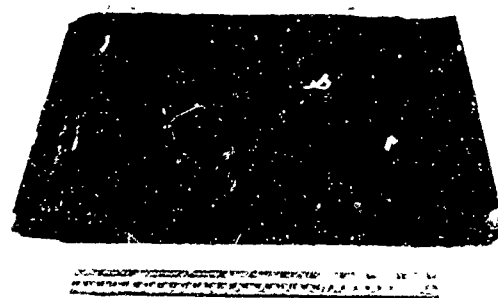


Figure 5. Cured Blank

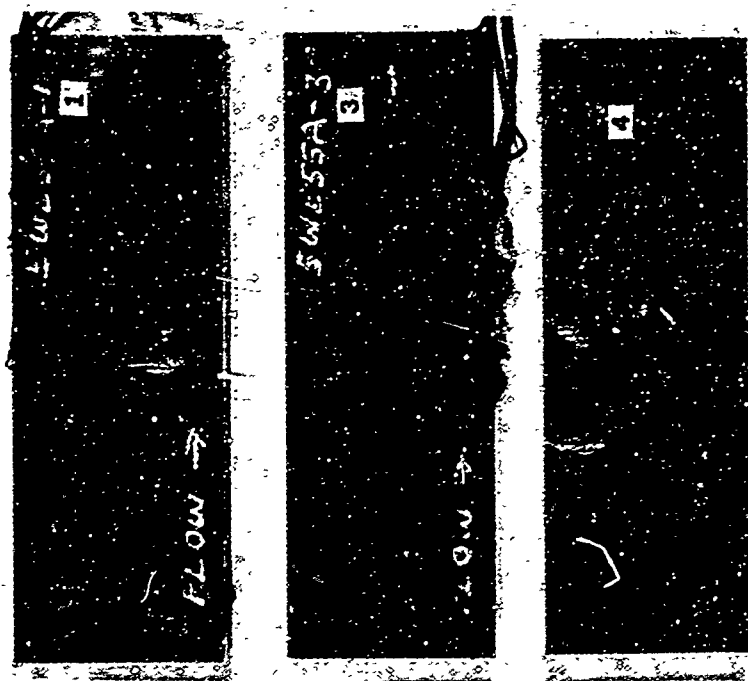


Figure 7. Machined Silica Phenolic Specimens

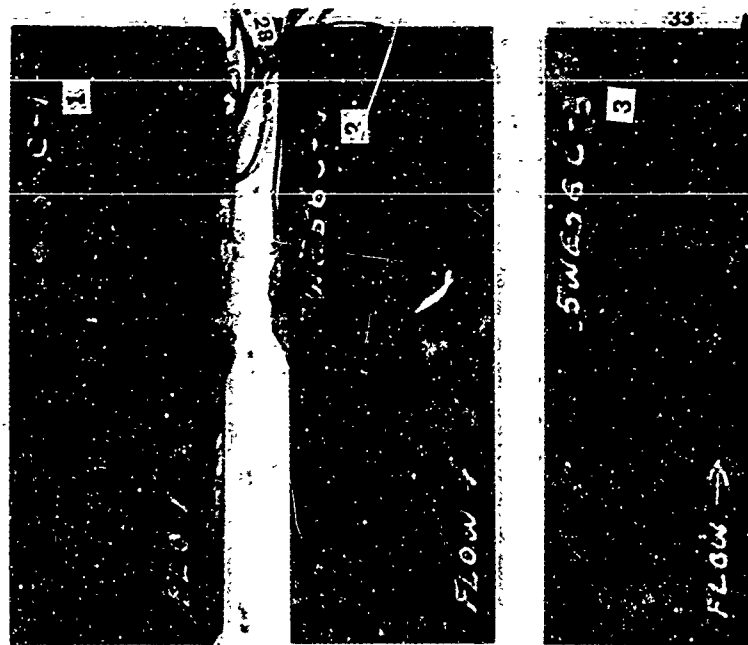


Figure 6. Machined Carbon Phenolic Specimens

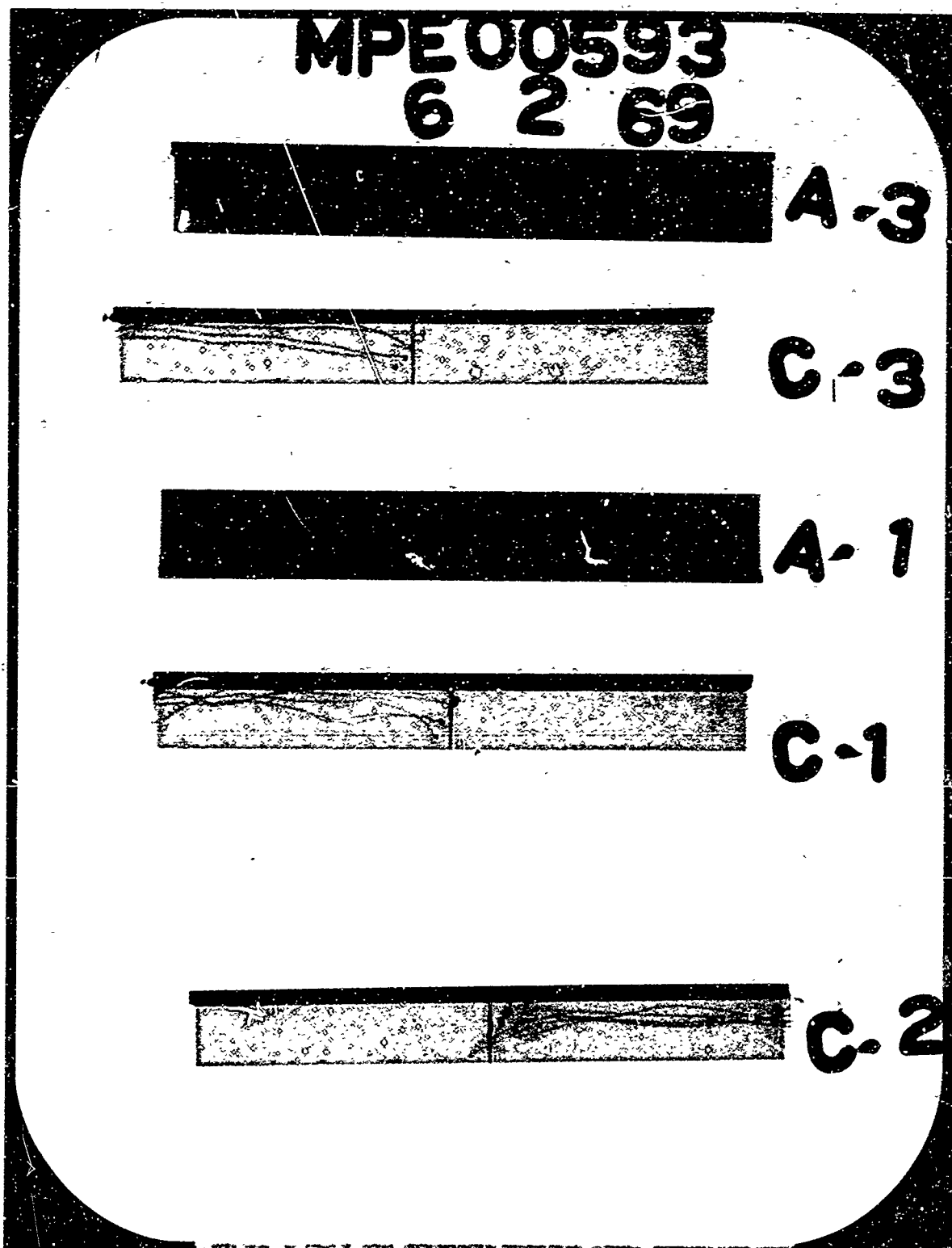


Figure 8. X-ray Views of Two Types of Instrumented Specimens

surface to be heated. Simple trigonometric calculations provide a measure of the point where the thermocouple junction will be located.

An estimate of error for a typical situation has been obtained (see Figure 9). Measurement of the location of the thermocouple depth with an error of ten mils, as installed at an assumed angle of 3 degrees, results in an error of 0.5 mils relative to the surface. It has been the experience of machinists that drills of the size employed cannot sustain a bow of more than two or three mils without breaking. Even this amount of flexure could not be sustained within a curved hole. Hence, hole enlargement of up to three mils could occur and negligible curvature would exist. Due to enlargement, the measurement of the true axis may contain an error of less than ten minutes of arc. This leads to a possible depth error of approximately 1.5 mils. Assuming the errors to be maximum and cumulative, an error of approximately two mils might be accumulated and added to the true absolute depth of the thermocouple relative to the heated surface of a specimen.

The represented errors are reasonable, even conservative, compared to those which might be accumulated in actual measurement. Hence, it is estimated that the measurements are of an accuracy superior to that obtainable from standard measurements of x-ray films. After test, the specimens were sectioned to locate the actual hole positions, and the drill-rod measuring technique weighed against the x-ray films. The drill rod measurement technique was found to be acceptable.

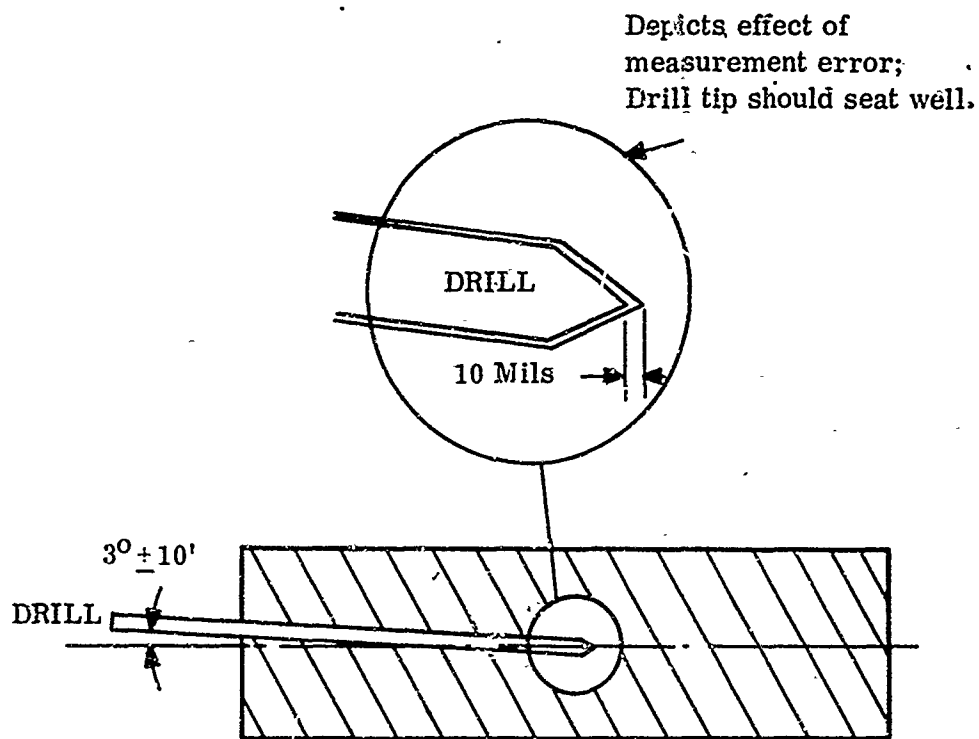
LABORATORY CHARACTERIZATION

Hyperthermal Arc Facility

A brief review of the characteristics of the arc heater employed for the test program is appropriate. The arc heater unit is of the Tandem Gerdien design as depicted in Figure 10. Gas enters the unit through two swirl chambers and the flow is divided. Part of the gas passes through the vortex stabilized arc column into the plenum chamber and is then discharged to the test chamber. The remainder of the gas passes over the electrodes, carrying off any trace of contaminants, and exhausts from the rear of the arc chamber. The arc unit, including electrodes, is watercooled copper with the exception of insulators. For the present program, the secondary plenum, the rectangular nozzle, the by pass assembly and other related components are added. Power to maintain the arc is furnished by two direct current generators, each of which is rated at 2000 amperes and 1300 volts. They are connected in parallel. At the Hyperthermal facility, the Gerdien heater has a plenum of the wedge design. The economy of internal surface area within the plenum results in the capability to achieve stagnation enthalpies approximately 20 percent greater than those attainable in the in-line electrode geometry.

Heat transfer and pressure are measured above the upstream half of the sample during each run (see Figure 12). These parameters are also read at the sample during calibration and correlated with upstream readings. Enthalpy is determined by energy balance and all other parameters are measured except shear stress. Shear is determined by using Reynold's analogy for turbulent flow together with measured parameters. Table IV summarizes the important parameters associated with ablation testing.

A family of trajectories has been generated which are compatible with the study program. Figure 11 shows a typical trajectory which has been selected to govern test conditions. In this characterization phase, a nominal heat flux of 25 Btu/ft²-sec was used for the first 230 seconds and 440 Btu/ft²-sec for the remaining 70 seconds. The latter heat flux was the highest obtainable for this type of long term ablation testing. Shear is low initially, but increases with an increase in heat transfer.



Note: Tolerance of 10 mils represents an enlargement of the hole by 3 mils

Figure 9. Method for Estimating Thermocouple Position

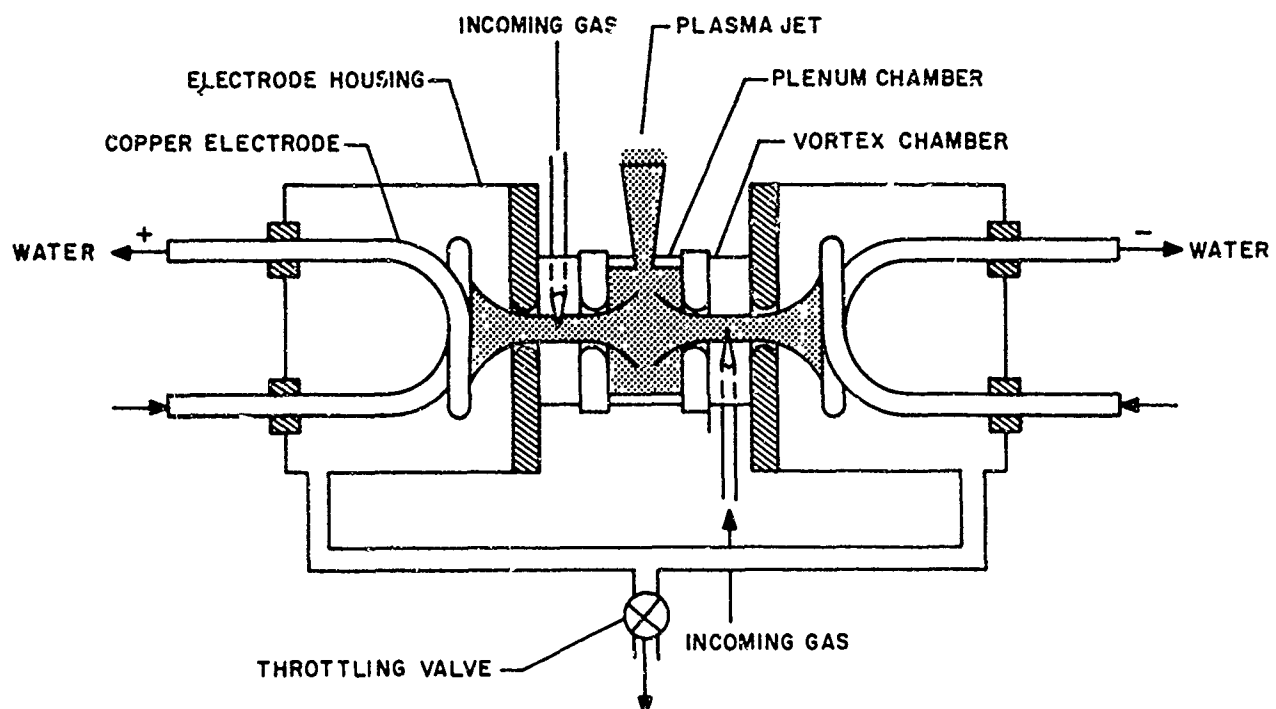


Figure 10. Tandem Gerdien Arc Chamber (Schematic)

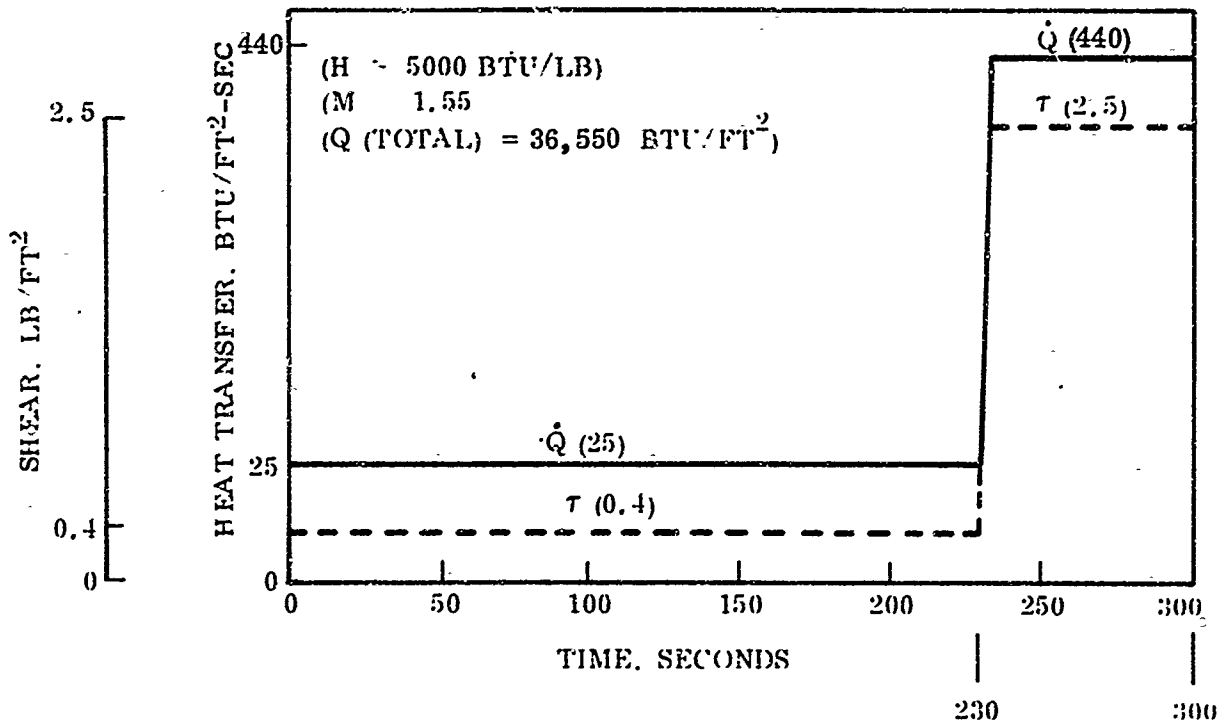


Figure 11. Nominal Shear and Heat Transfer Ablation Test Program

Standard procedures for conducting tests and handling models are utilized. Samples are examined before and after testing to determine pertinent data and assure quality control. All facility conditions and test are accompanied by calibration data which present sufficient information to verify flow conditions and perform further analysis.

CHRONOLOGY OF ABLATION TEST PROGRAM

The water cooled channel was designed to produce the capability to change the mass flow distribution through auxiliary hardware and alter the heat transfer in a manner prescribed by the requirements of the test program (see Figure 12). The solution of the design problem was obtained by introducing a second plenum between the arc plenum and the rectangular nozzle of the water cooled channel (see Figure 13). The secondary plenum was equipped with an alternate cylindrical by-pass channel. All components were water cooled. An assembly consisting of a cylindrical graphite plug driven by a reciprocating air cylinder was mounted co-axial with the by-pass channel. The graphite plug functioned to close the by-pass which carried most of the mass flow when open. Closure of the by-pass forced all air to pass through the rectangular nozzle producing supersonic flow conditions.

The throat of the rectangular nozzle was sized to be 0.1000 square inches. Used in conjunction with the conventional nozzle of the arc facility, it was intended that when the by-pass was closed, virtually no change in arc heater conditions should occur. The nozzle throat of the arc heater measured 0.1104 square inches. Subsequent use of the system showed that no corresponding change in arc plenum pressure resulted when the by-pass was closed.

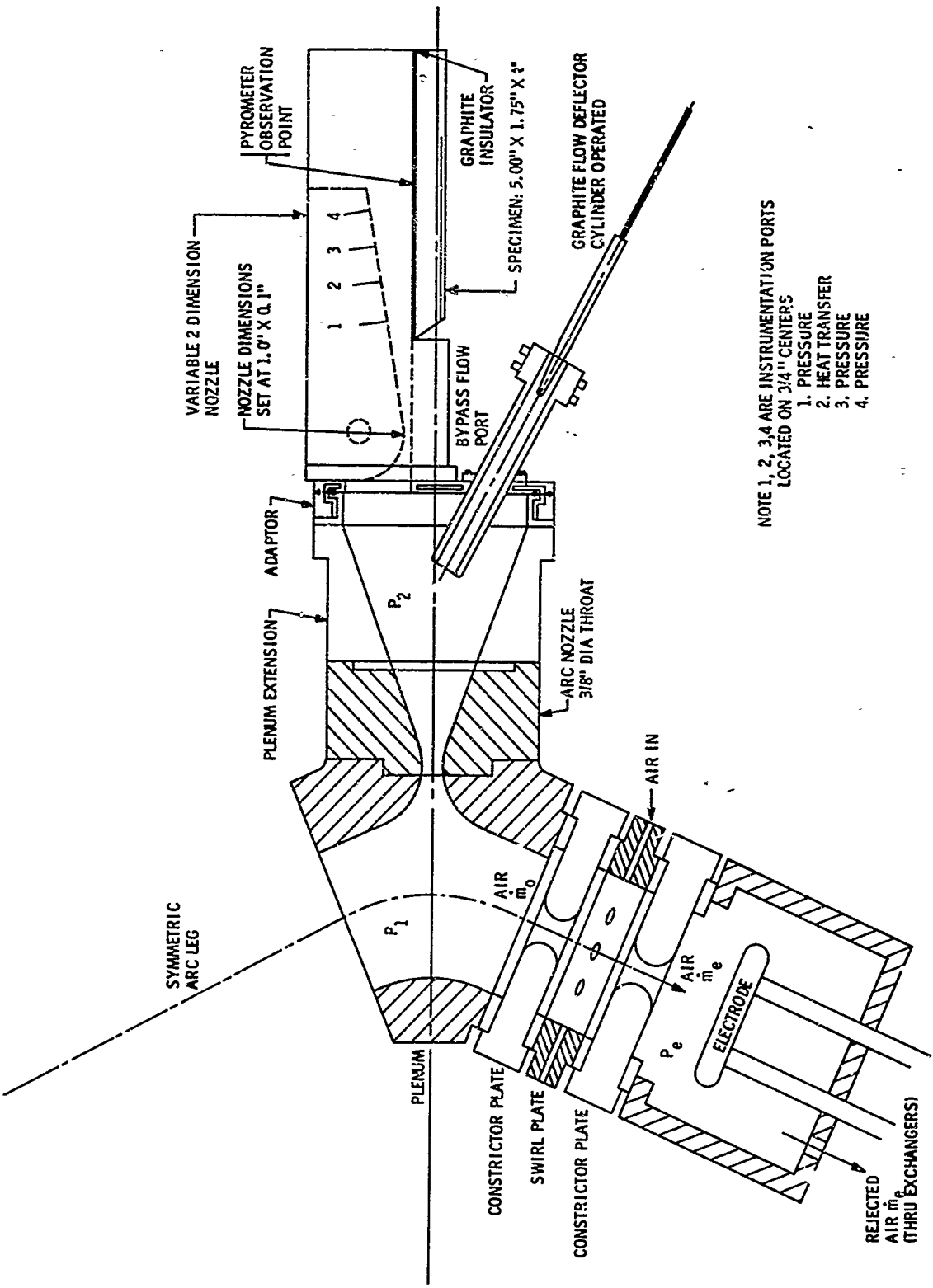


Figure 12. Arc and Channel Ablation Test Fixture

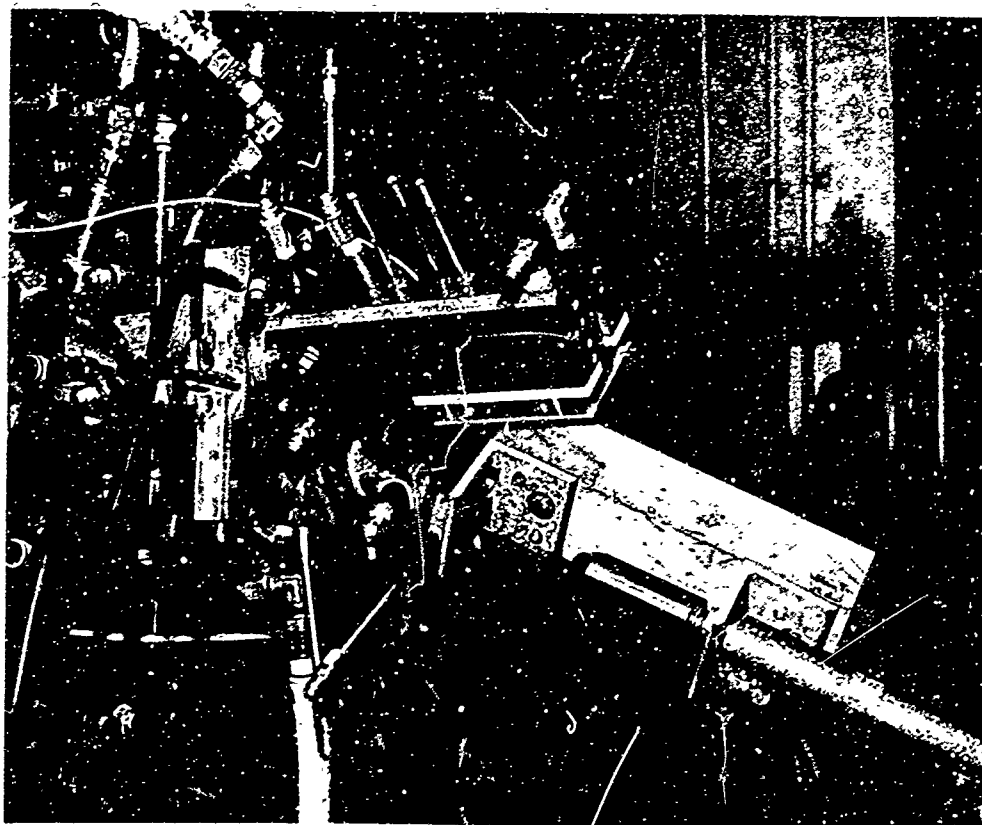


Figure 13. Equipment Installed at the Arc

When the hardware had been fully qualified, tests were conducted, first without employing the by-pass and later inserting the graphite plug to require pressurization of the second plenum and the development of supersonic flow. Various problems arose, leading to improvement of the by-pass plug mechanism. Finally calibration runs were conducted. It was intended that asymptotic (Gardon) gauges should give a continuous record of the rate of heat transfer being delivered at several stations along the wall of the channel. After several attempts to evaluate the signals from the asymptotic gauges, which displayed abnormalities attributed to spurious signals from the arc plasma, calibration procedures were modified to include a water cooled gauge electrically insulated from the metallic parts of the nozzle. The signals generated by this gauge appeared to be normal and heat transfer rates approaching the values sought were recorded. The intention in using the water cooled calorimeter which was installed in place of a specimen was to calibrate the signals generated by the asymptotic gauges. Thereafter, the generation of signals from the asymptotic gauges were planned to be used to evaluate heat transfer based on these calibrations. Unfortunately, the gauges were not capable of sustaining the long time heating required for the specimens. It appears probable that deterioration may have begun during earlier long tests (e.g., run 80, 130.6 seconds).

In any case, the gauges ceased to respond at all during run 89, the first of the specimen tests. Concurrently, other solutions to the problem of continuous recording of heat transfer have been sought. While it is probable that further experimentation would probably result in a match of measured heat transfer rates with those set as objectives, the expenditure of additional time and effort seemed unprofitable. Therefore, testing of specimens was initiated. Initially, the long tests, totalling some 300 seconds, created various problems and several aborted model tests. Some of these will be discussed in this report. Toward the end of testing of the Phase One specimens, the testing was progressing more routinely.

MECHANICAL REDESIGNS

The initial experiments employed a graphite plug supported by a coil spring. The spring was intended to avoid a bottoming impact of the plug. It was considered likely that severe impact might fracture the plug and force premature termination of the test. Early, relatively short tests showed that despite the significant distance between the end of the by-pass nozzle and the retracted graphite plug, the latter acquired significant heating. In one case, the length of the test was sufficiently long to bring the graphite to a temperature yielding significant visible radiation (perhaps 2000°R) before it was inserted. Indeed, the spring lost its temper, and metal parts inside were melted. Consequently, the system of attaching the graphite to the cylinder was modified and an arrangement of expendable O-rings was used to cushion the seating impact. More important, however, a shield was constructed to deflect the by-pass flow and minimize premature heating of the graphite. An auxiliary air cylinder was attached to a shield plate positioned between the by-pass nozzle exit and the retracted graphite plug. Early experiments employed ESM (silicone rubber based heat shield material). This method was shown to be capable of successful application, but the severity of the heat produced significant ablation and required frequent replacement of the shield. Furthermore, the ESM was not totally reliable in this application. However, it was used as an interim method until water cooled components could be constructed and mounted on the shield plate and the support beam for the graphite plug and related equipment. Since its installation the water cooled shield equipment has performed faultlessly.

During tests of long duration, the interior leading edge of the by-pass nozzle, which lies approximately on the centerline of the flow from the arc plenum, is burdened with intense heating. The free jet issuing from the arc plenum is supersonic. The first attempt to develop the full test time resulted in a failure of the by-pass nozzle. The failure was traced to erroneous fabrication tolerances. The damaged part was removed by machining and a replacement which had been fabricated to meet the design tolerances was affixed to the assembly. The replacement accumulated a significant amount of exposure time, but eventually failed because the high enthalpy gas stagnation on the nozzle had gradually eroded the metal. A replacement was again installed using Elkonite, an alloy combining the advantage of good thermal conductivity with that of higher melting point. The second nozzle replacement has been employed for all remaining tests.

Figure 12 is a schematic diagram which shows a cross-sectional view of the modified arc, and gives operational details. Figure 13 is a photograph of the actual installation. Figure 14 shows the changes that were made to the by-pass insert in order to insure reliable operation.

SPECIMENS

All specimens were constructed with flat surfaces. They measured 1.750 inches wide by 5 inches long. The location of the model in the arc is shown in Figure 12. Thicknesses depended on the type of model employed. Three broad classifications evolved in the course of development of the program. The R-series were specimens constructed for test as references. The C-series was comprised of two layer composites of which the subsurface layer was an insulator and the surface material was an ablative shield material of the R-series. A third group, the A-series was constituted of prospective candidate shield materials. Each specimen was instrumented with five nominally equispaced thermocouples. Early in the program, it was demonstrated that a system of physical measurements gave accuracies as great as those obtainable by x-ray techniques. These measurement techniques have been employed consistently to measure the actual locations of the thermocouple junctions. Although the nominal plan was to equispace the thermocouples, it was found that drill misalignment and positioning error seldom resulted in the thermocouples being located in their nominal positions. However, the actual depths are measured to estimated accuracies of two mils. The thermocouples are chromel alumel with wire diameters of five mils.

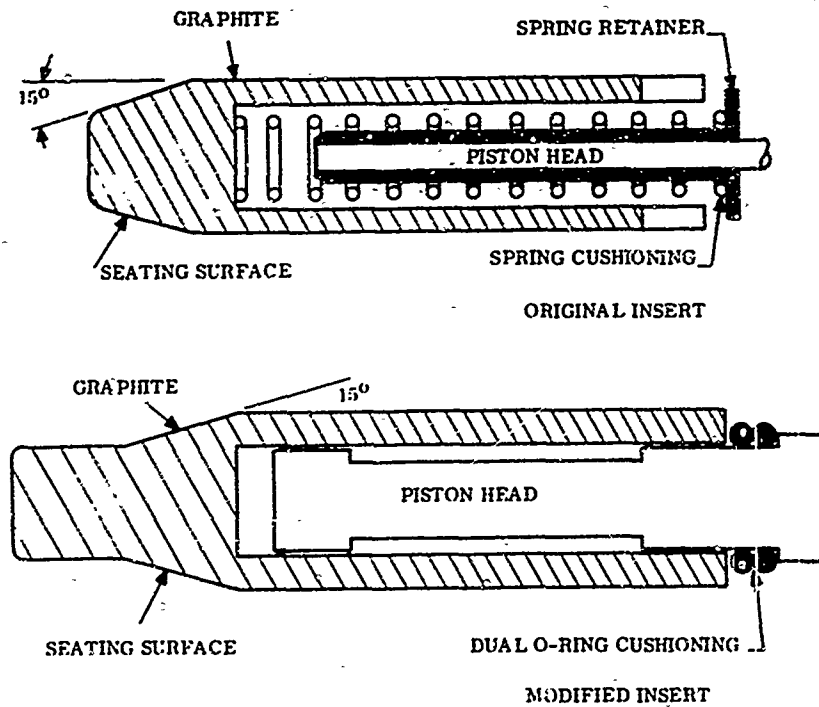


Figure 14. Modification of Graphite Inserts for Bypass

ARC HEATER PERFORMANCE

The performance of the arc heater is normally assessed in terms of the enthalpy attainable in gases passed through the arc plenum. Various methods exist for determining the gas enthalpy, and of these, the Hypersonic Arc Facility employs the heat balance to determine enthalpy. The heat balance merely sums all of the measurable values of rejected thermal energy, subtracts them from the known input energy and uses the difference to represent the amount of energy contained in the air. The Gerdien arc has a multitude of individual lines furnishing cooling water from an inlet manifold and a similar number returning the water to the outlet manifold after it has passed through the components of arc hardware. It would be advantageous with respect to data acquisition to monitor the flow rate and temperature rise of water flowing through each individual component, but the number of measurements required becomes prohibitive. An acceptable alternative is to record the bulk water temperatures in the inlet and outlet water manifolds. It was demonstrated experimentally at NASA Houston for the Gerdien arc installed there that the small temperature changes developed do not contribute significant heat to the hoses and fittings joining individual parts with the manifold. Within the accuracy of the measurements, heat losses compiled from all individual components corresponded to bulk heat loss measurements in the manifold. The Gerdien Arc used in the present program is monitored for temperature change in the inlet and outlet water manifolds. While the results may be representative, there is one area in which erroneous readings may be obtained. In the event that mixing of the individual water streams from hose lines joining the outlet manifold is not thorough, it is possible to postulate the existence of strata of hot and cold water. Inadequate thermocouple instrumentation within the water passage can lead to erroneous hot water temperatures. In the present program, this situation exists and may account for some of the scatter in the enthalpy data. This scatter is evident because it has been demonstrated from an accumulation of experimental data that for a constant mass flow in a fixed geometry, the energy contained in the gas exposed to the arc column is approximately proportional to the energy consumed by the arc. Statistical plotting of prior tests at similar conditions have demonstrated the approximation. Of course, such things as arc column behavior and the effectiveness of stabilization may produce effects which perturb the proportionality. Furthermore, the variations may be aggravated by the more complex exchange of heat and redirection of mass flow in the high integrated heating apparatus. Certainly there was more than usual scatter of the data.

An additional problem created by the heat balance method is the effective scatter introduced by measurement errors of the recorded water temperature difference. The differences measured have in general been about 25°. An error of one degree represents a four percent temperature change. Depending upon the measured value of delivered energy and the mass flow rate of the water, enthalpy variations of 20 percent are not unusual. Hence all measurements have been reviewed carefully. Measurement errors have been minimized, but possible system errors associated with recorded data (such as those introduced by insufficient thermocouple instrumentation) can not be quantitatively identified. Recommendation has been made, however, that an array of thermocouples be installed to provide an averaged outlet water temperature.

The water cooled channel design was based upon gas of an enthalpy of 5000 Btu/lb driven by a plenum pressure of 60 psia. Early exploratory tests revealed that in order to achieve values approaching those of design, a significantly higher enthalpy and pressure must be generated in the arc plenum. When acceptable operating conditions were achieved in the secondary plenum, which furnished the driving potential for the fully operational rectangular nozzle, the pressure in the arc plenum was in the vicinity of 100 psia. Although the arc plenum pressure is not normally sufficiently high to produce a choked flow at the arc plenum nozzle exit when entering the second plenum, it is extremely interesting to note that rarely during the specimen testing was there an observed change in P_1 which reflected alteration in P_2 the secondary plenum pressure.

The conditions of operation achieved during each test have varied appreciably. One contributing factor of importance is the furnished power and its division between the electrical voltage and the current from which it is evaluated. The exact current and voltage cannot be furnished by the GE Switchgear operators with precision control. However, while direct control is not within the province of the RESD facility personnel, it has been shown that once the arc is operating, it is possible to modify current (and hence voltage) to a degree and hence adjust operating power toward the same level on every run. Thus, within limits, there exists the capability to improve the repeatability of successive runs. It is expected that this technique will be applied to subsequent testing. The adjustments can be made in the early portion of the low heat transfer segment of a run. Thus it is anticipated that little effect will be imposed on the integrated heat transfer.

SOME ASPECTS OF TESTING

One of the principal objectives sought in designing the water cooled channel was to provide an environment in which the flow was expanded to one atmosphere at the exit plane of the nozzle. Achieving such conditions provides a parallel flow such that shock reflection and interaction effects are minimized. In many of the tests (referring to the high heat transfer portion of the tests) the pressure achieved approached the one atmosphere design value. Several tests produced pressure values different from one atmosphere. Generally, in these cases, the pressures were subatmospheric and the pressures were required to shock up to one atmosphere. It follows that when pressure mismatch occurred, the resulting interactions produced irregular ablation on the specimen. Of course, the maintenance of an absolutely uniform channel cross section is impossible in the presence of an ablating specimen. Hence the optimum solution is to create local pressure slightly in excess of atmospheric at the upstream station. Ablation of the specimen will increase the channel cross-section locally, resulting in a decline in the static pressure. Overexpansion in the channel is not desirable because of its adverse effect on heat transfer. Fortunately, the plan to attempt to control the input power to the arc should yield positive advantage with regard to pressure stability. The contributions of ablation effects appear to be unavoidable and incapable of being compensated. Poor ablators will obviously aggravate the decline in pressure, but control of the power will tend to confine pressure changes to those produced by ablation, since pressure conditions are variable as a function of power.

One area which created problems initially was the selection of insulators to isolate the test specimens from the water cooled hardware. Several conventional ceramics were tried, but evidence pointed to their inability to withstand the severe heatloading when all flow was directed through the nozzle. Alumina plates became very brittle and tended to crack under the severe gradients. A low density foamed silica was tried, but it failed dramatically. Within a few seconds after closing the bypass, it glowed whitely and melted. The flow was dispersed and the run aborted. The failure of conventional insulators forced a compromise selection of graphite. The graphite has the capability of withstanding the high integrated heatload. Because it is appreciably more conductive than the ceramic materials, the geometry of the holder was modified in order to minimize conduction paths between the graphite and the water cooled equipment. Thus, although it may conduct more heat from the specimen, the geometric considerations tend to offset excessive heat loss. Of paramount importance, the compromise solution assures survival of the insulator throughout the run. Finally, a brief comment about another possible objection to graphite as the insulator is appropriate. It has been demonstrated that when heated to high temperature, the graphite is quick to combine with free oxygen. The possibility presents itself that the graphite will deplete the oxygen in the air and thus inhibit the ablation process on the surface of the specimen. However, it can be shown that carbon-oxygen reactions will be confined essentially to the boundary layers which develop above the graphite plates. At the operating conditions employed, boundary layer growth is confined to small dimensions. Hence oxygen consumption by the graphite insulators is not a serious problem.

Surface temperature responses have been recorded with a Millitron two-color pyrometer. In general, pyrometer responses indicated black surface temperatures of the order of $2,500^{\circ}\text{R}$ during the low heating portion of the test and values approximately twice as high during the high heating portion of the test. In a few instances, the recorded temperatures indicated a very erratic high frequency signal. It has been suggested that in the low heating portions of the tests, this variation may have been produced by an unstable flow which did not continually maintain contact with the surface. However, both the shortness of the intervals and the magnitude of the variations tend to refute this hypothesis. A more logical explanation consistent with the observed behavior revolves around the sensitivities of the two detectors as well as their relative response rate. Local surface changes evolving as the surface heats (degradation of the resin) may result in the formation of surface materials which vary in departure from the assumed grey/black conditions on which the theory of two color pyrometry is based. Such postulated variations in the local spectral emissivities are potentially rapid and the sensors in the pyrometer can respond with electronic rapidity. Rapid "hunting" of the detector signal may result. Data reduction involving the emissivities and surface temperature of test specimens is simplified by introducing the assumption that the emissivity is a constant 0.8 for all test surfaces. A ± 25 percent variation in emissivity (i.e., $0.6 \leq \epsilon \leq 1.0$) gives a temperature variation of approximately ± 6 percent. Obviously, appreciable error in emissivity can be tolerated in applying data for surface temperatures.

DATA EVALUATION

The responses of the system pressures were measured from the oscillograph records and pressure data were obtained as a function of time. Due to the length of connecting tubing between the plenum and the plenum transducer, the response of the sensor is slow. Hence, although the recorded responses indicate that plenum pressure has not equilibrated, in actuality, a maximum pressure is attained in a short interval. Comparison of the current and voltage records during the course of a test confirm this. Both, being interrelated in the arc column, are responsive to pressure change. In general, they stabilize and remain relatively constant within a very few seconds of start-up.

The pyrometer, which is directed toward a region ($\sim 1/4$ -inch diameter) just outside the water cooled nozzle exit makes a continuous record of the temperature of the surface. It cannot identify effects due to emissivity change or departures at either wavelength from the grey body condition. Nevertheless, the data acquired suggest that changes in one or the other of these conditions may have occurred. In several runs, the recorded surface temperature curves generated during the low heat transfer portion of the test showed a drooping characteristic. Since the specimen was receiving an increasing amount of thermal energy during the interval, the decline of surface temperature appears to be contrary to the heat accumulation. Hence, one of the two phenomena cited may be contributory to the changes observed. Other explanations of the characteristic curve are also possible.

Motion pictures were taken during each test run. In order to attempt to cover the entire test sequence, time lapse pictures were taken (one frame per second). The footage obtained was very unsatisfactory. Heating during the low heat transfer portion of the run produced little visible radiation, so the frames were underexposed. The high heat transfer portion of the tests had mixed successes with the degree of exposure because of the intensity of the radiation. The framing device, external to the camera, apparently failed to fully trigger the exposure and advance the film properly. Consequently, filmed sequences frequently "rolled" in the manner of a poorly adjusted television picture. The use of time lapse sequences permitted several tests to be exposed on a single roll of film, thus several models had been photographed. It was necessary to await the use of a reasonable amount of film before processing to reduce wastage. Therefore, changes could be introduced in the filming procedures only after several runs had been completed. Since the arrangement was not satisfactory, future filming will be confined to exposure during the high heating portion of each test and framing rate will be adjusted to obtain maximum utilization of the roll of film. With the higher frame frequency, it is possible that more detail regarding the ablation process may be identified on the films.

The first four specimens tested were not exposed for the full period of time to the appropriate heat fluxes because of failures of the arc equipment. The data that were obtained were reduced and are reported. R2-1 was the first specimen tested. After 201 seconds the test was terminated. Pressure and temperature data are reported in Figures 15 and 16 respectively. The ablated specimen, and a section, are shown in Figures 17 and 18. The second test specimen, (R1-1) was exposed for 264 seconds. The results of this test are summarized in Figures 19, 20, and 21. Figure 22 shows the ablated test specimen, and Figure 23 is a section. Tables V and VI show model measurements.

A third run was performed on a carbon phenolic sample (R2-2) without refurbishment of test hardware after the previous test. The anode of the arc heater eroded after 170 seconds and the arc was extinguished by the intruding of coolant water. This was a demonstration of the inability of the arc hardware to withstand repeated exposure to the generated environment without the replacement of parts. The results of this aborted test is illustrated in Figures 24, 25 and 26. Figures 27 and 28 illustrate the ablated test specimen and Table VII indicates model measurements.

After the arc hardware was rebuilt, a silica phenolic test specimen (R1-3) was subjected to the two step ablation test for 289 seconds. The flow appeared to produce severe heating, since the side wall insulators were badly eroded. This resulted in the distribution of heat over the entire surface of the test specimen indicated by the observation of the effect of ablation over most of the sample surface. The graphite plug for the bypass appeared to have failed to seat uniformly. As the test progressed, gas escaping past the plug appeared to have eroded it unevenly. As a result, the plenum pressure (P_2) declined. Figures 29, 30 and 31, describe the pressure and temperature profiles of this test. Figures 32 and 33 show the ablated test specimen, while Table VIII is a tabulation of model measurements.

In order to further assess the durability of the test hardware, a specimen of ATJ graphite was used. The test ran the full length of time, with no hardware failure. When the arc was disassembled after the test, it was found that the equipment had barely survived. A firm decision was then made to overhaul the arc hardware after each high integrated ablation test. The ablated test specimen is shown in Figure 34, while a tabulation of model measurements is included in Table IX.

A third replicate carbon-phenolic test specimen (R2-3) was exposed to ablation testing (see Figures 35 and 36). The test was terminated early when it was observed that the graphite plug failed to seat when inserted. Table X shows the measurements obtained on this specimen.

Six additional test specimens were instrumented and dimensioned. These included duplicate specimens of C1, C3 and R3.

Post Ablation Test Measurements

After being photographed, the test specimens were sectioned to facilitate the determination of recession characteristics. Recession and char measurements were made using a cathetometer. The recession profiles, illustrated in Figures 37, 38, and 39 were determined from pre-test and post-test measurements. While there are marked differences among the various profiles, they are, basically, consistent with respect to the types of environments to which they were exposed. The graphite specimen (Figure 34) provided a representative result for the nominal environment. The peak recession at the mid-region of the test specimen is a typical result of flow expanding through the rectangular nozzle. Although there is a decline in enthalpy, and thus, heat transfer along the sample surface, it is relatively smaller than the shear effect which increased almost proportionally with the gas velocity.

The same pattern was found with the two phenolic-refrasil (R1) reference specimens, which were subjected to both elements of the test environment. The second specimen of this type (R1-3) was subjected to a higher heating environment. Peak recession was less because of lateral leakage. A trace of the central peak may also be found in carbon-phenolic test specimen (R2-3) which was subjected to higher heating conditions, but was modified by the presence of water vapor in the mass flow of the hot gases.

The remaining two specimens of carbon-phenolic reference material (R2-1 and R2-2) produced recession profiles typical of a low flow, low heating environment which was losing energy as it moved along the specimen surface. Both specimens, in general, and R2-2, in particular, were degraded and expanded and the expanded portion was not completely ablated at the aft end of the specimen. Table XI shows raw ablation data from this test sequence.

After this first series of tests was run, a re-design of the arc (previously explained) permitted operation of the arc without any further equipment failures occurring. A second series of tests was performed, with the results analyzed in the following section. Tables XII through XXIII show measurements made on the tested specimens.

Data Analysis

Among the data reported, at least one of every type of specimen made available for Cycle I has been tested for the total test time. It should be emphasized, however, that specimen A4-2A, Figures 77, 78, 79, 80, 81 and 82 (CCA1-1641/Skybond 700) is not considered a prime specimen because of its

relatively low density. Because of this factor, as well as the difficulty in the fabrication of a low porosity test specimen using this polyimide resin, samples A3 and A4 have been prepared using the newly developed GE polyimide resin. These test specimens appear to be excellent with respect to minimal porosity and they will be subjected to ablation testing during Cycle II.

Specimen R1-4 (Figures 40, 41, 42, 47, 48, 49, 50, 51, 52) was exposed to obtain a representative sample of the reference refrasil shield material. Previous samples had not been exposed for the entire planned test period. The sample is exemplified by average recession of approximately 80 mils and a char layer averaging in the range of 200 mils. Conditions of the test were slightly lower than nominal. An interesting comparison can be made with R1-1. The latter was run for a time less than intended, about half of the higher heating rate interval was obtained. Note that recession was correspondingly lower, averaging about 50 mils. Char thickness averaged about 145 mils; the results appear reasonable. All other things being essentially equal, it can be estimated that the net recession is approximately proportional to the test time, weighted for the corresponding level of heating. On the order of 15 percent of the length loss occurs during the low heating portion of the cycle providing only the integrated heating is considered.

The sample of carbon phenolic, R2-4 (Figures 43, 44, 45, 46) will serve as a comparison standard for similar materials developed later. In-depth heating of the carbon material was significantly lower than the silica base material. Prior to the high heating step, no thermocouple response exceeded 1,000°R. This contrasts to R1-4 where the first two thermocouples exceeded this value. Note that the drooping surface temperature is again apparent. While char depth was greater than for the silica, the net recession averaged less. Since the enthalpy and the heat transfer were slightly greater, a preliminary preference can be given the carbon base material on the bases of both gross recession and of internal temperature response.

A preliminary examination of the behavior of R3-6 (Figures 59, 60, 61, 62, 63, 64) the standard reference model of Pluton carbon base material, indicates it has the best insulative characteristics of the three reference specimens. However, its resistance to the ablative environment appears to be inferior to the other materials. The upstream end of the model was deeply eroded and the subsequent diminution of the recession downstream may be attributed to the blocking action of the large amount of material added to the boundary layer. However, the local ablation appears abnormally excessive. It is estimated that the most representative recession values are those near mid specimen.

The "C" series specimens employ each of the reference materials, assembled atop a low density quartz fiber lattice. The tests of these materials were designed to examine whether or not the substructure has any appreciable effect on the shield material when they act together as a composite system. Specimen C1-1 (Figures 44, 83, 84, 85, 86, 87, 88) was exposed to an environment more severe than that of its non-composite counterpart. Although the in-depth response was higher, for the low heating portion of the run, the first two thermocouples failed exactly in the manner of the reference specimen. Note that these were about 25 percent deeper than those installed in the thinner reference specimen. The effectiveness of the insulative layer and uniformity of its temperature gradient can be seen by mating the responses of the remaining two thermocouples. The ablation profile exhibits an abnormally large upstream recession similar to the reference specimen of Pluton carbon. Note that values on the aft half of the specimen are essentially similar (combined graph). Significantly, the depth of char corresponds to the thickness of the shield material. This suggests that the presence of the efficient insulative material may have modified the recession pattern.

Corresponding to the Pluton carbon reference specimen C2-2 (Figures 46, 94, 95, 96, 97, 98, 99) was subjected to the complete heating profile. As the data tables show, enthalpies in the two tests were nearly identical. Recession in the composite was smaller, primarily in the region of higher ablation on R3-6. The downstream ends of the two specimens show comparable recession averaging about 100 mils and both exhibit similar char characteristics. Note that surface temperature responses are nearly coincident. The last of the composite group, C3-2, was tested at an enthalpy below nominal. The thermocouple responses are marked in this silica based composite. A comparison of recession profile with R1-4 (Figure 42) shows the upstream portions to be equitable, but the aft half of C3-2 (Figures 105, 106, 107, 108) appears to have grown. This is due to accumulation of the molten glass on the aft end of the specimen. For reasons not clear, the liquid phase solidified here and was not swept off. Notice that both had low enthalpy and the values were not drastically different. The char layers were quite comparable. A brief discussion of the three experimental combinations follows below.

The shield material employed in A1-2 (Figures 65, 66, 67, 68, 69, 70) appears to be characterized by rather high conduction at higher heat transfer rates. During exposure, two thermocouples failed and the third was brought to incipient failure. It can be noted that during the low heating portion of the exposure, thermocouple responses were not particularly different from those installed in other specimens. Recession was not excessive compared to reference materials but char thickness averaged close to 0.25 inch.

Specimen A2-1 (Figures 71, 72, 73, 74, 75, 76) was subjected to an environment of higher enthalpy. In part, the relatively high surface temperature may be attributed to the more energetic gas impinging on the model. Internal conduction was similar to other silica based models, when consideration is given to the lesser thickness of the sample (0.46 inch compared to 0.50 inch). The ablation was not severe, but the pattern of recession and char suggests that perhaps the char is much weaker than the parent material and that the flow may have removed some char in chip form. This is suggested by the inverse symmetry of the two curves.

Specimen A4-2A (Figures 77, 78, 79, 80, 81, 82) suffered badly in its environment. Conduction was rather severe and, according to information on fabrication, the fissures in the material may have been present prior to the test. In this case they may have aggravated the movement of heat into the center of the model. Char had progressed essentially through the entire specimen. In this case, the full penetration of the char gives rise to the inverse char-recession patterns. It is merely a geometric aspect of the model which is, that char plus recession will total thickness in the central portion of the model. It appears that the specimen provided was not thick enough and it is probable that better performance can be achieved on a thicker and more carefully fabricated specimen.

The results obtained on R1-1 and R1-3 are generally consistent with circumstances involved in the tests. Although both ran normally up to the closure of the by-pass, nozzle, the latter specimen suffered abnormal conditions immediately thereafter. Note that the surface temperatures obtained during the low heating portion of the cycle both average about 2,300°R, although the higher enthalpy obtained on run 97 induced slightly higher initial effects and produced somewhat greater response changes during test. It is inferred that the decline in surface temperature during the low heating portion of the test is a result of changes in the surface characteristics. Speculation suggests two possibilities. 1) the glassy surface formed by liquid phase silica has a lessening emissivity, and 2) the onset of ablation introduces increased mass to the boundary layer, effectively blocking an increasing portion of the available thermal flux. Either concept is consistent with the relative decline of the response curve. For example, in the environment of greater enthalpy, ablation will

initiate earlier and suppression of heat transfer to the surface will occur earlier. On the other hand, a lower enthalpy (and related heat transfer) will require a longer time in which to develop the liquid layer. Because the recorded surface temperature is above the softening range of quartz, the theory of ablative mass addition being the cause tends to be more acceptable.

During the second portion (the "high heat rate" portion), only R1-1 was exposed to a representative environment. Two failures tended to degrade the results on R1-3. First, the seal of the bypass nozzle was not maintained. The effect is evident in the decline of P_2 , the pressure which serves as the driving potential for the flow through the rectangular nozzle and across the specimen. While the pressure remains high enough to produce a choked flow, the Mach number of subsequent nozzle flow must decline. In this particular run, however, a second failure aggravated the circumstances. The insulator was not sealing properly and flow was not confined to the channel. The lateral escape of the flow was not detected and the test ran its course, but obviously, the available gas energy was dissipated over much larger areas than that of a normal test. The resulting lower surface temperature concurs as does the net lower recession values. However, the more energetic gases caused an over-all greater mass loss, taking material from the specimen in the regions of leakage as well as in the normal channel and continuing for a greater test time. Therefore, it is clear that the two results are consistent with the circumstances of the tests and that the first specimen is more representative of the optimum test conditions.

The surface structure of the specimens varied widely. The carbon-cloth materials were generally characterized by a porous char with clearly visible cloth edge patterns. The porosity and irregularity of the ablated surface tend to create the illusion that the char penetration is irregular. Such is not the case. For example, specimen R2-4 (Figure 54) exhibits a relatively smooth line of demarcation between the char and the virgin material. Since char thickness is taken between this interface and the ablated surface, the surface irregularities are frequently transferred to the char thickness profiles. In some cases it can be seen that the char profile is approximately a mirror image of the recession contour.

It is appropriate to obtain intercomparisons of the char profiles. Despite the irregularities of the profiles, some trends can be observed. The intercomparisons were made among four categories. First, the general aspects of chars among the three reference specimens were noted. All three reference specimens were subjected to nominally equal integrated heat transfer. Of the three, the carbon CCA1-1641 exhibited the thickest char. In general, it appeared that the char developed by the Pluton B1 with DP-2510 phenolic was very similar in thickness to that developed in (R1-4) the silica phenolic reference specimen. All three specimens evolved char layer thicknesses in excess of 200 mils, on the average.

A second group examined compared the basic reffrasil models employing two different resins. Included in this category was C3-2, a two layer composite. Evidence was sought indicating any change in char which might be attributed to the presence of the insulative layer. The use of DP-2510 appeared to yield a thinner char than the USP95 resin. Specimen A2-1 had a char layer consistently thinner than the reference specimen. It averaged less than 200 mils in thickness. The performance of the standard reffrasil phenolic appeared to be essentially unchanged when mounted atop the LDQ insulative layer.

A third comparison examined the relative performance of the CCA1-1641 carbon in the presence of USP95 phenolic and of Skybond 700 polyimide. The two specimens (R2-4 and A4-2A) both exhibited relatively deep chars. As was pointed out in the first group comparison, the char of R2-4 was the deepest. In general, however, the Skybond does not appear to have significantly improved

the char resistance. The composite, C1-1, was charred completely through the shield material. This suggests that the LDQ insulation may have modified the char resistance of the shield layer. However, it must be observed that the integrated heat transfer to this specimen was much greater than the other two specimens. Hence, the complete charring of the shield material is more probably the result of the increased integrated heat load.

A final intercomparison examines the performance of Pluton B-1 and VCX carbon fiber, both using the same resin. The VCX carbon showed a thinner char layer. The carbon pluton reference material and the corresponding composite (C2-2) performed very similarly. By considering the more severe ablation suffered by the VCX carbon, it can be concluded that the thinner char layer is the result of the more rapid ablation removal of the surface, rather than improved char resistance.

In all cases, the evaluation of the relative performance of the char layer is affected by the surface recession. Obviously, the interplay of these two factors introduces difficulty in interpreting the changes resulting from the use of a different material (fiber or resin). In general, a basic fiber will withstand ablation essentially the same for different resins, but, coupled with the fiber conduction, the constituents of the resin system may develop thicker or less thick char layers. In this vein, the data available suggests the DP-2510 is a little less char prone than USP95. When design considerations require control of the char thickness, the difference in resin resistance may be of importance.

THERMAL CALCULATIONS

Introduction

A portion of the program has as its objective the evaluation of the ablation resistance of the materials in terms of the environmental properties. In order to provide as complete a profile of interrelated data as possible, numerical evaluation of specimen recession for calculating ablation resistance will be obtained from the region lying within the pyrometer viewing area. Thus, recession (and char depth) observed at this point have surface and subsurface temperatures as direct supporting data. It is intended that effective heats of ablation be calculated for the observed recession values.

Most test programs examine material performance in a "constant" environment. Unlike the prior studies, the present program deliberately subjects each specimen to a varied environment. The present test environment consists of essentially two distinct levels of heat transfer at a nominally invariant enthalpy. The heat transfer rates differ by more than an order of magnitude. The problem is one of devising a logical expression for evaluating the effective heat of ablation. In its simplest form the heat of ablation is defined as the ratio of the heat transfer rate to the mass removal rate, thus:

$$q^* = \frac{\dot{q}}{\dot{m}} = \frac{\dot{q}}{\rho S} \quad (1)$$

The equation is evidently quite simple, but its interpretation leads to various, more complex representation. A choice of a suitable definitive expression must be governed by the objective of describing realistically the actual distribution of energies at the specimen-environment interface and the ultimate disposition of those energies.

Data Analysis

In evaluating the general behavior of the test specimens, there are several ways in which the response of the materials may be considered. An intercomparison of those specimens which are nominally identical ablators can, of course, be made directly. However, the variations in test conditions which have been discussed in other sections of this report prevent the comparisons made in this direct manner from being absolute. One of the most common systems of attempting to measure performance of a material in varied ablative environments is to evaluate its "Heat of Ablation". Several forms of the heat of ablation have been introduced in an effort to consider all factors contributing to the process. The heat of ablation attempts to identify the amount of energy consumed in removing a unit quantity of material from the ablator. Obviously the total energy brought to the vicinity of the surface is expended in different processes or rejected. Hence, the lack of discrimination in obtaining a cold-wall heat of ablation makes it at best a convenient expedient. The values are useful and reliable only when applied to a similar environment.

The definition for heat of ablation which perhaps comes closest to describing the true distribution of available energy is called the "Thermochemical Heat of Ablation".

Expressed in its most common form,

$$q^* = [\dot{q}_{cw} (1 - h_w/h_r) - \dot{q}_{rr}] / \dot{m} \quad (2)$$

it served as the basis for calculations in the present program. The modification of the cold wall heat transfer was based on the ratio of enthalpy difference between the hot gas (h_r) and the hot wall (h_w) to the enthalpy difference between the hot gas and the cold wall (h_{cw}). The net heat transfer to the specimen was further reduced by reradiative loss.

$$\dot{q}_{net} = \dot{q}_{cw} \left(\frac{h_r - h_w}{h_r - h_{cw}} \right) - \dot{q}_{rr} \quad (3)$$

When introduced into the basic heat of ablation expression and combined with the related expressions, an equation was derived to describe the thermochemical heat of ablation:

$$q_1^* = \frac{\dot{q}_1}{\rho s} \left\{ t_1 + r t_2 \left[\frac{(\Delta H)_1}{(\Delta H)_2} \right] \right\} \quad (4)$$

In Equation (4), the symbols are identified as:

q^* = Thermochemical heat-of-ablation

\dot{q} = Rate of heat transfer

ρ = Material density (ablator only)

s = Total recession

t = Time

r = \dot{q}_2/\dot{q}_1

ΔH = Enthalpy difference, $(h_r - h_w)$

The subscripts, 1 and 2, refer to the low and high-heat transfer rate portions of a test, respectively. Note that the heat of ablation calculated is proportional to the enthalpy difference. The calculation appears to be the only method by which the net recession can be interpreted as a heat of ablation.

After the method applicable to the calculation of the thermochemical heat of ablation had been determined consideration was given to its application to the data accumulated in the various ablation tests. Inasmuch as the heat transfer rates reported were perforce based on calculated values, particular attention was given to a review of these values. The original heat transfer rate calculations, proportioned to the heat transfer rates obtained in the calibration runs had employed the pressures reported at the first channel station. In reviewing the entire group of data it appeared appropriate to use values representative of the station at which the original calorimeter measurements has been made. Furthermore, in the preliminary evaluations, a single value had been used for pressure. It is evident that pressure along the channel walls varied appreciably during every test run. This behavior can be attributed to the increase in channel cross section resulting from ablation of the specimen. In a few identifiable cases, the drop in pressure was due to failure of the insulator with attendant lateral leakage. The former cases are amenable to evaluations but large uncertainties in the channel mass flow make correct heats of ablation difficult to obtain. Future improvement will include more positive sealing around the specimen. In any case, to accommodate the effect of varying pressure the heat transfer for a point two inches from the forward edge of the specimen was determined as a function of time. The heat transfer corresponding to each evaluated pressure was then determined using the modified version of the Gilbert-Scala correlation. Since the expression is applied as a ratio at a nominally corresponding point of the specimen, the basic relationship is independent of dimension:

$$\dot{q} = \dot{q}_{cal} \left[\frac{h_r}{h_{r_{cal}}} \right] \left[\left(\frac{\epsilon}{\epsilon_{cal}} \right)^{1/4} \left(\frac{P_{\infty}}{P_{\infty_{cal}}} \right)^{1/2} \right]^f \quad (5)$$

However, since the Gilbert-Scala relationship is fundamentally a laminar correlation, the factor f reintroduces dimension through the Reynolds Number and provides the conversion required to interpret changes in turbulent flow. The variation in heat transfer during the high-heat transfer portion of the test cannot be employed conveniently in the heat of ablation equation described earlier. Therefore, the variable curve was re-evaluated and an equivalent mean value of heat transfer was determined. It is these values, together with the less variable values of lower heat transfer which have been tabulated in the revised data Tables XXIV, XXV and XXVI. Also included are summaries of the net integrated heat transfer accumulated during the tests. These tabulations show that the high heat transfer rate, when integrated yields the larger variations in its contributed share of the heating. Note that in many instances the average values of heat transfer based on the variable pressure are substantially below those evaluated at the upstream location. The thermochemical

heats of ablation, using the summarized heat transfer rates have been calculated in those cases where it was practical (Table XXVII). The net recession values in which the heats of ablation are based accompany the calculated values. In each case, the recession used corresponds to areas just forward of the middle of the specimen (approximately at Station 10).

In order to illustrate more graphically the performances of the various materials, the thermochemical heats of ablation have been assembled on a bar graph (Figure 113). The upper limits shown are values corresponding to the environment of greater enthalpy difference and the lower limits to the environments of lesser enthalpy difference (higher heat transfer). The values are based on the postulation that the heat of ablation is proportional to the enthalpy difference available to drive the ablation process.

Figure 114 compares the cold wall heats of ablation of the carbon fiber specimens. Figure 115 shows the thermochemical heats of ablation of both silica and carbon specimens, summarizing data to illustrate scatter.

A very convincing bit of evidence has been noted which demonstrates effectively that heat transfer is dependent on the local pressure to a pronounced degree. In examining the data, it was observed that surface temperature response tended to change as local pressure changed. Since pressure changes modify the heat transfer rate, a corresponding alteration of surface temperature is an obvious corollary. The evidence tends to validate the contention of that corollary.

Further Improvements

In subsequent testing, several changes in technique will be introduced in an effort to develop improved data. One change will be the introduction of local voltage control to attempt to get more uniform power demand from run to run. A second modification, which has been requested, is the introduction of multiple junctions in the outlet water manifold. Use of such a pile will more accurately determine the mean outlet water temperature. In turn, better enthalpy evaluations should be available. Thirdly, motion picture sequences in real time will be obtained in lieu of time lapse pictures and will cover the high heat transfer portion of each run.

Fourth, a study is underway to improve sealing around the specimens. Lateral leakage, however small in quantity, introduces uncertainties which make difficult the calculation of a meaningful thermochemical heat of ablation. Figures 111 and 112 show transverse cross-sectional views of specimen R1-4 (silica phenolic) and specimen R2-4 (carbon phenolic). The effectiveness of the sealing technique in localizing the heat flux is readily apparent. Finally an effort will be made to determine representative values of the insulative index for each material of interest.

III. SUMMARY AND CONCLUSIONS

The principal objective of the program was to seek new material concepts capable of sustaining a high integrated heat load. The developmental materials were designed to provide lighter weight and more efficient thermal protection than conventional tape wrapped constructions. The program thus far has examined the thermal response of three reference materials and six developmental materials. Each of the test specimens was exposed to a long time two step heat flux environment in the five megawatt arc heater. Despite some rather wide variations in the response of the materials, it was possible to make comparative evaluations of the groups of specimens. The following summary outline highlights the details of program. Brief paragraphs are employed to describe the progress and observations made thus far.

- a. It was the objective of the program to evaluate the ablation performance and insulative properties of a group of composite candidate materials subjected to a high integrated heat load. To this end, performance goals consisted of high resistance to thermomechanical surface erosion, good insulative characteristics for structural thermal protection and low total weight per unit area. Detailed study was planned for asymmetrical ablation char instability, and dimensional changes resulting from pyrolysis, in-depth heating, lack of physical integrity, spallation or other thermomechanically induced deleterious phenomena.
- b. An investigation was made of the adequacy, limitations, and materials problems associated with the use of conventional tape wrapped carbon and silica reinforced phenolic resin materials. Consideration was given the specific components, fiber sizes, weave patterns and resin systems as well as the geometrical orientation of the cloth fibers in the conventional materials. Three were selected as reference materials. These were a silica cloth/phenolic resin (C-100-48/USP95, Code R1) and two different carbon cloth/phenolic resin systems: 1) CCA1-1641/USP95, Code R2 and 2) Pluton P1/DP-2510, Code R3.
- c. To compare with these reference heatshield materials, four developmental heatshield combinations were considered. Different carbon cloths and the silica cloth were combined with phenolic resins and polyimide resin. The combinations consisted of VCX/DP2510 (Code A1), C-100-48/DP-2510 (Code A2), C-100-48/Skybond 700 (Code A3), and CCA1-1641/Skybond 700 (Code A4).
- d. In order to effect a structure of lower weight per unit area, the heatshield materials were incorporated into two layer composites. The subsurface layer was designed to be highly insulative and of a low density. It consisted of a loom woven low density quartz (LDQ), which was bonded to each of the shield materials. The LDQ was made with silica phenolic strands alternating at right angles to give a square wall pattern simulating a filament wound structure. The composites described in this report were R2/LDQ (Code C1), R3/LDQ (Code C2) and R1/LDQ (Code C3).
- e. Specimens for ablation test were obtained from larger fabricated plates of the various materials. The finished specimens measured 5.0 x 1.75 inches. Thicknesses were appropriate to the materials and material combinations. All specimens were processed to simulate a tape wrapped heatshield element. An aluminum plate was bonded to the shield or the LDQ insulative layer. Each specimen was equipped with five thermocouples. They were installed in isothermal planes at progressively increasing depths.

- f. The specimens were tested in a facility powered by a five megawatt arc. The equipment was arranged to provide an integrated heat transfer of $36,550 \text{ Btu/ft}^2$ in two discrete heating pulses during a 300 second interval. The nominal conditions achieved during the 230 and 70 second heating intervals were 5,000 and 5,000 Btu/lb enthalpy, 25 and 440 Btu/sec-ft², heat transfer and 0.4 and 2.5 lb/ft² shear stress. The stepwise change in heat transfer was obtained by redirection of portions of a constant net mass flow of air.
- g. The test facility equipment was constructed around a rectangular two dimensional flow nozzle. The nozzle was designed to provide an expansion ratio of four from a plenum pressure of 60 psia at an enthalpy of 5,000 Btu/lb. The corresponding Mach Number was approximately 1.5. Calculations were based on an assumed frozen flow. The specimens were mounted to form one wall of the rectangular nozzle during test.
- h. After test, recession profiles and char depths were determined from the longitudinally sectioned specimen. The material performance was determined as a function of distance along each specimen. The most representative, average values were those obtained near the middle of the specimen. In each case, a time resolved history of surface temperature, subsurface temperatures and local pressures was also obtained.
- i. The three reference specimens can be intercompared for relative performance. Test results indicate that for ablation resistance they can be ranked R2, R1, R3. The relative char resistance is not so clearly defined. Although the first two are very similar with respect to char depth, the apparent ranking is R3, R1, R2. Because recession was smaller while char thickness was very similar (in R1 compared to R3) it appears that the char resistance of R3 may be interpreted as progressing at a more rapid rate through the specimen material. Interpreted in this way, it may be rated as inferior to the resistance of R1.
- j. Based on the thermocouple responses, it is possible to rank the ability of each of the three reference materials to provide insulative advantage. With no equivocation the ranking may be established as R3, R2, R1. However, it is interesting to note that the relative performance of the materials has been established primarily on the responses occurring during the low heat transfer portion of the tests. In each case, the first two thermocouples only were destroyed during the remainder of the run at the high heat transfer rate.
- k. A similar group of evaluations can be made for the composites constructed with identical heat shield atop LDQ construction. In the presence of the insulative second layer, the performance of Carbon CCA1-1641/USP-95 appears to be diminished. Thus the specimen ranking is altered: C3, C1, C2. Char layers are nominally the same and the same ranking as for the reference materials was determined: C3, C2, C1.
- l. A distinct difference in the performance of internal thermocouples was apparent due to the insulative layer of the composites. Although the C3 specimen lost only one thermocouple the remaining composite specimens each lost two. However, the temperatures of the deeper thermocouples were lower in all cases. The ranking becomes C3, C2, C1. With respect to internal heat penetration, the specimens

constructed as composites performed in the same pattern as the corresponding reference specimens.

- m. The variant materials constructed as candidates for heat shields were consistently less satisfactory in performance than the reference materials most similar to them. In the cases of A1 and A4, much lower densities were achieved in preparing the specimens. As may be seen, the effective heats of ablation for these specimens are not very disparate when the low density is considered. It can be concluded, that with a thicker shield of approximately the same weight, the low density material would give approximately the same performance. If volumetric limitations are a consideration however, the low density materials would not be satisfactory.
- n. Specimen A1-2, with a variant fiber contained in DP-2510 resin was compared with R3, which possessed the same resin. Recession was similar, but a thicker char developed. During the low heating pulse, back face thermocouples behaved similarly, but the high heating pulse was more damaging to the A1 specimen. Considering that the density is about 7 percent lower for A1-2 its ablation resistance was relatively good. However, the specimen was able to show neither good char resistance nor good resistance to the penetration of heat.
- o. Specimen A2-1 employed a silica fiber. It was compared to R1-4. The two differed in the type of resin employed in their fabrication. Ablation resistance appeared to have been adversely affected although a much thinner char was developed on specimen A2. It appears that the increased recession rate may be responsible for the apparently thinner char. For specimen R1-4, recession plus char is 287 mils. For A2-1, the sum is 265 mils. These values differ by less than 10 percent, and, significantly, the sum is smaller for the deviant material. The backface thermocouples show A2-1 to be less conductive than the reference specimen during the low heating pulse. Performance in the high heat transfer environments is approximately comparable.
- p. Specimen A4-2A was constructed of CCA1-1641 carbon and a polyimide resin. It was compared to R2-4 which employed the same fiber but differed in that the phenolic resin was used. The variant material had significantly greater recession, a thicker char layer and much poorer resistance to the conduction of heat. As with A1-2, the ablation performance is consistent with the lower density. However, in general this specimen performed worst of the three variants.
- q. Irregular erosion was found at the specimen-nozzle edge. This was possible due to a combination of irregular flow and thermochemical erosion. It may be noted that the disturbed region is less pronounced in the more ablation resistant materials.
- r. A second disturbed region frequently occurs at the nozzle exit. This region is dependent on the pressure gradient within the nozzle. If the pressure within the nozzle departs greatly from one atmosphere, a shock will be created at the exit. Enhanced local heat transfer will result. The ability of the system to maintain approximately one atmosphere is strongly influenced by the amount of specimen erosion which occurs. Obviously the ablation changes the area of the nozzle exit, the effective area ratio, and the characteristics of local conditions furnished by the heated gas.

- s. A very interesting phenomenon was observed on specimen C1-1. This specimen was a carbon phenolic and carbon removal is in part an oxidation process. A feature of the specimen was a tungsten wire installed on the centerline and normal to the surface. In this particular test, the tungsten oxidized strongly (white deposit downstream of wire, Figure 83). In consuming the oxygen, it depleted the gas downstream. Oxidation of the carbon was inhibited and a small region remained raised in the wake of the wire. The hump between 3 and 4 inches (Figure 88) is a local condition in the region of the center line. Although not its function in these tests, the use of tungsten (or another material) as a preferential ablator could be considered to modify heat shield ablation for various purposes.
- t. The design of the two-step heating nozzle can be improved. Presently the design conditions are achieved in the second plenum by operating the arc heater at higher pressure. This is necessitated by the appreciable transfer of heat to the water cooled equipment. An optimization of the design could be achieved by incorporating elements tending to reduce the surface area through which heat is transferred to the cooling water. This in turn would lower the requirements of arc heater operation and provide longer operating life for the arc heater components.
- u. Improvements installed in the equipment to date include the use of Elkonite to tip the air bypass tube and a redesign and reconstruction of the secondary plenum. In addition, the introduction of water cooled elements on the bypass plug mechanism has produced a system free from subsequent failures.

IV. RECOMMENDATIONS

Based on the results obtained thus far in the program, the following recommendations are made.

- a. Develop a more readily processable polyimide composite system, and investigate high density carbon and silica based polyimide composites.
- b. Re-examine the VCX fabric ablation system, using a more thermally stable resin.
- c. Investigate the improvement to be achieved by using quartz fabric in place of silica in ablative composites tested under long term, high heating conditions.
- d. Continue to upgrade the performance of the arc facility to provide a more realistic simulation of actual trajectories.

FIGURES 15 THROUGH 115
TEST SPECIMENS

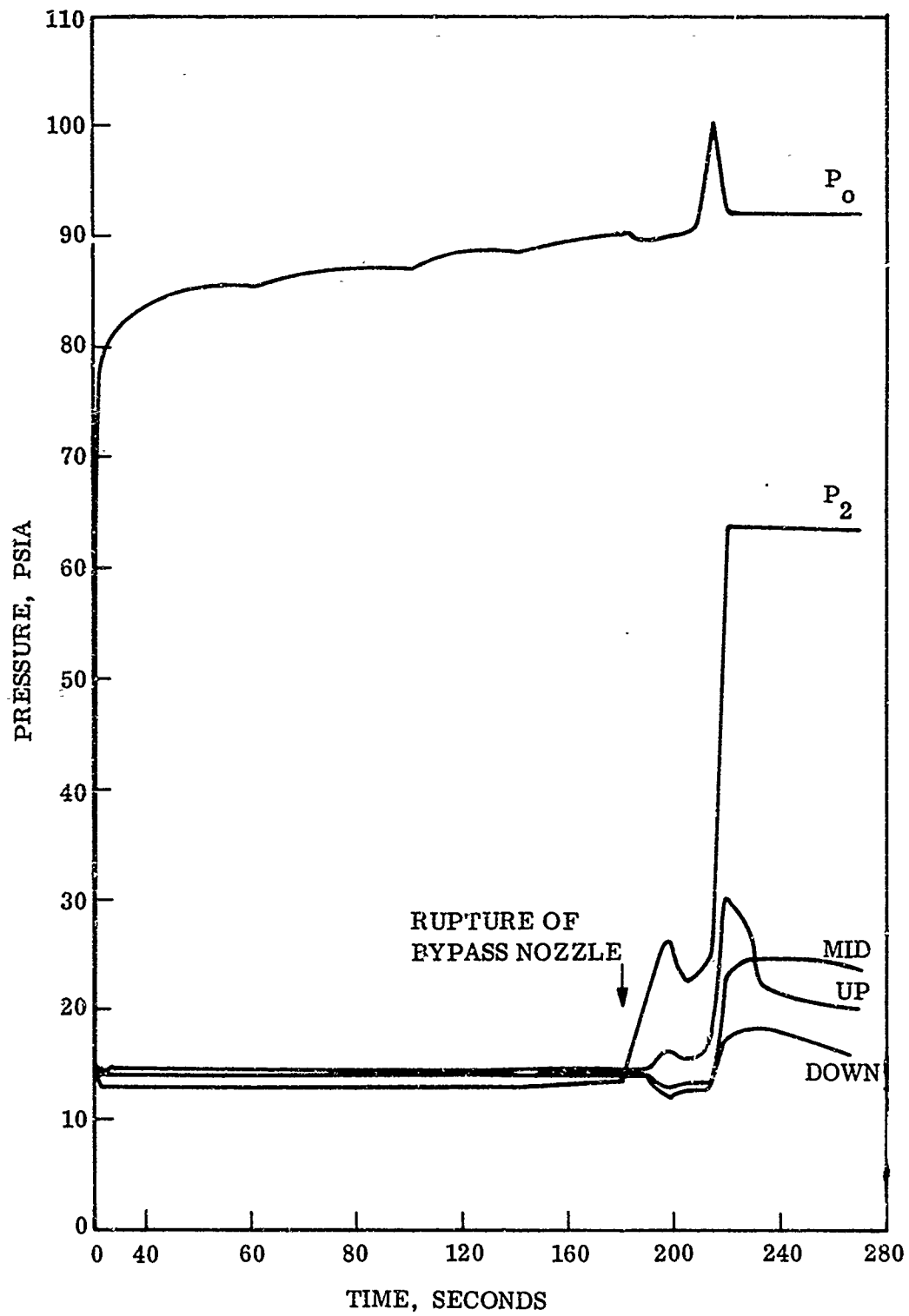


Figure 15. Pressures Run 89-69, Specimen R2-1

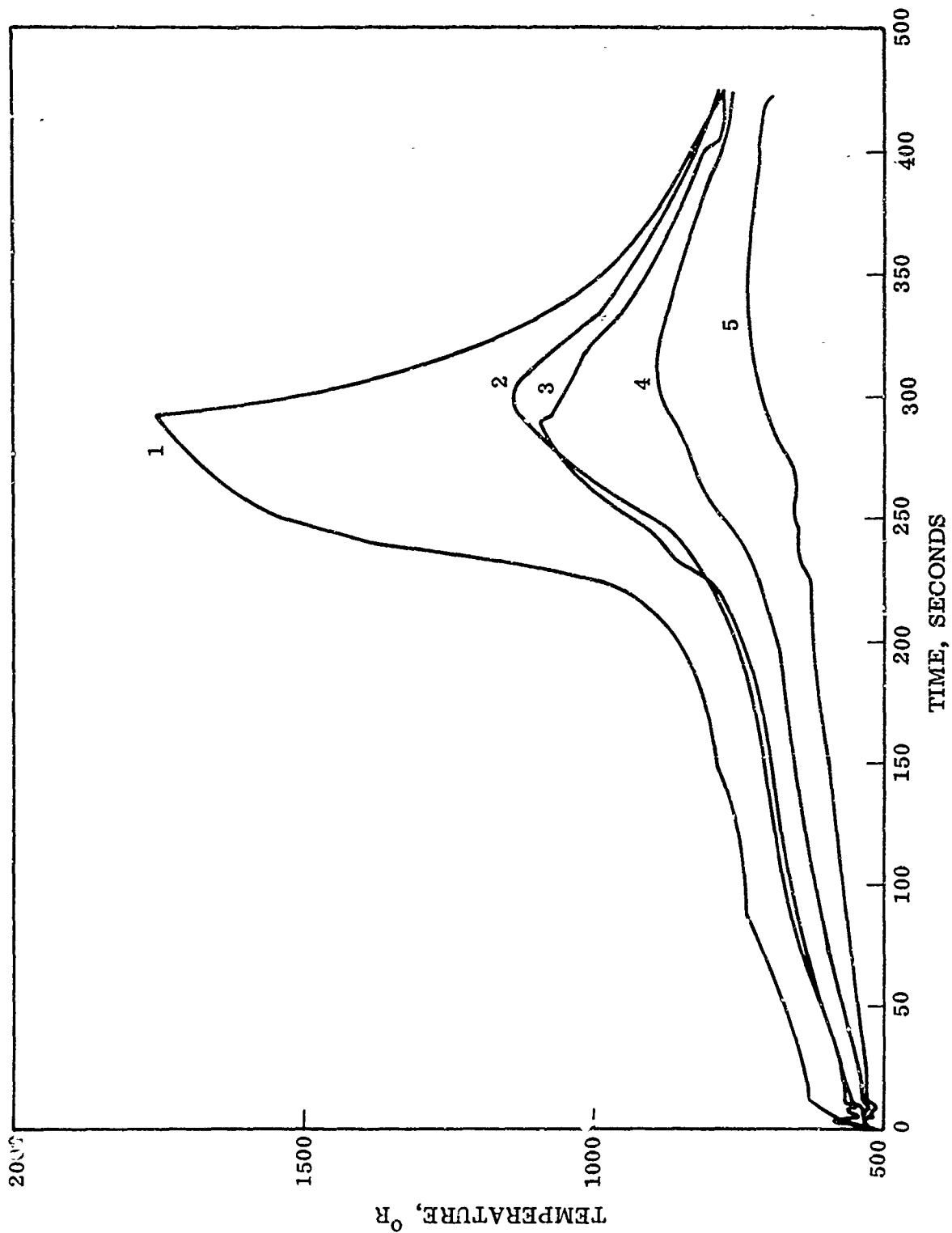


Figure 16. Internal Temperature, Run 89-69, Specimen R2-1

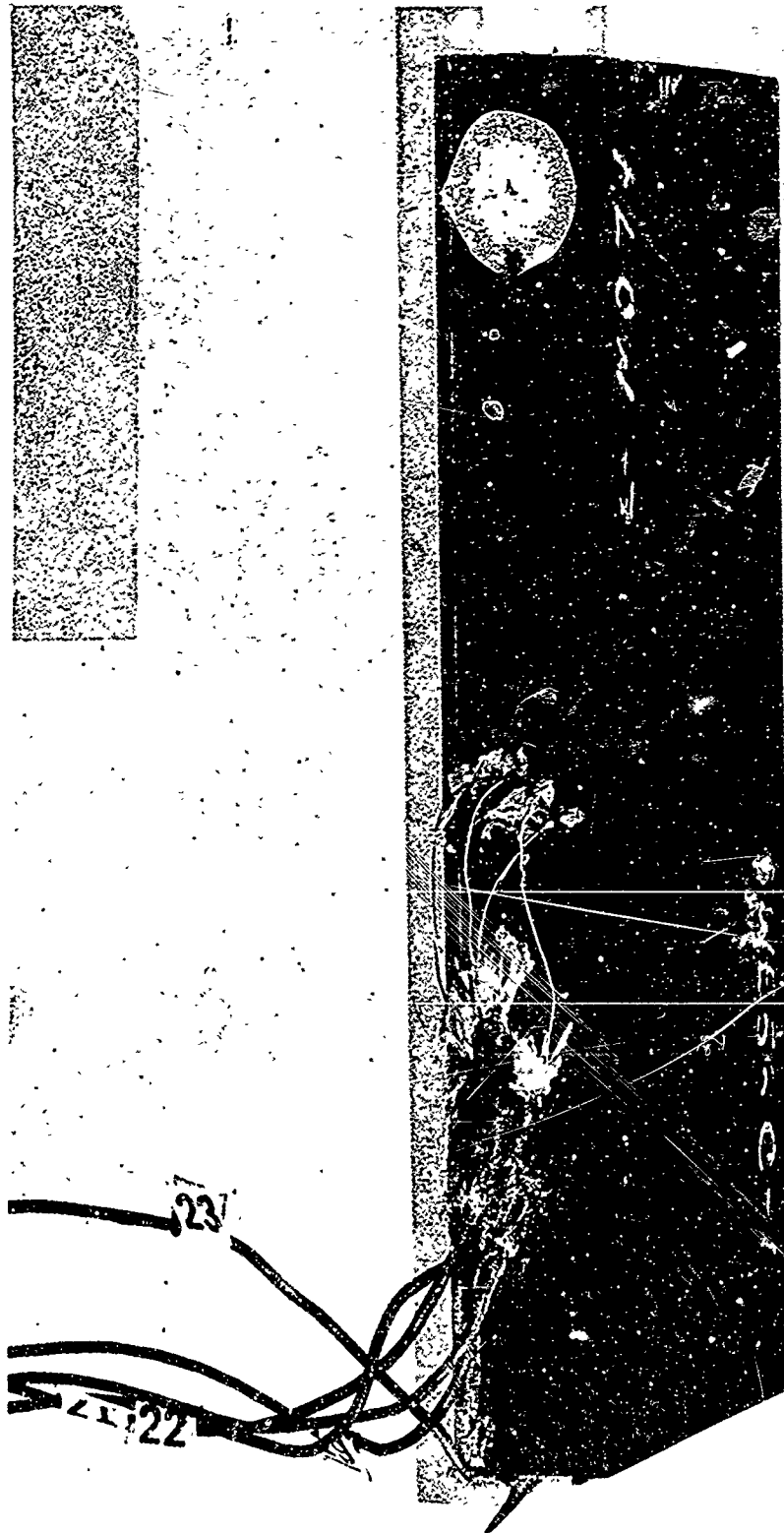


Figure 17. Ablated Test Specimen R2-1 (Run 89-69)

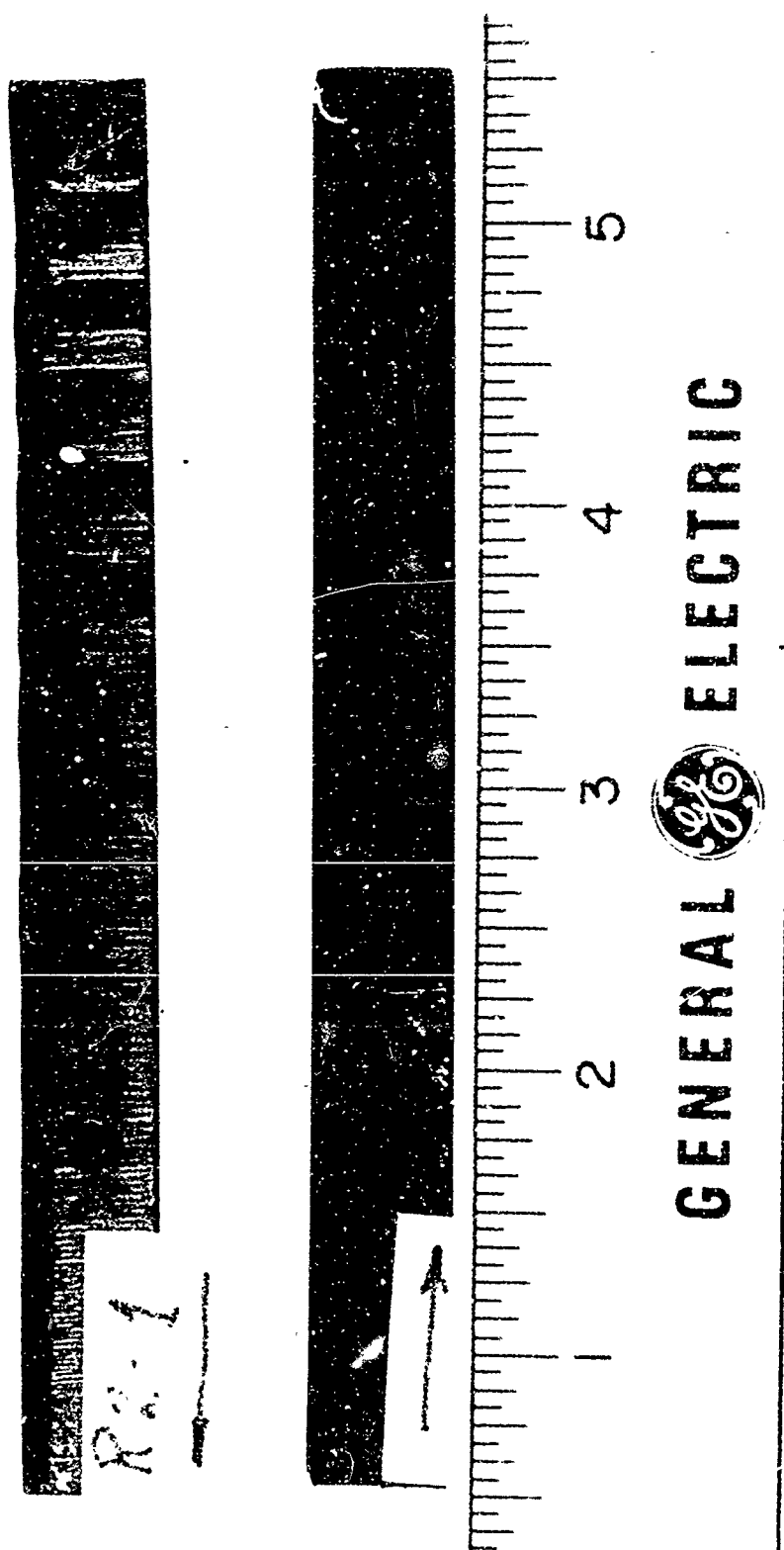


Figure 18. Ablated Test Specimen R2-1 (Sectioned)

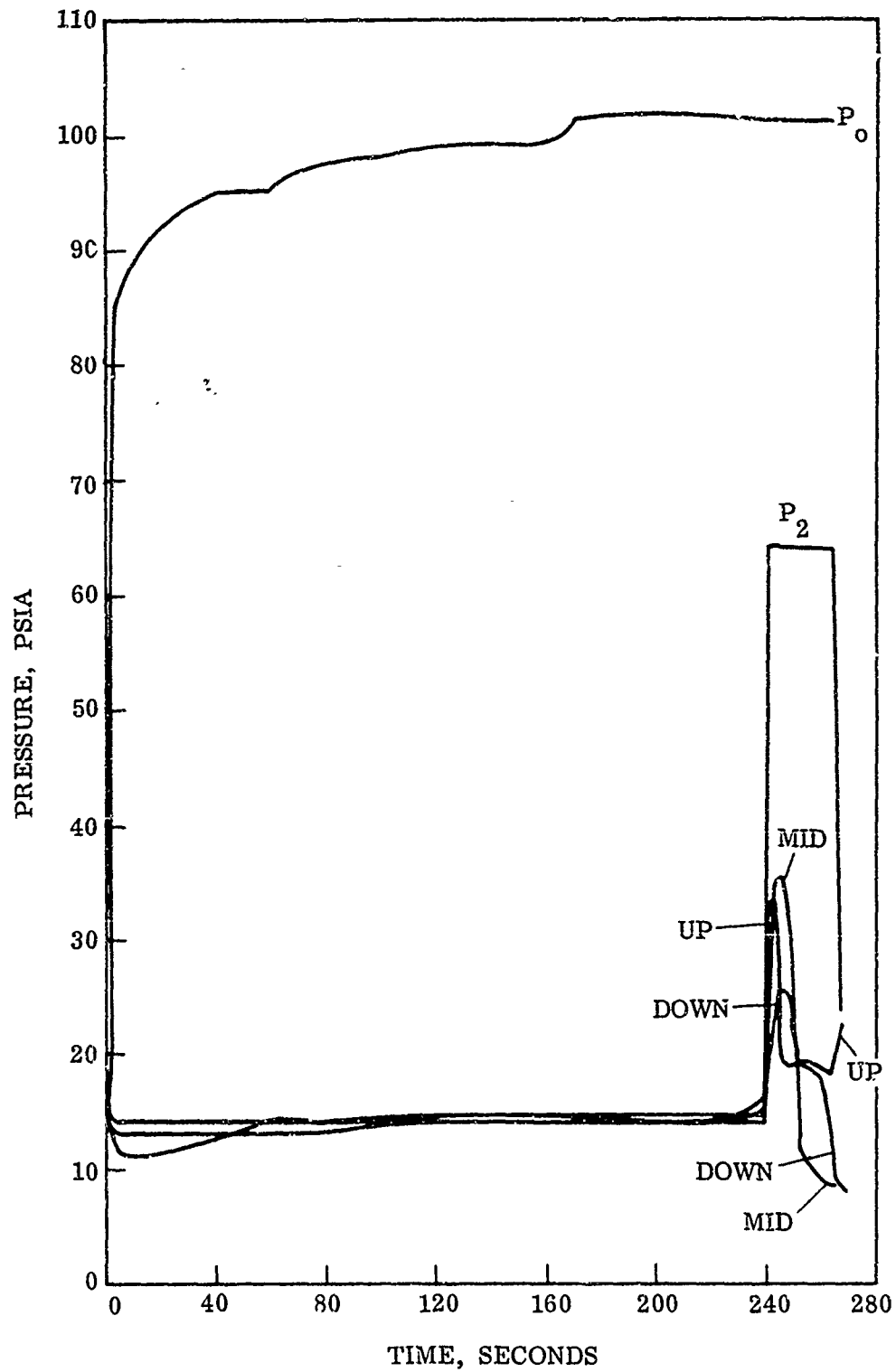


Figure 19. Pressures Run 95-69, Specimen R1-1

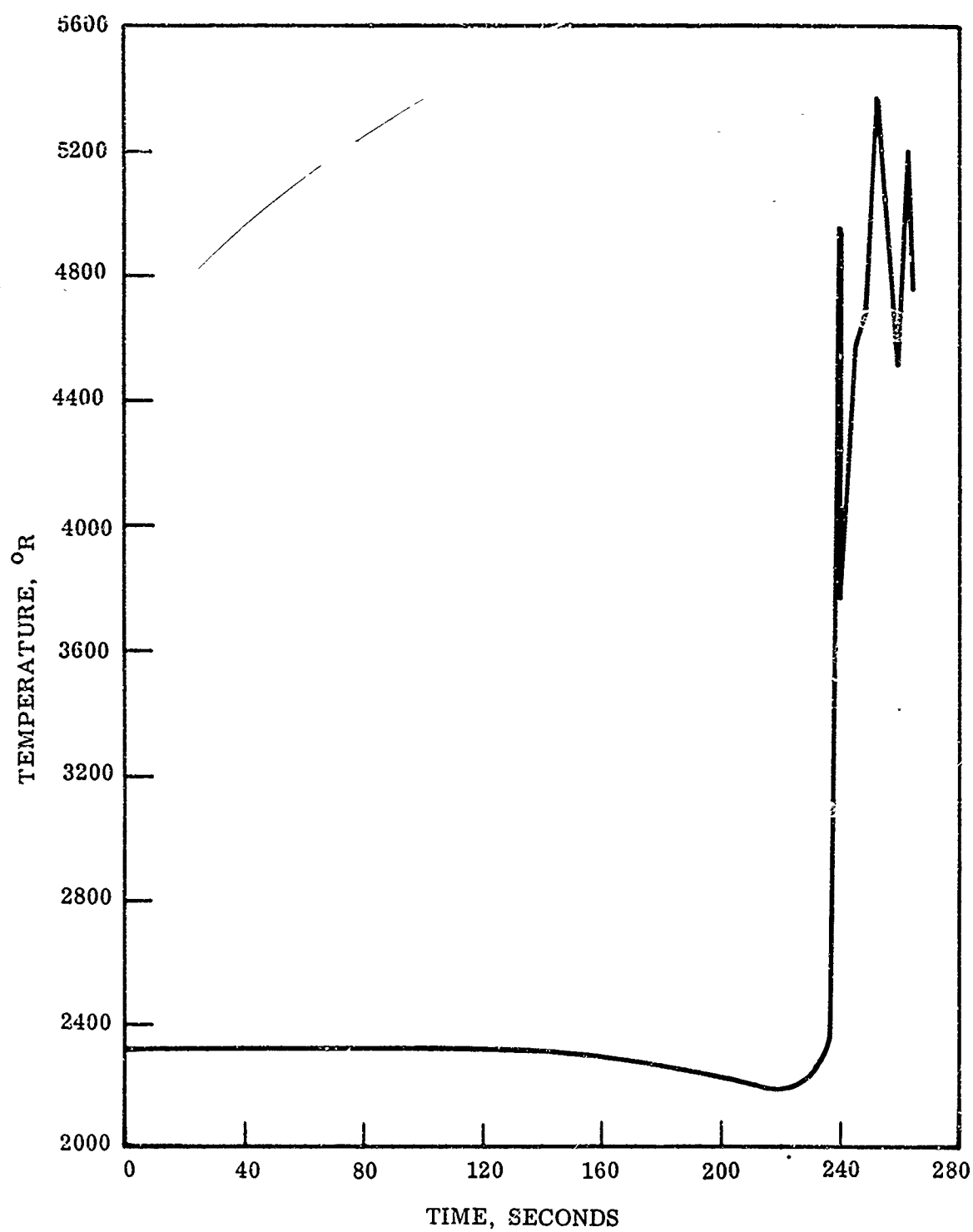


Figure 20. Surface Temperature, Run 95-69, Specimen R1-1

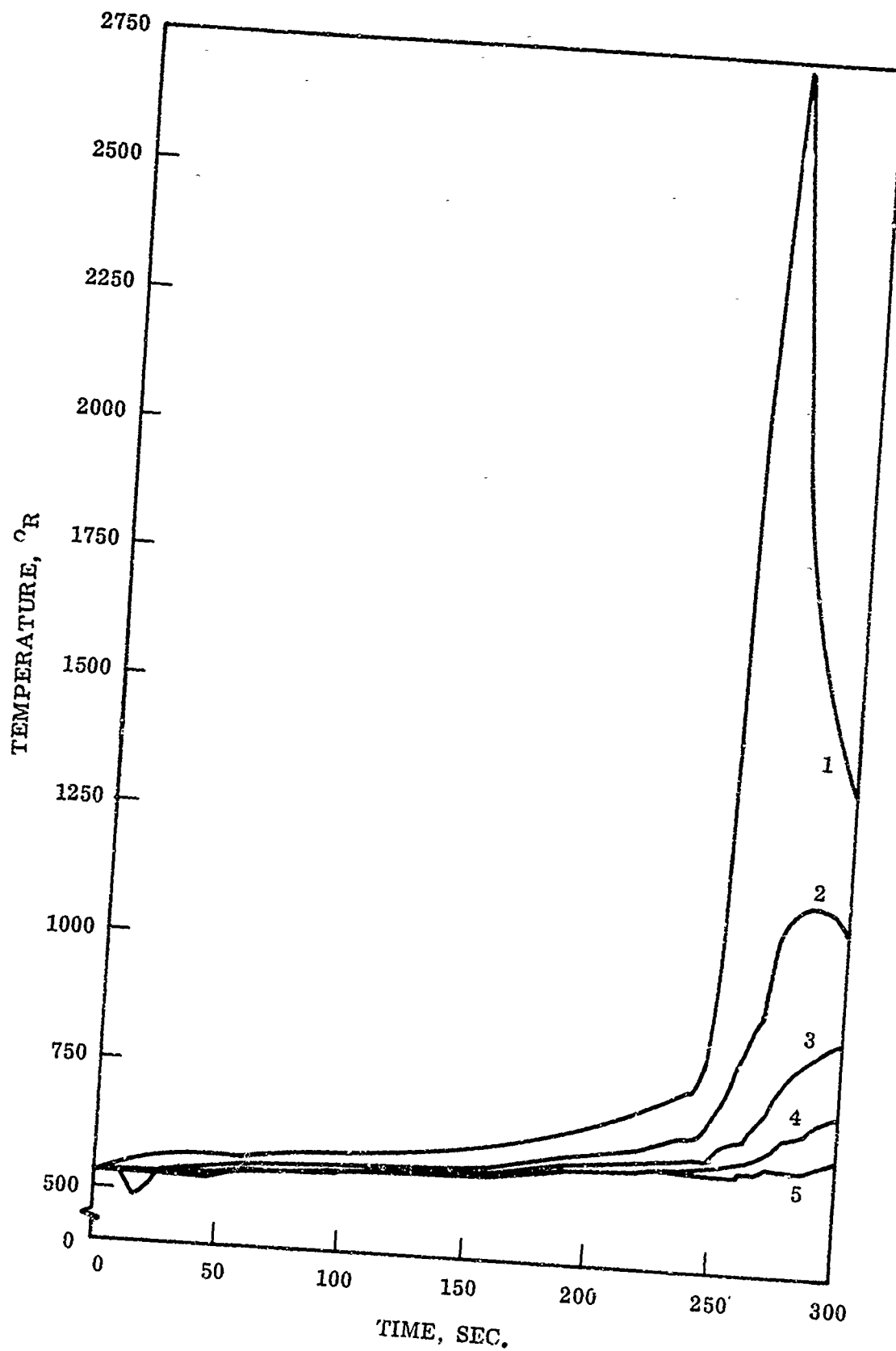


Figure 21. Internal Temperatures, Run 95-69, Specimen R1-1



Figure 22. Ablated Test Specimen R1-1 (Run 96-59)

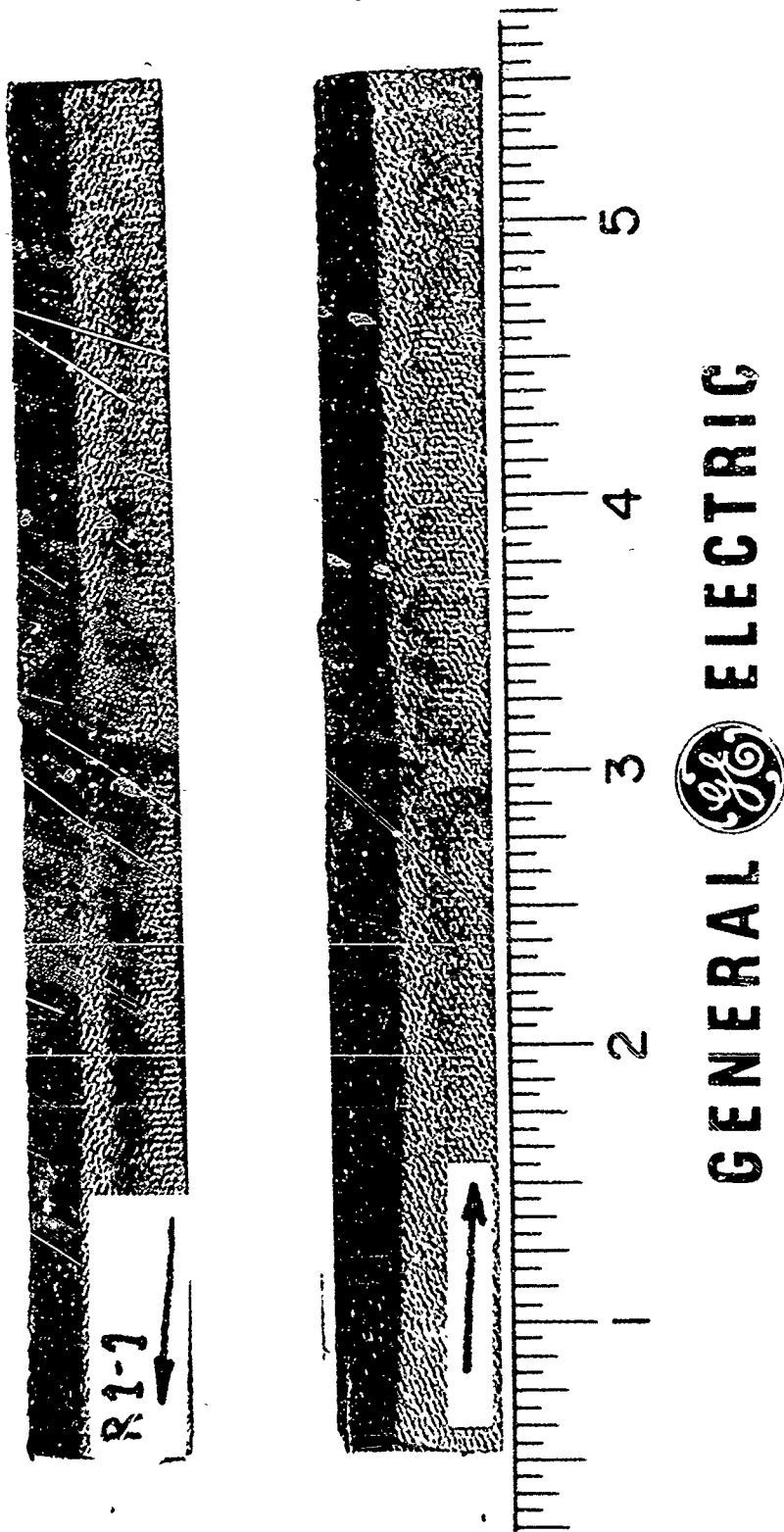


Figure 23. Ablated Test Specimen R1-1 (Sectioned)

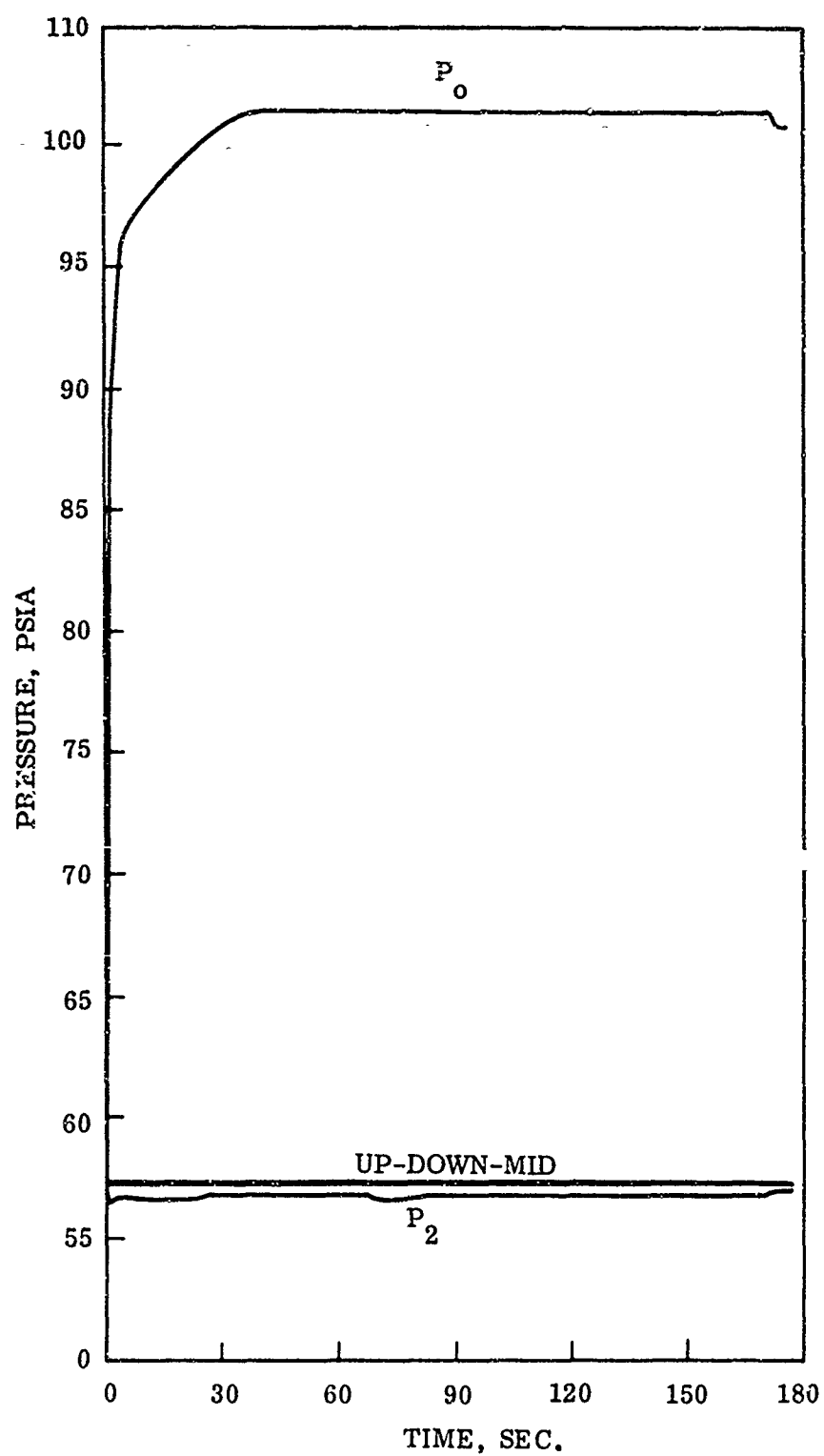


Figure 24. Pressures Run 96-69, Specimen K2-2

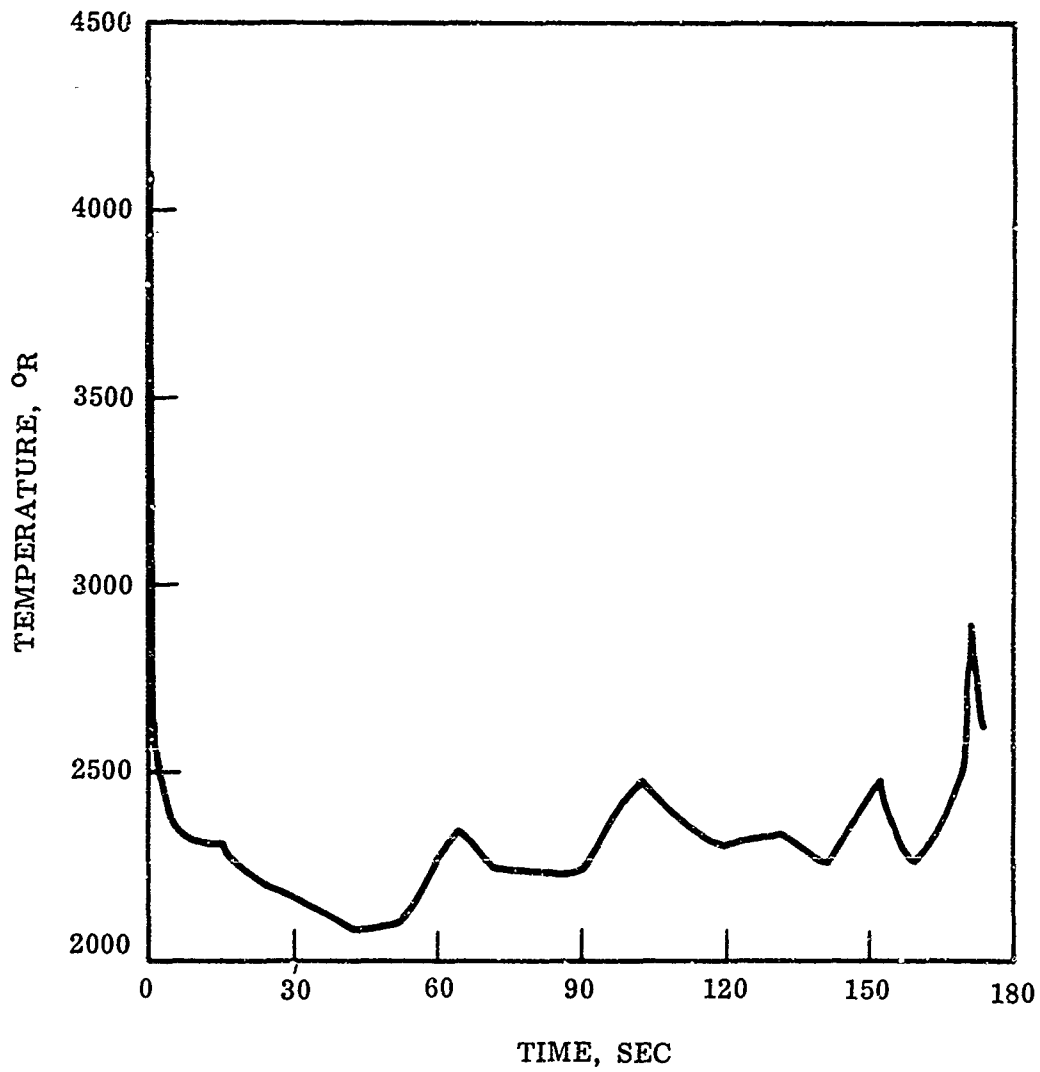


Figure 25. Surface Temperature, Run 96-69, Specimen R2-2

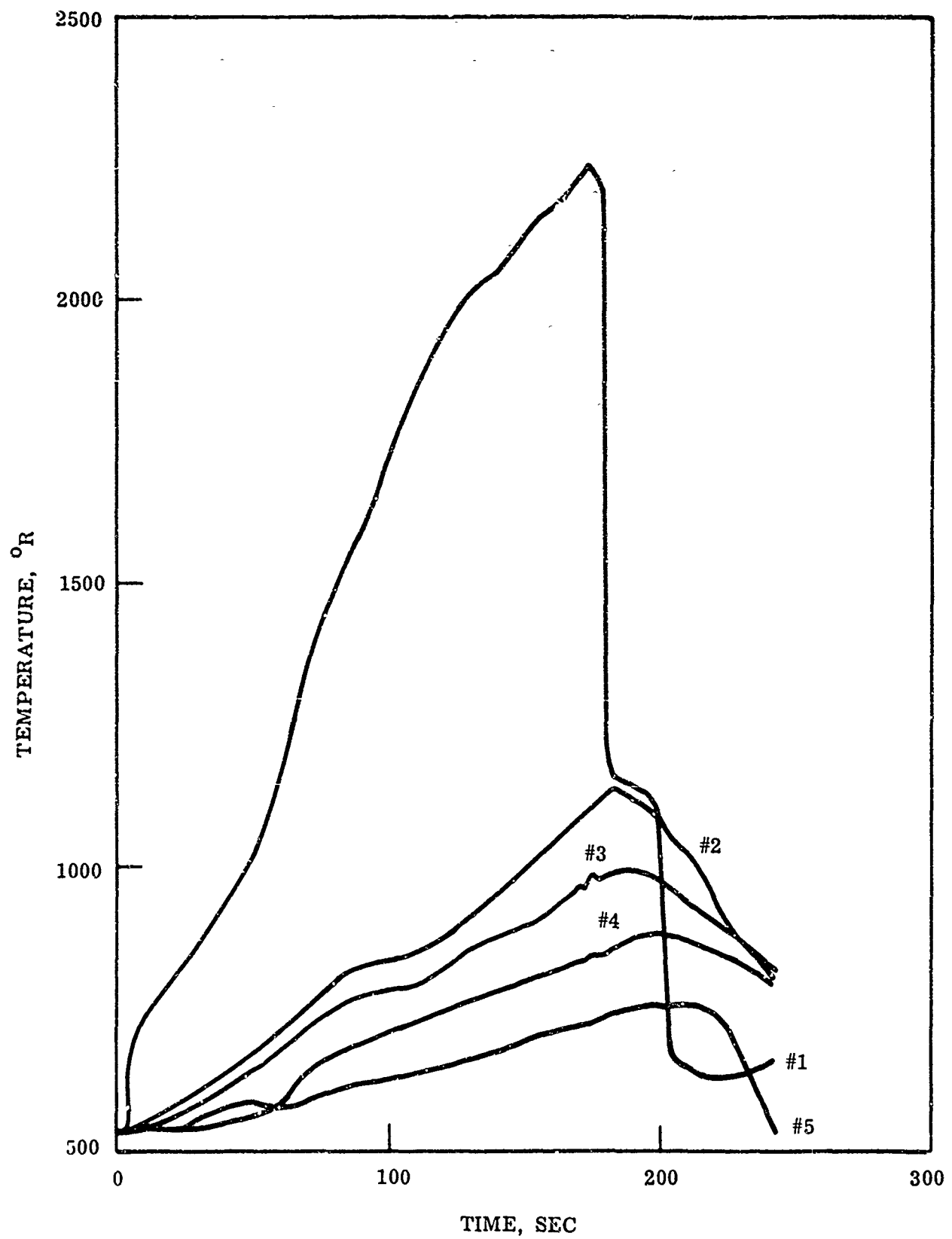


Figure 26. Internal Temperatures, Run 96-69, Specimen R2-2



Figure 27. Ablated Test Specimen R2-2 (Run 96-69)

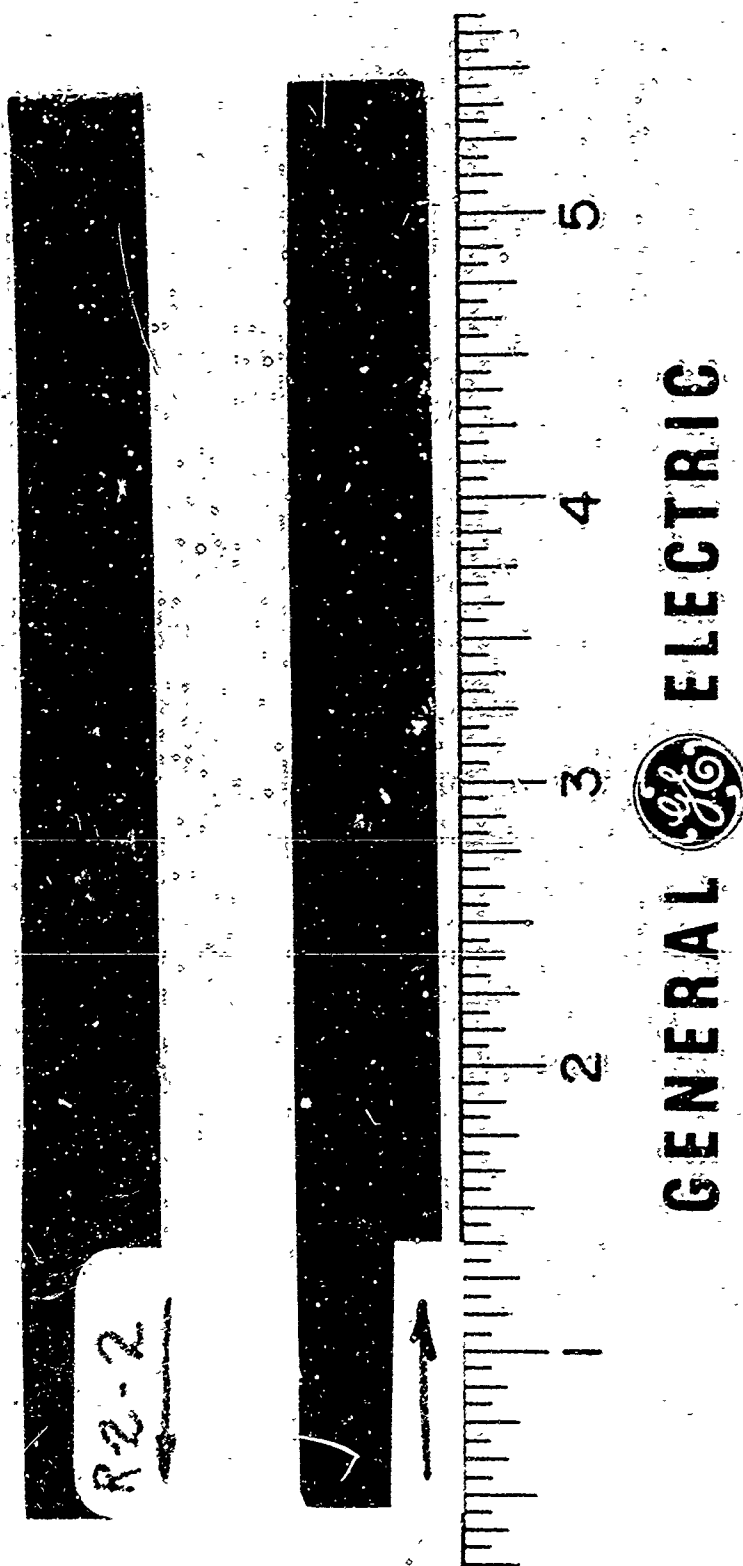


Figure 28. Ablated Test Specimen R2-2 (Sectioned)

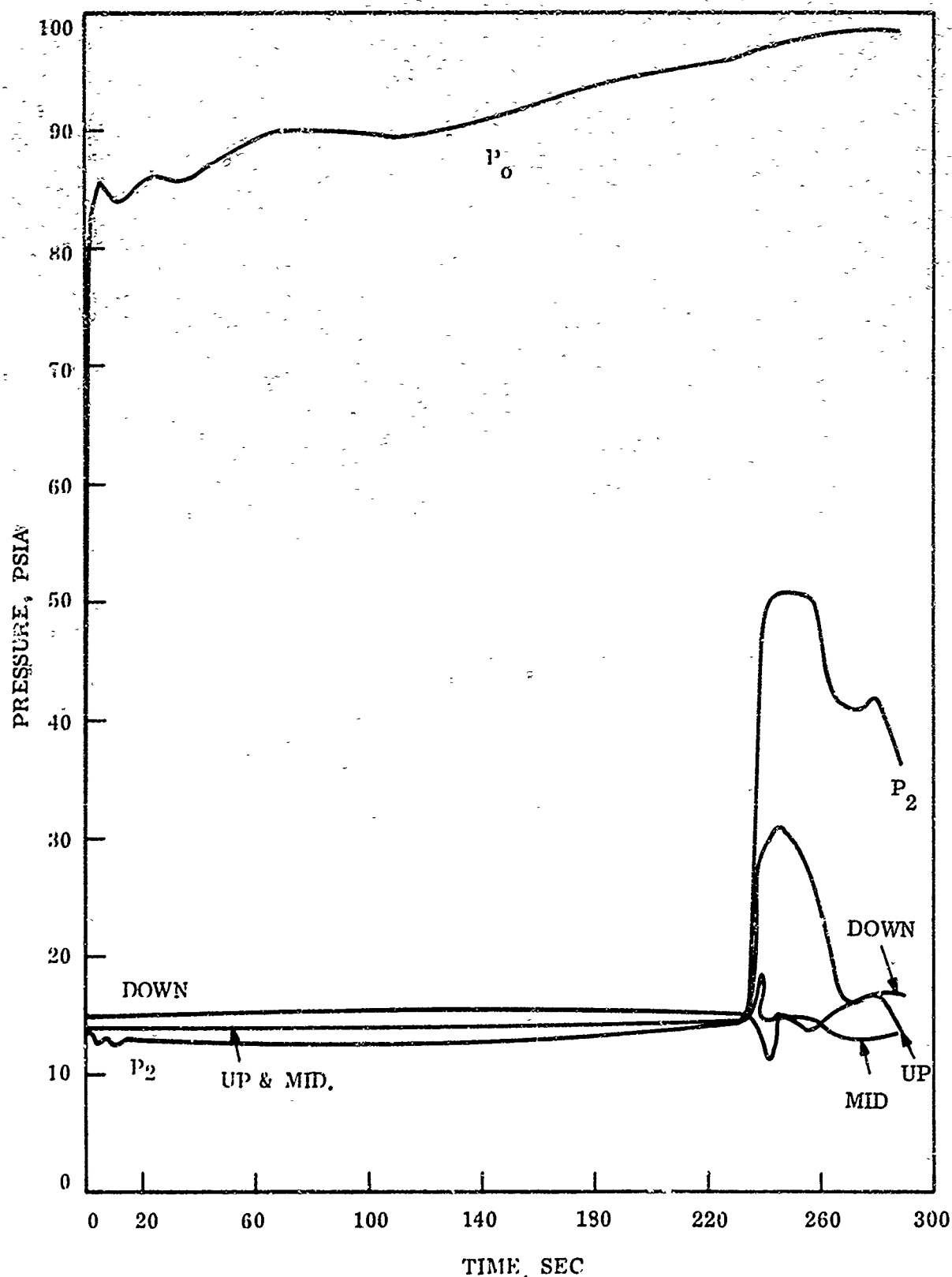


Figure 29. Pressures, Run 97-69, Specimen R1-3

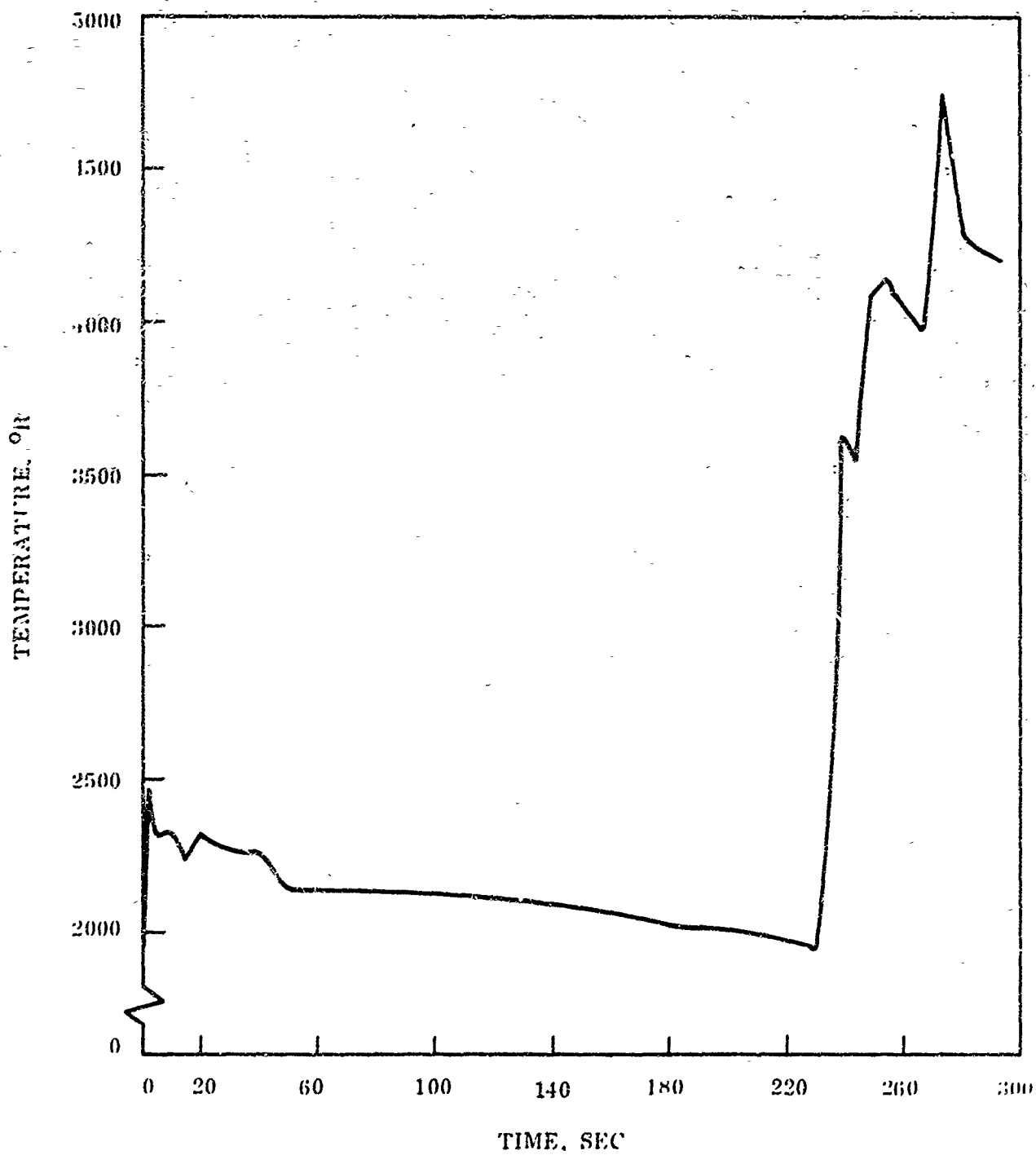


Figure 30. Surface Temperature, Run 97-69, Specimen R1-3

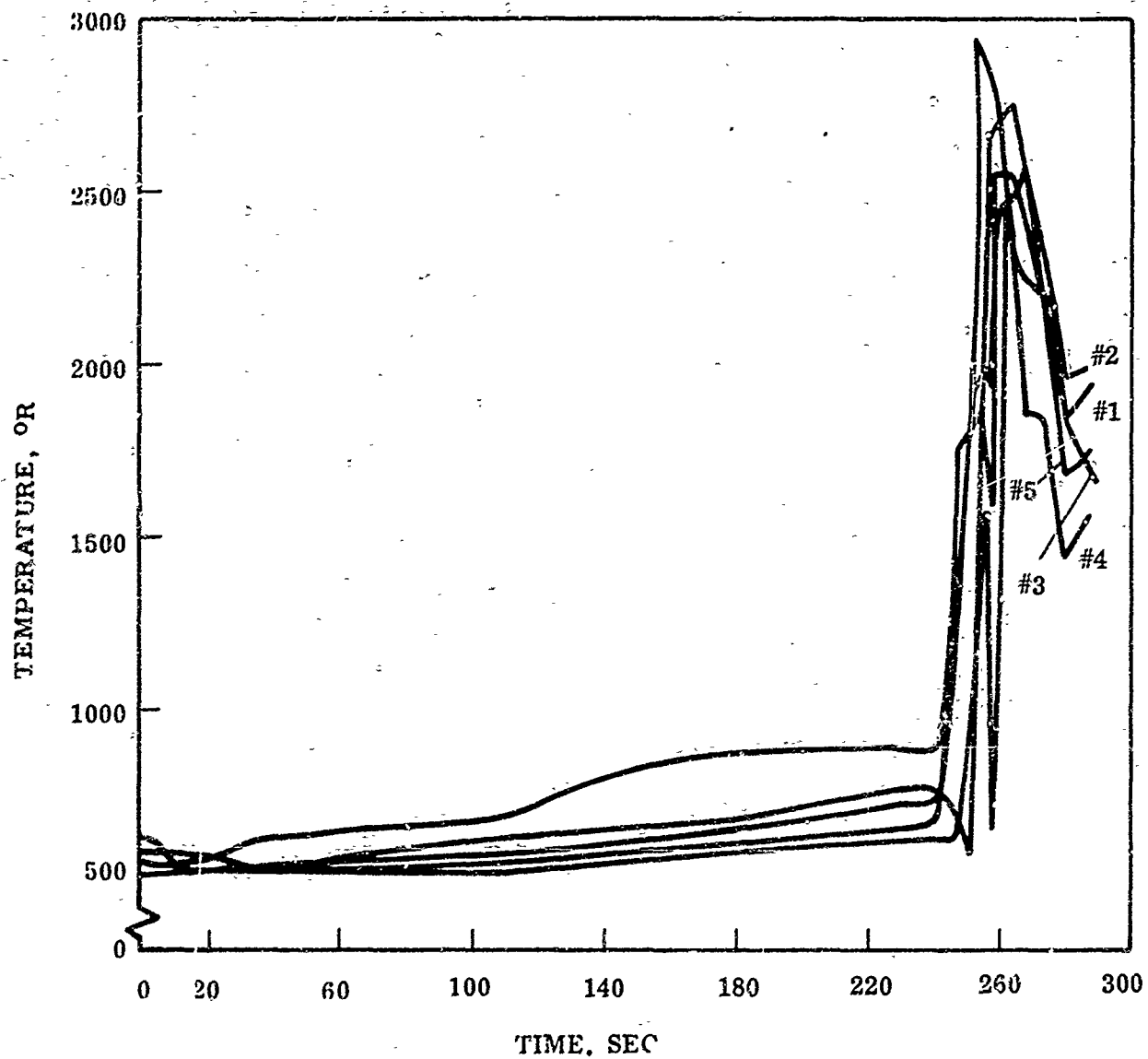


Figure 21. Internal Temperatures, Run 97-69, Specimen R1-3



Figure 32. Ablated Test Specimen R1-3 (Run 97-69)

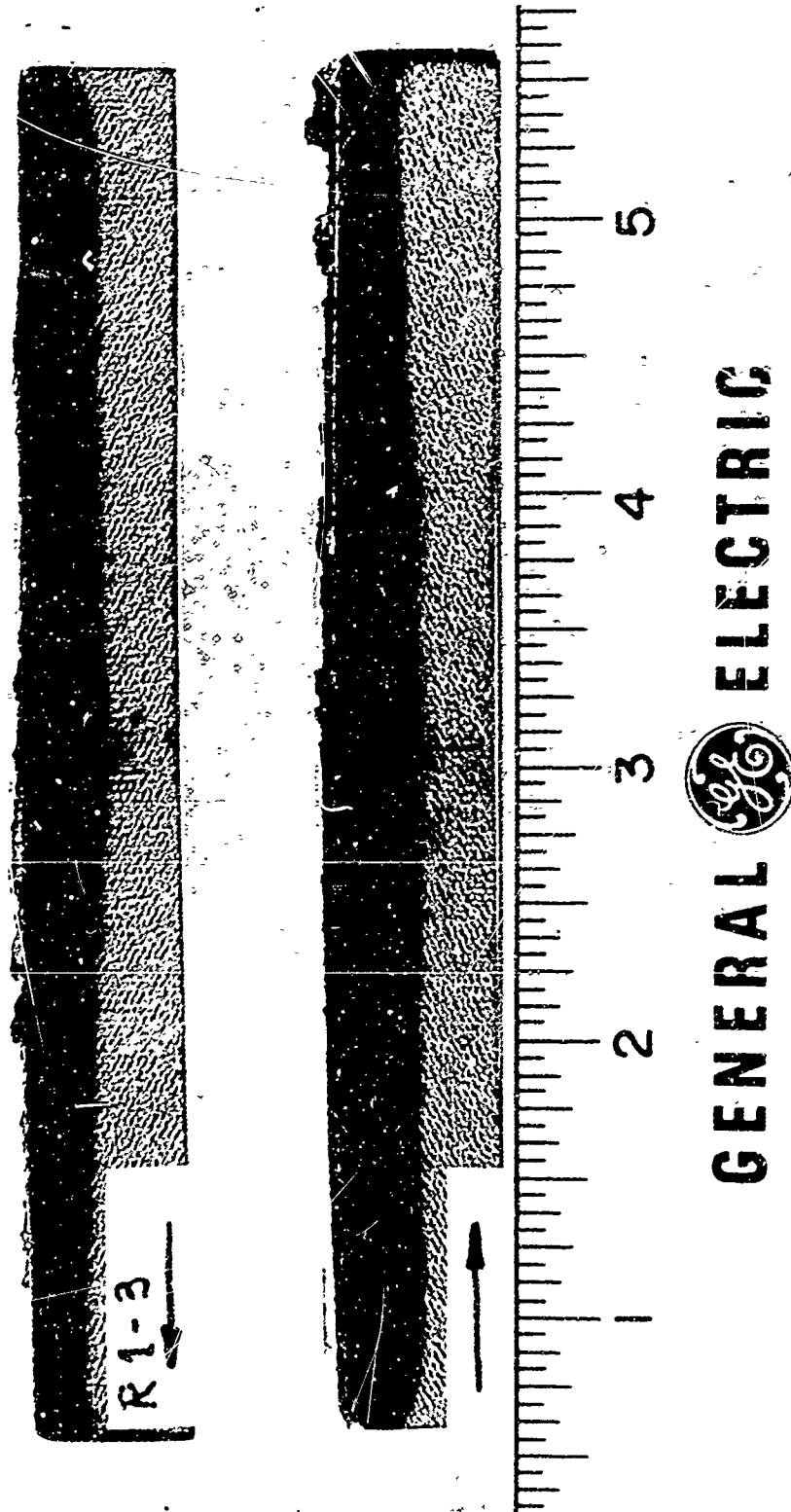


Figure 23. Ablated Test Specimen R1-3 (Sectioned)

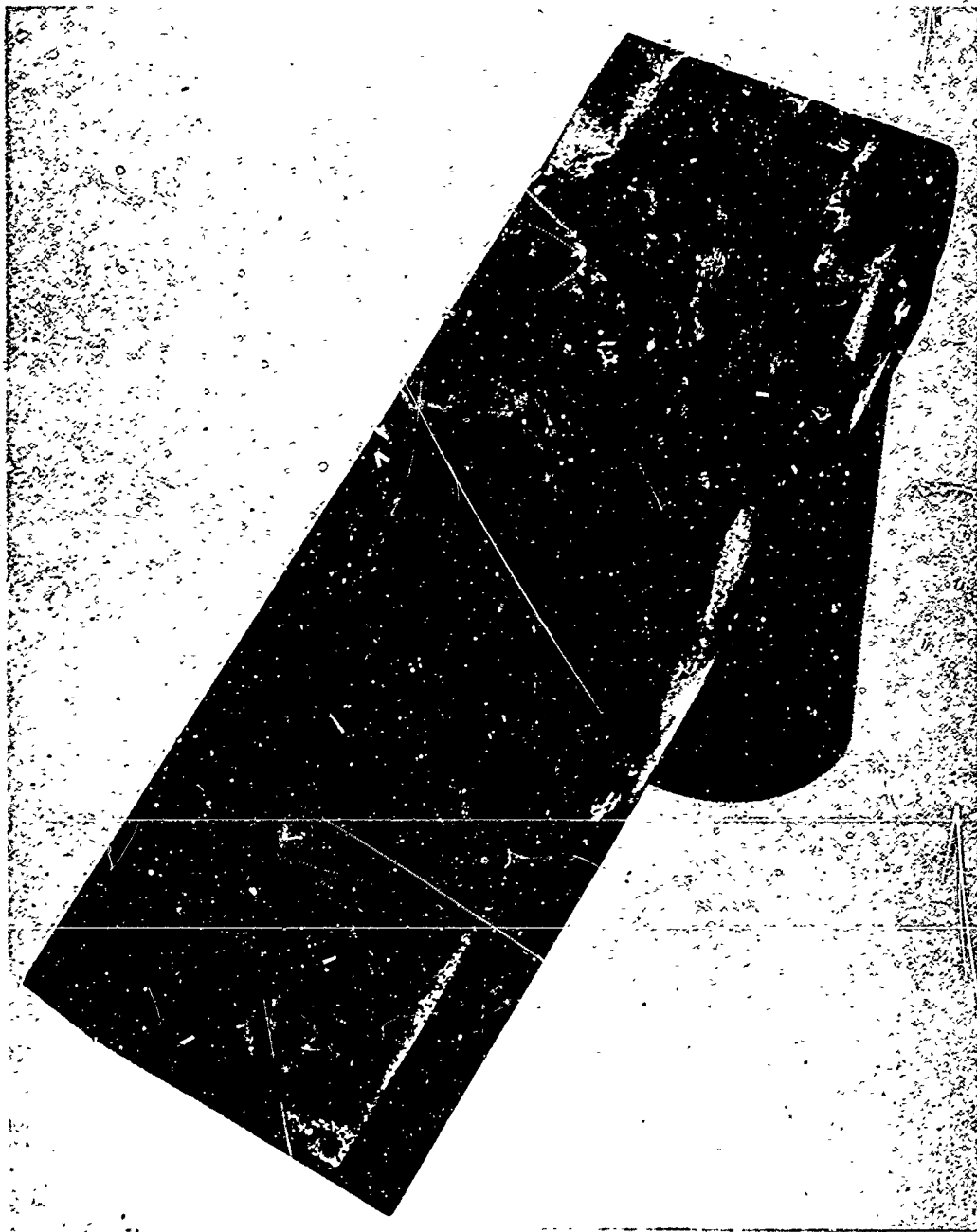


Figure 34. Ablated ATJ Graphite Test Specimen (Run 98-63)

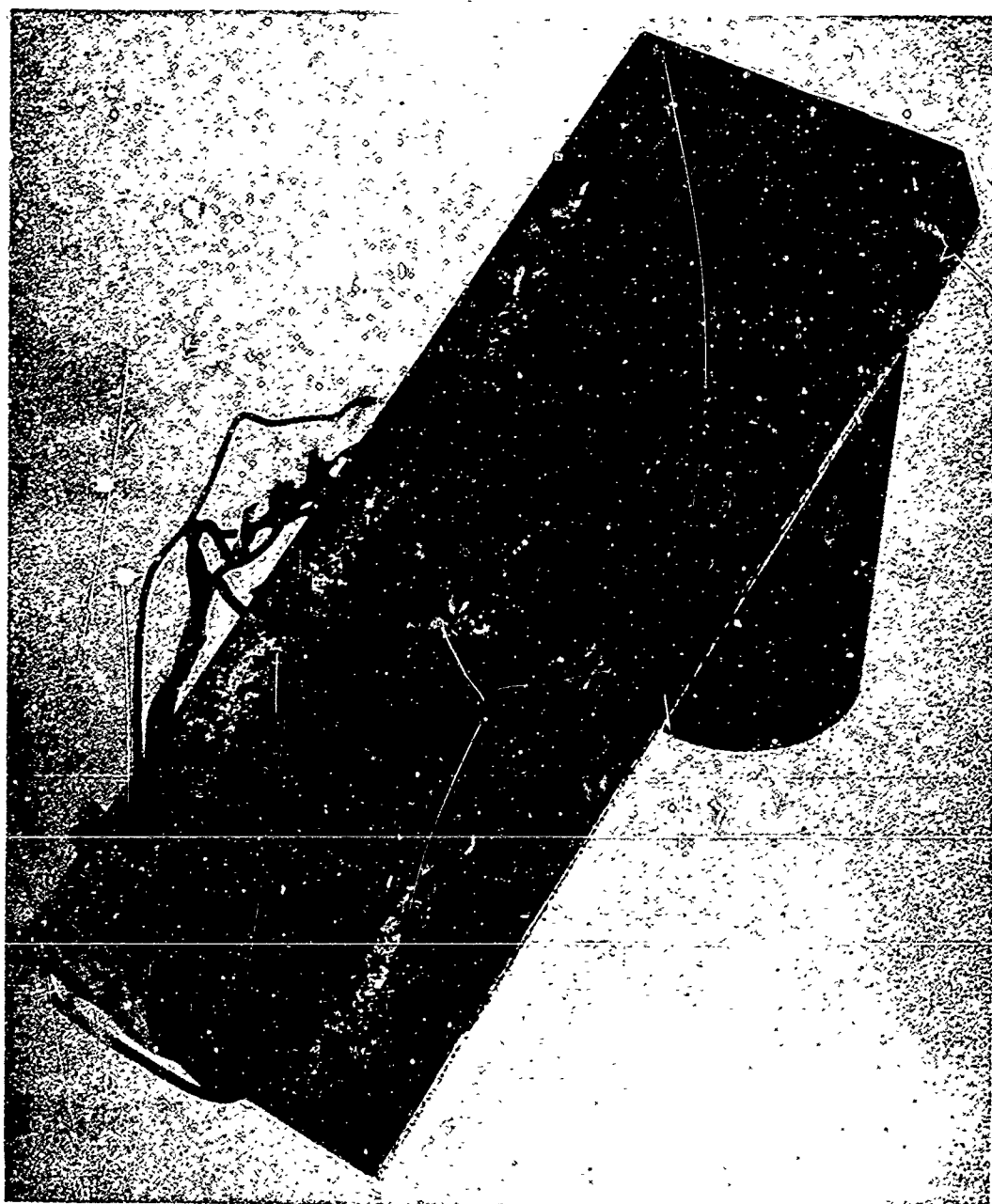


Figure 35. Ablated Test Specimen R2-3 (Run 102-69)

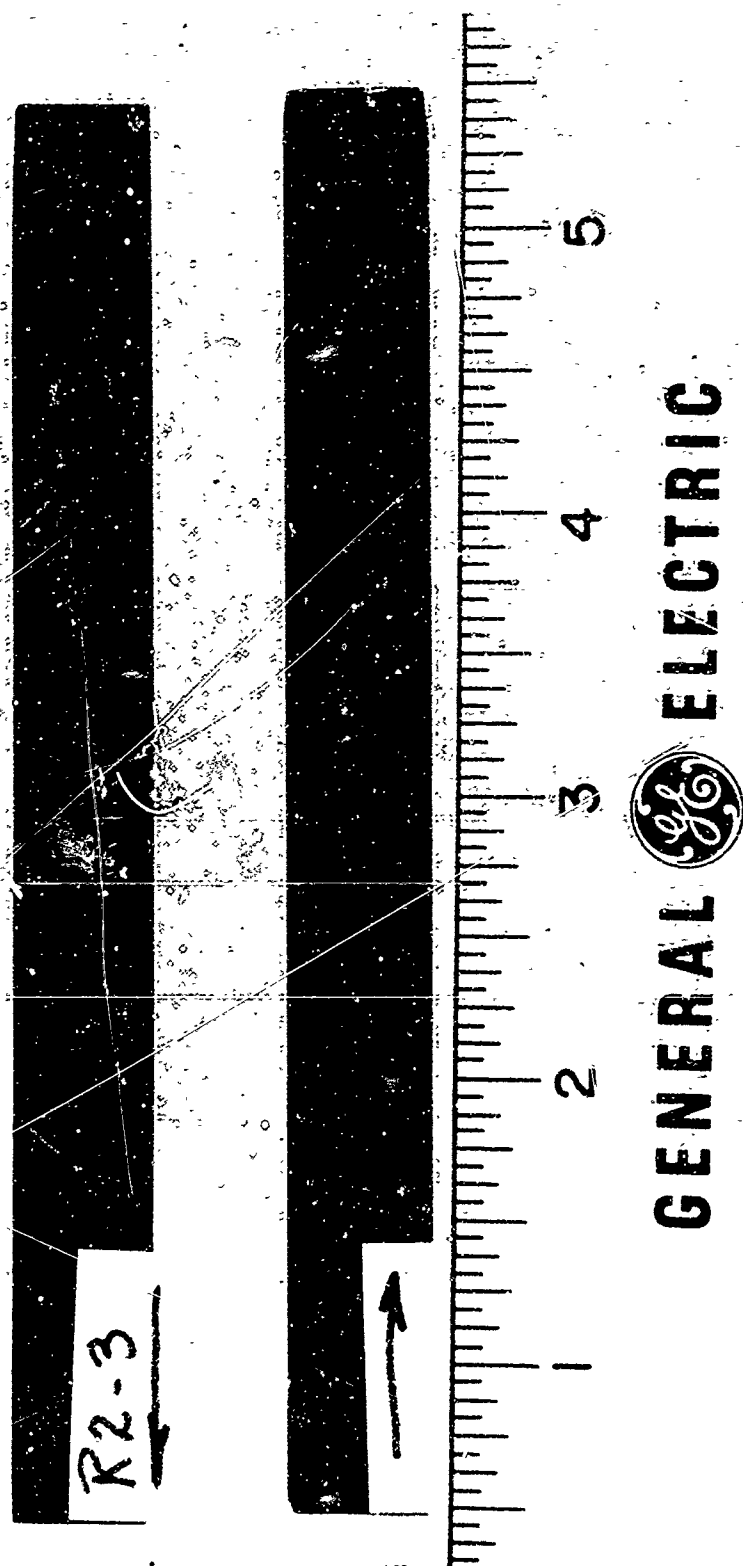


Figure 36. Ablated Test Specimen R2-3 (Sectioned)

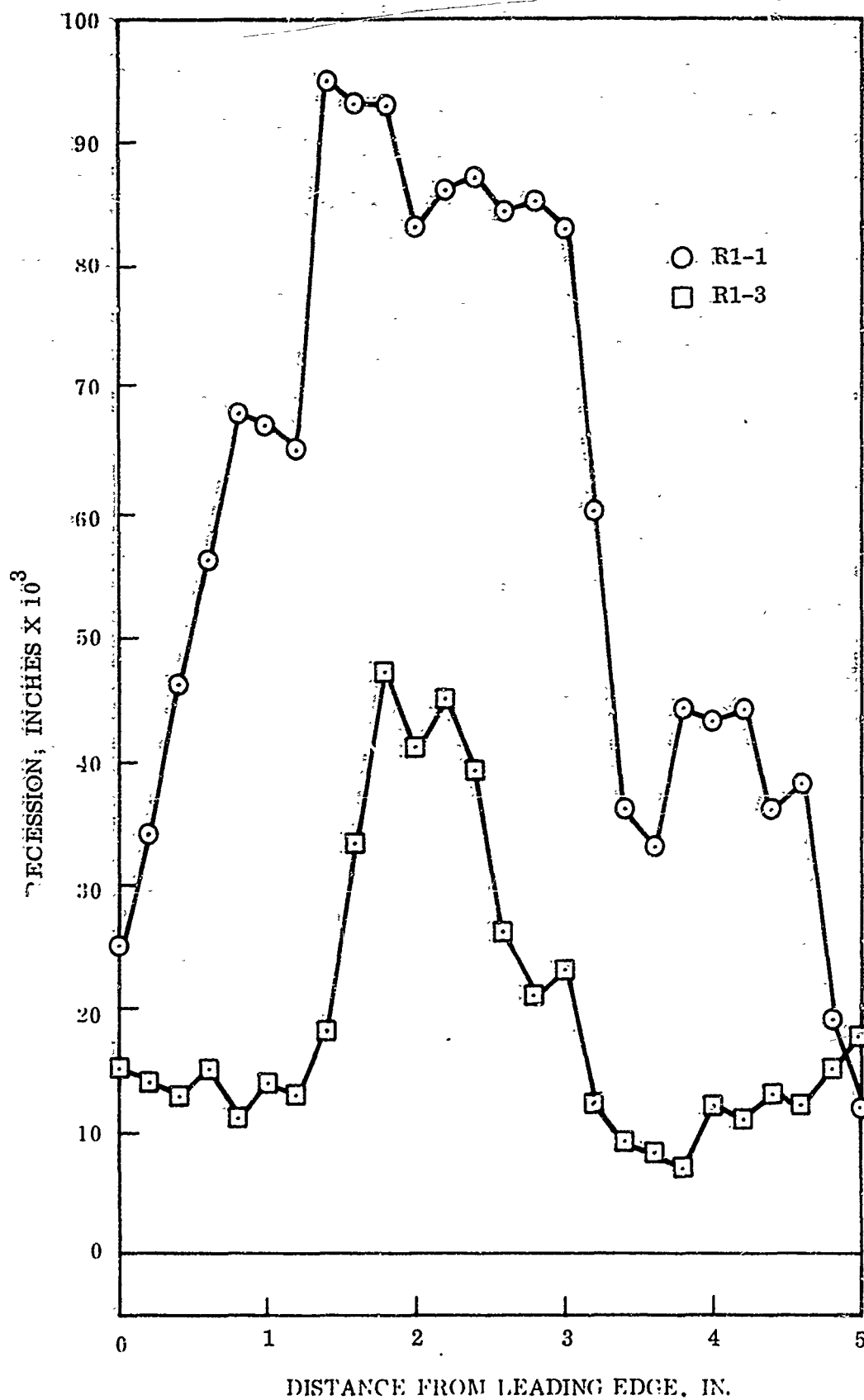


Figure 37. Ablative Recession Profiles, Specimens R1-1 and R1-3

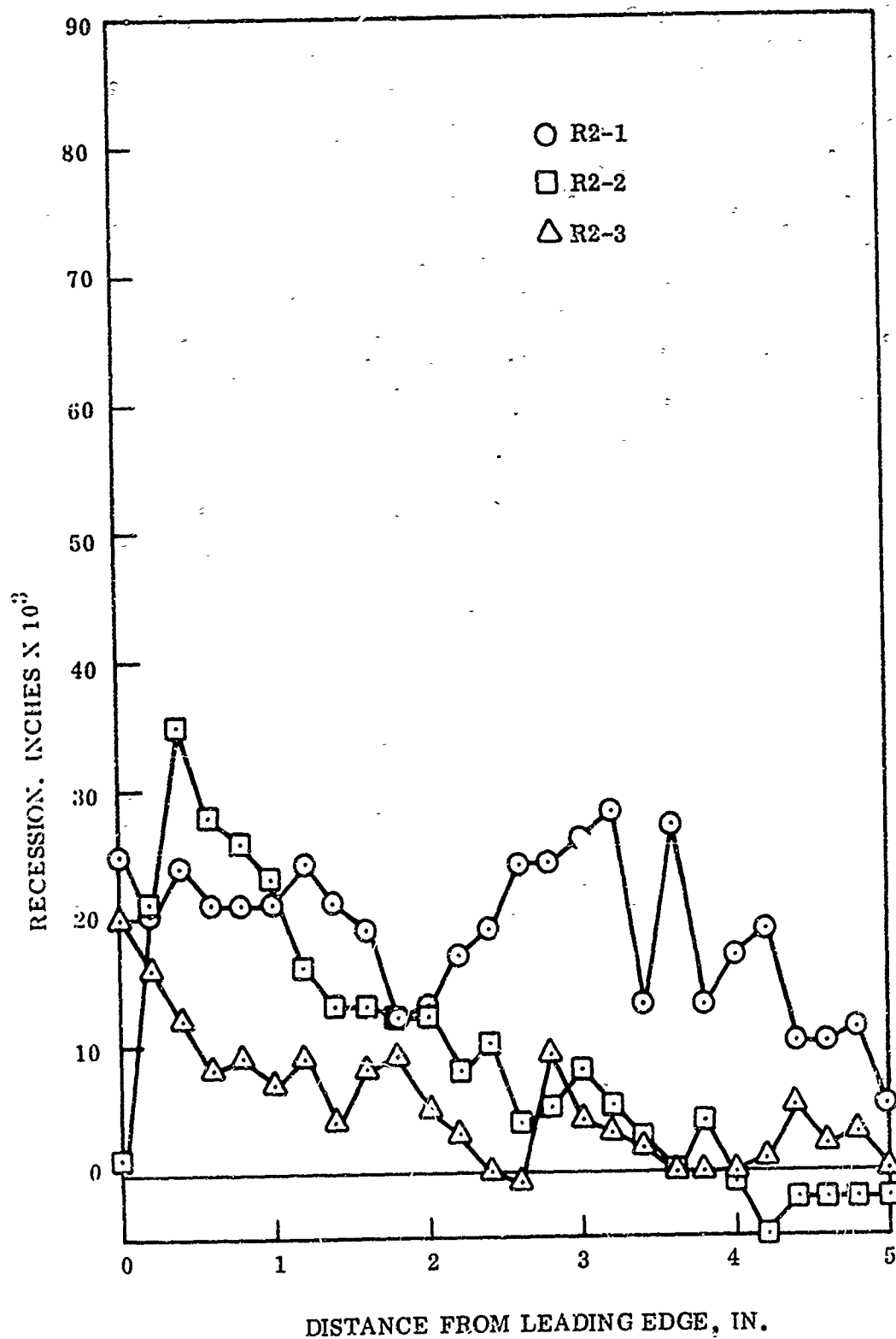


Figure 38. Ablative Recession Profiles, Specimens R2-1, R2-2 and R2-3

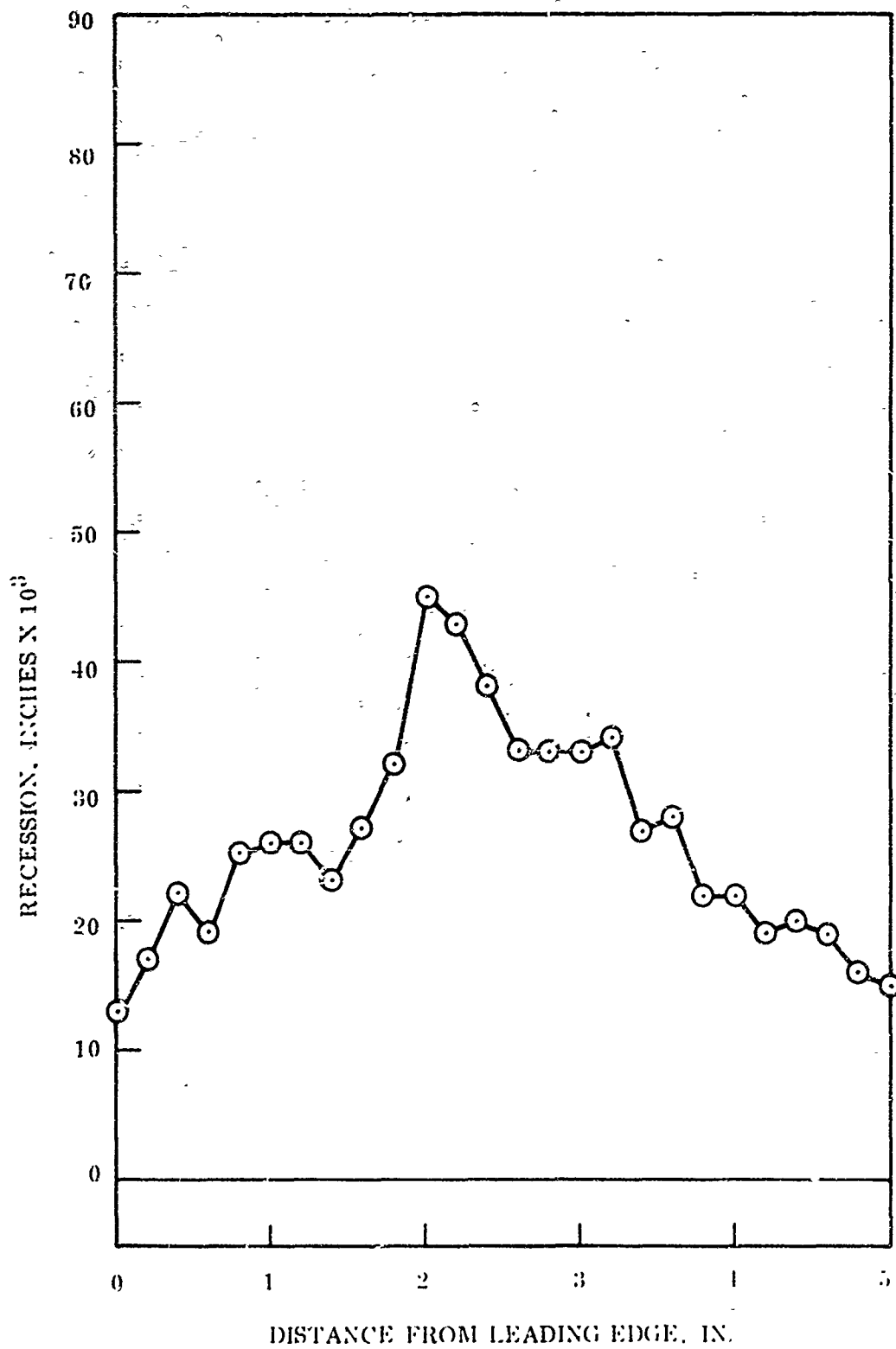


Figure 39. Ablative Recession Profile, ATJ Graphite Specimen

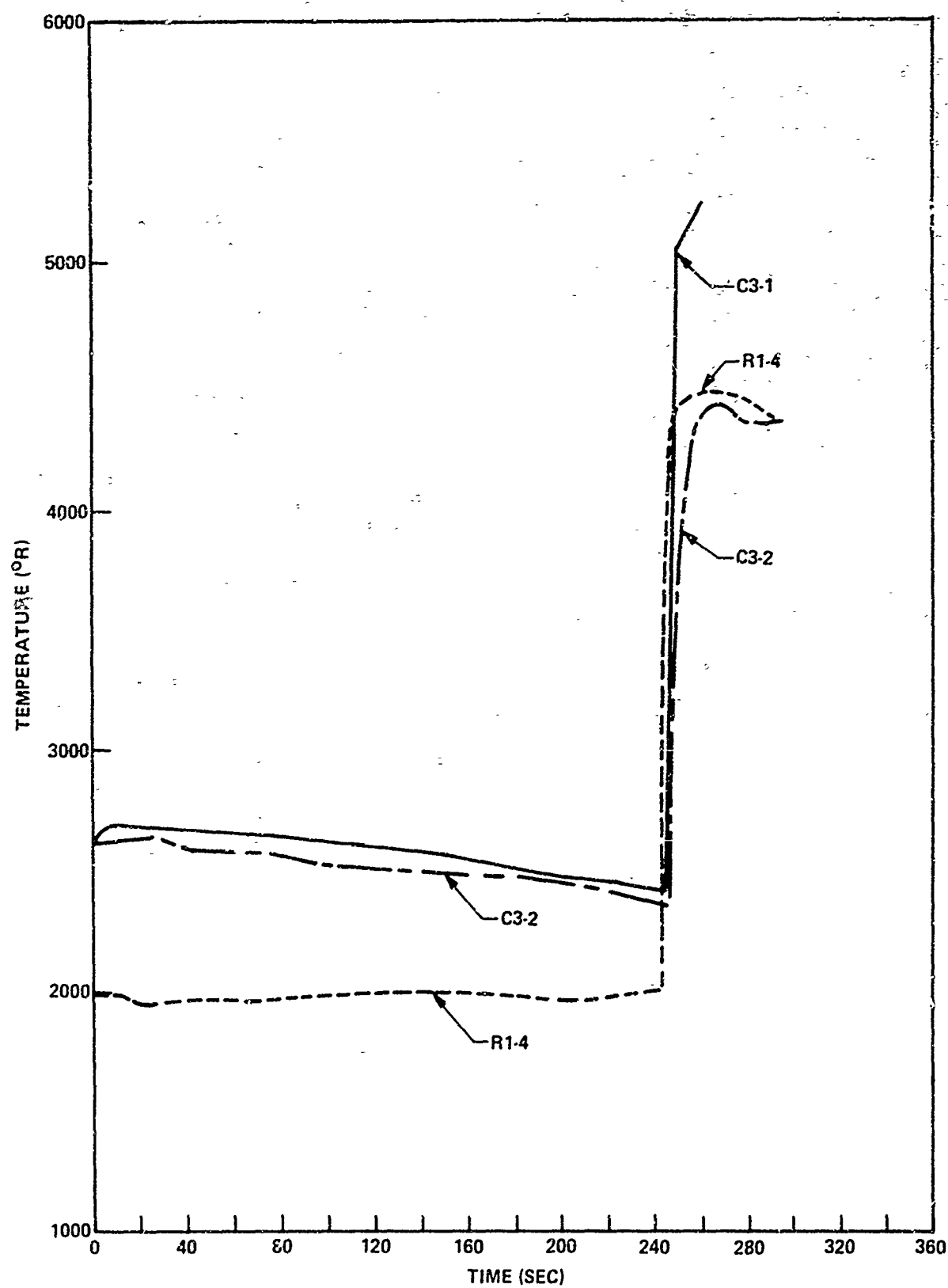


Figure 40. Surface Temperature - Silica Phenolic C3-1; C3-2; R1-4

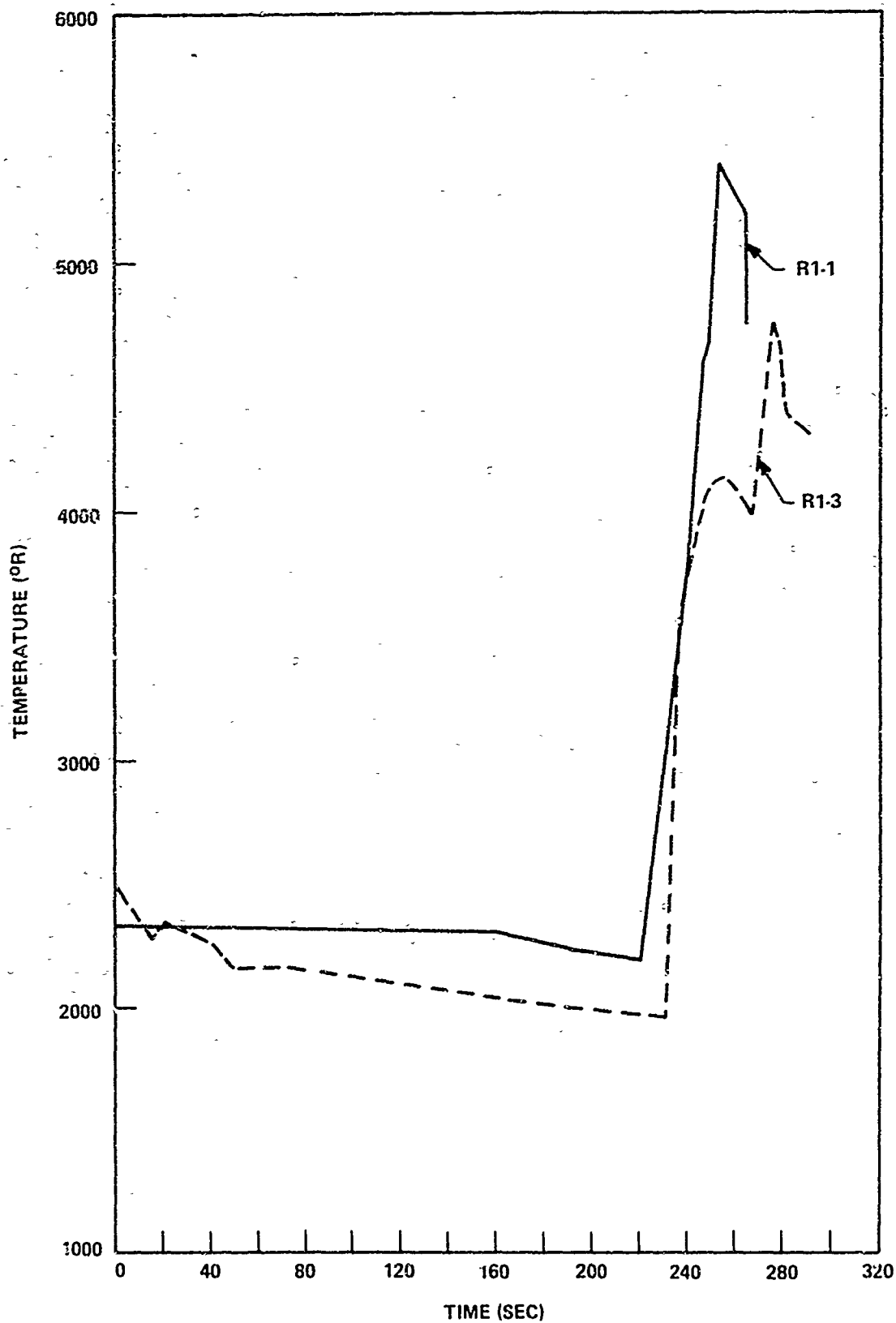


Figure 41. Surface Temperature – Silica Phenolic R1-1; R1-3

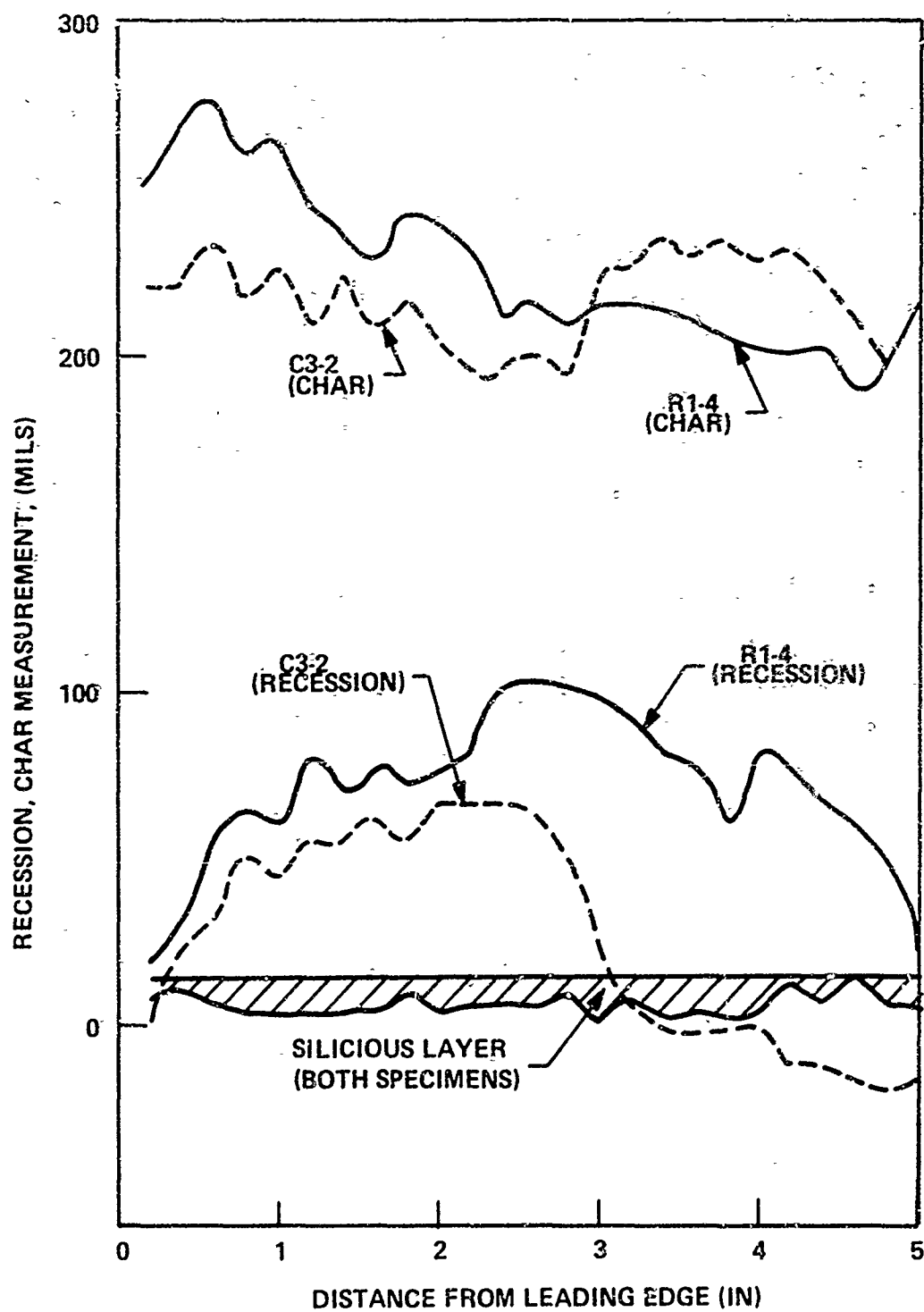


Figure 42. Ablative Profile - Silica Phenolic C3-2; R1-4

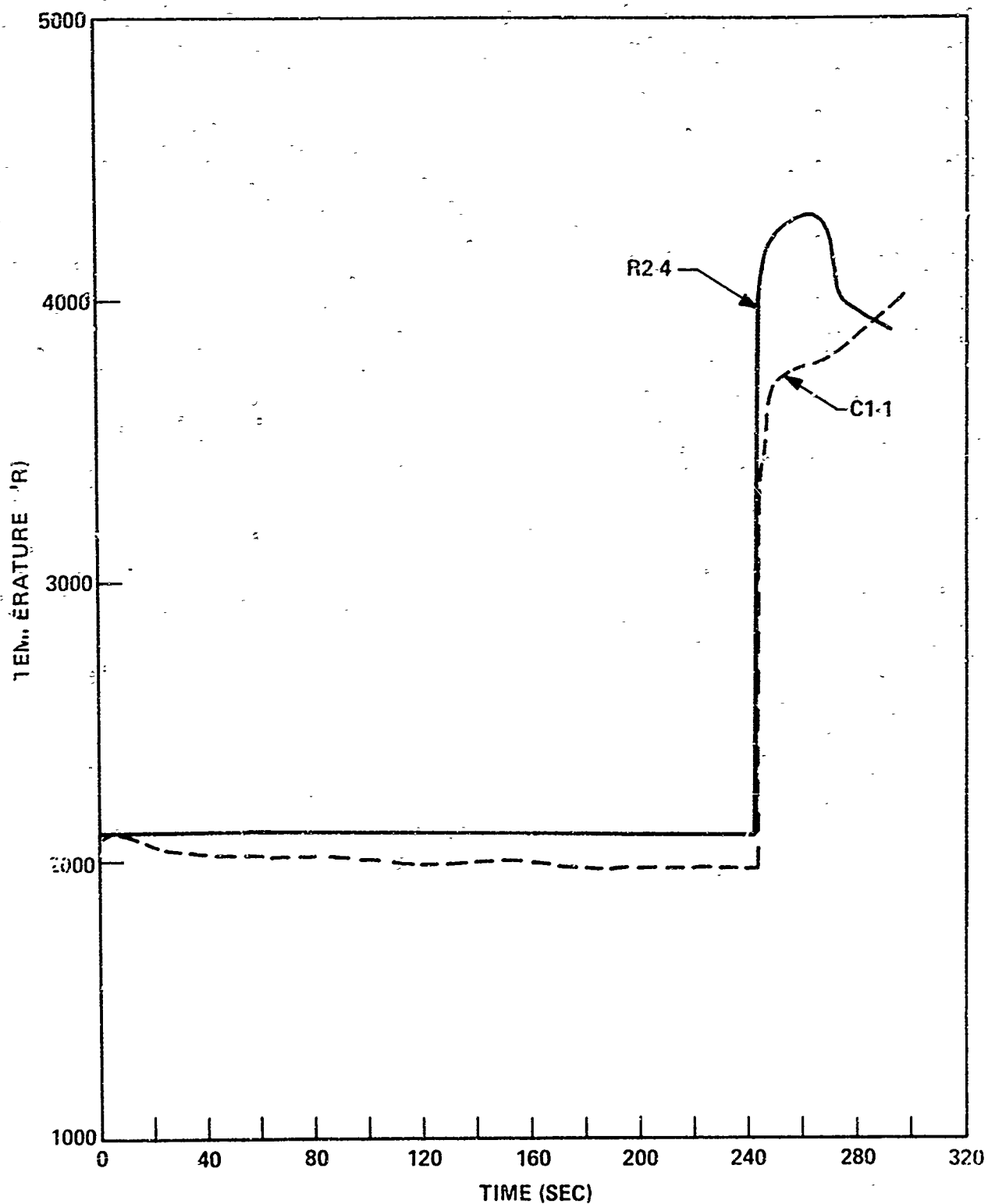


Figure 43. Surface Temperature - Carbon Phenolic C1-1; R2-4

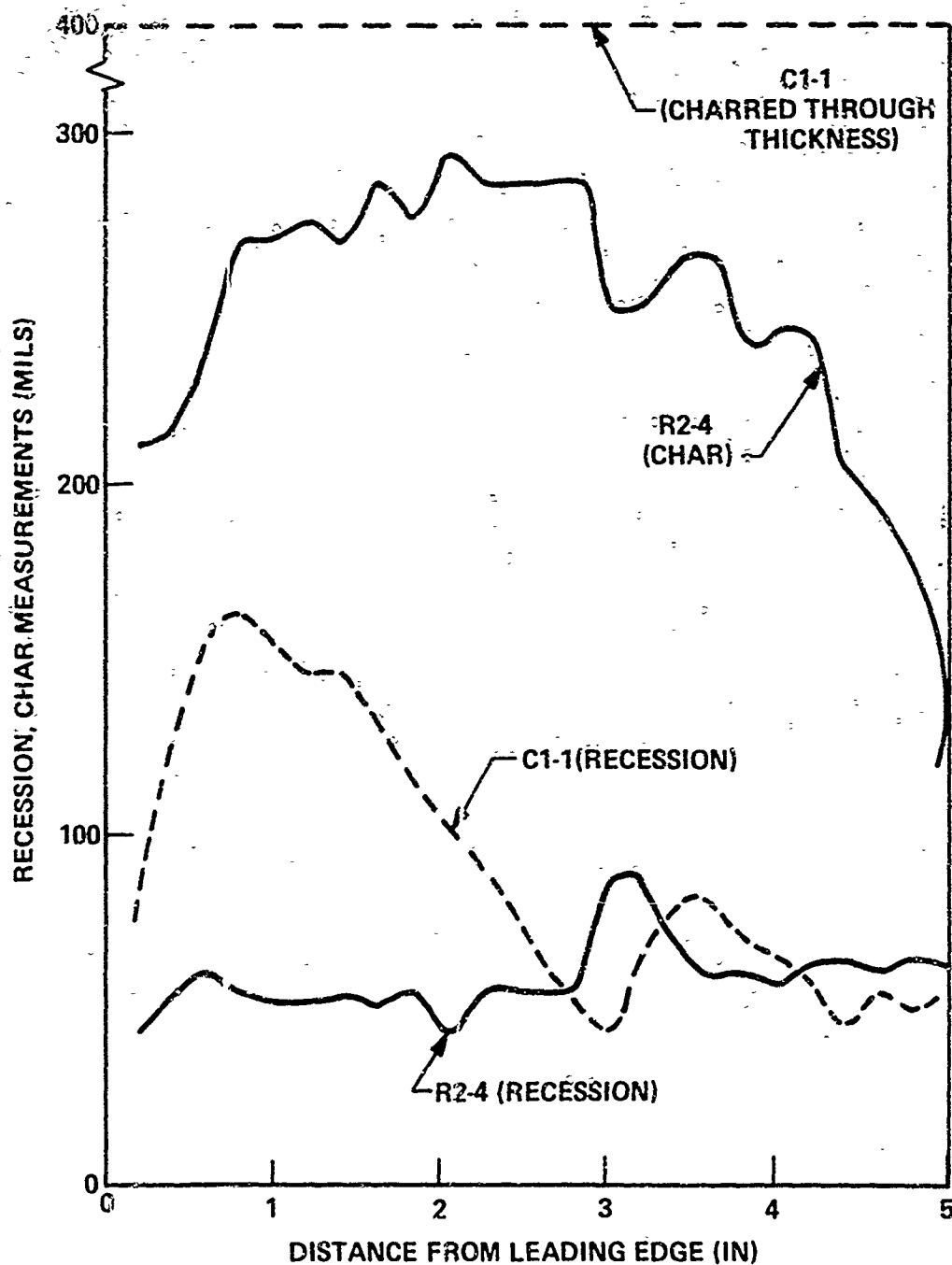


Figure 44. Ablative Profile - Carbon Phenolic C1-1; R2-4

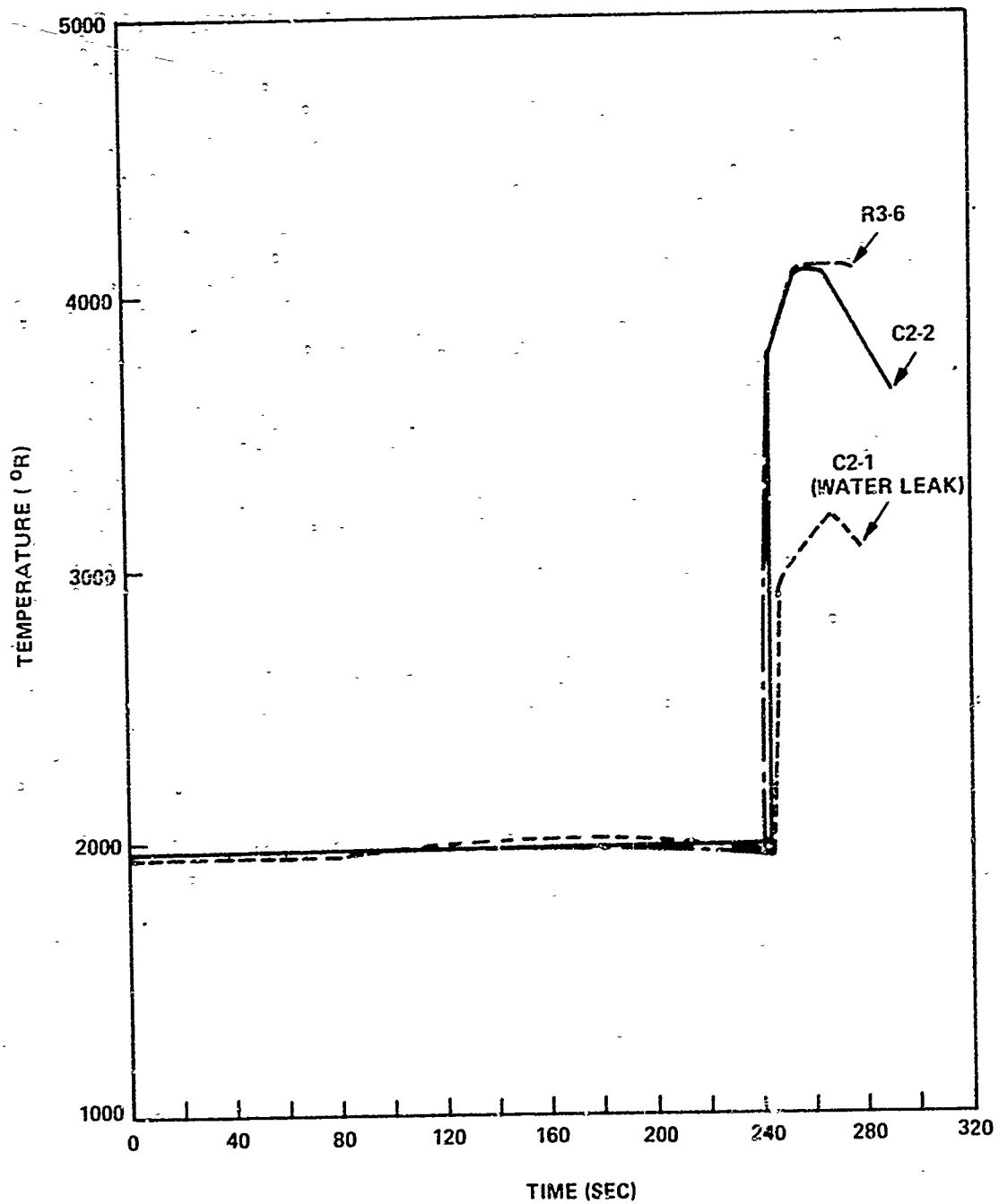


Figure 45. Surface Temperature — Carbon Phenolic C2-1; C2-2; R3-6

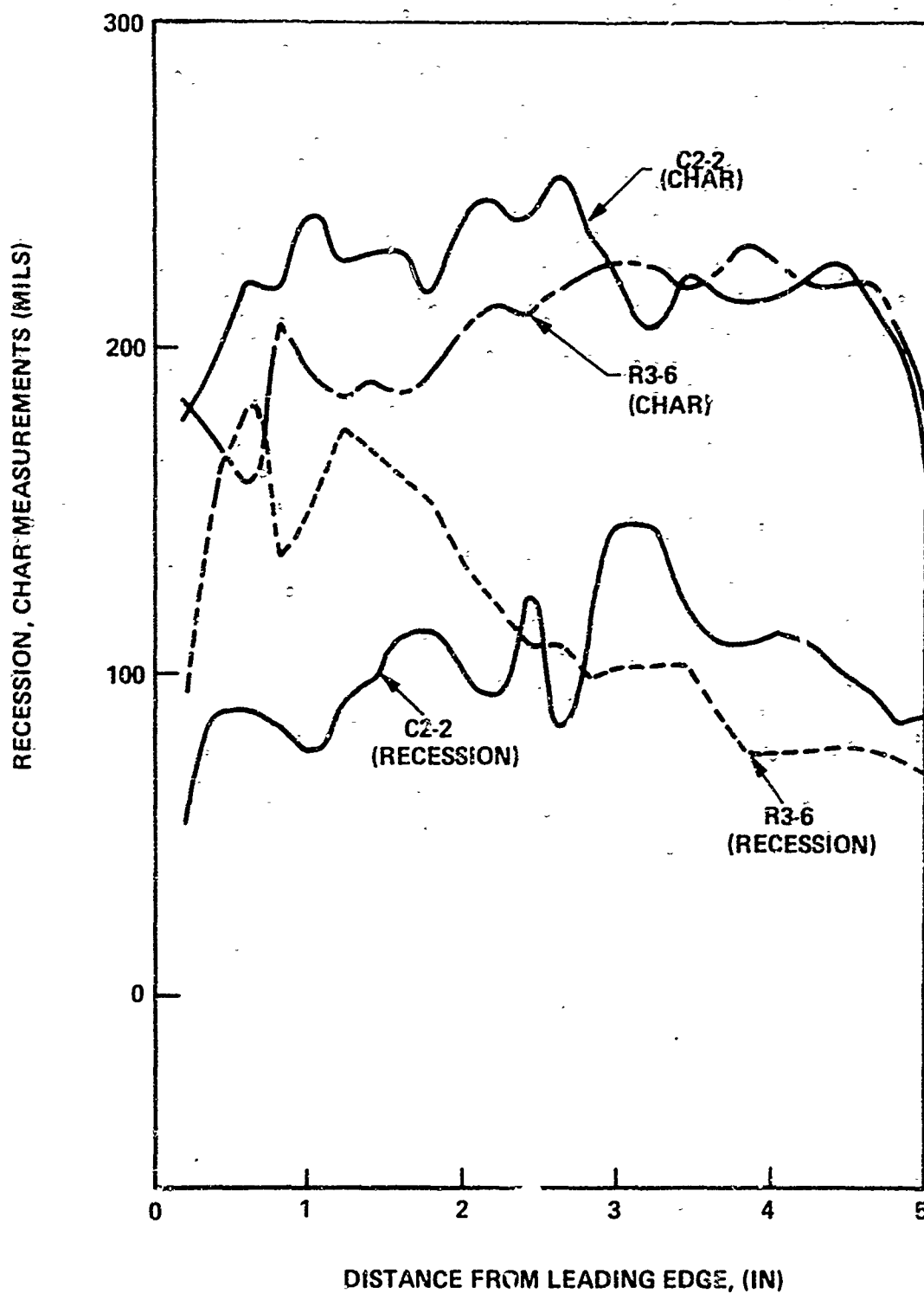


Figure 46. Ablative Profile - Carbon Phenolic C2-2; R3-6



Figure 47. Silica Phenolic -- Post Test R1-4

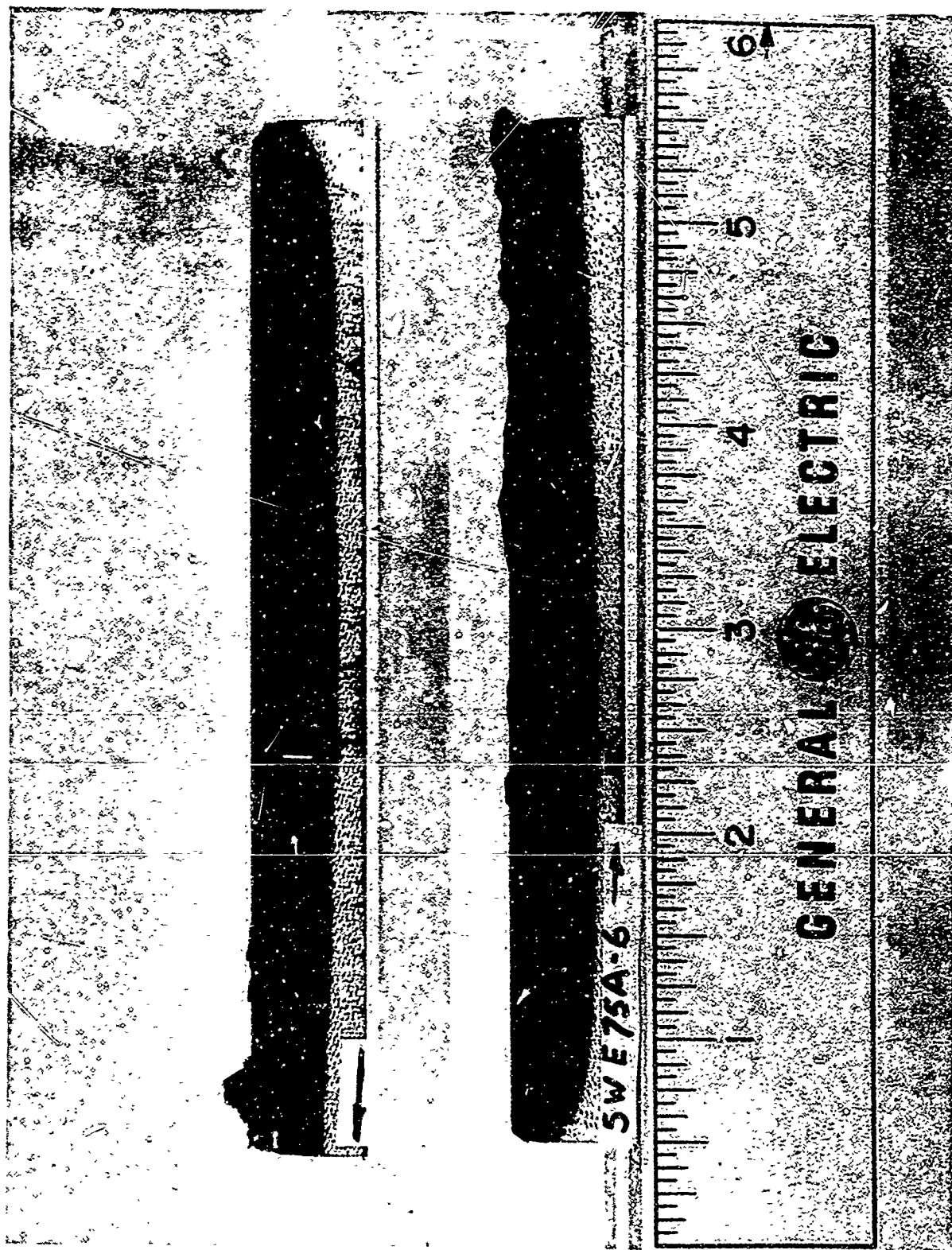


Figure 48 Silica Phenolic - Post Test R1-4 (Sectioned)

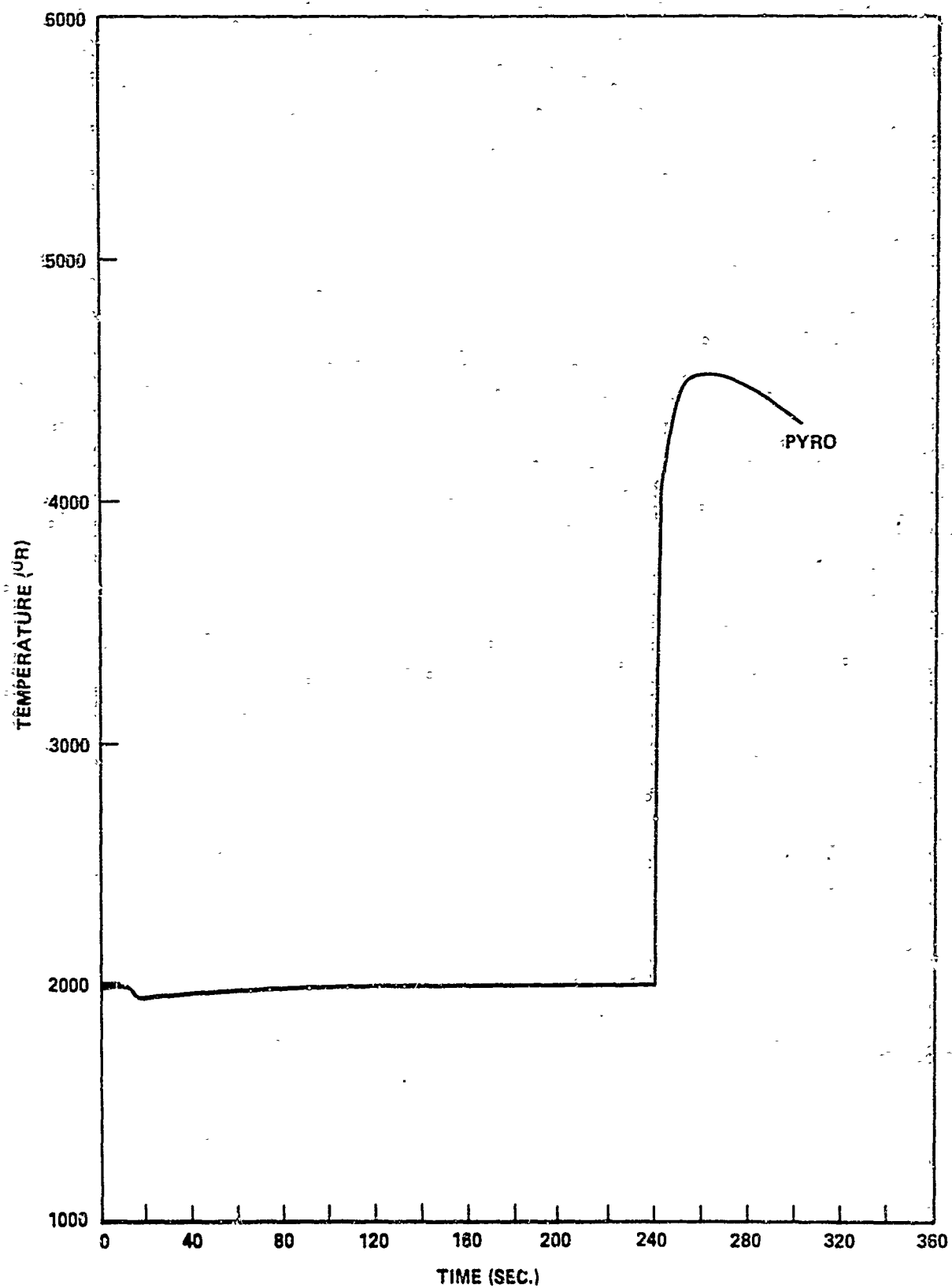


Figure 49. Surface Temperature — Silica Phenolic R1-4

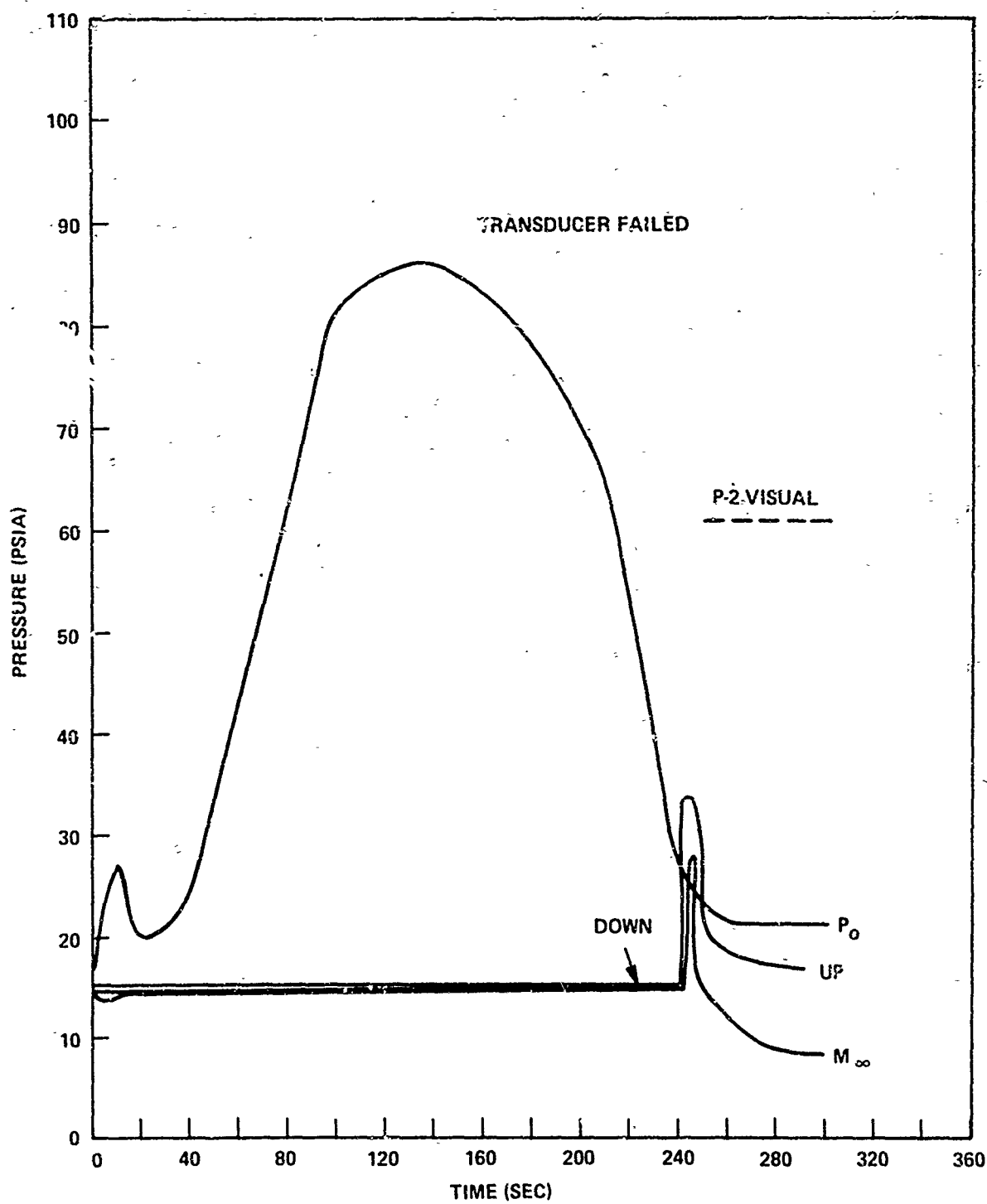


Figure 50. Pressures - Silica Phenolic R1-4

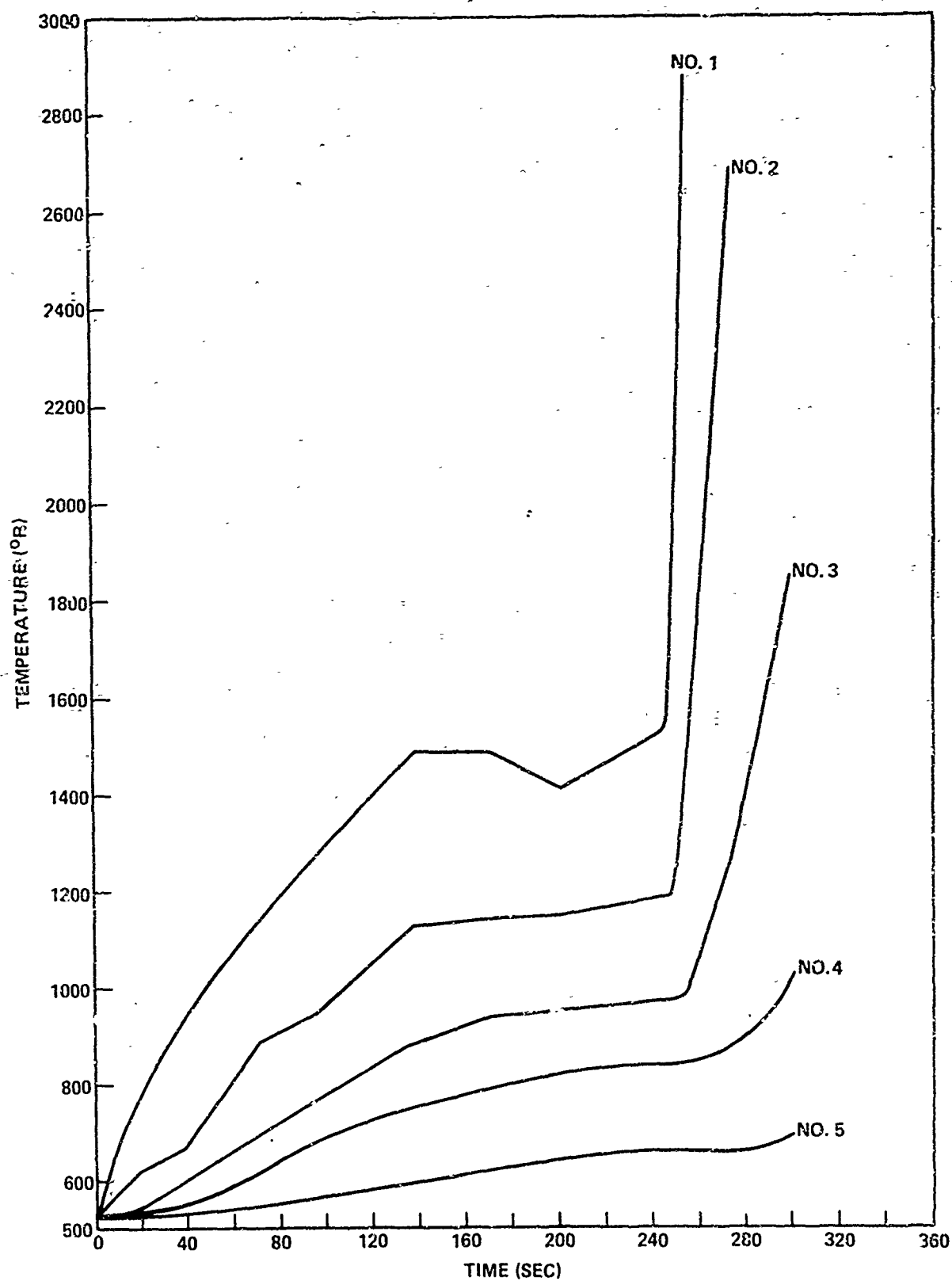


Figure 51. Internal Temperatures - Silica Phenolic R1-4

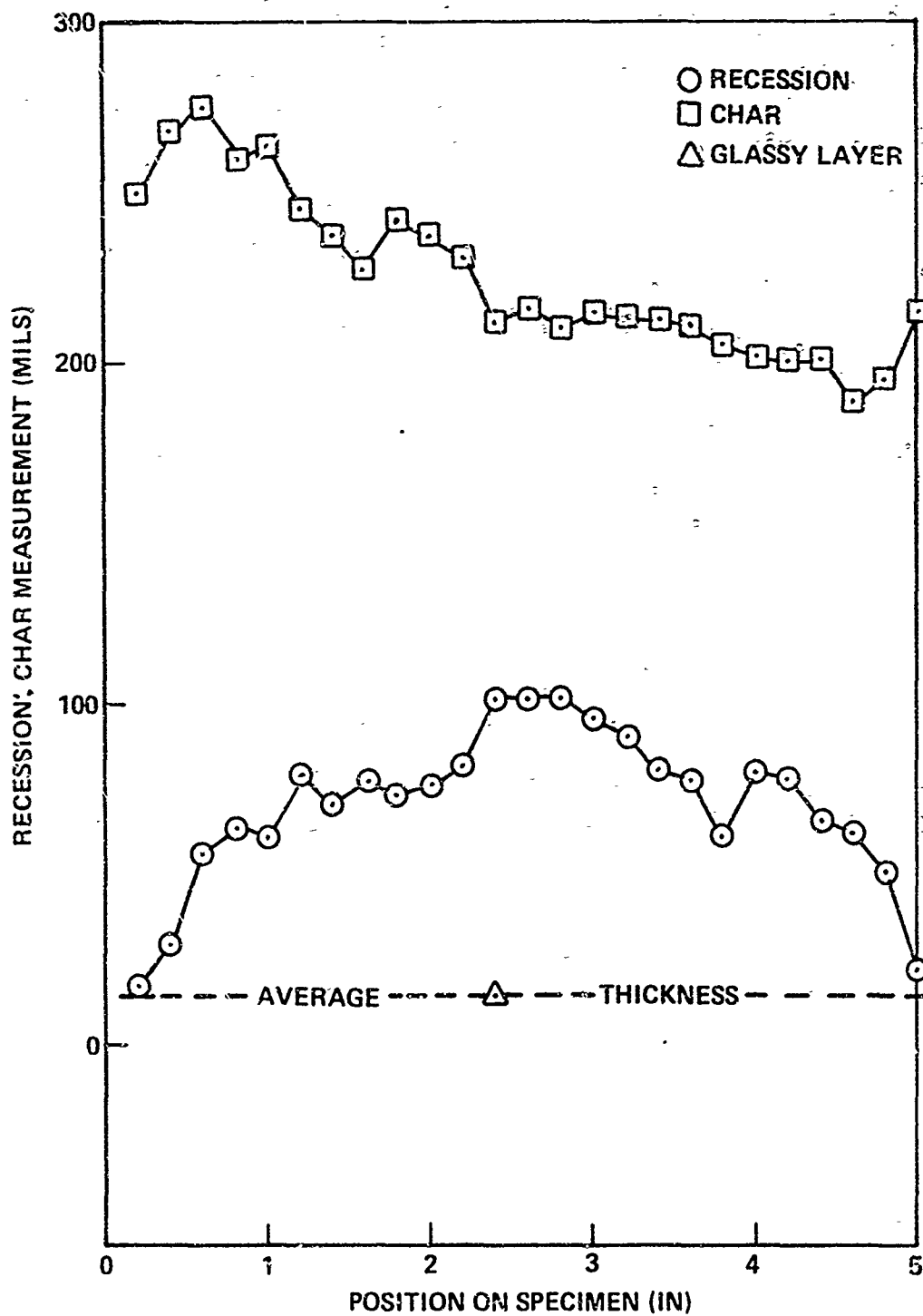


Figure 52. Char Measurement — Silica Phenolic R1-4



Figure 53. Carbon Phenolic - Post Test R24

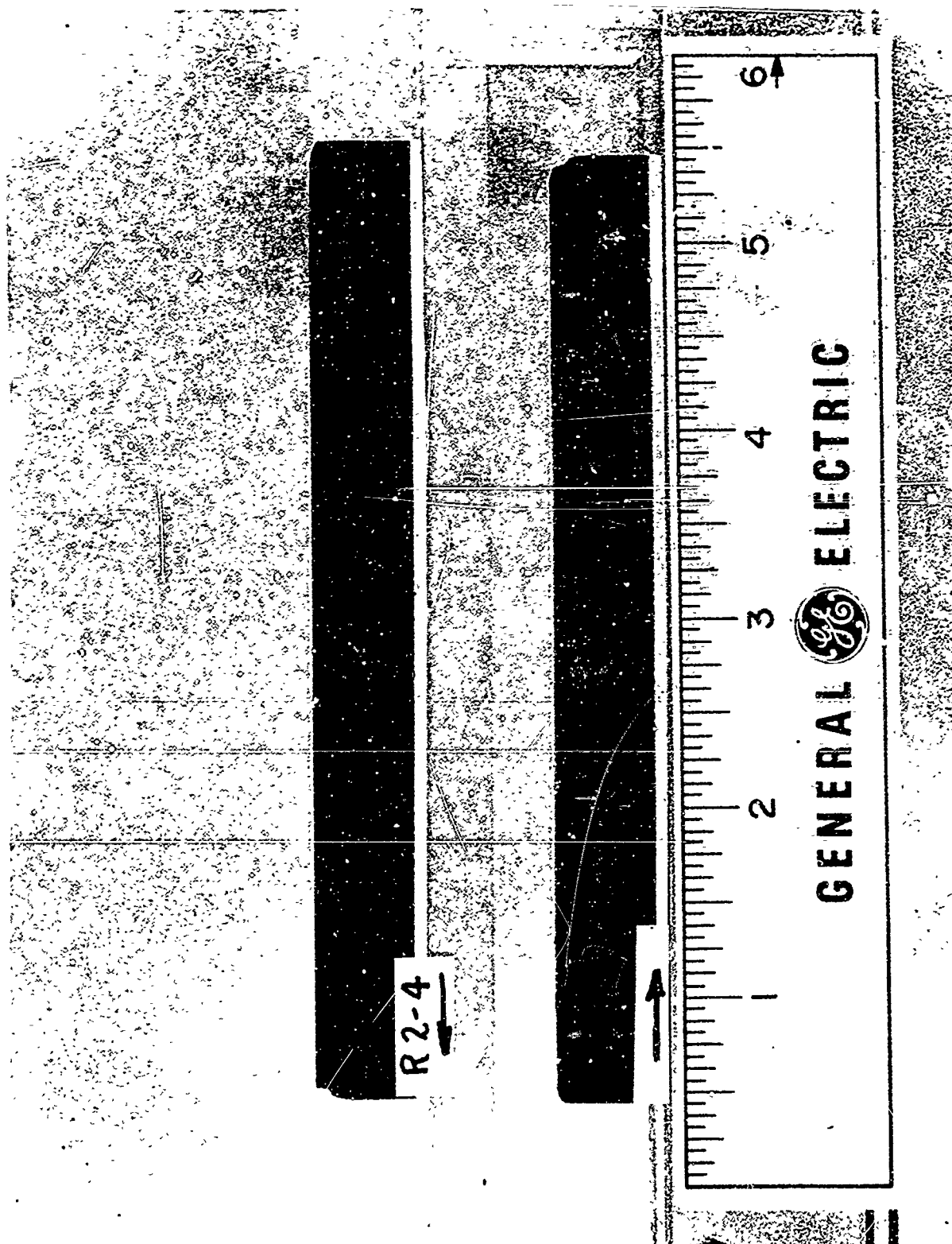


Figure 54. Carbon Phenolic - Post Test R2-4 (Sectioned)

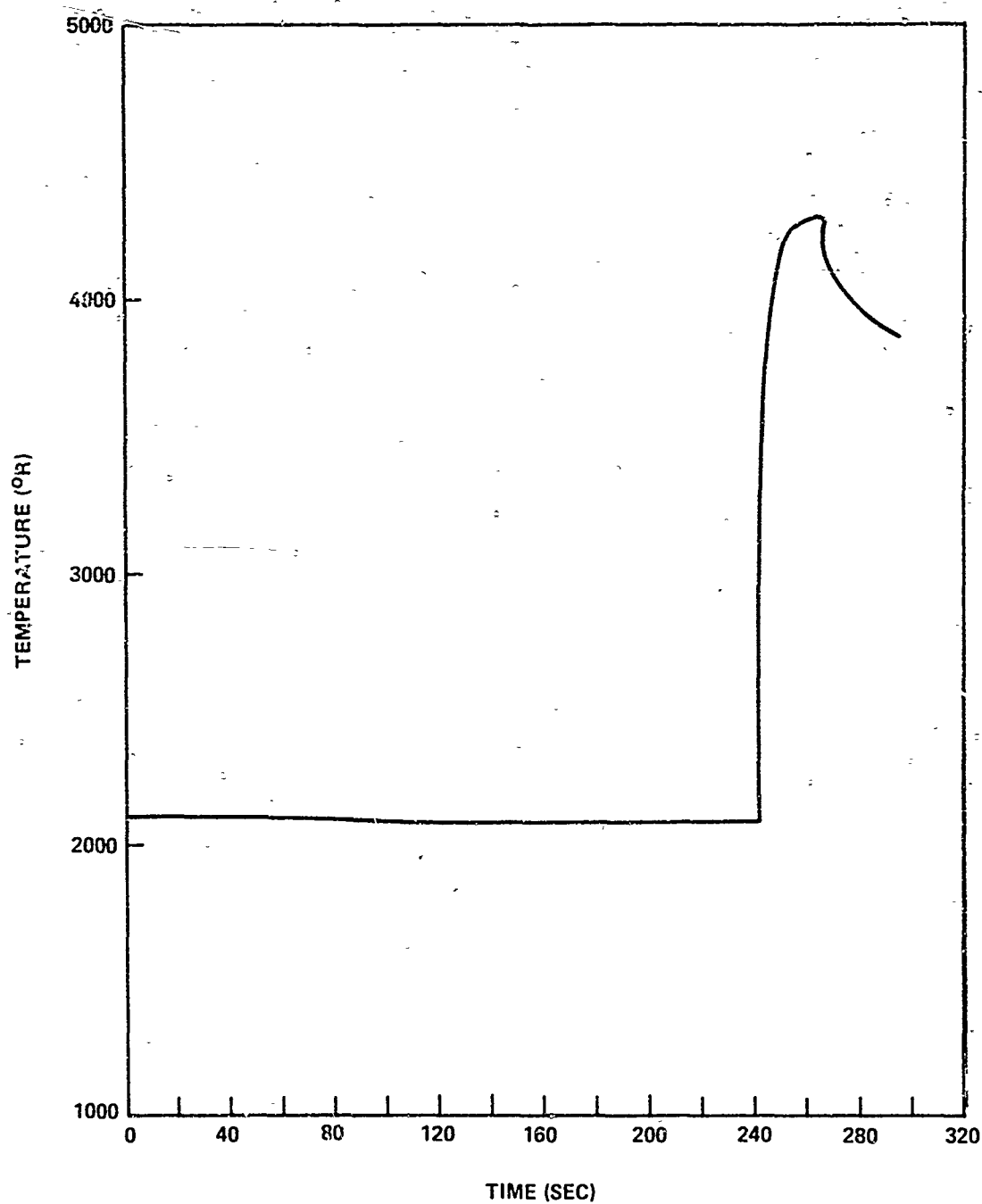


Figure 55. Surface Temperature – Carbon Phenolic R2-4

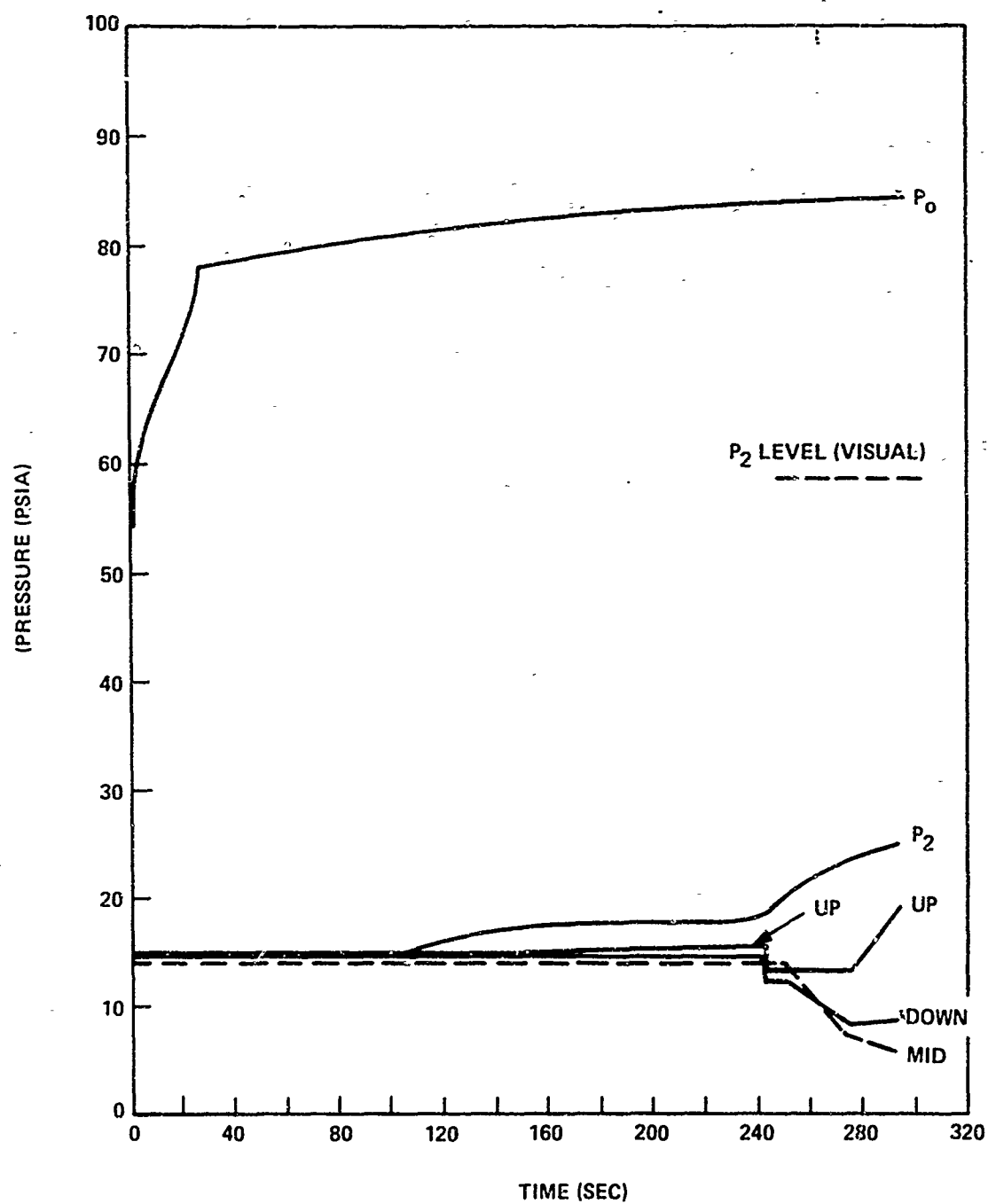


Figure 56. Pressures - Carbon Phenolic R2-4

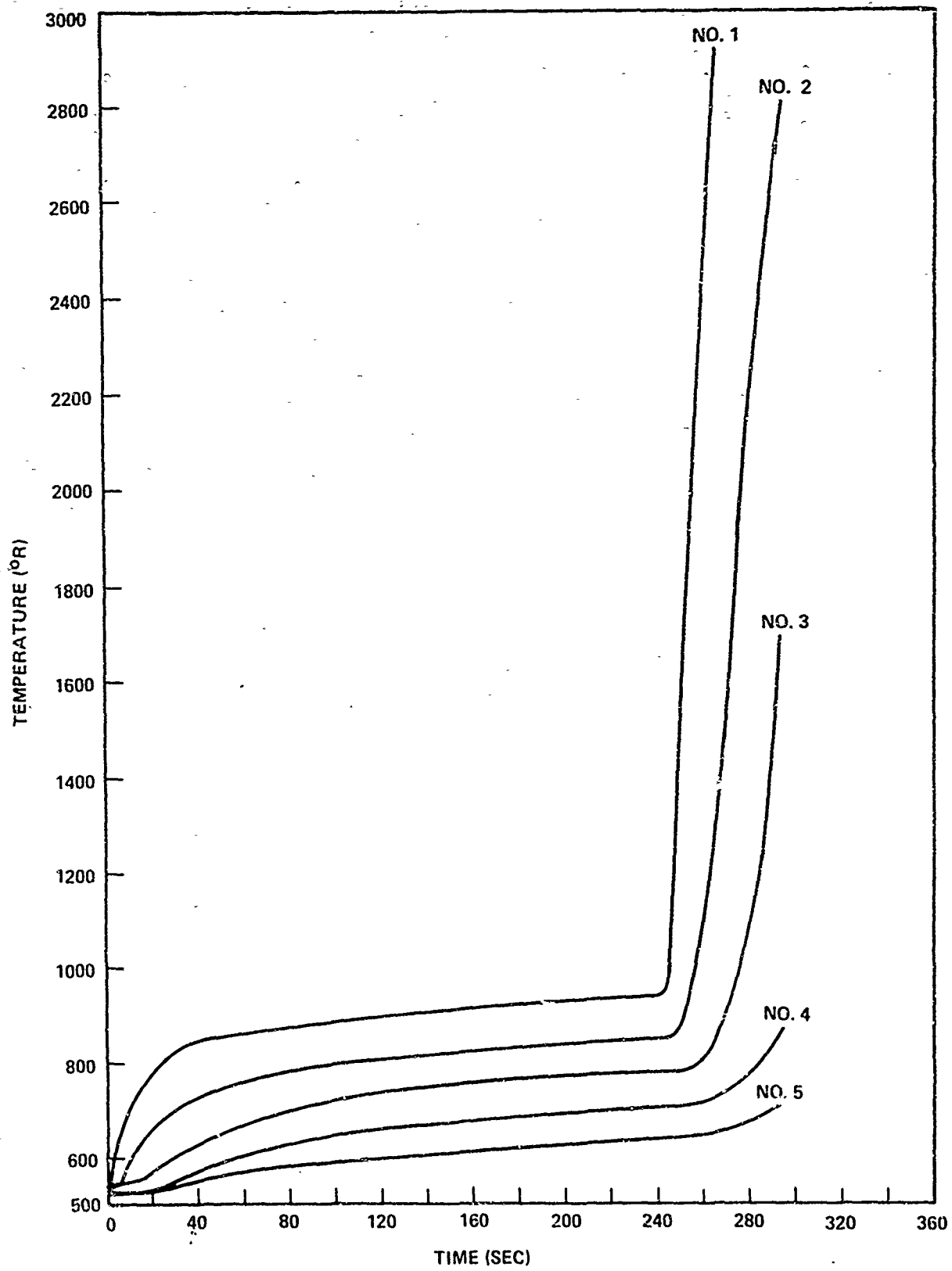


Figure 57. Internal Temperatures – Carbon Phenolic R2-4

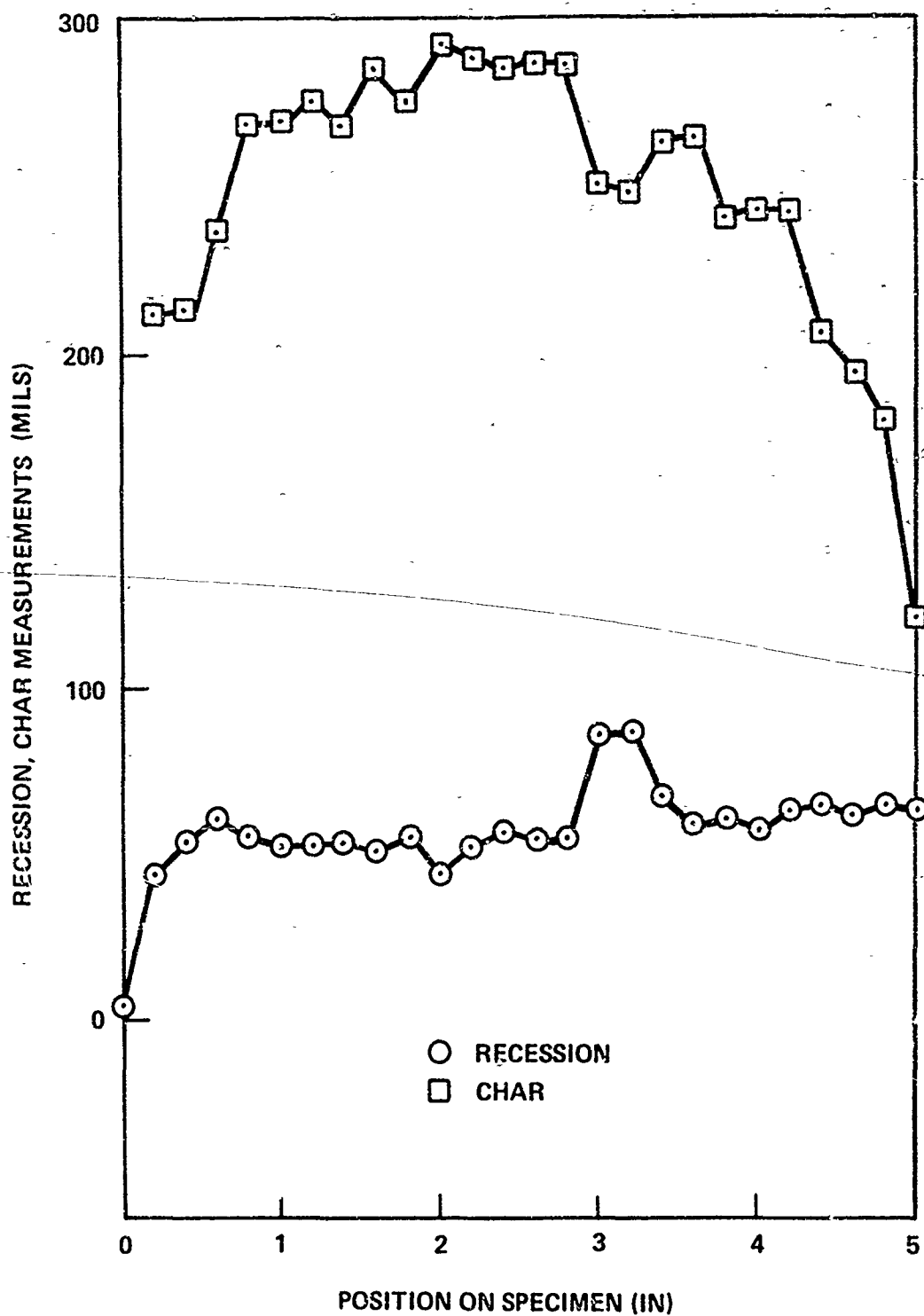


Figure 58. Char Measurements - Carbon Phenolic R2-4



Figure 59. Carbon Phenolic — Post Test R3-6

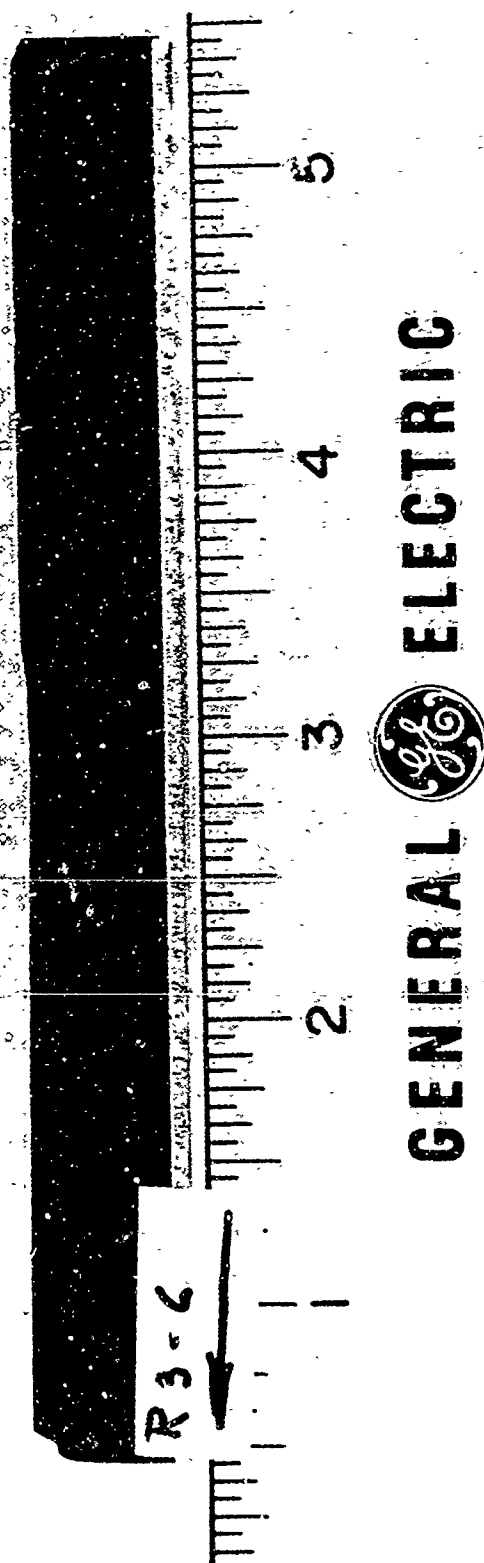


Figure 60. Carbon Phenolic-Post Test R3-6 (Sectioned)

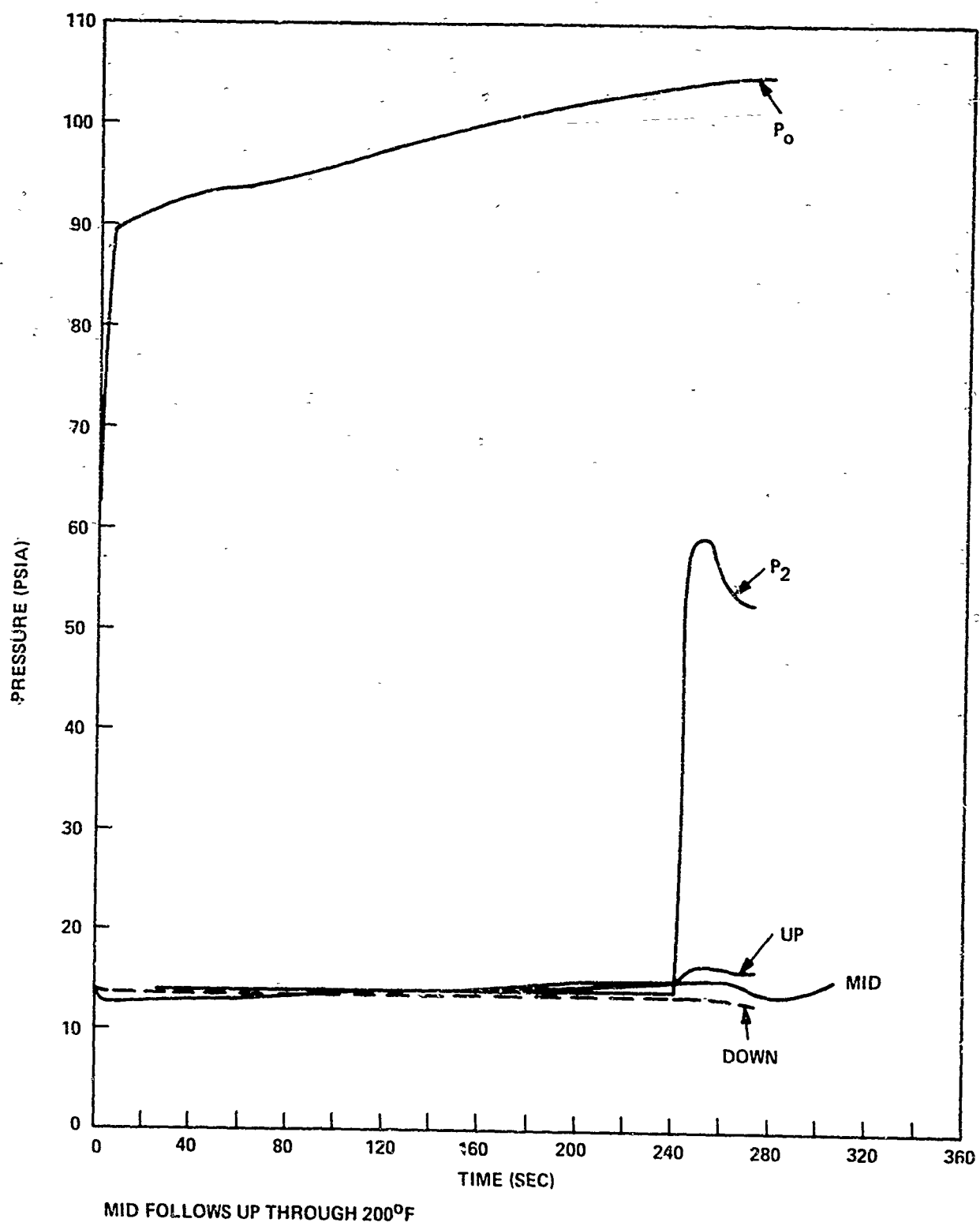


Figure 61. Pressures - Carbon Phenolic R3-6

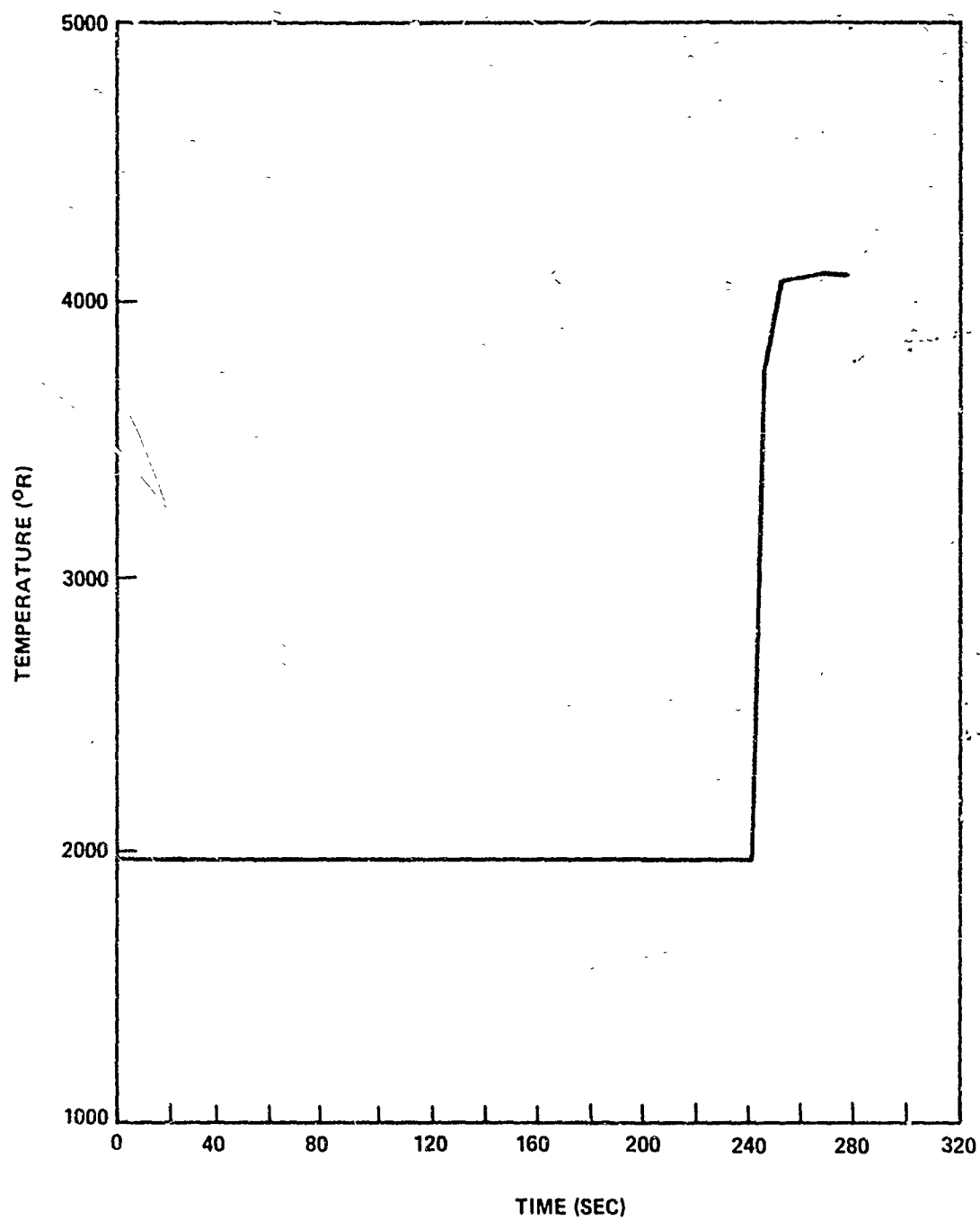


Figure 62. Surface Temperatures – Carbon Phenolic R3-6

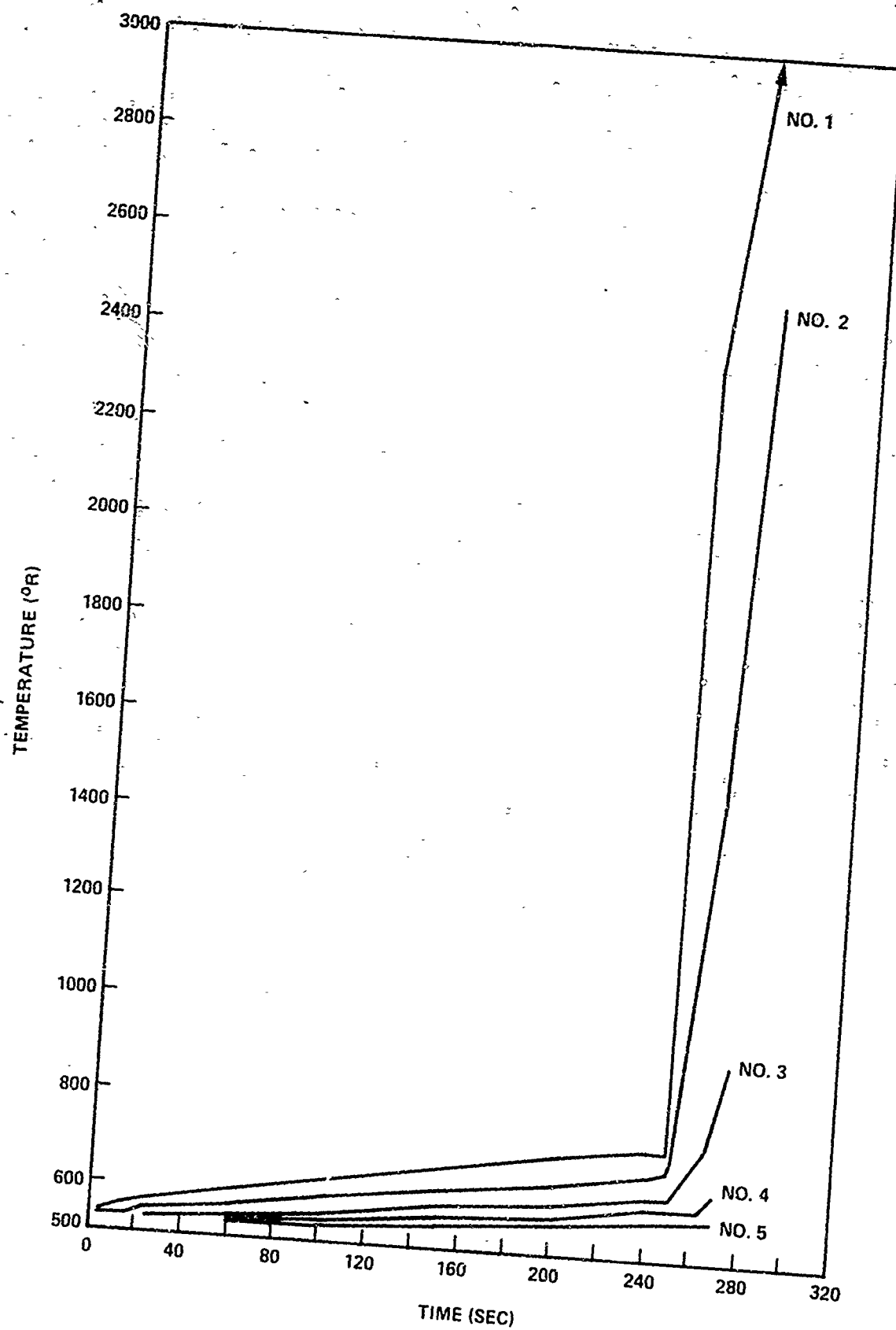


Figure 63. Internal Temperatures -- Carbon Phenolic R3-6

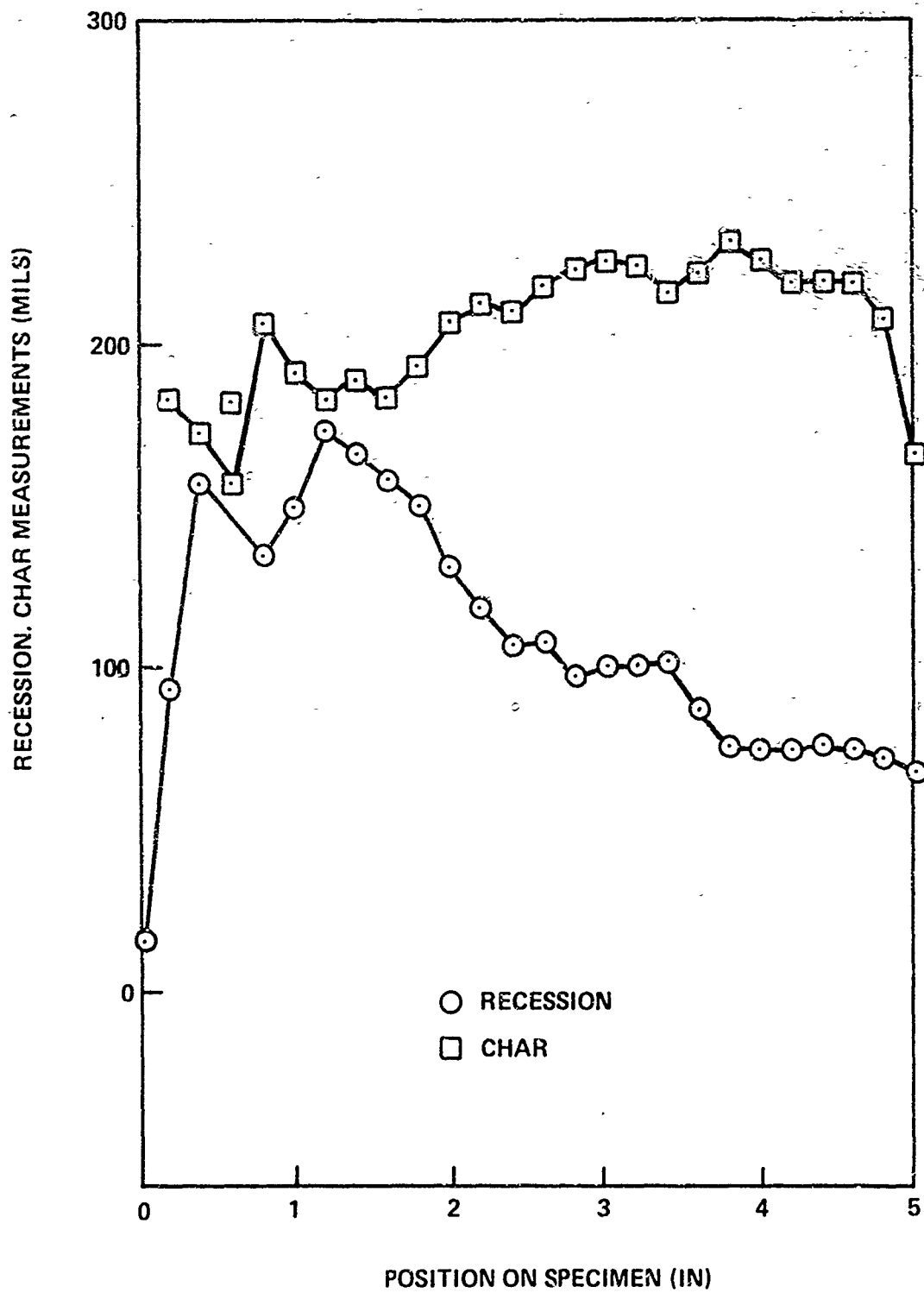


Figure 64. Char Measurements - Carbon Phenolic R3-6

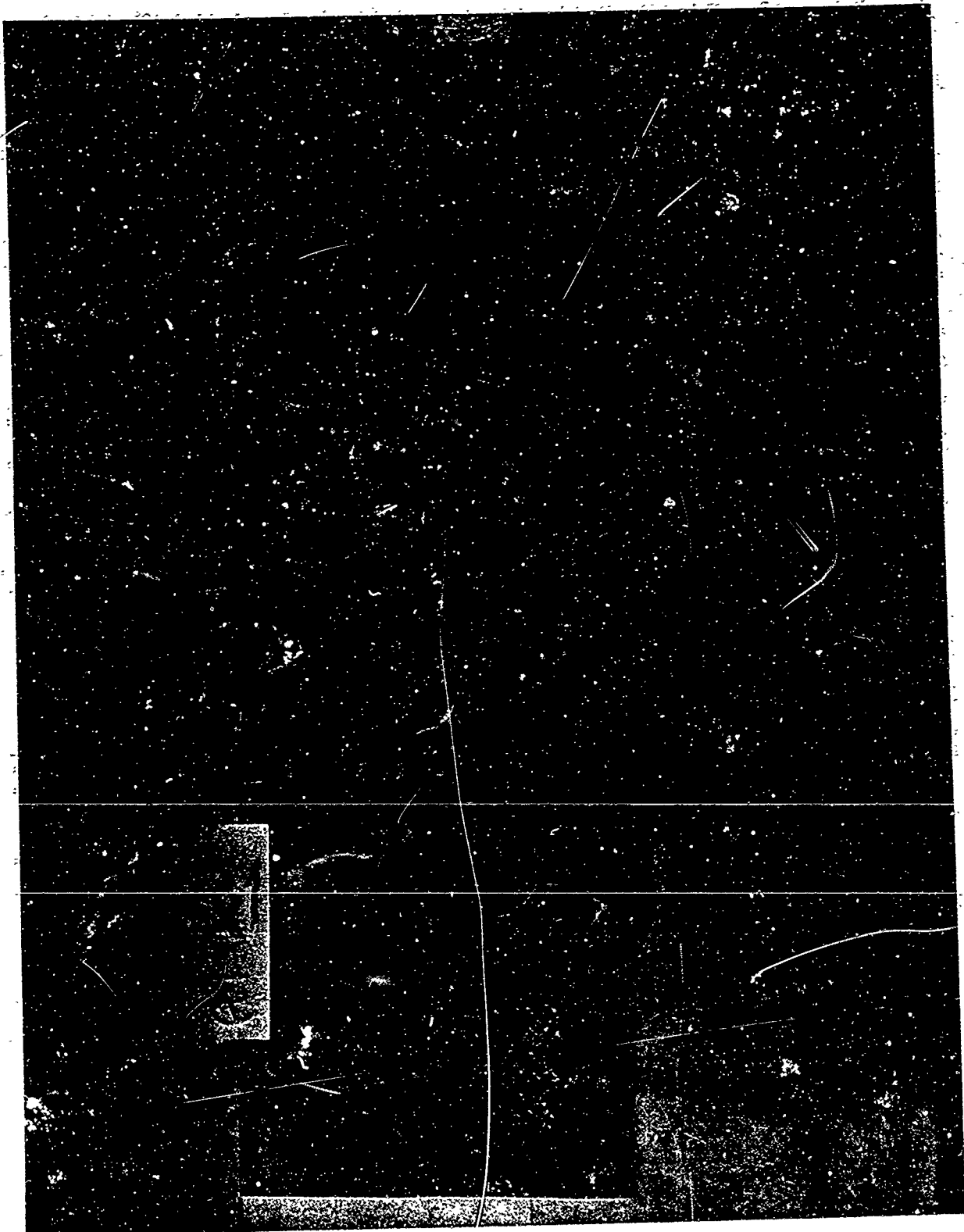


Figure 65. Carbon Phenolic — Post Test A1-2

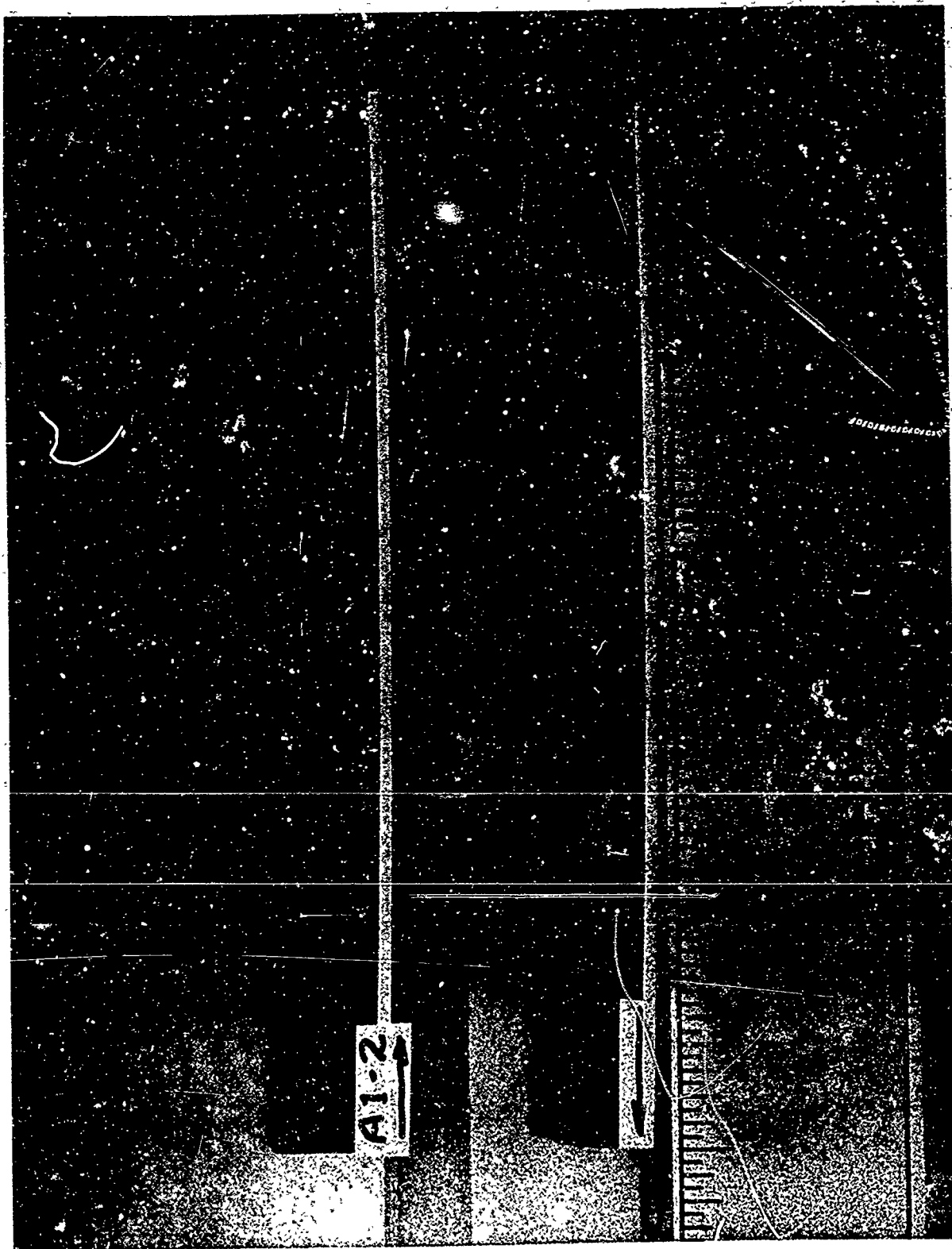


Figure 66. Carbon Phenolic — Post Test A1-2 (Sectioned)

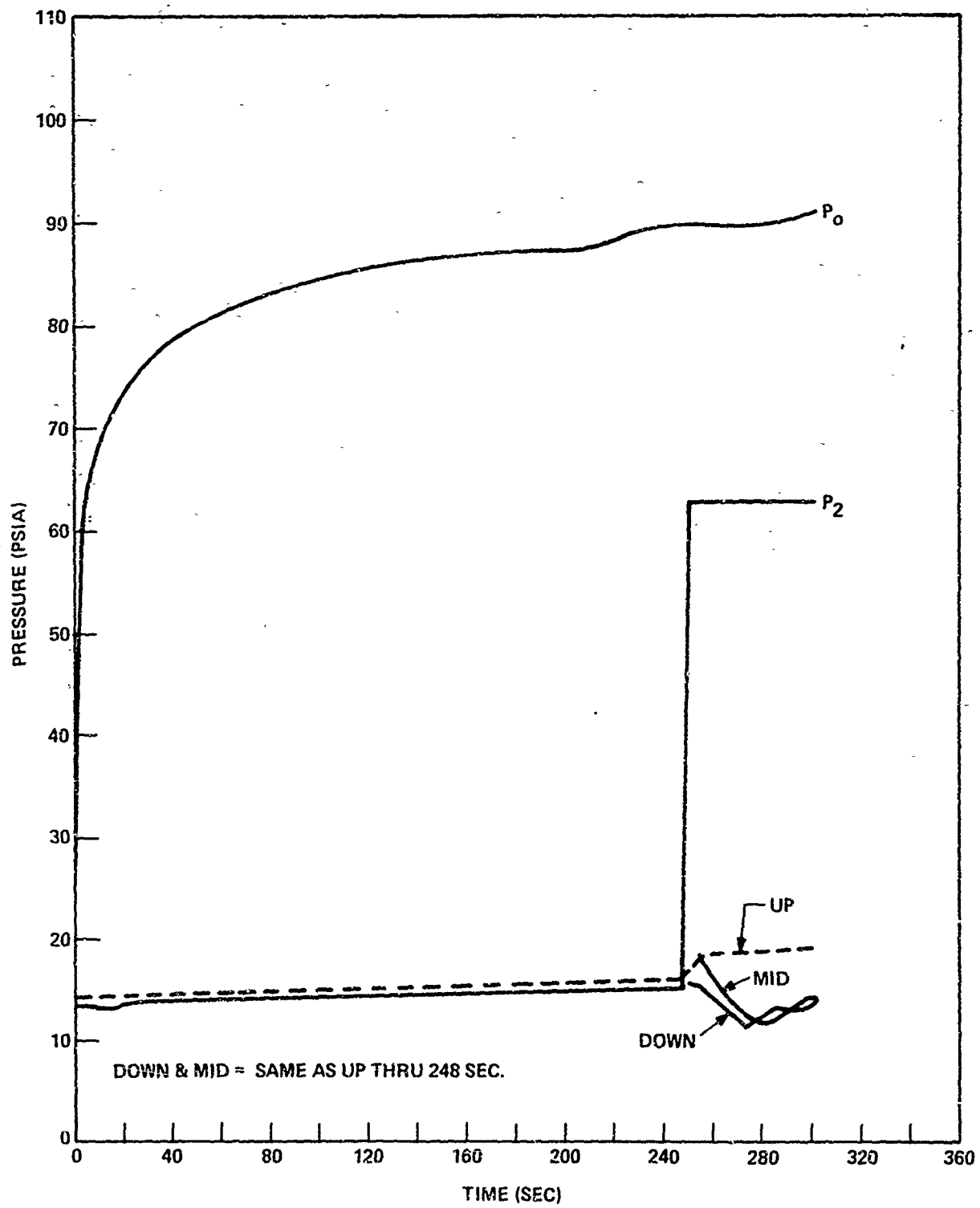


Figure 67. Pressures - Carbon Phenolic A1-2

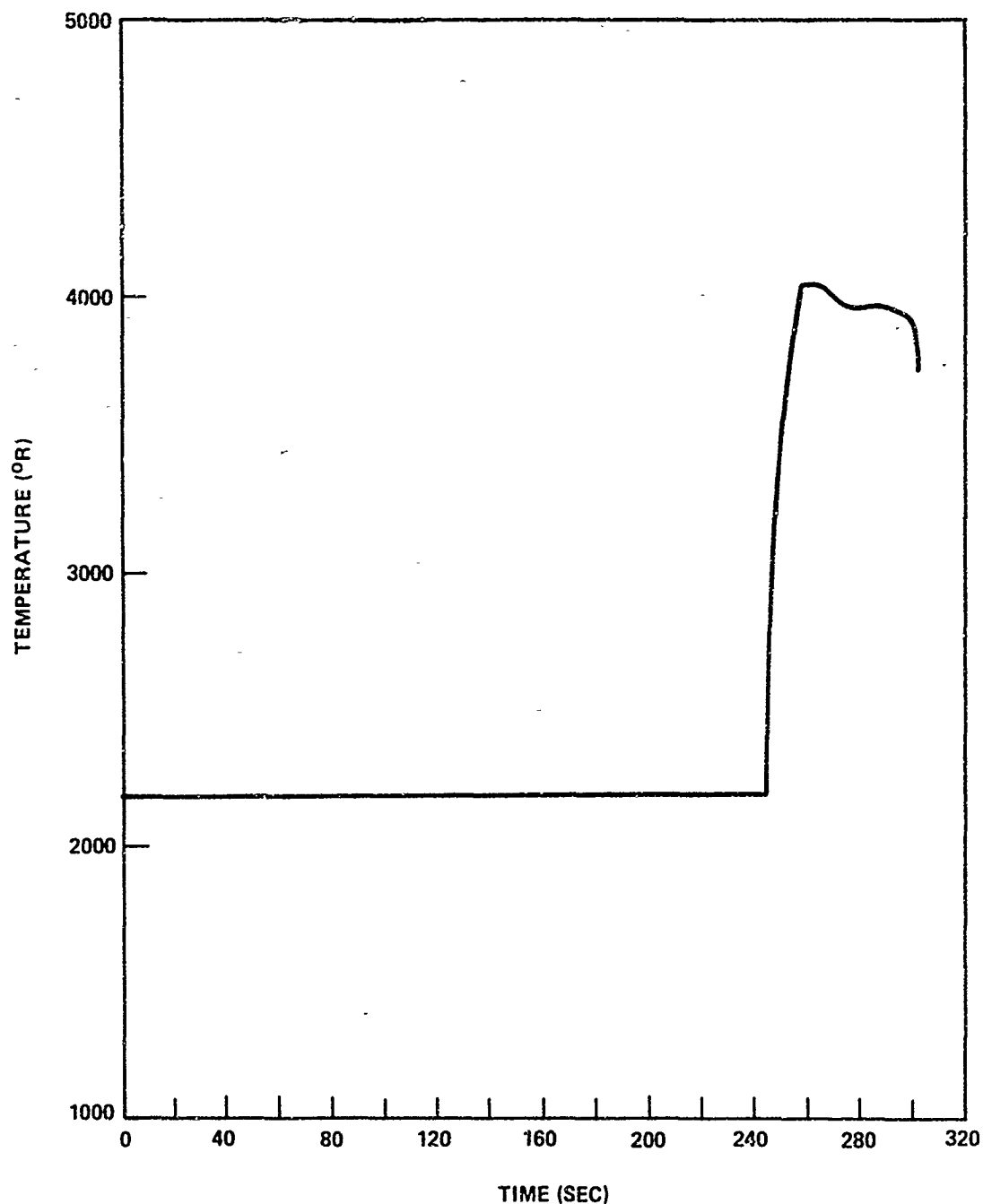


Figure 68. Surface Temperatures - Carbon Phenolic A1-2

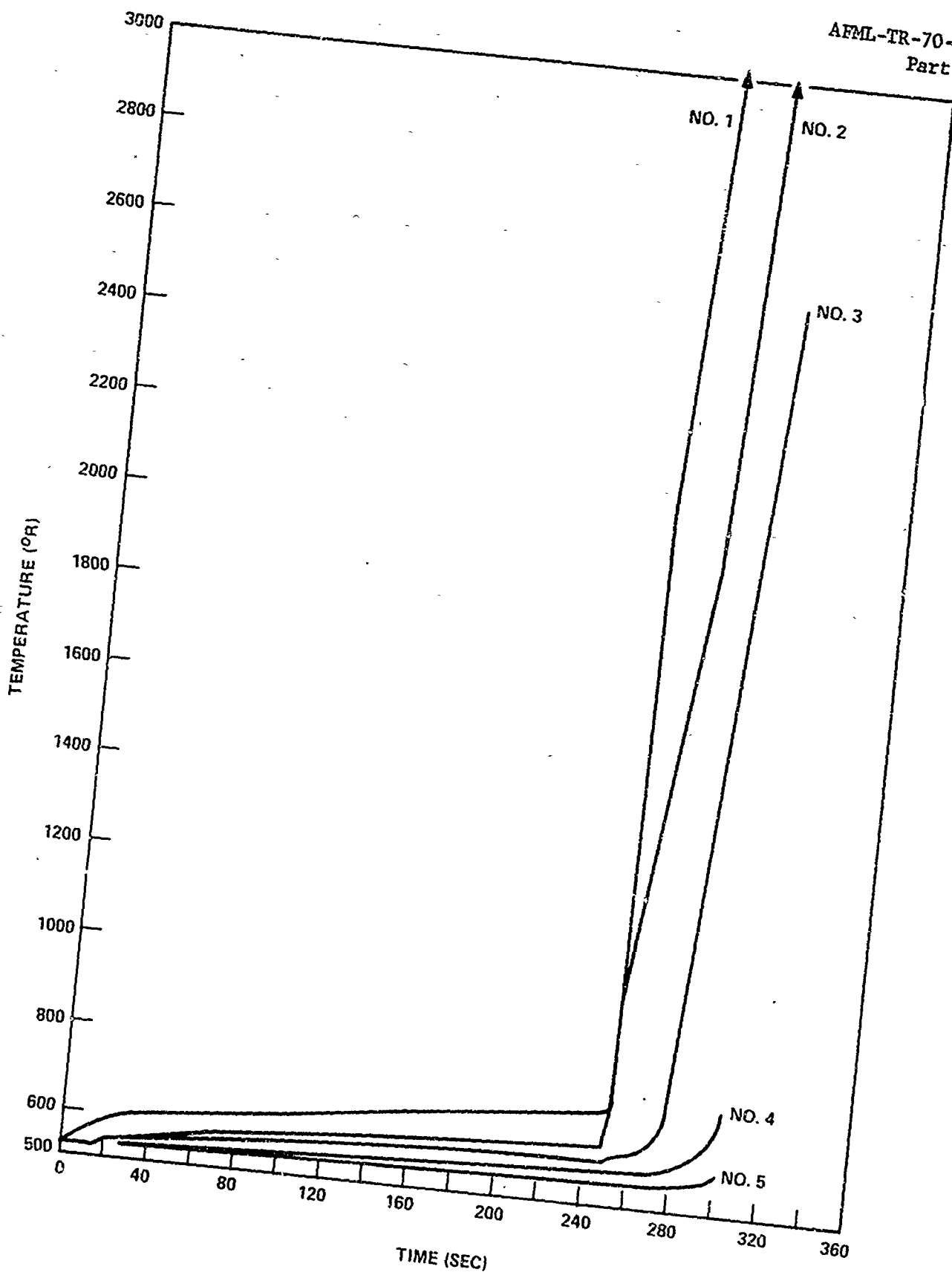


Figure 69. Internal Temperatures - Carbon Phenolic A1-2

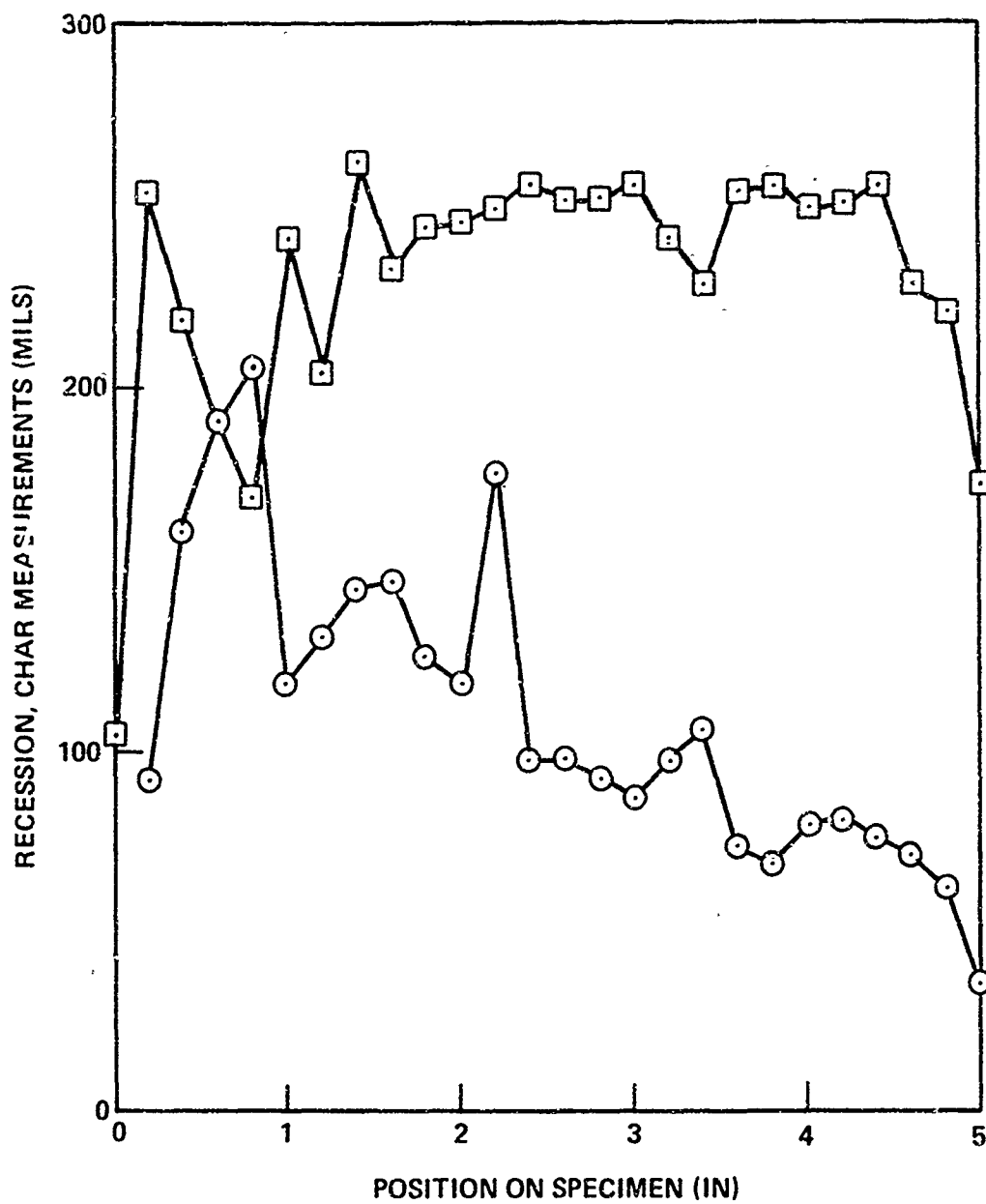


Figure 70. Char Measurements - Carbon Phenolic A1-2



Figure 71. Silica Phenolic — Post Test A2-1

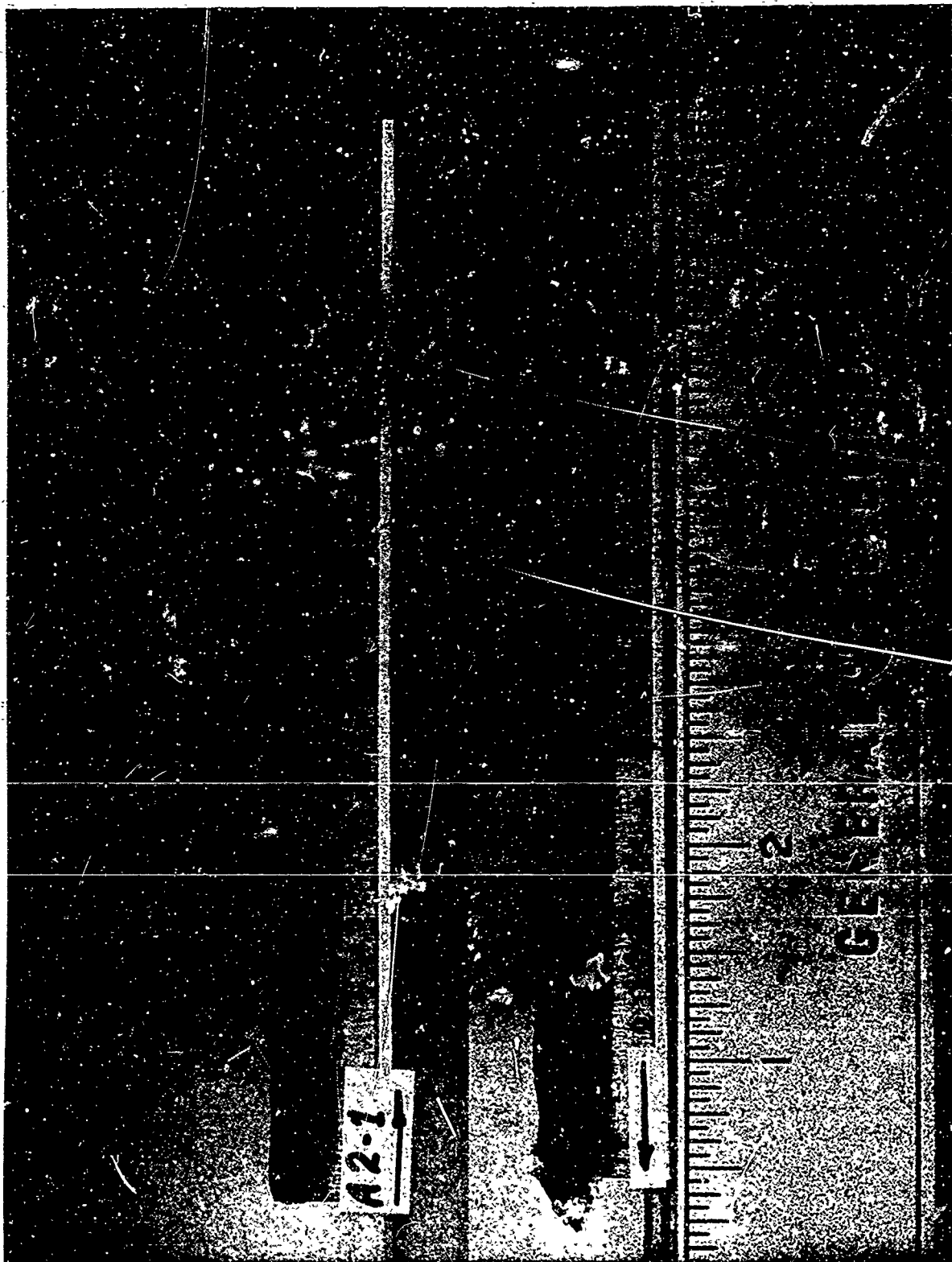


Figure 72. Silica Phenolic — Post Test A2-1 (Sectioned)

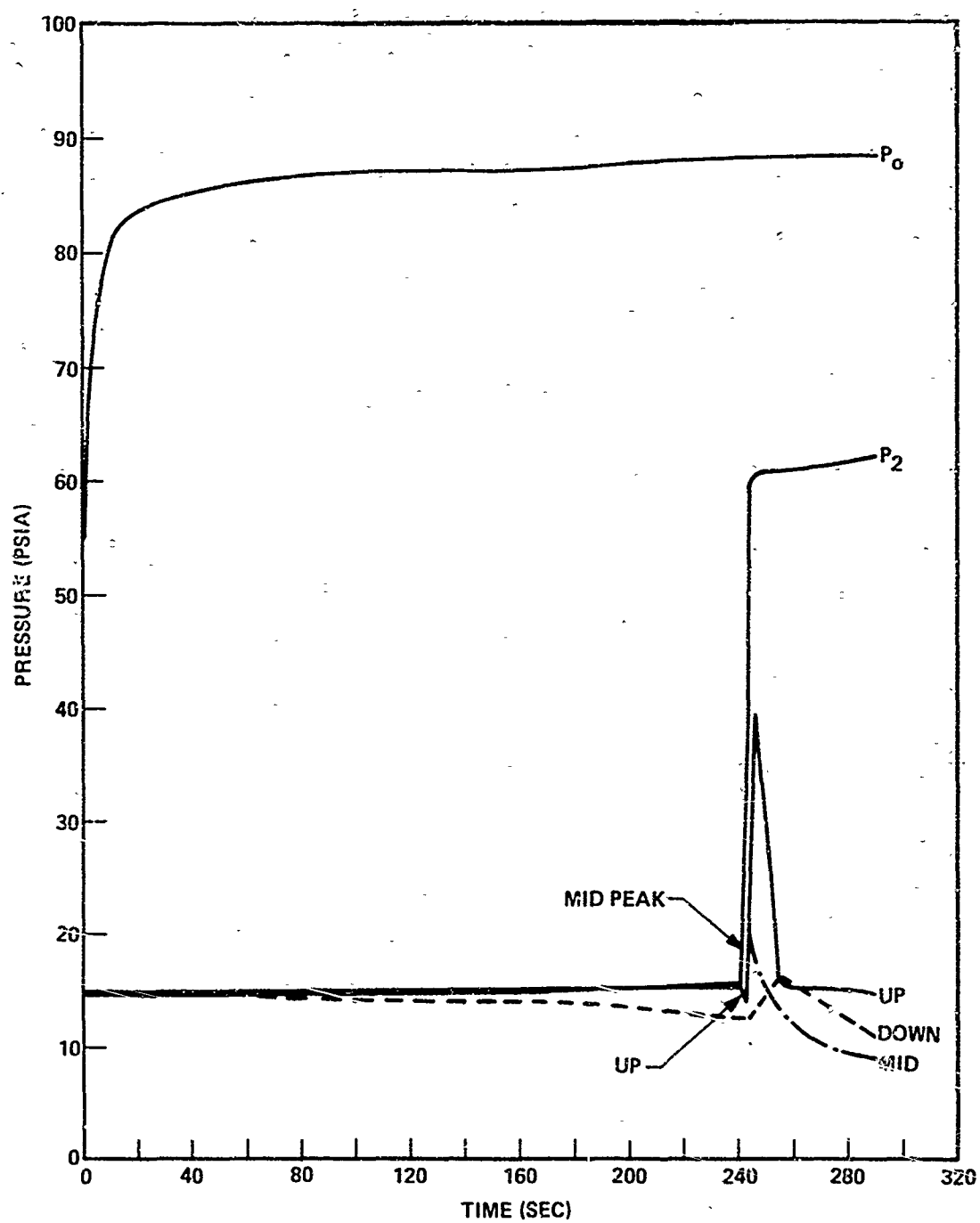


Figure 73. Pressures - Silica Phenolic A2-1

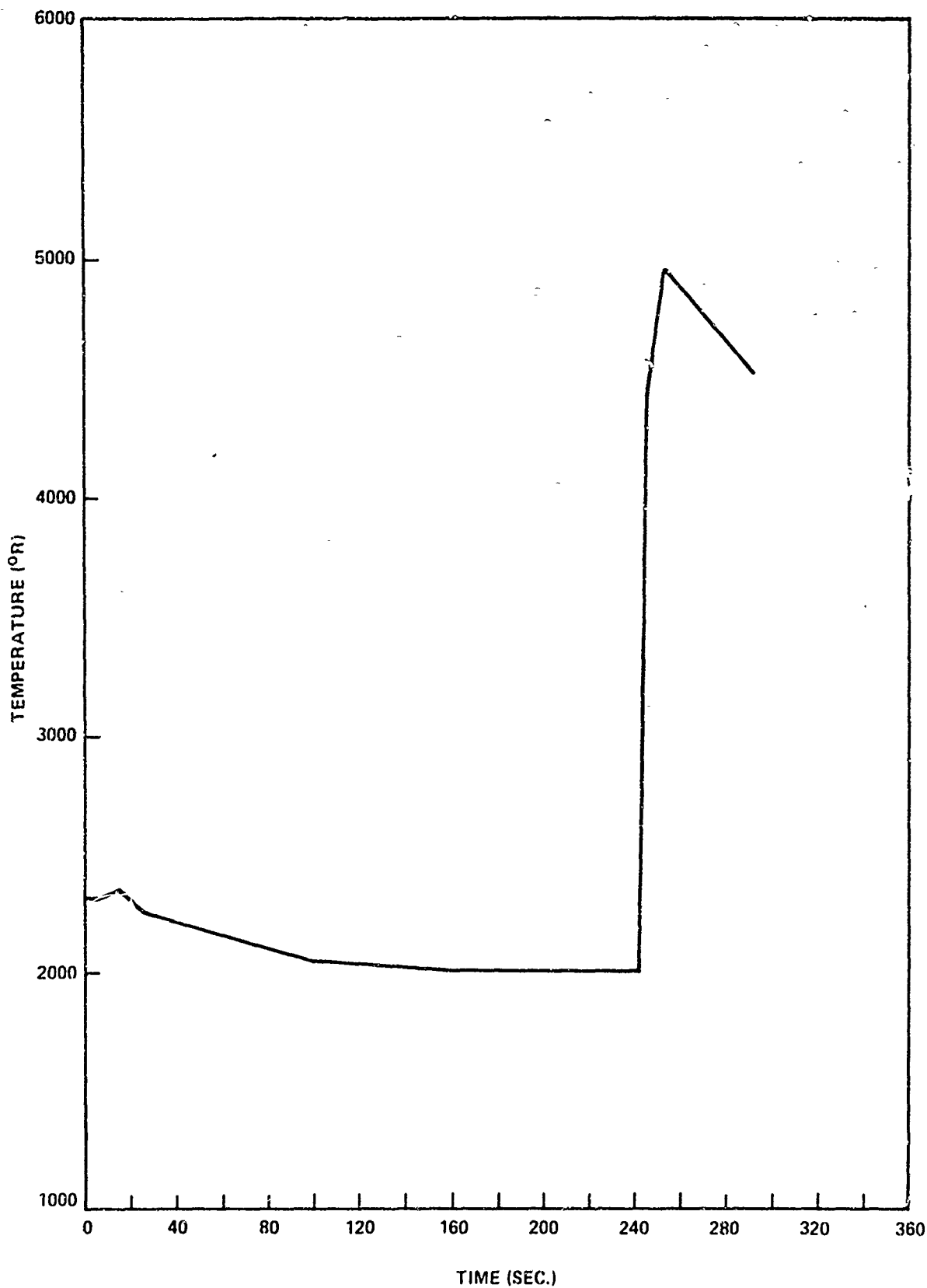


Figure 74. Surface Temperatures - Silica Phenolic A2-1

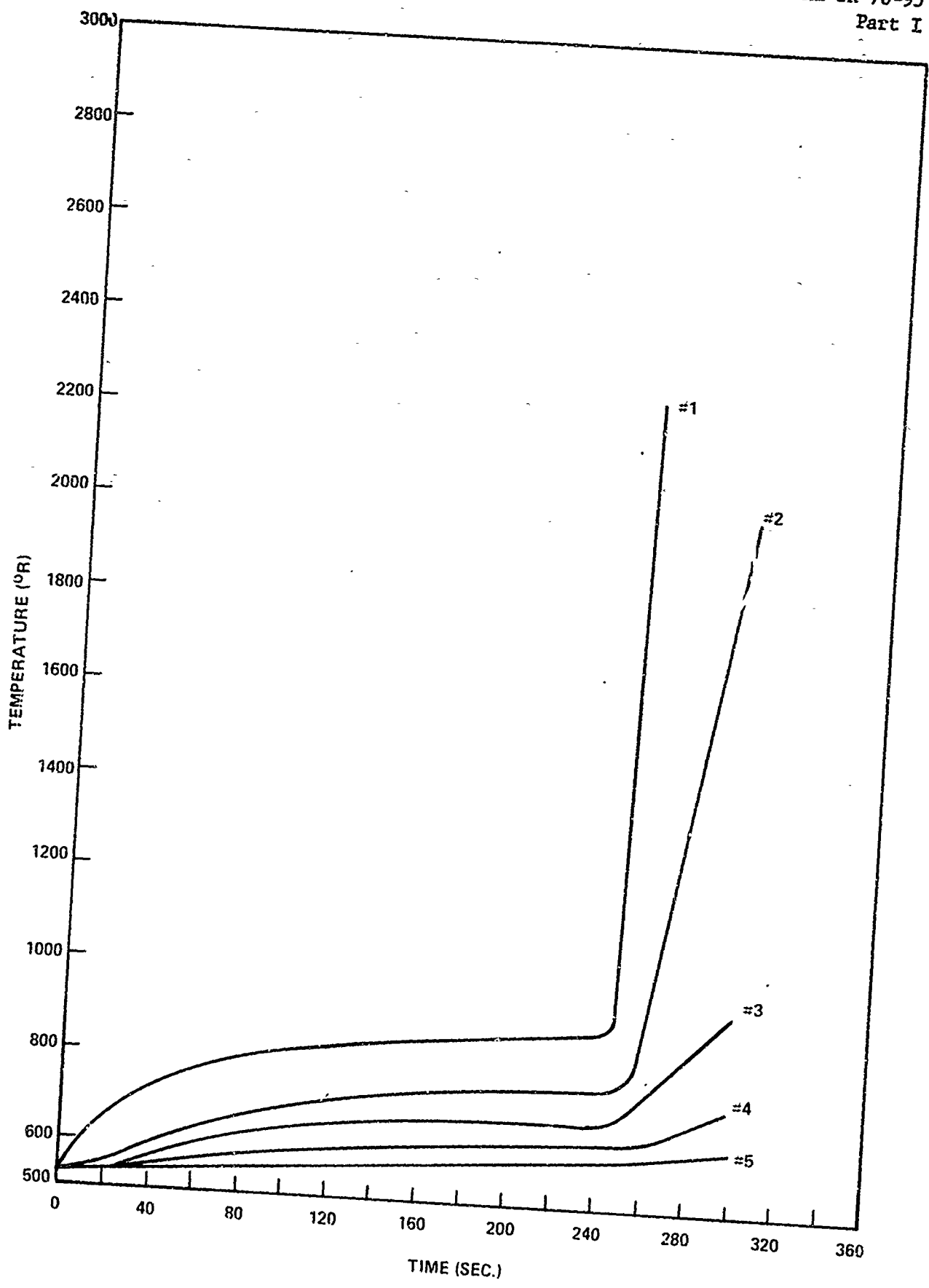


Figure 75. Internal Temperatures - Silica Phenolic A2-1

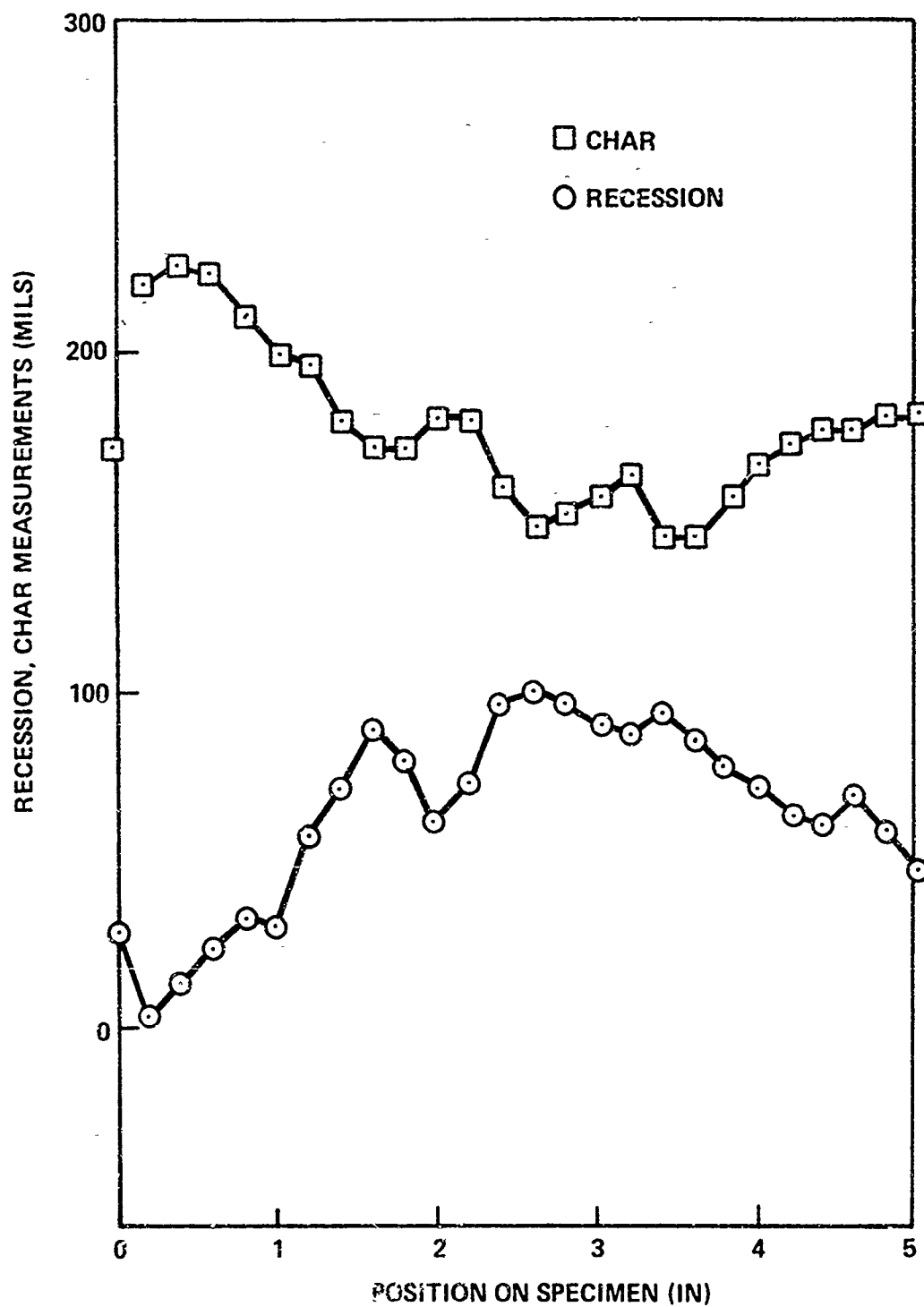


Figure 76. Char Measurements — Silica Phenolic A2-1



Figure 77. Carbon Polyimide Post Test A4-2A

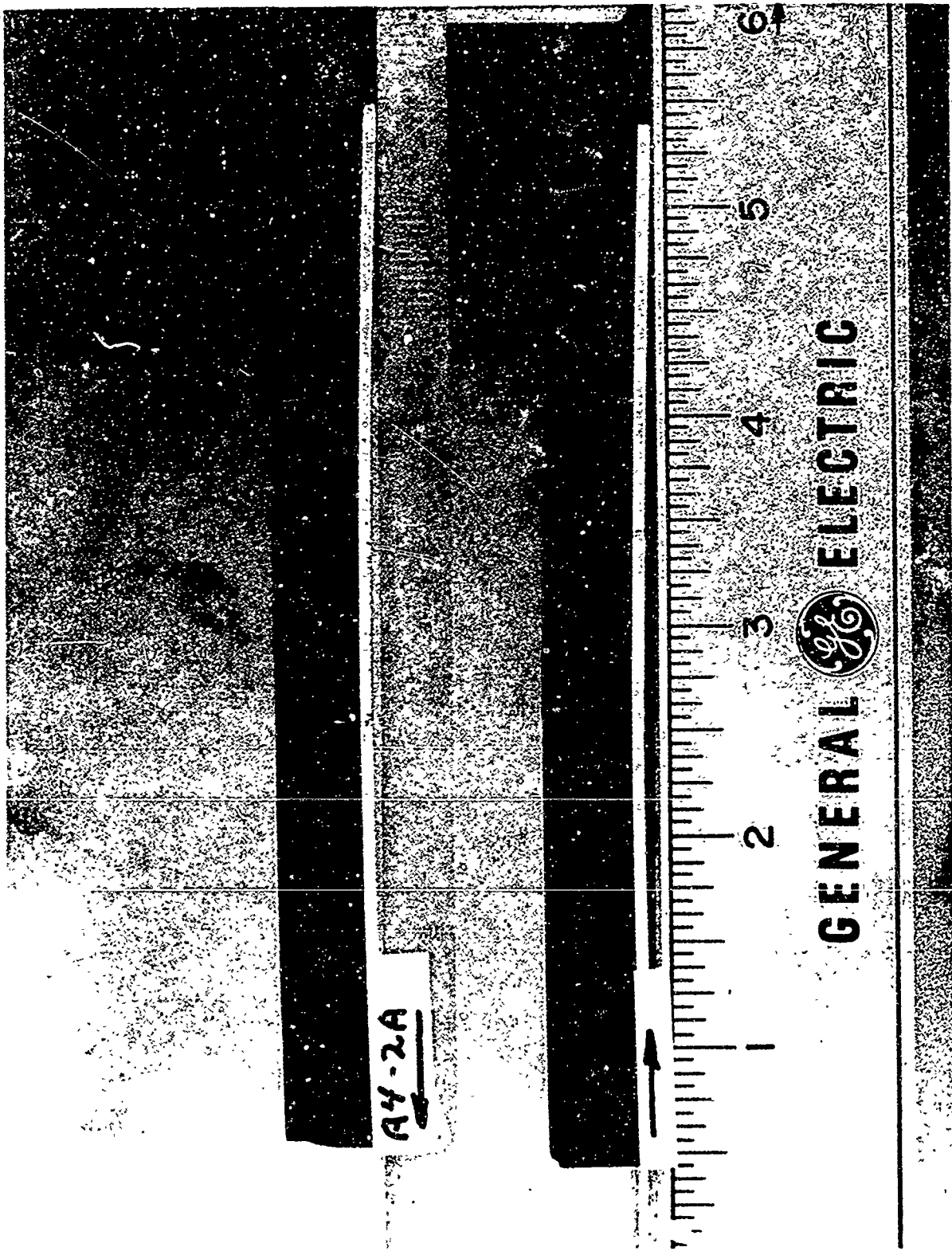


Figure 78. Carbon Polyimide – Post Test A4-2A (Sectioned)

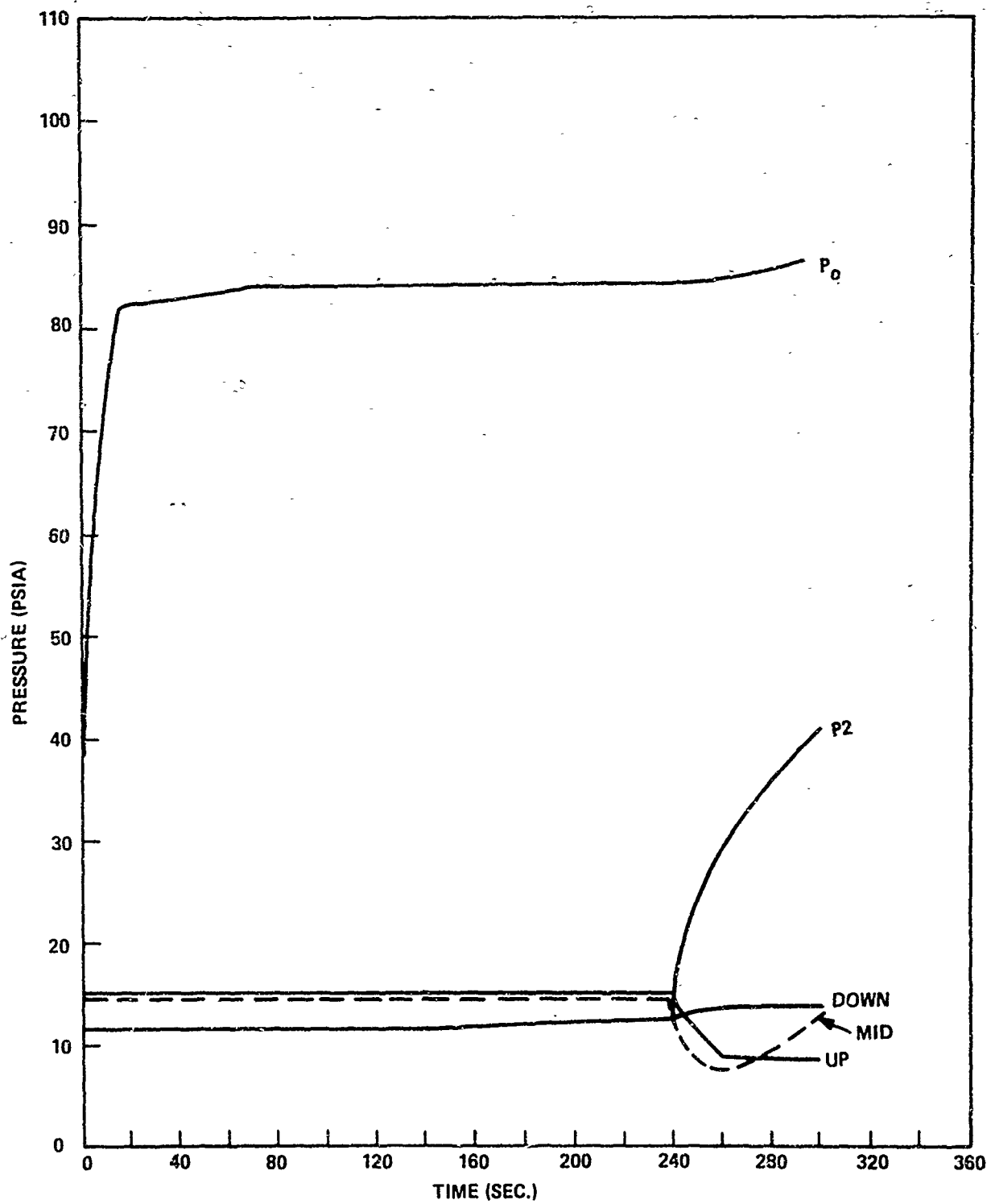


Figure 79. Pressures - Carbon Polyimide A4-2A

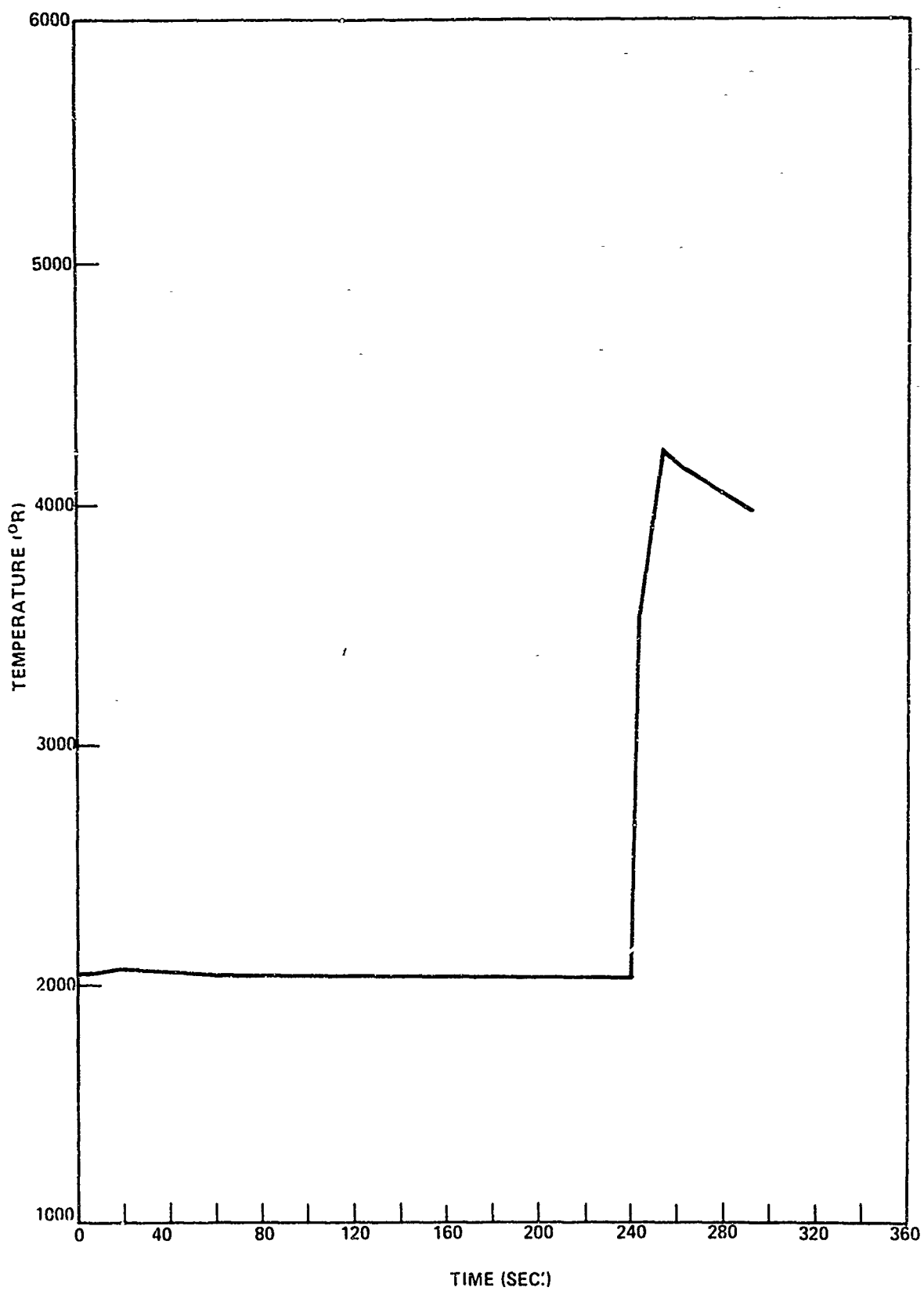


Figure 80. Surface Temperatures - Carbon Polyimide A4-2A

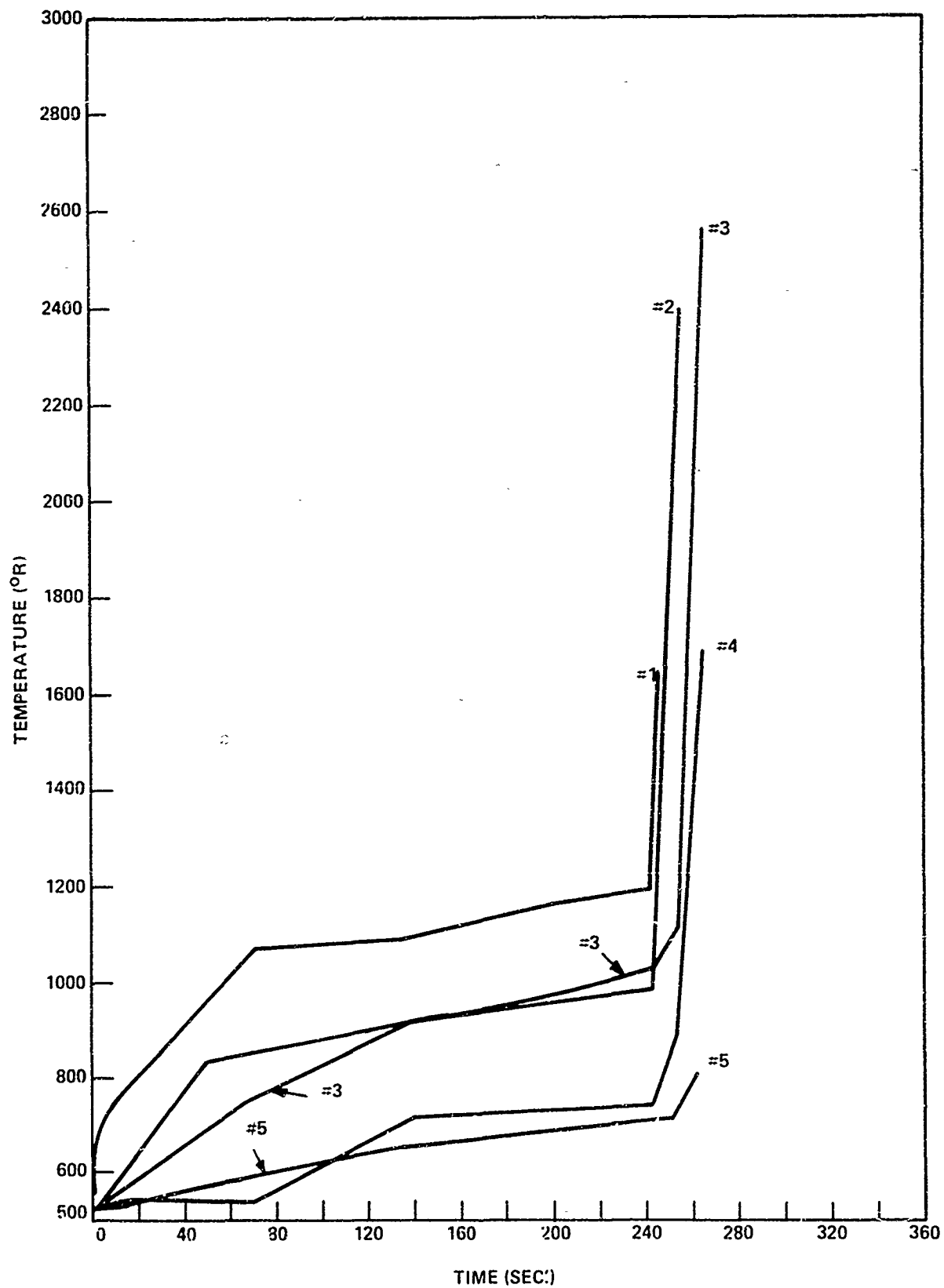


Figure 81. Internal Temperatures - Carbon Polyimide A4-2A

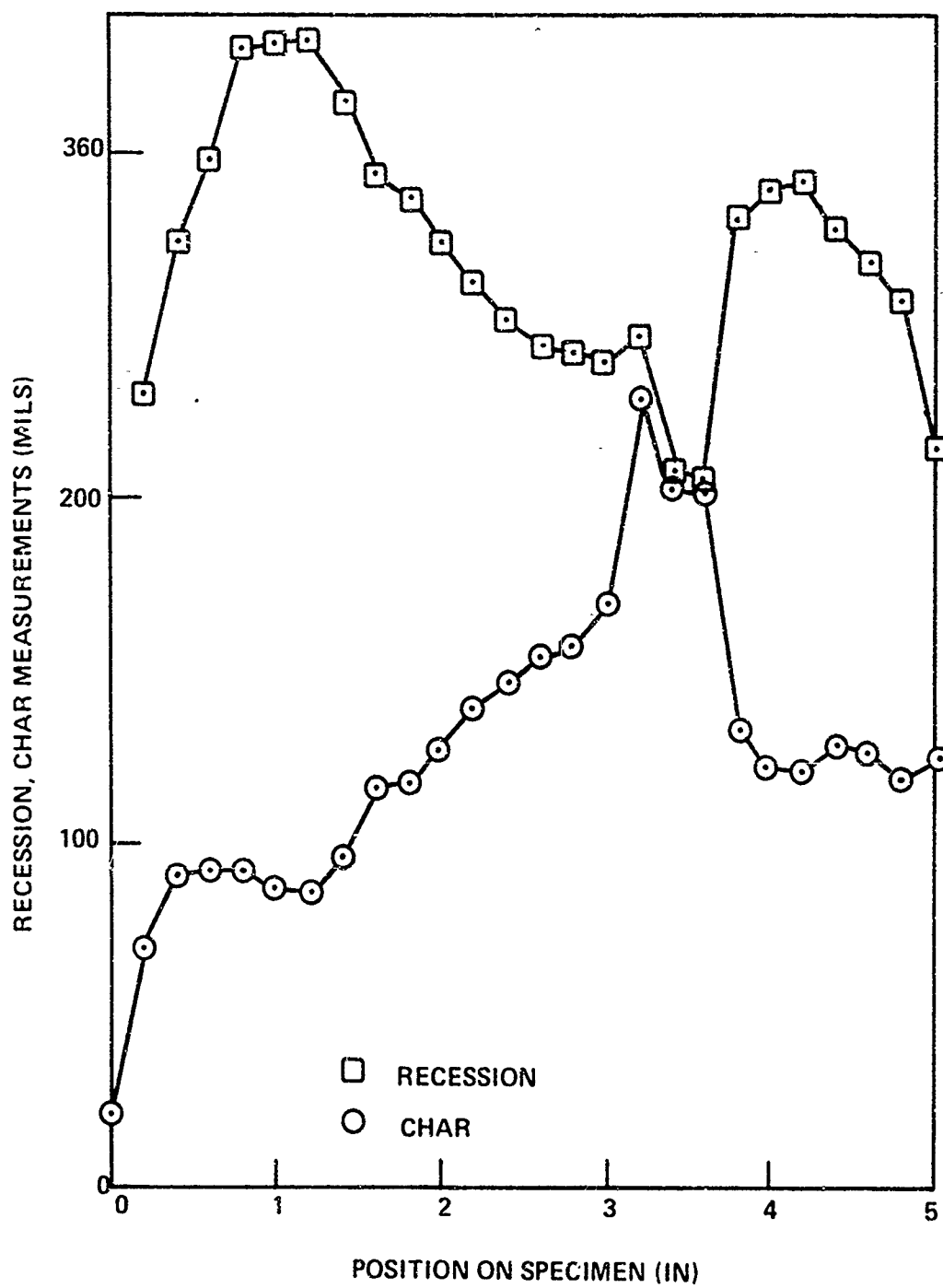


Figure 82. Char Measurements - Carbon Polyimide A4-2A

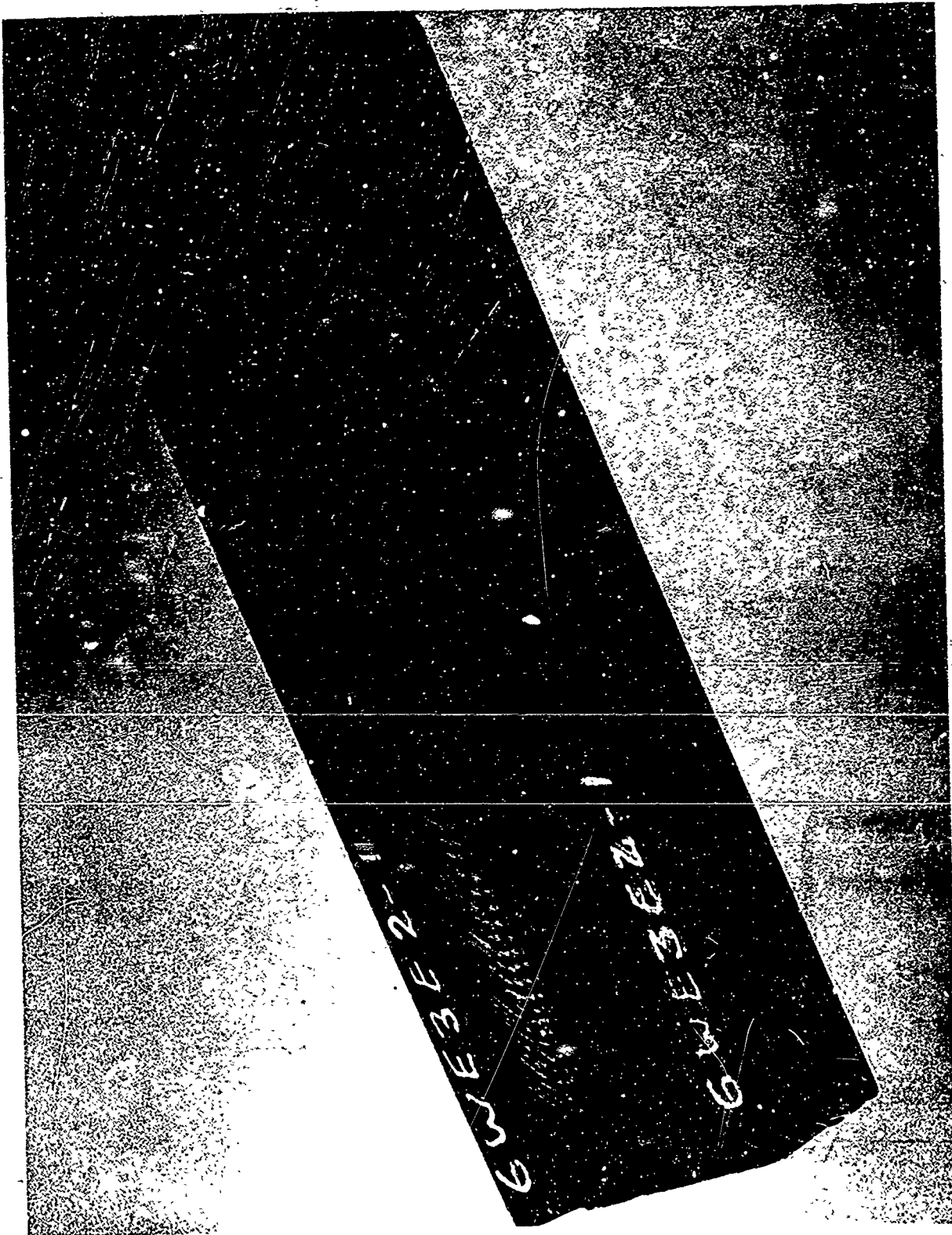


Figure 83. Carbon Phenolic — Post Test C1-1

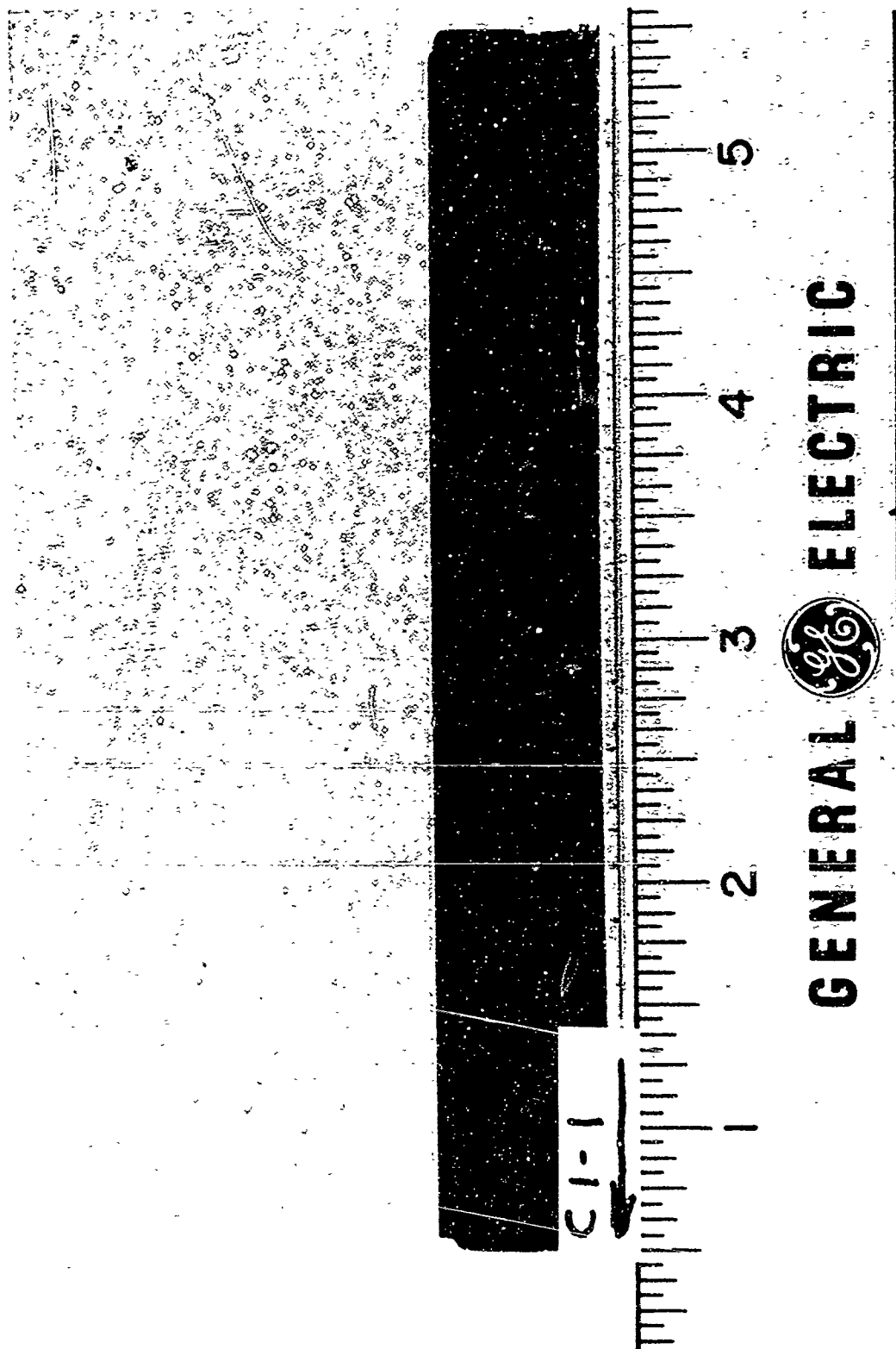


Figure 84. Carbon Phenolic-Post C1-1 (Sectioned)

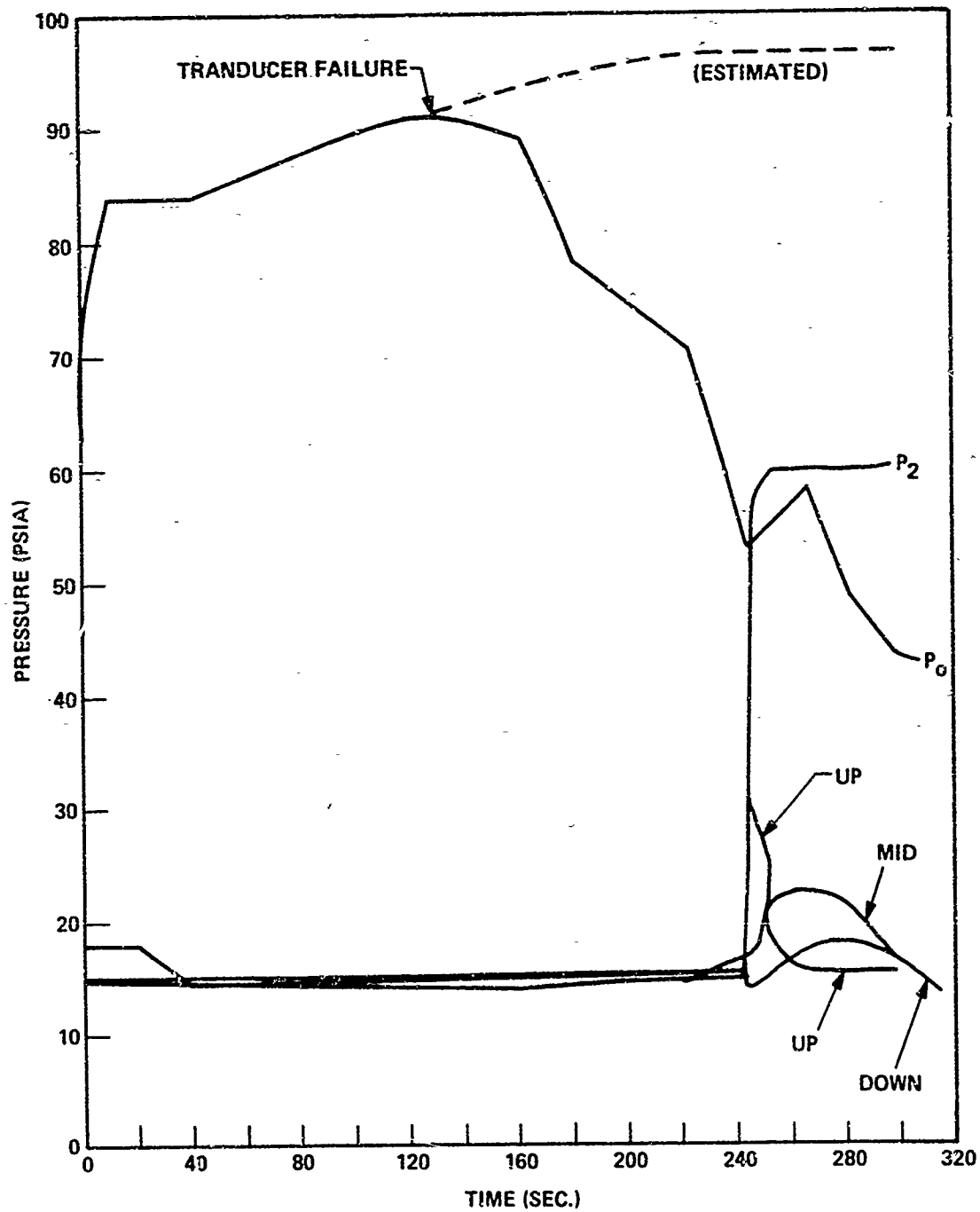


Figure 85. Pressures - Carbon Phenolic C1-1

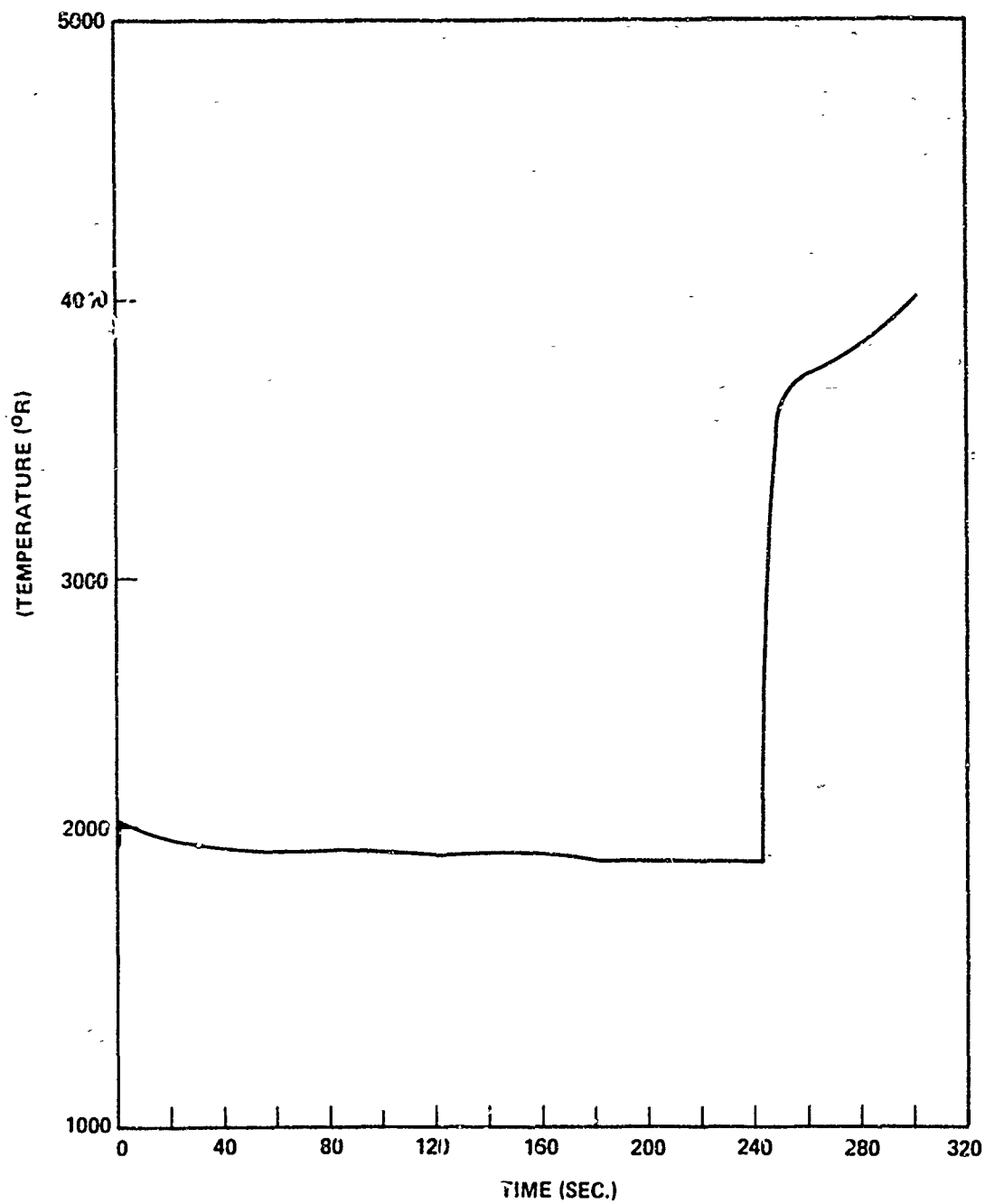


Figure 86. Surface Temperature -- Carbon Phenolic C1-1

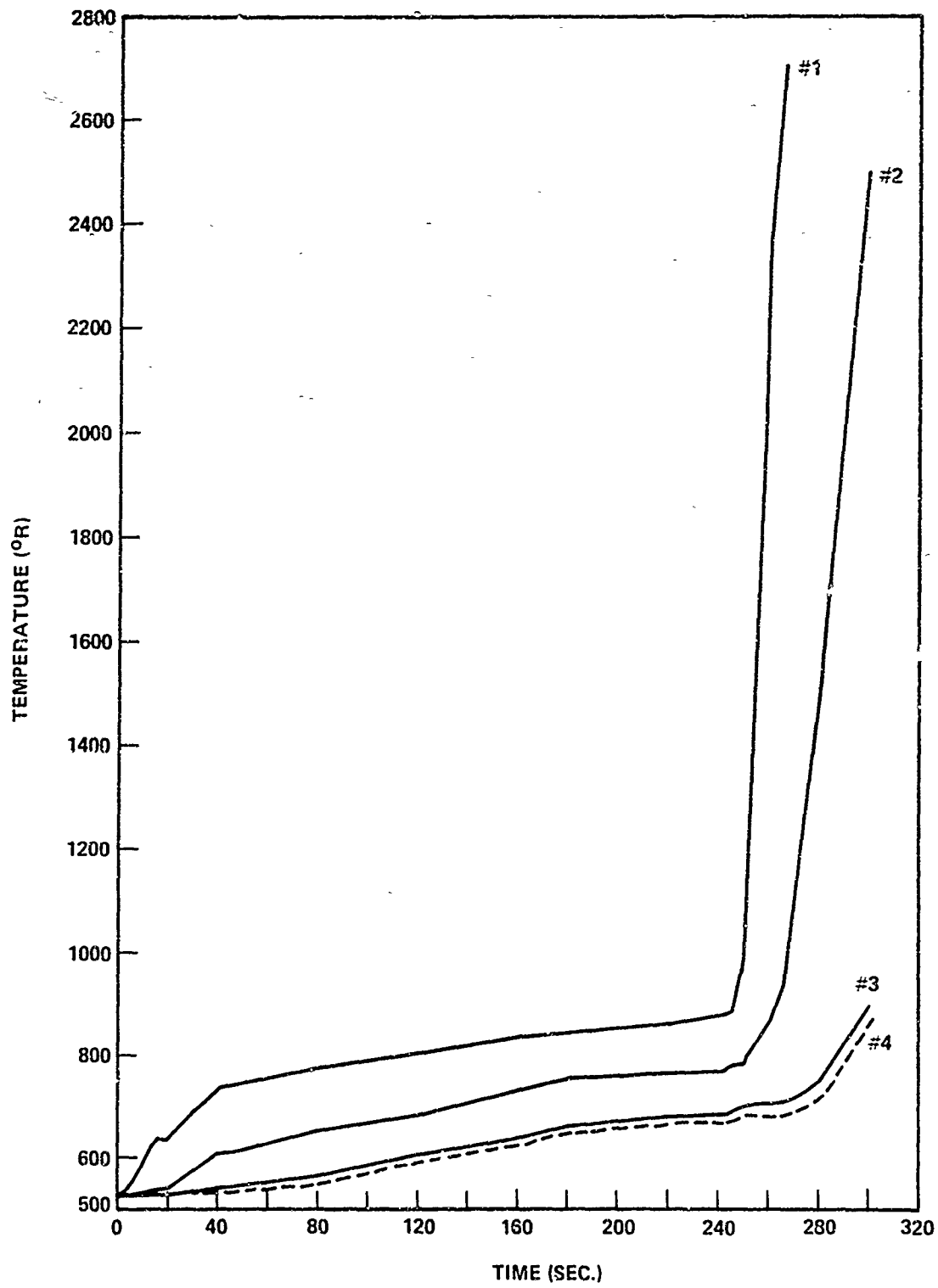


Figure 87. Internal Temperatures – Carbon Phenolic C1-1

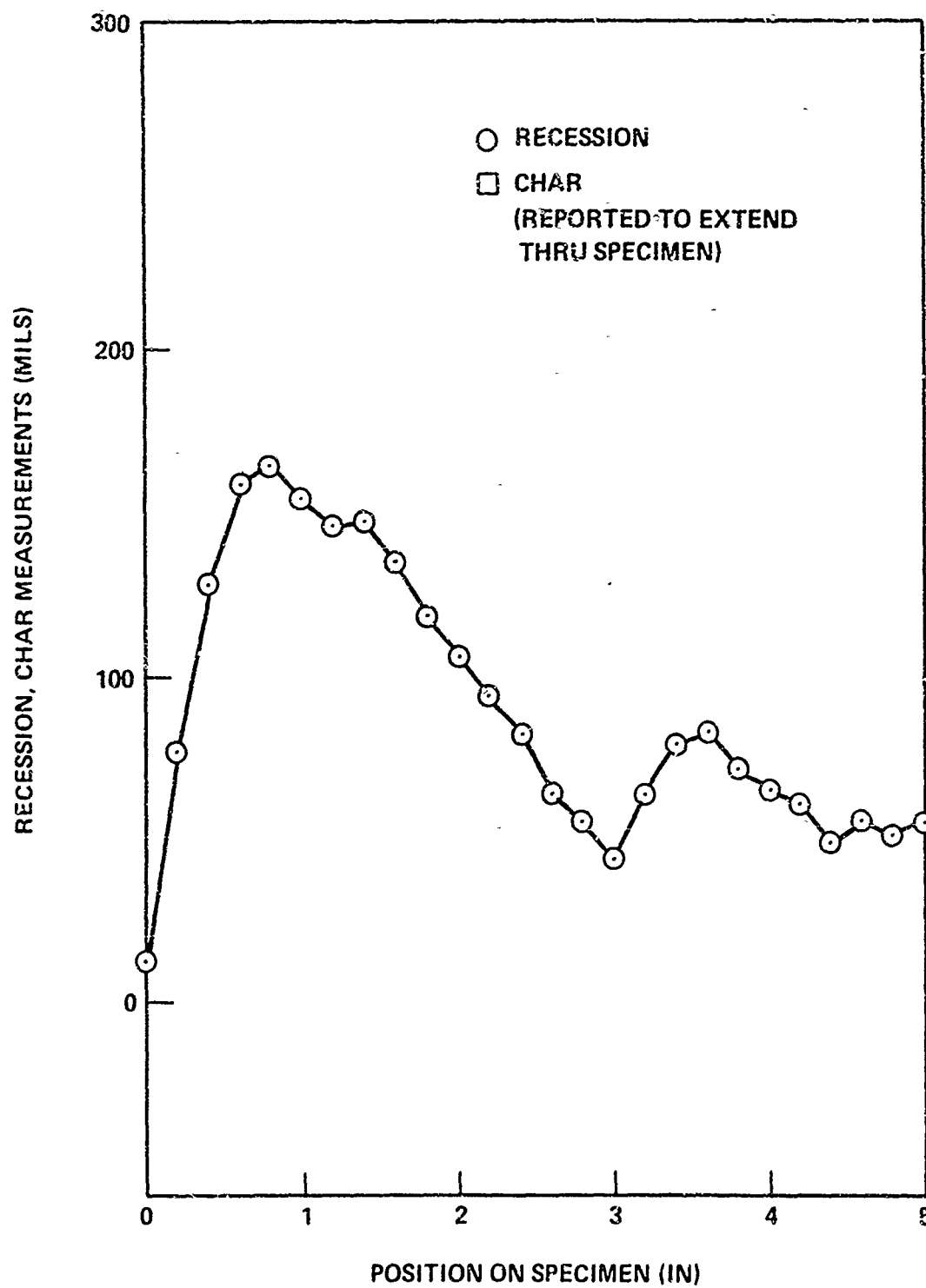


Figure 88. Char Measurements - Carbon Phenolic C1-1

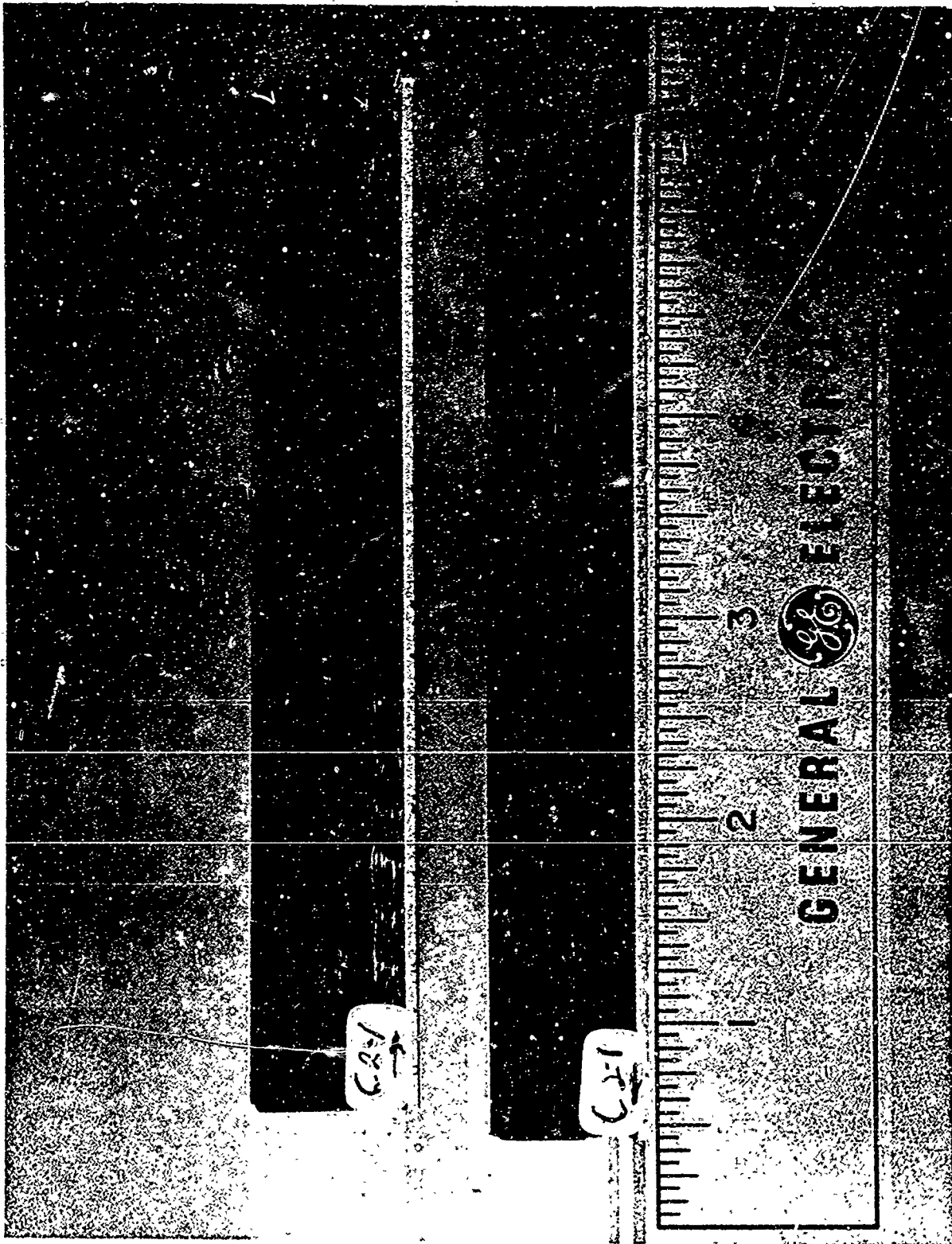


Figure 89. Post Test — Carbon Phenolic — Insulative Layer C2-1 (Sectioned)

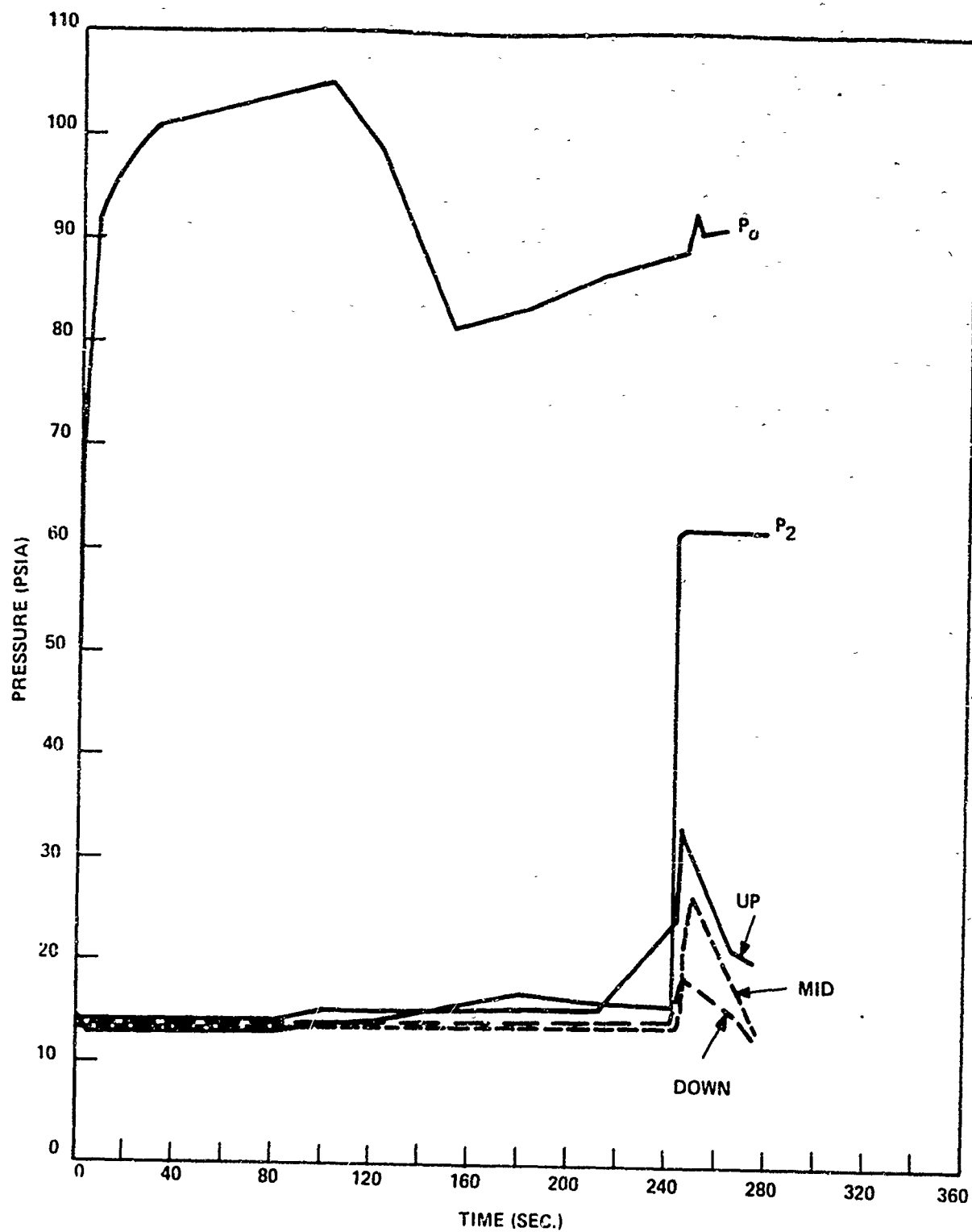


Figure 90. Pressures - Carbon Phenolic - Insulative Layer C2-1

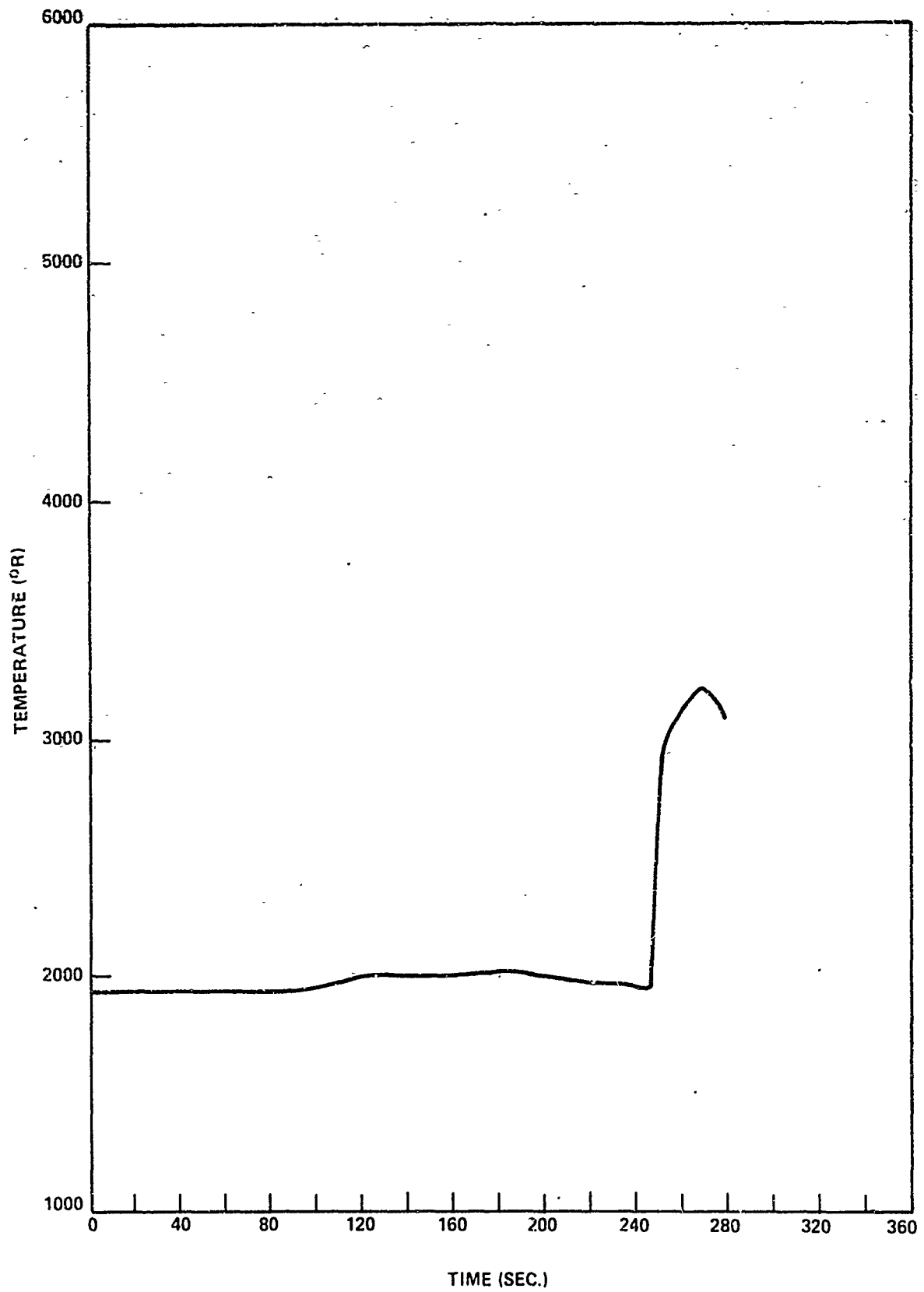


Figure 91. Surface Temperature - Carbon Phenolic - Insulative Layer C2-1

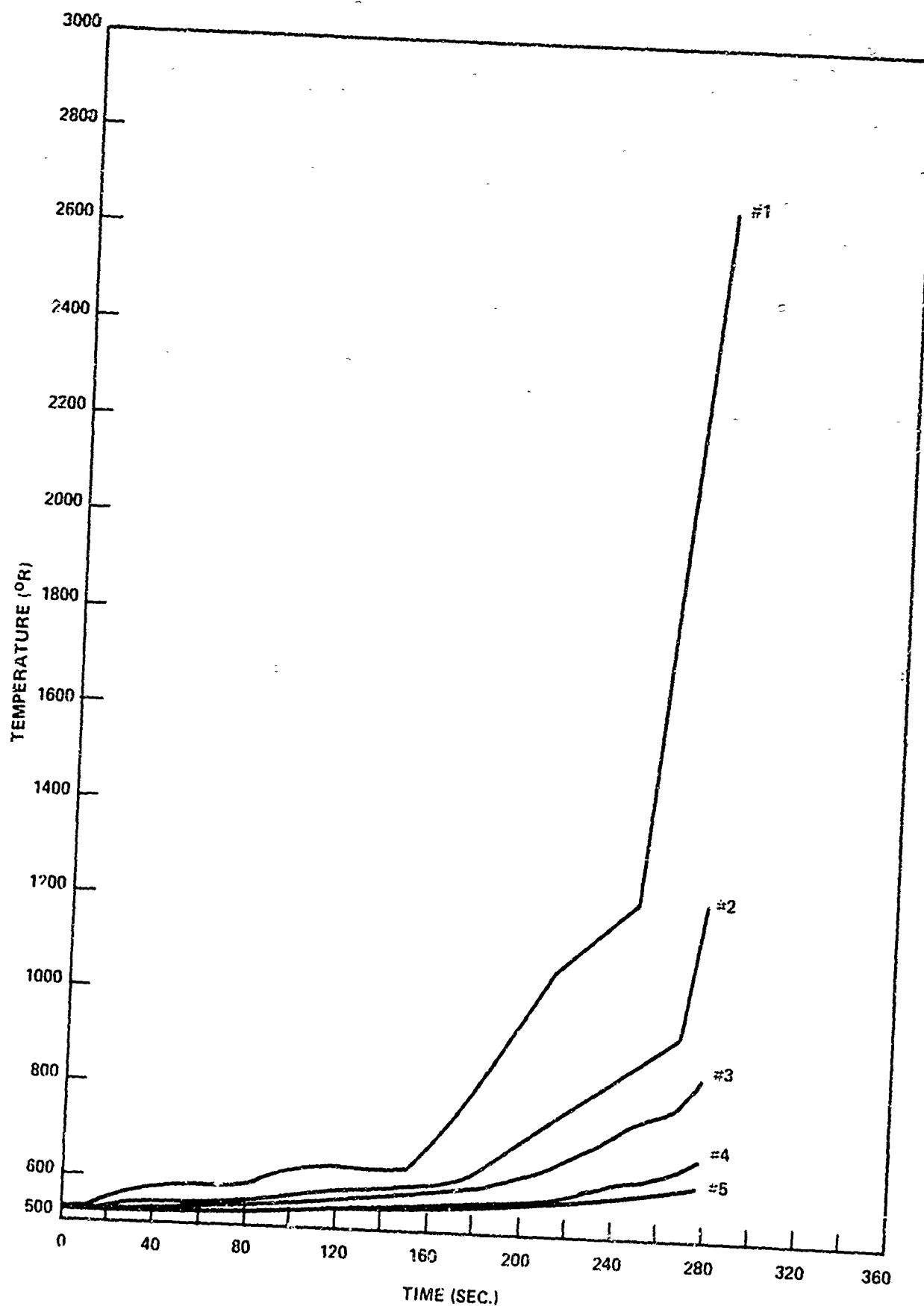


Figure 92. Internal Temperatures - Carbon Phenolic - Insulative Layer C2-1

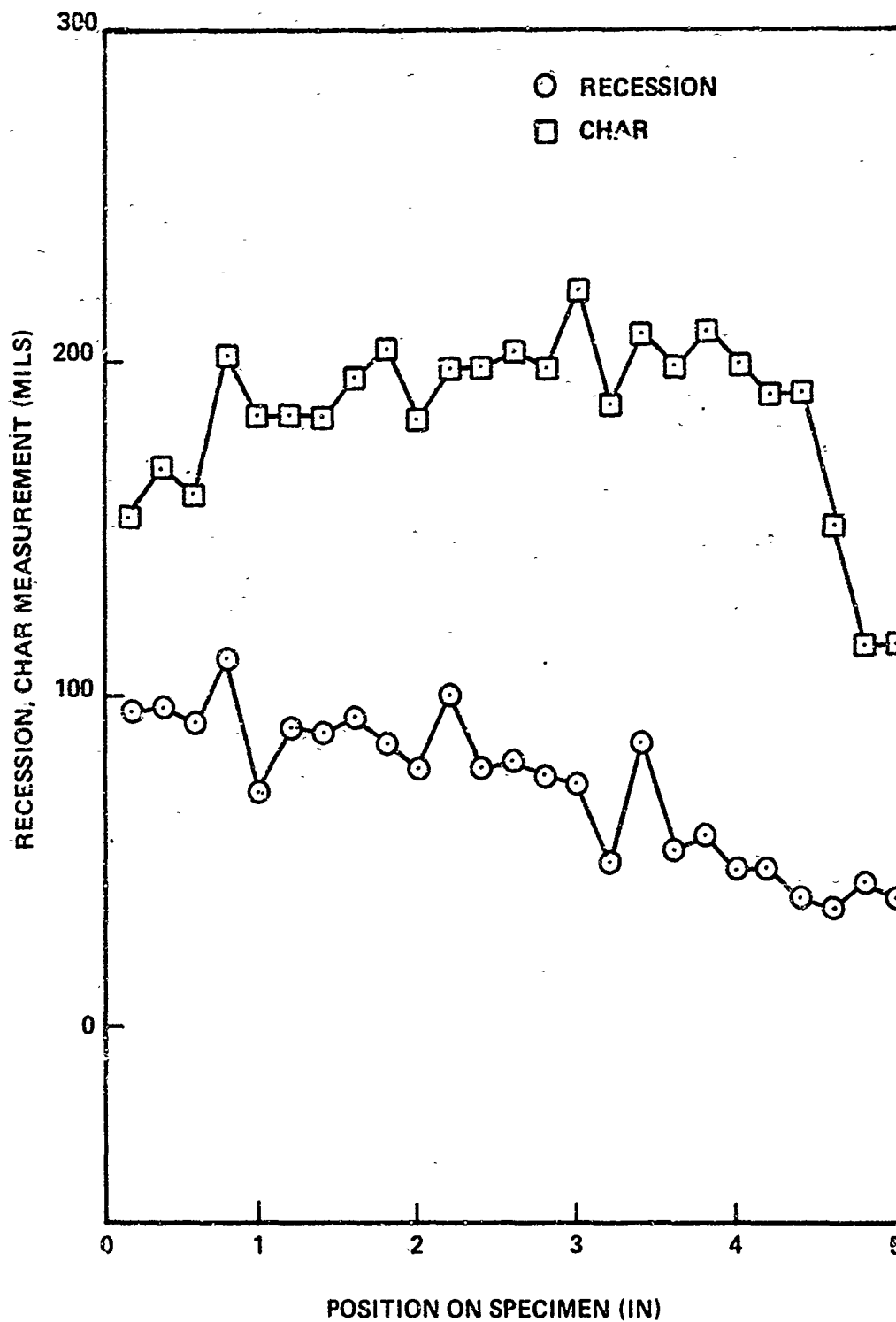


Figure 93. Char Measurements - Carbon Phenolic - Insulative Layer C2-1

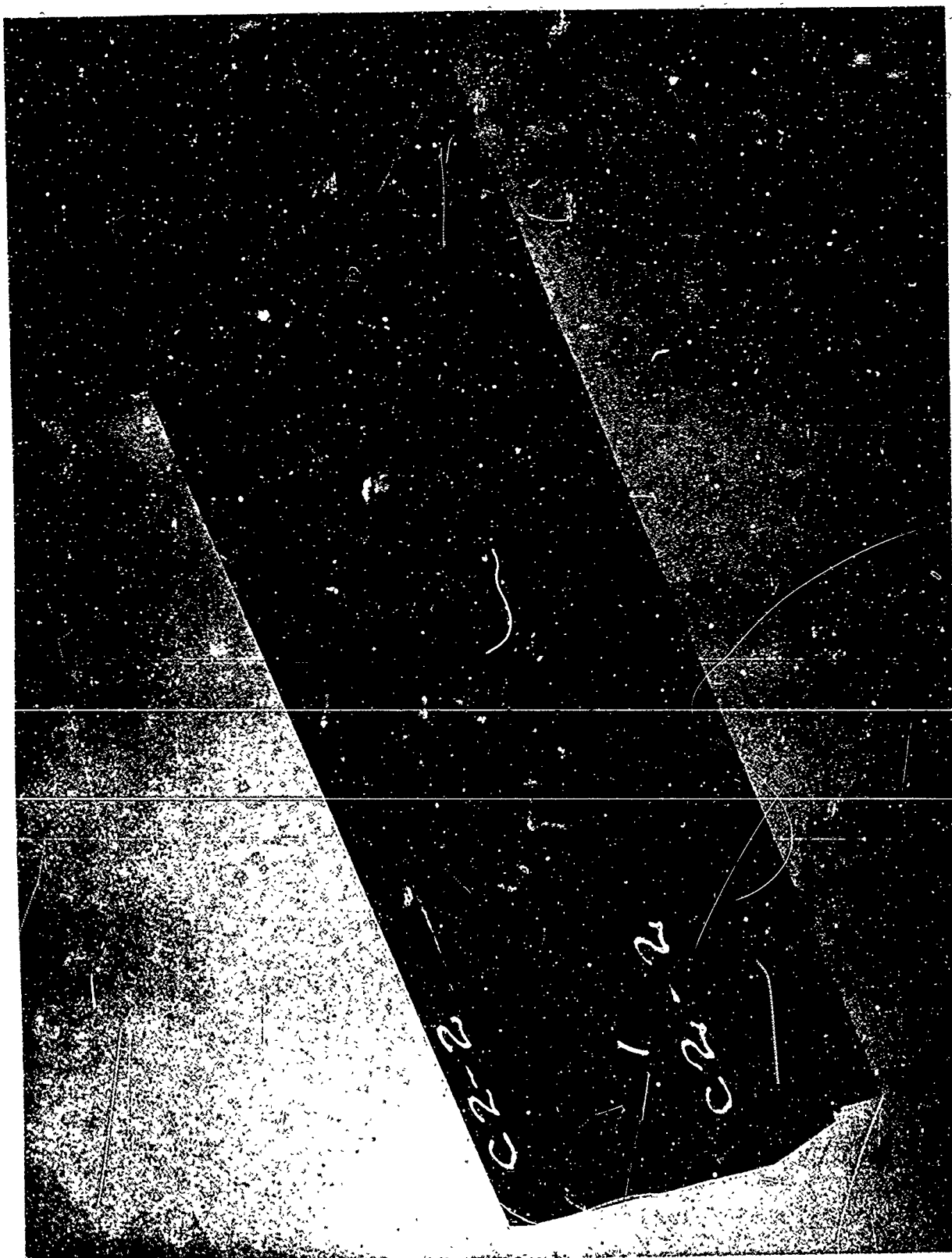


Figure 94. Post Test -- Carbon Phenolic -- Insulative Layer C2-2

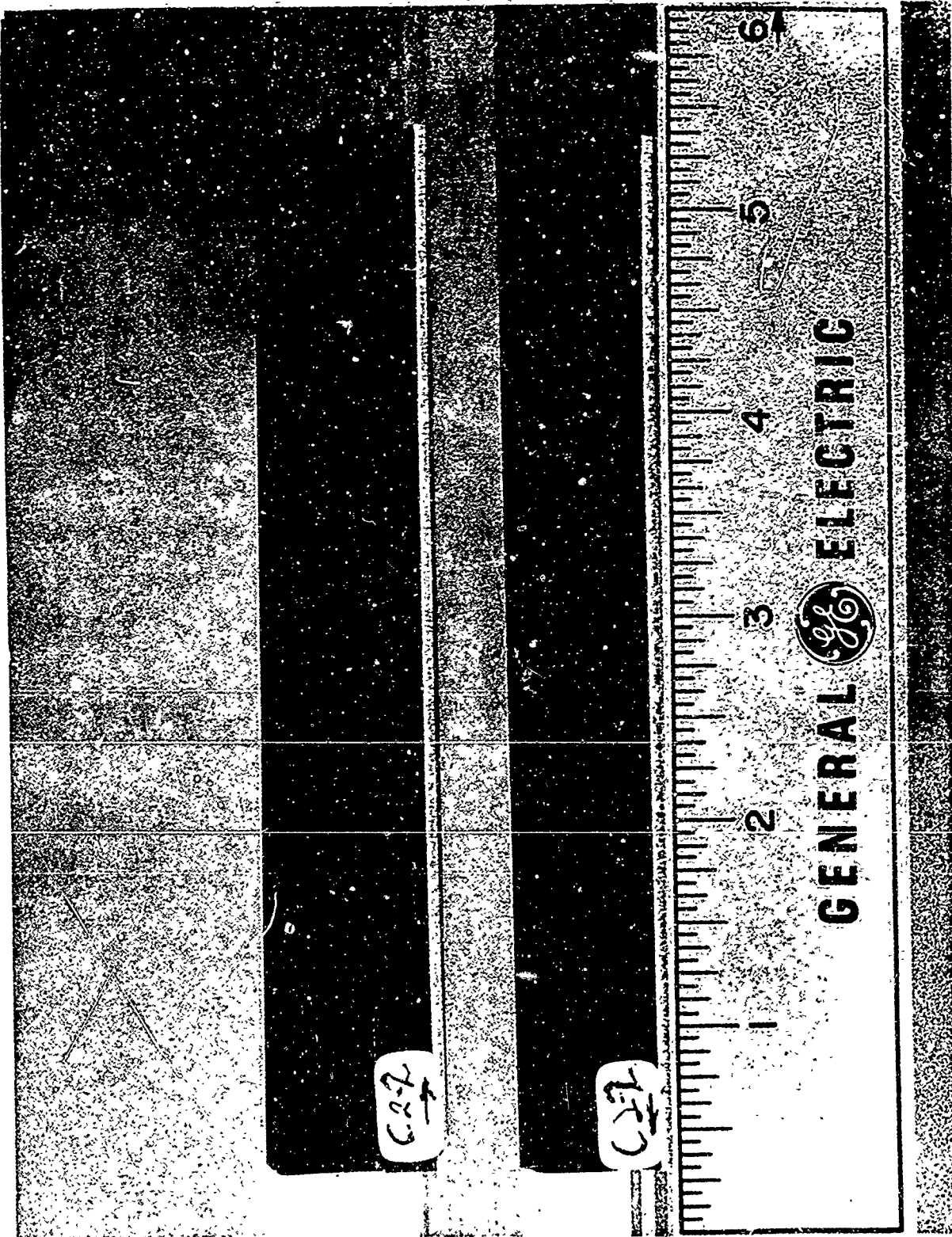


Figure 95. Post Test -- Carbon Phenolic -- Insulative Layer C2-2 (Sectioned)

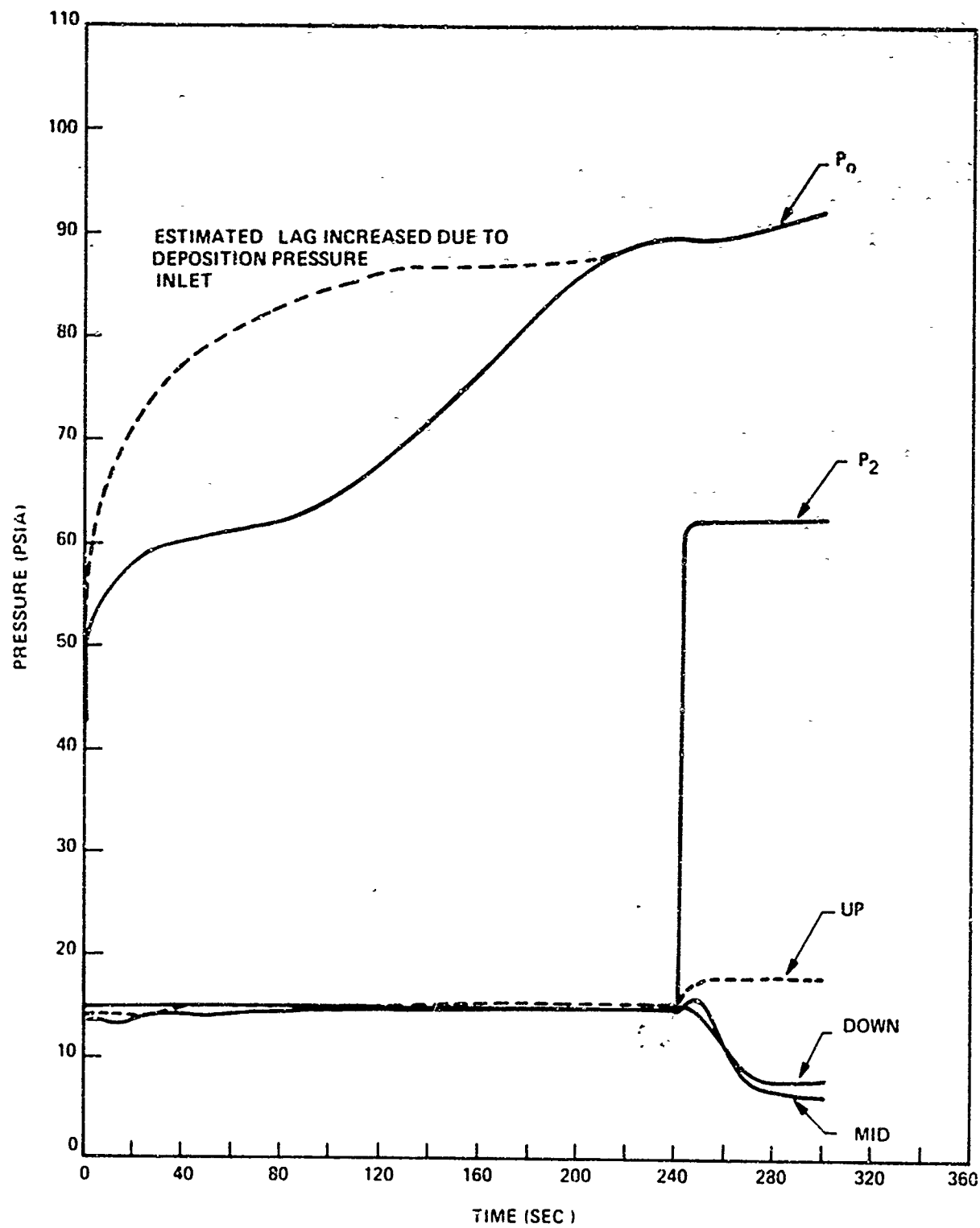


Figure 96 Pressures - Carbon Phenolic - Insulative Layer C2-2

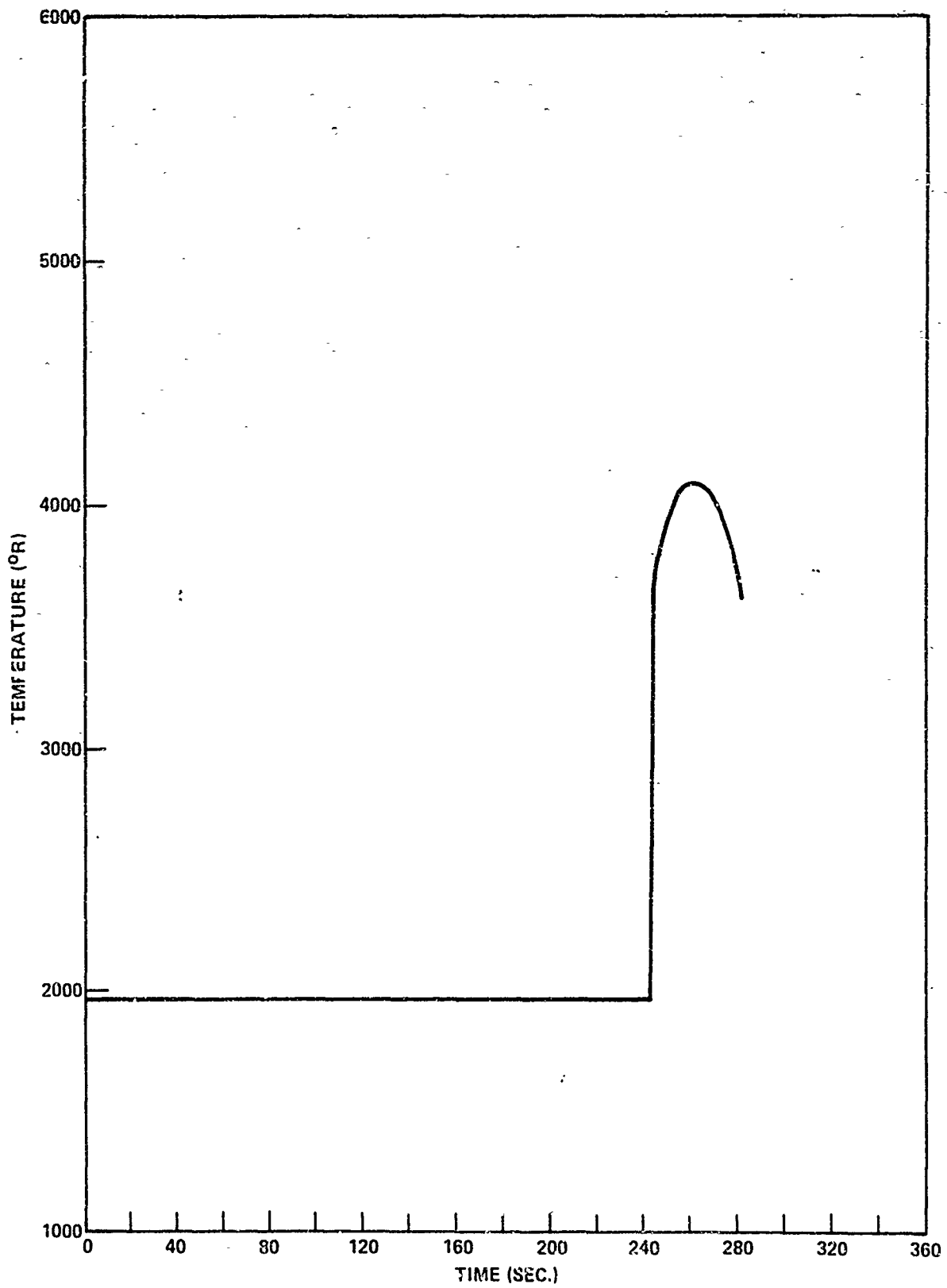


Figure 97. Surface Temperature - Carbon Phenolic - Insulative Layer C2-2

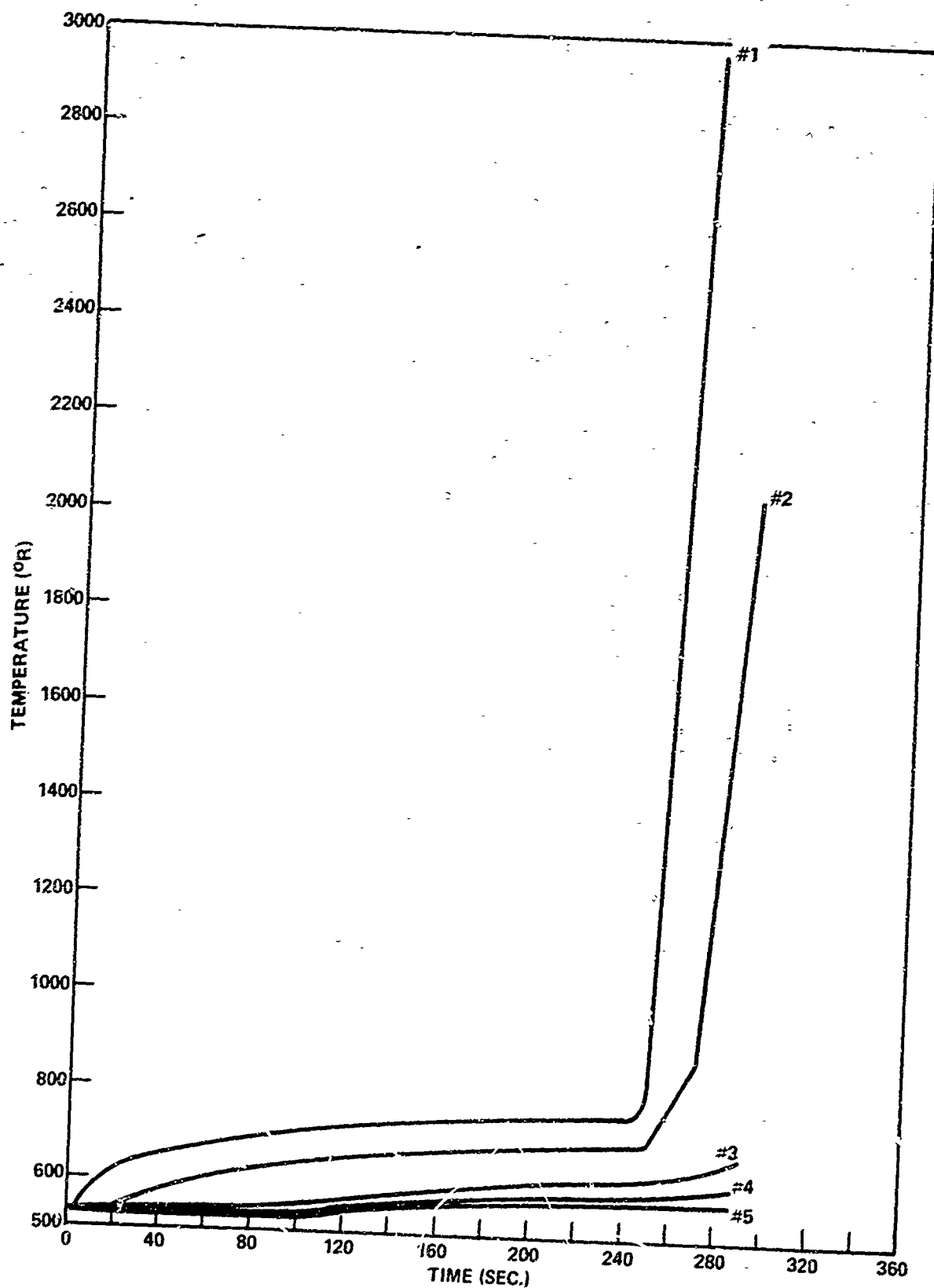


Figure 98. Internal Temperatures - Carbon Phenolic - Insulative Layer C2-2

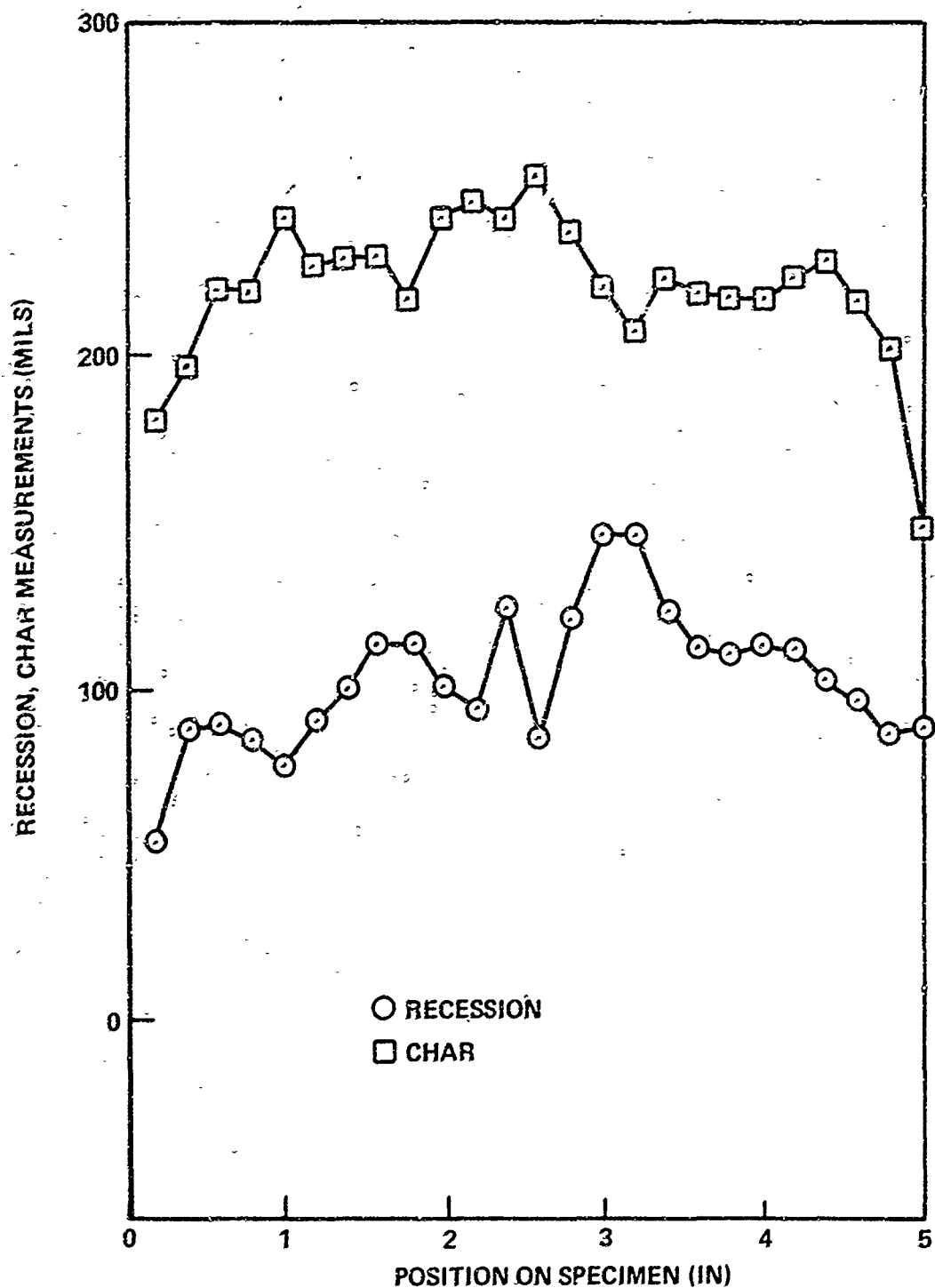


Figure 99. Char Measurements - Carbon Phenolic - Insulative Layer C2-2



Figure 100. Post Test - Silica Phenolic - Insulative Layer C3-1

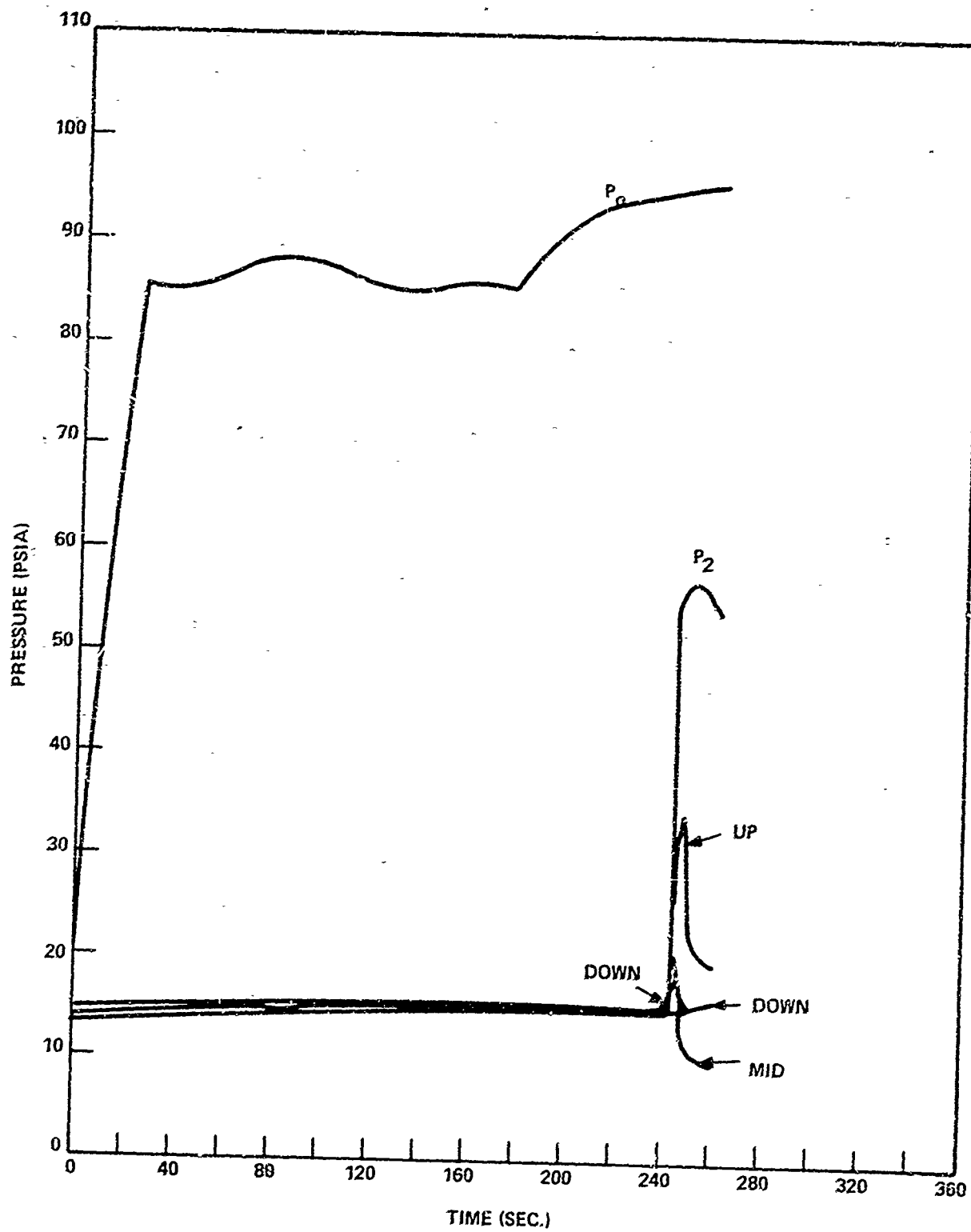


Figure 101. Pressures - Silica Phenolic - Insulative Layer C3-1

Part I

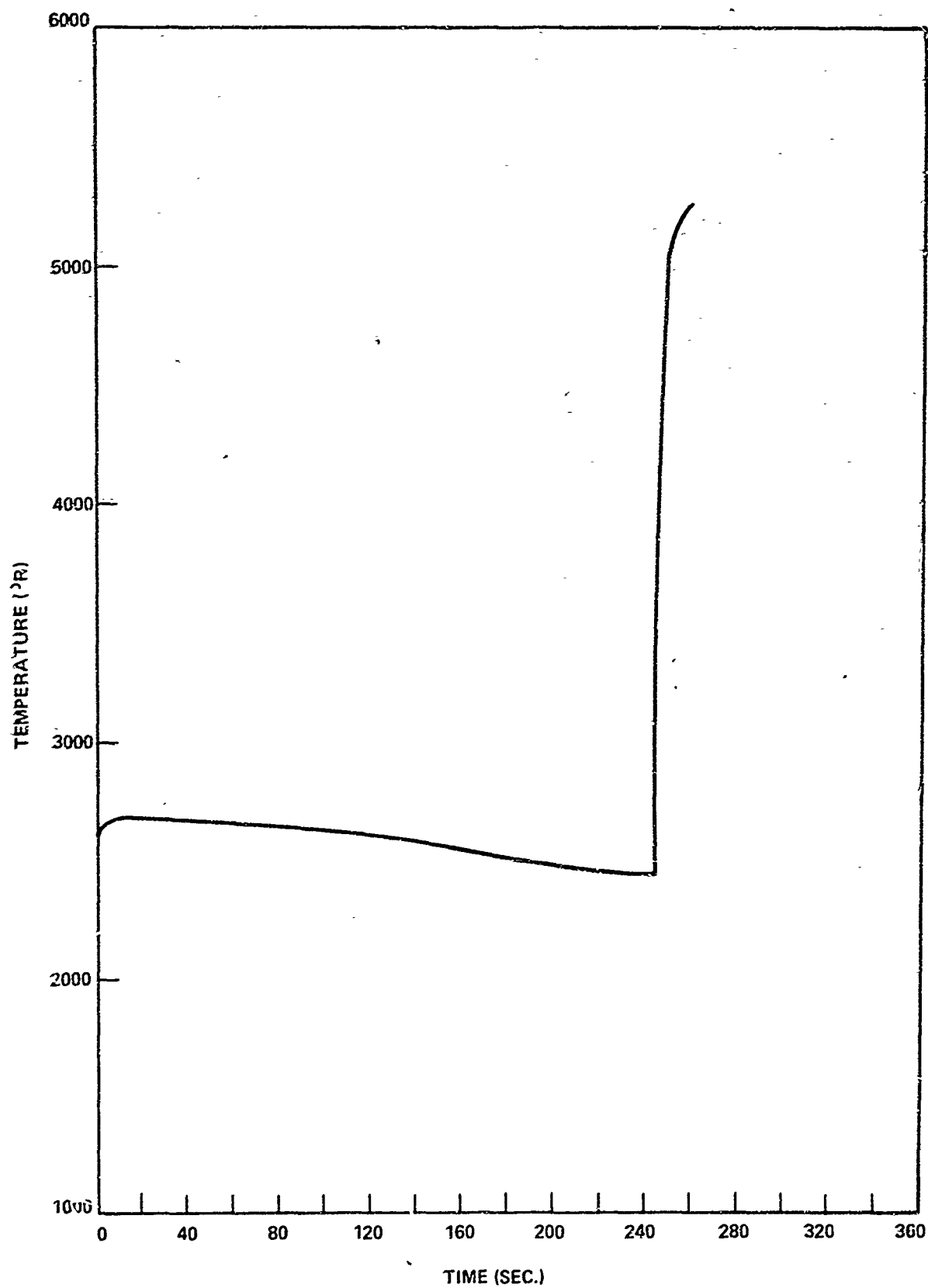


Figure 102. Surface Temperature - Silica Phenolic - Insulative Layer C3-1

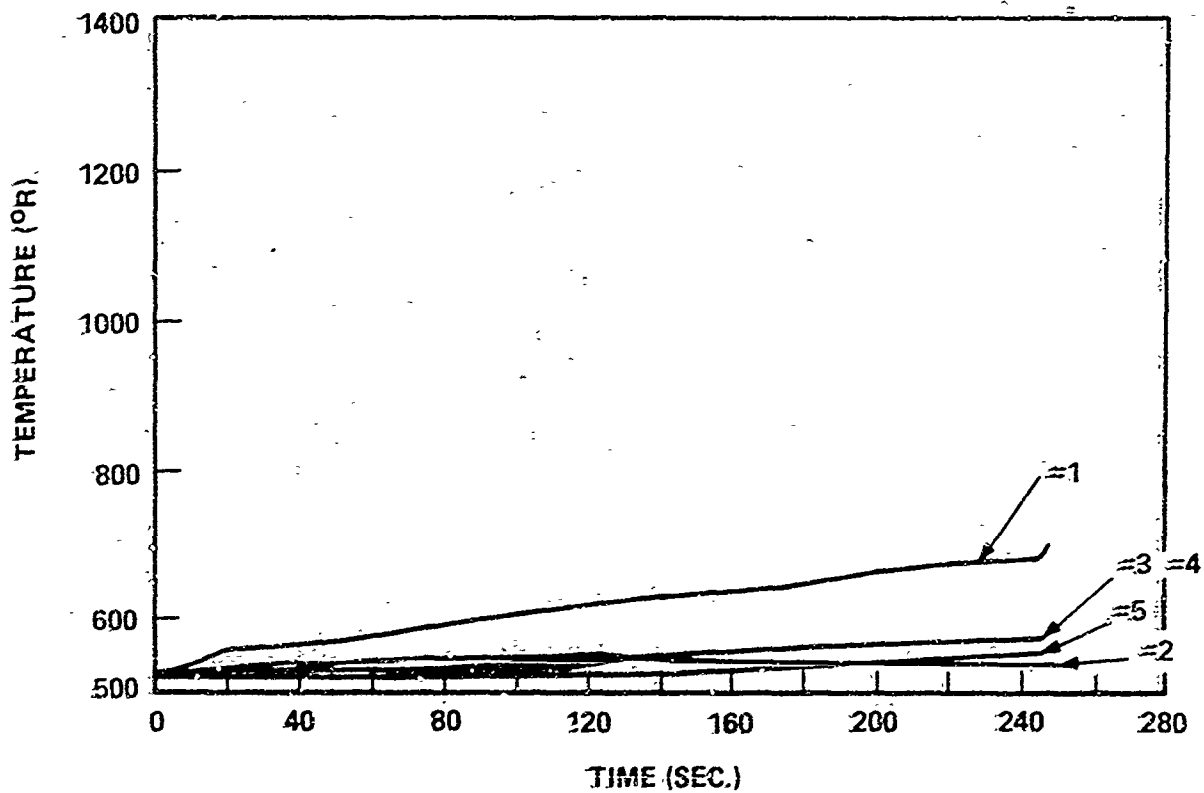


Figure 103. Internal Temperatures - Silica Phenolic - Insulative Layer C3-1

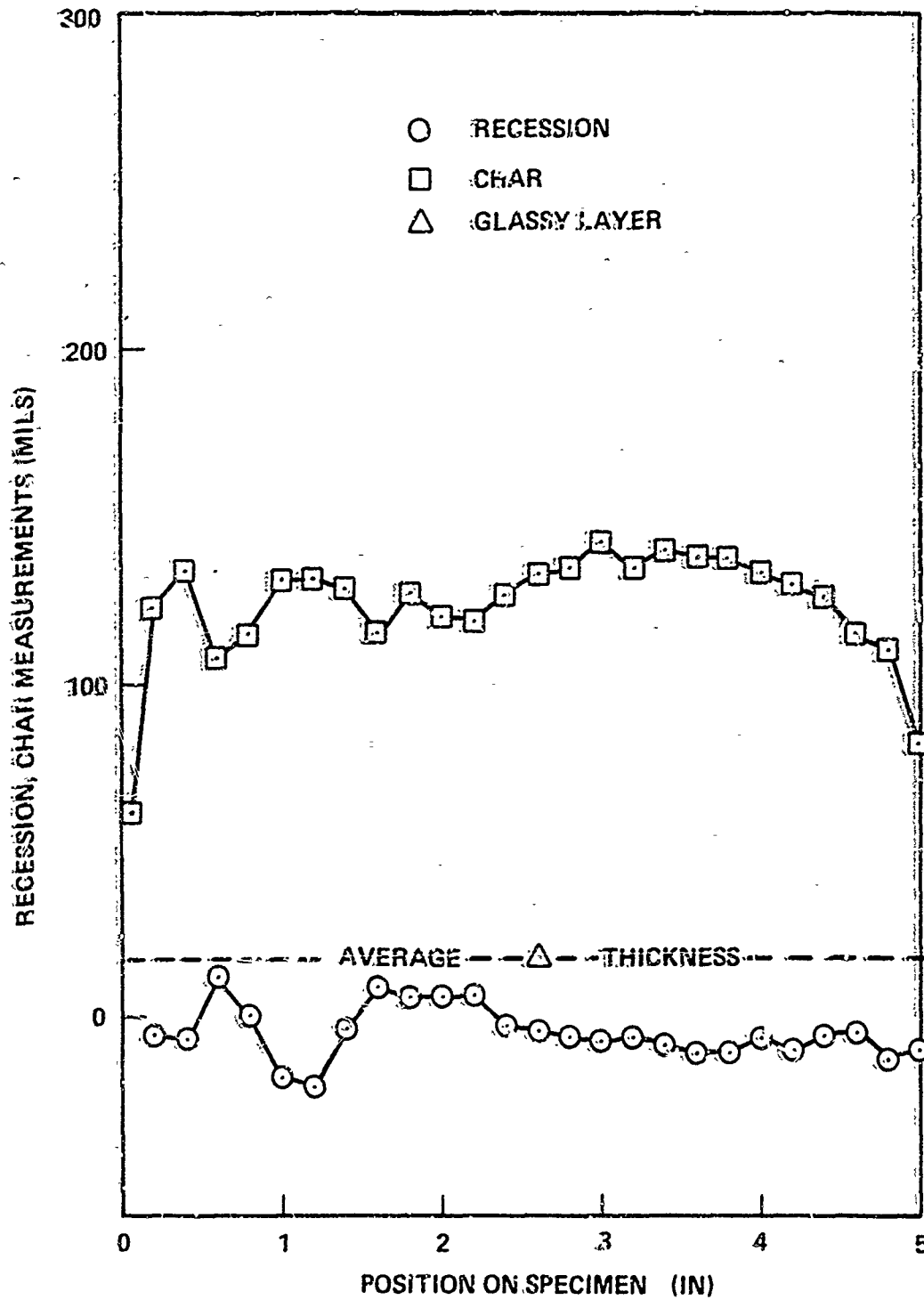


Figure 104. Char Measurements - Silica Phenolic - Insulative Layer C3-1



Figure 105 Post Test -- Silica Phenolic -- Insulative Layer C3-2

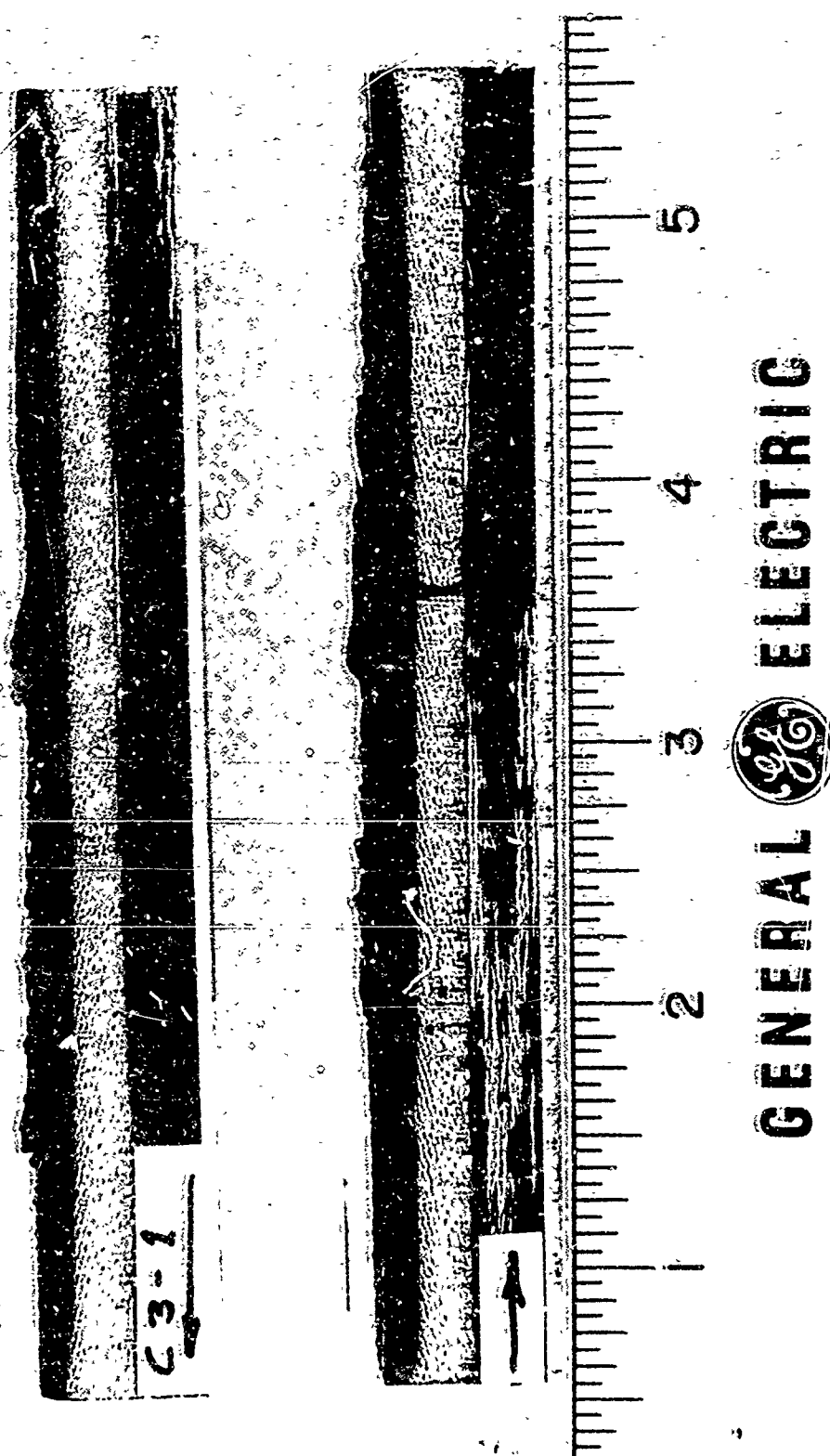


Figure 106. Post-Test Silica Phenolic-Insulative Layer C3-2 (Sectioned)

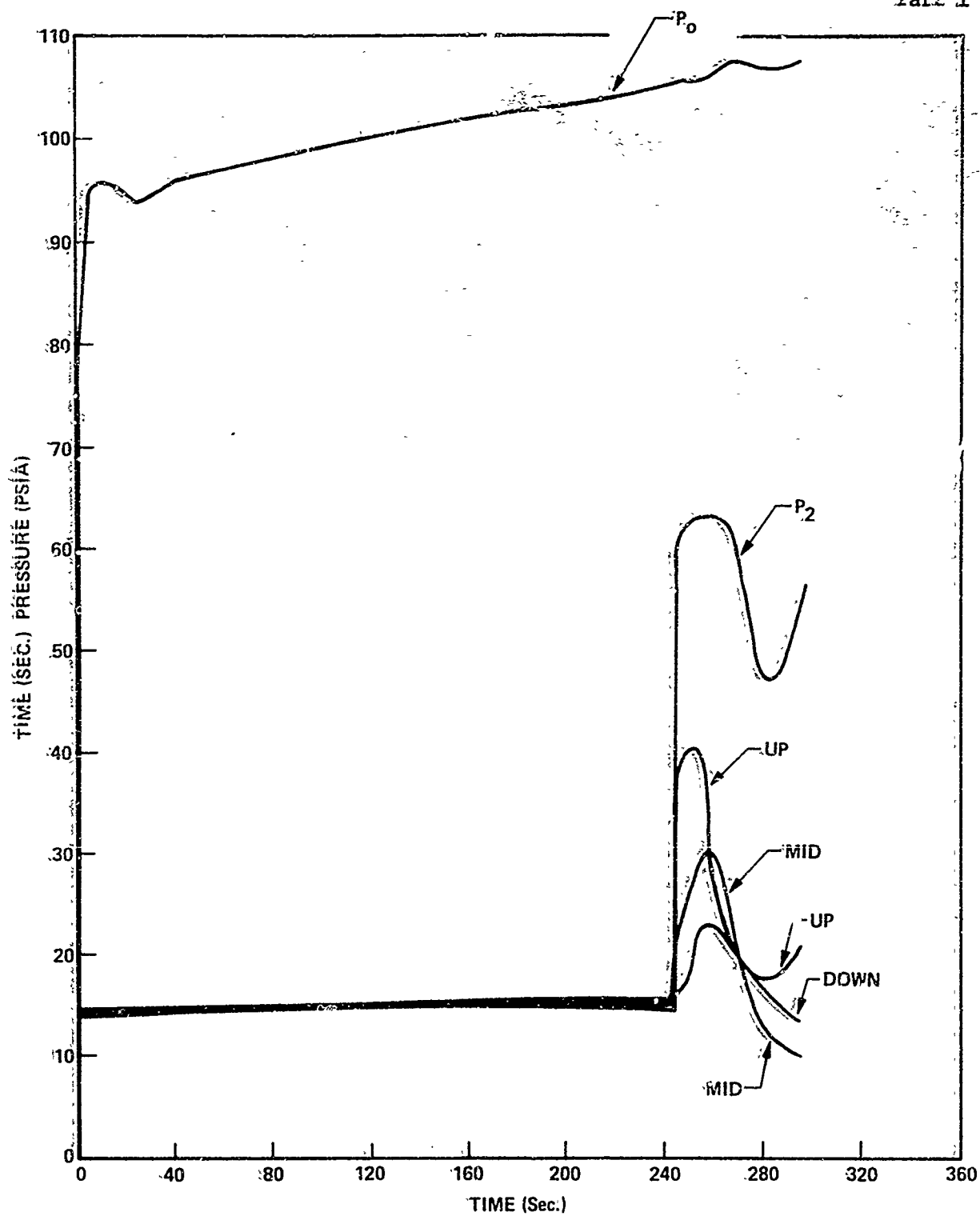


Figure 107. Pressures - Silica Phenolic - Insulative Layer C3-2

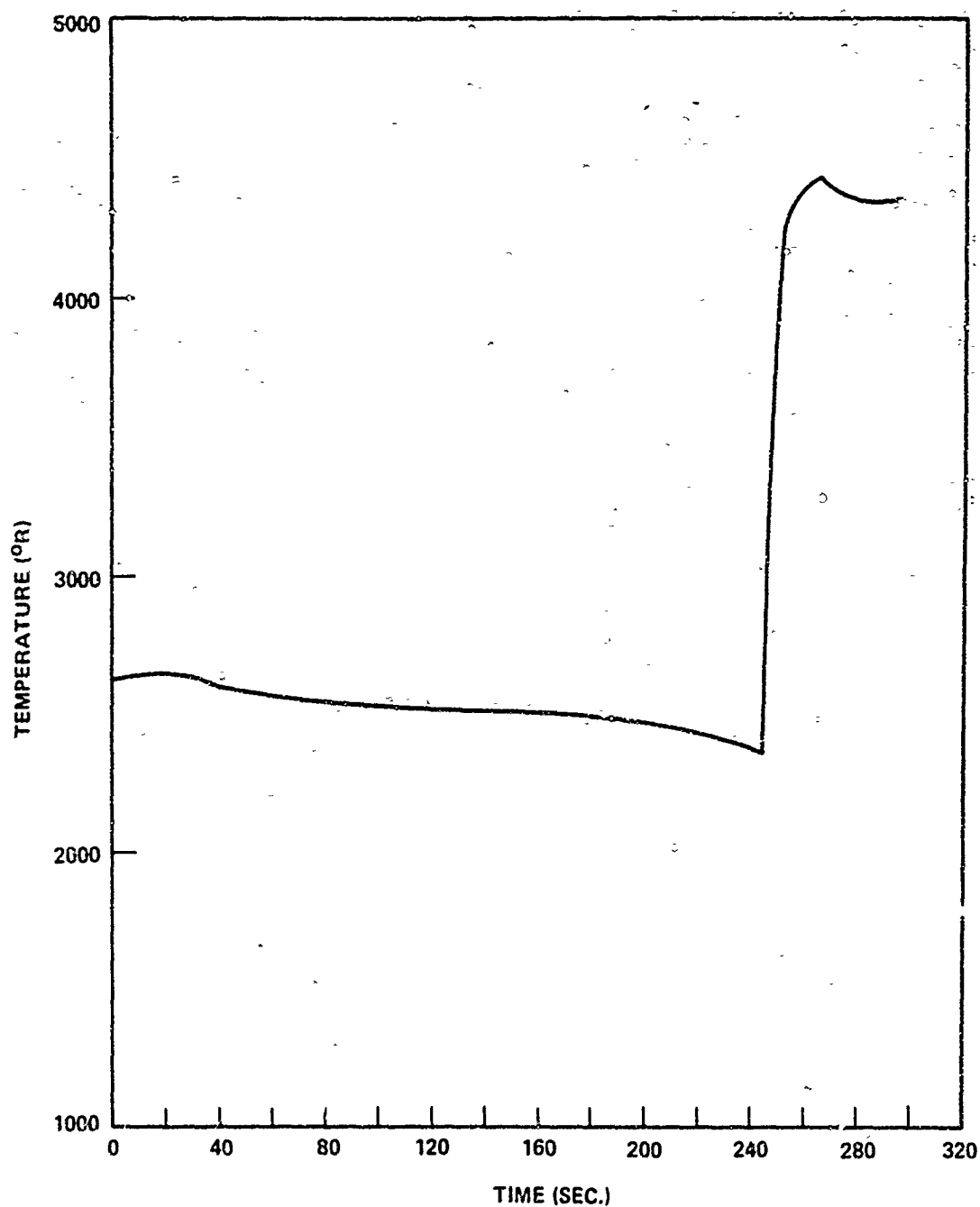


Figure 108. Surface Temperature - Silica Phenolic - Insulative Layer C3-2

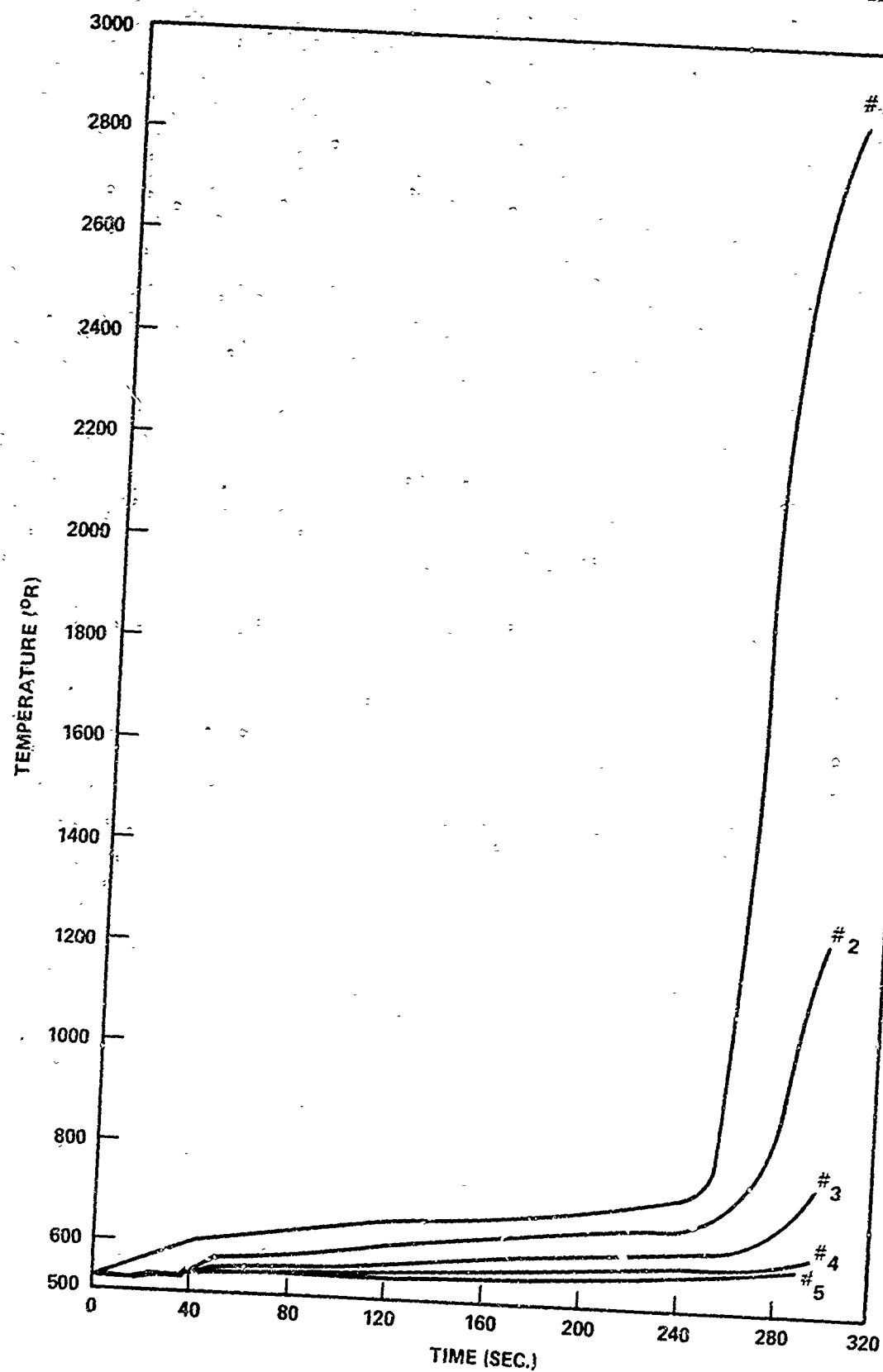


Figure 109. Internal Temperatures - Silica Phenolic - Insulative Layer C3-2

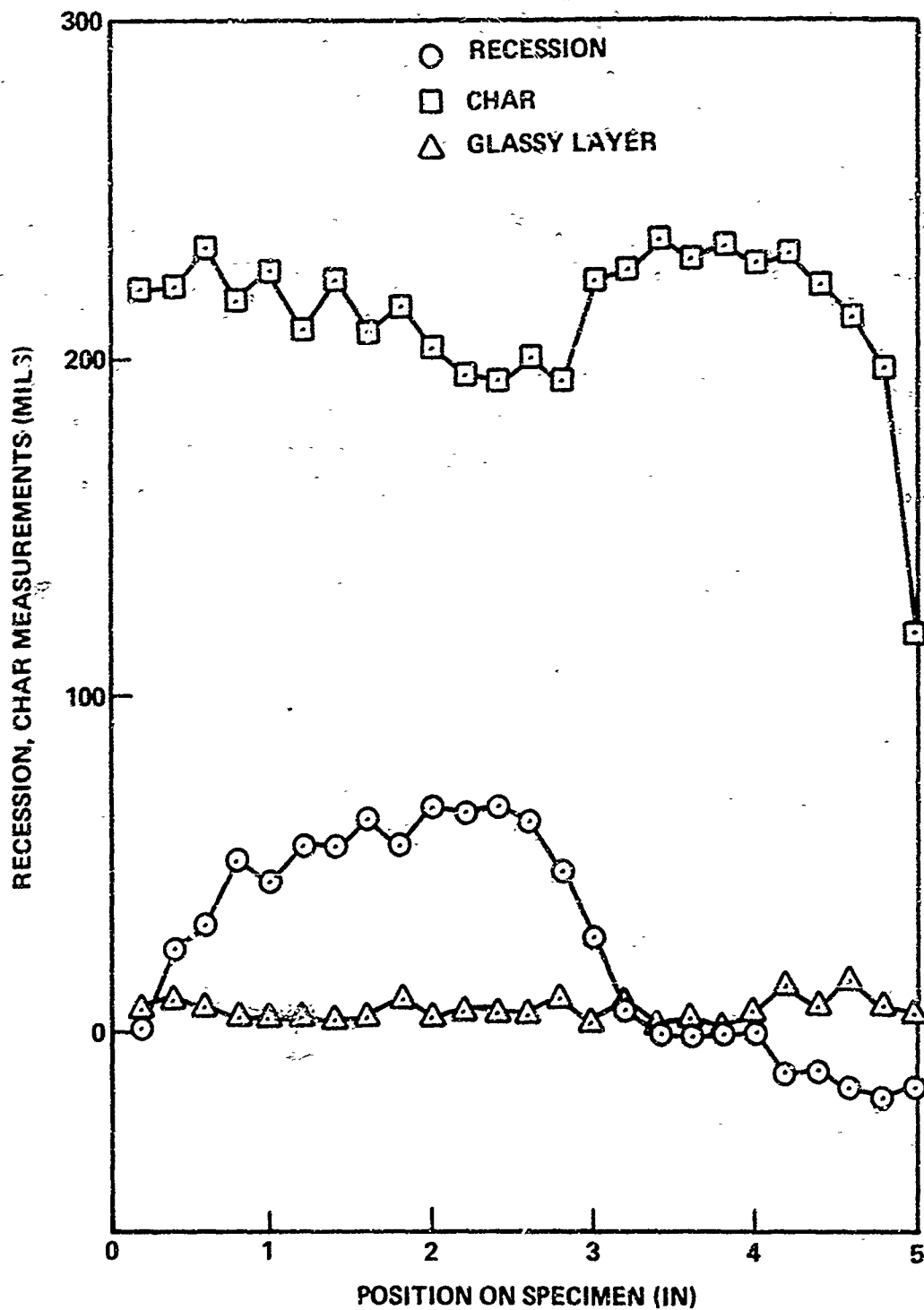


Figure 110. Char Measurements - Silica Phenolic - Insulative Layer C3-2

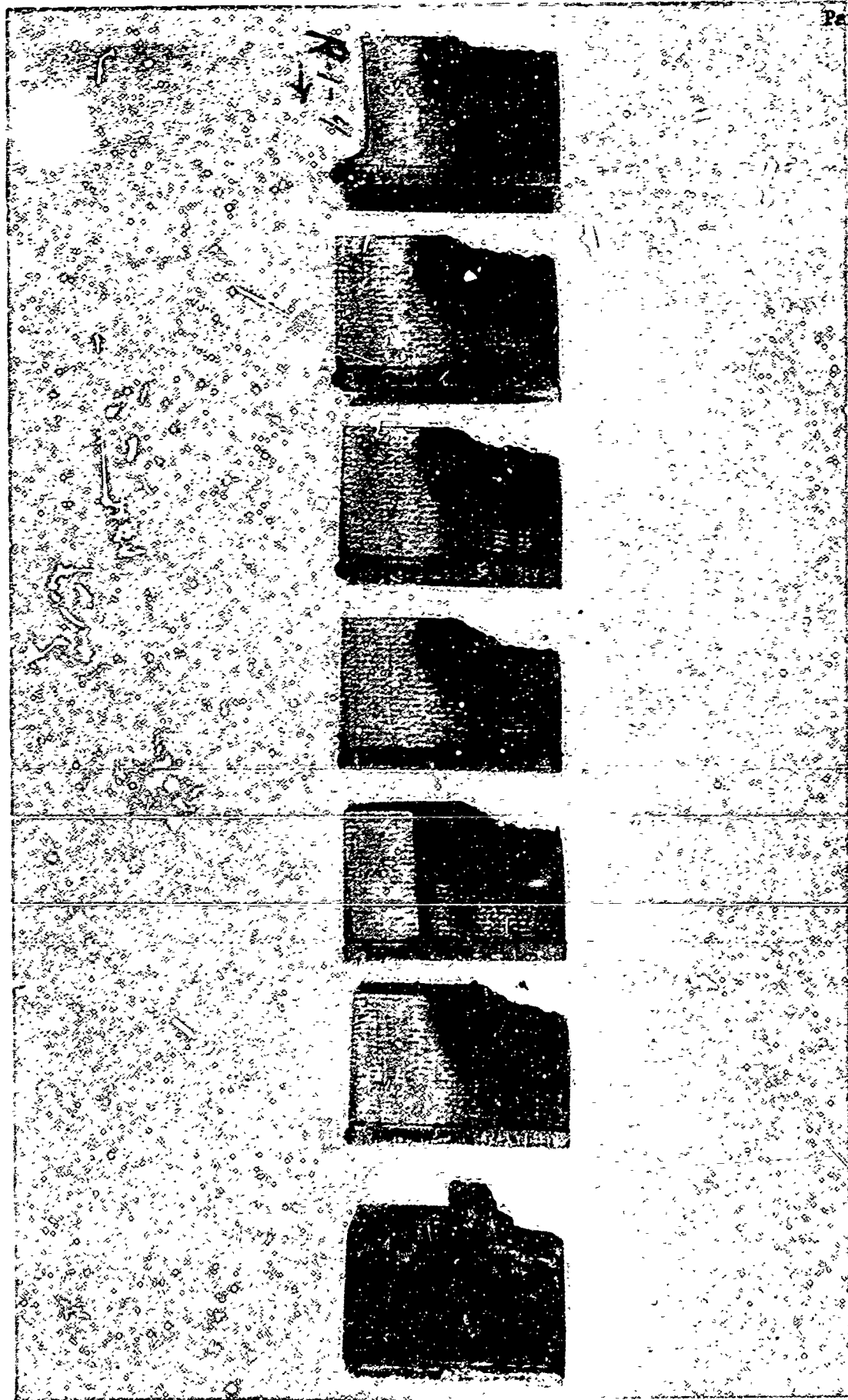


Figure 111 Transverse Cross Sections, R1-4

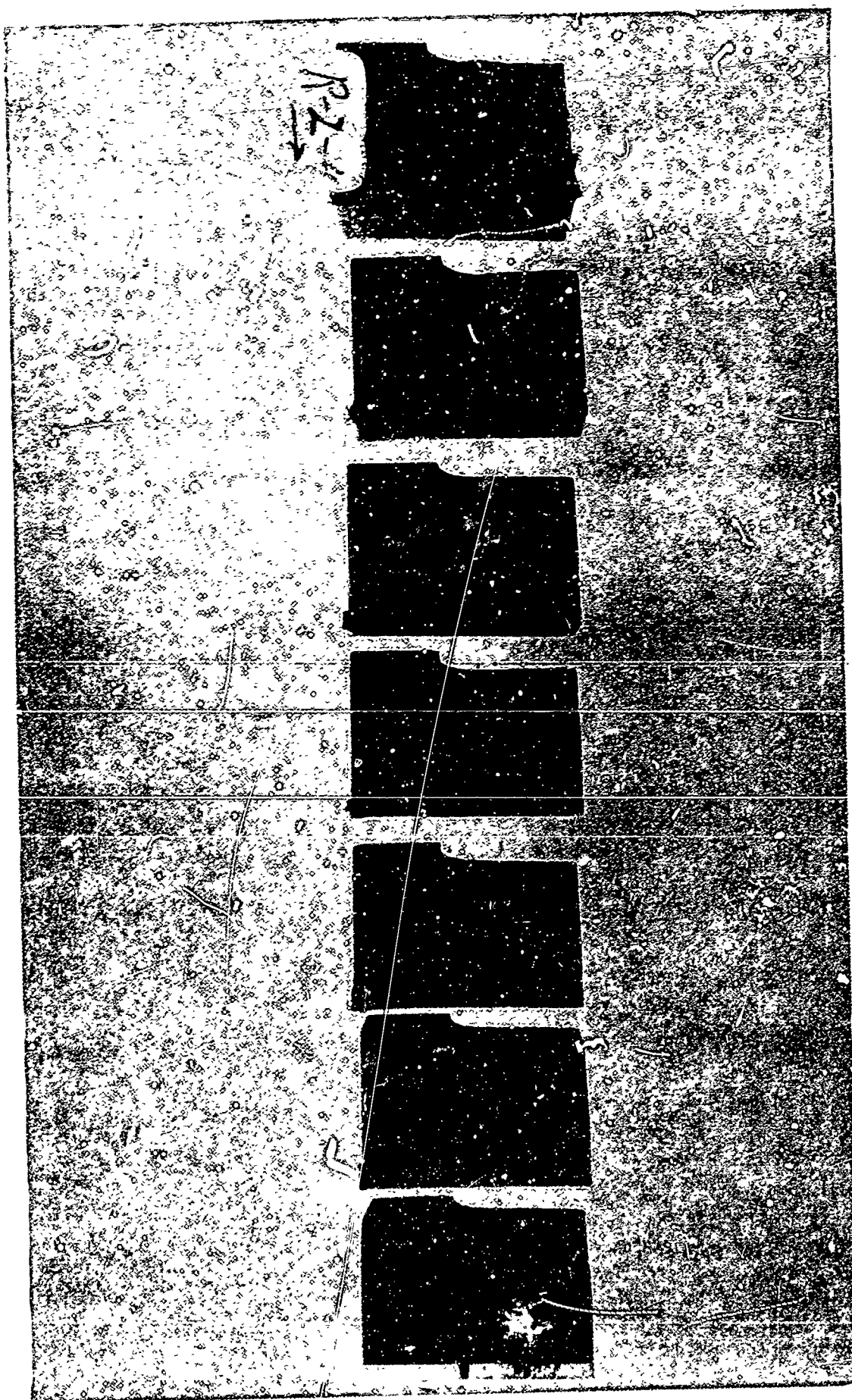


Figure 112 Transverse Cross Sections, R-2-4

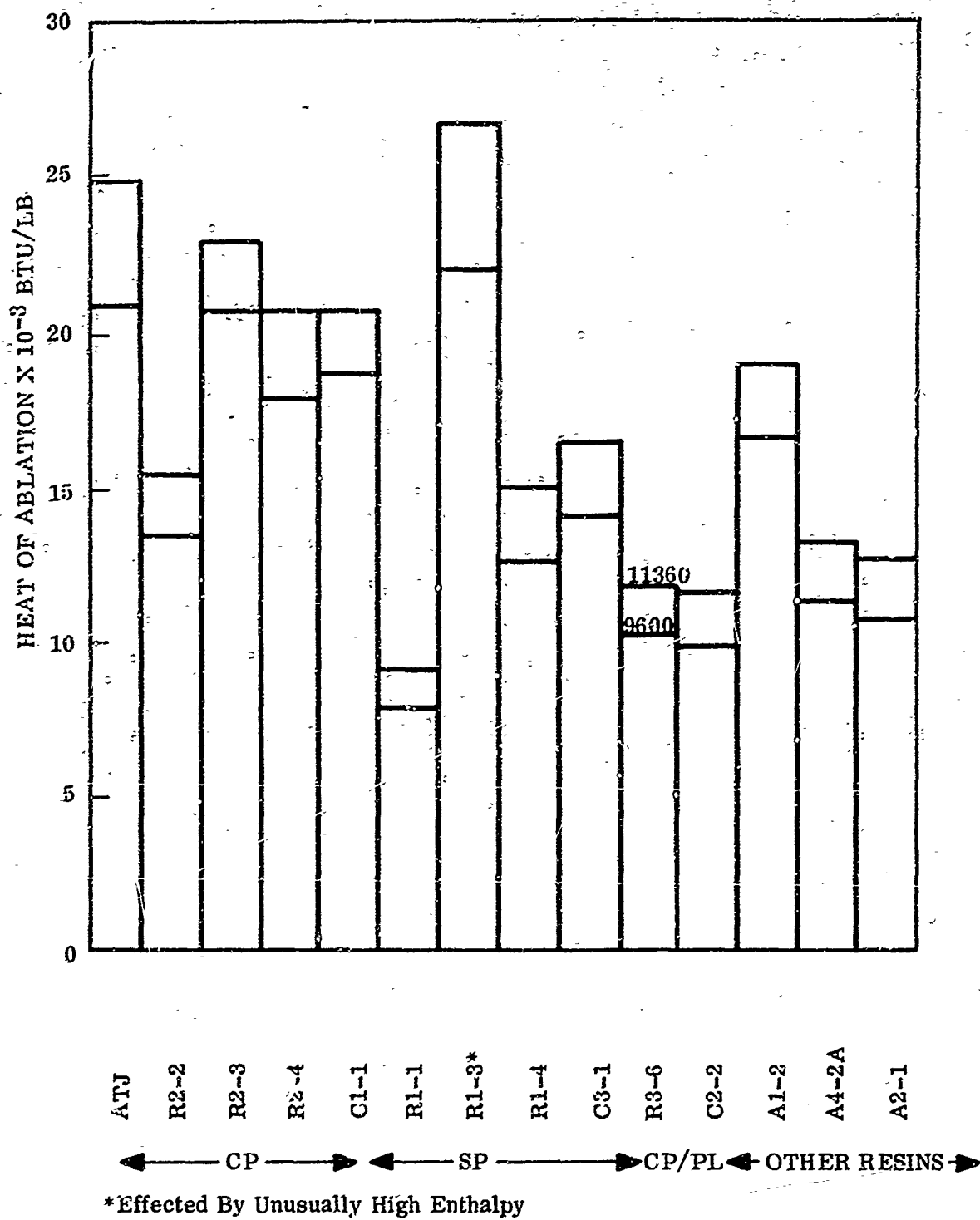


Figure 113. Integrated Heats of Ablation

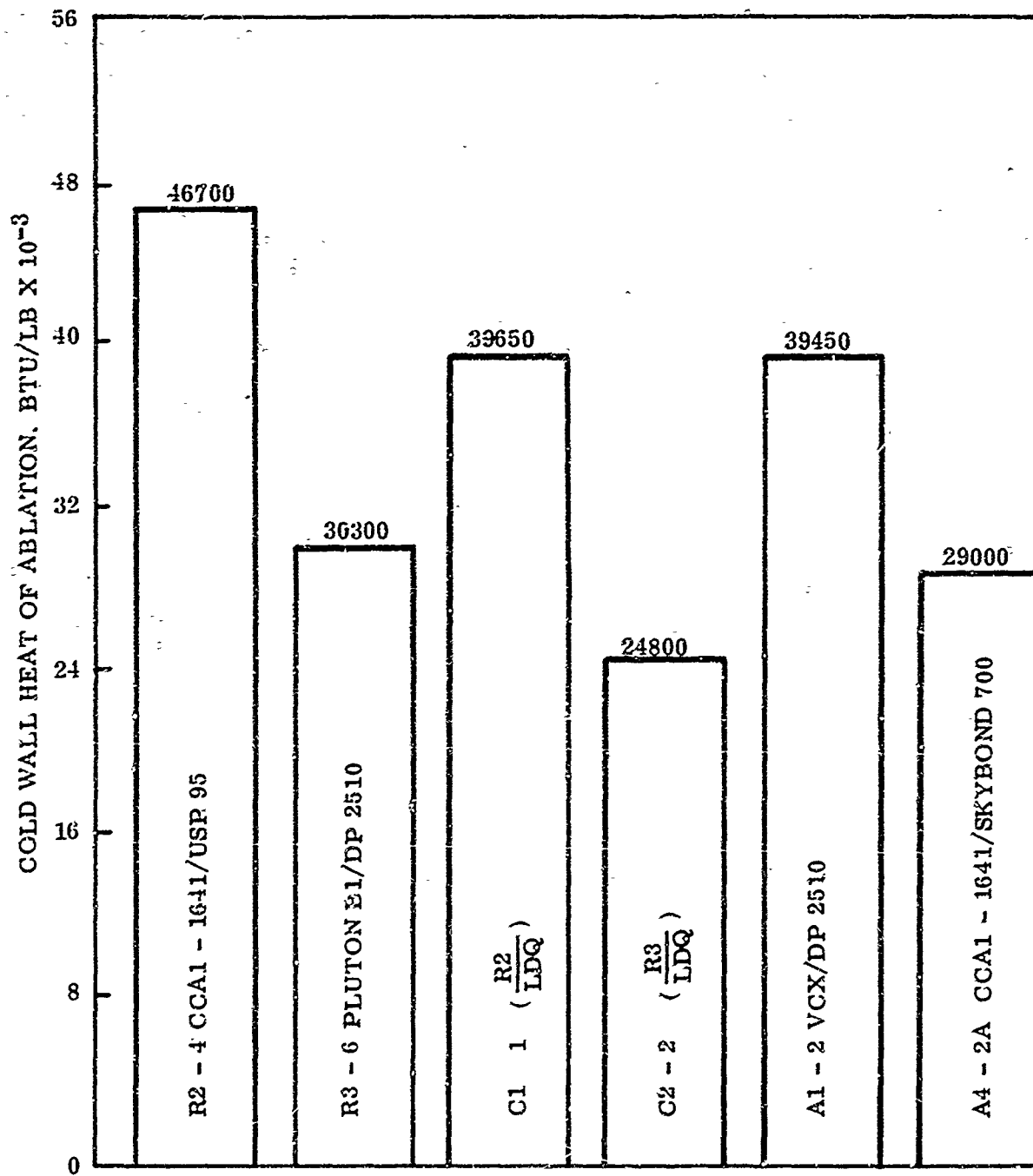


Figure 114. Cold Wall Heats of Ablation Carbon Fiber Specimens

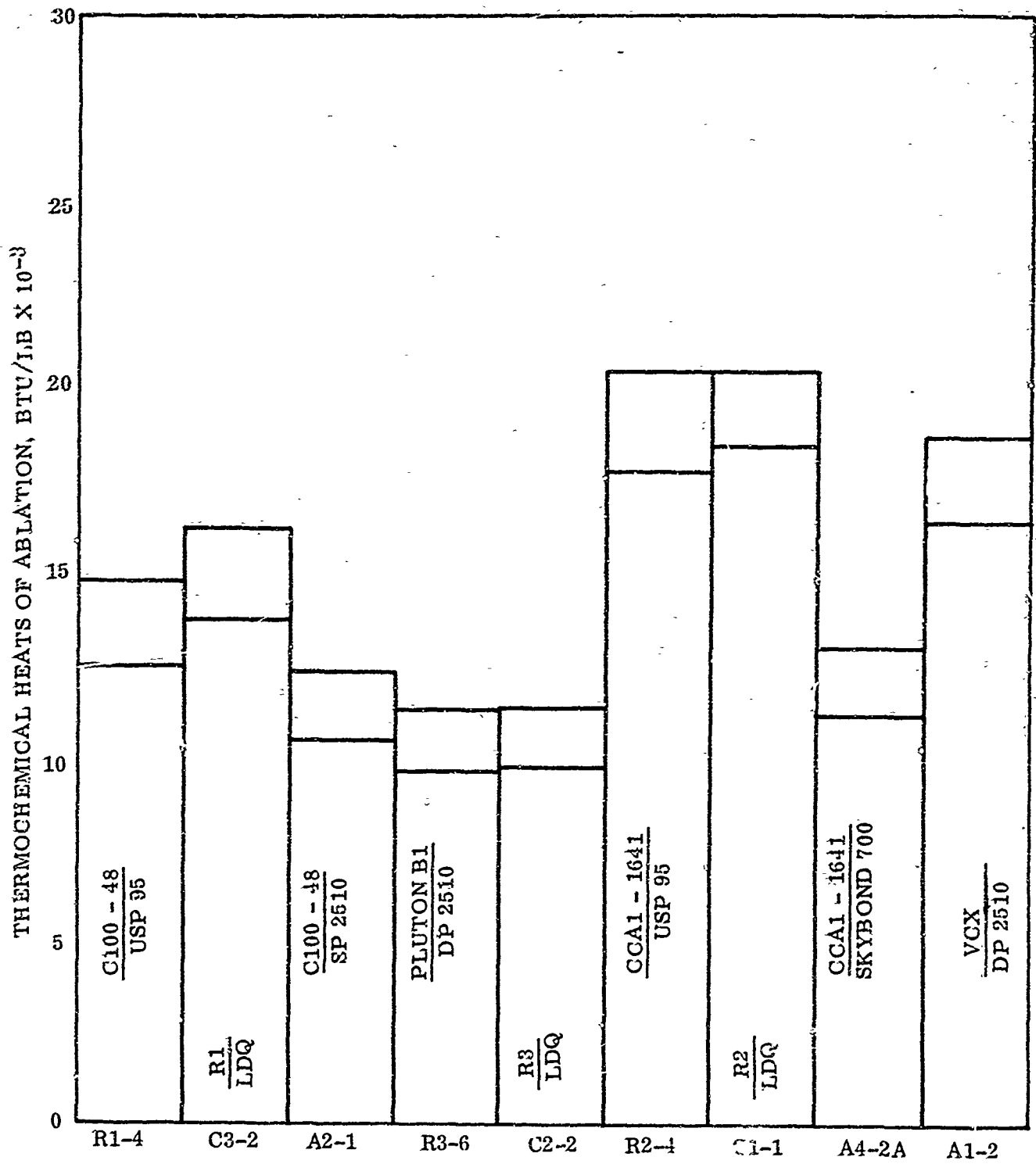


Figure 115. Thermochemical Heats of Ablation

AFML-TR-70-95
Part I

TABLES I THROUGH XXVII

TABLE I. CYCLE 1 TEST SERIES

AFML-TR-70-95

Part I

Sample Designation	Ablative ¹ Layer	Insulative ² Layer	Structural ³ Layer
R1	Silica/Phenolic (C-100-48/USP-95 FM 5020	—	2024-T3 Aluminum ↓
R2	Carbon/Phenolic (CCA1-1641/USP 95 FM 5055A	—	
R3	Carbon/Phenolic (Pluton B1/DP-2510 MXC-31HP	—	
A1	Carbon/Phenolic (WCX/DP-2510	—	
A2	Silica/Phenolic (C-100-48/DP-2510	—	
A3	Silica/Polyimide (C-100-48/Skybond 700	—	
A4	Carbon/Polyimide (CCA1-1641/Skybond 700	—	
C1	Carbon/Phenolic (CCA1-1641/USP95 FM5055A	Loom Woven Low Density Quartz	
C2	Carbon/Phenolic (Pluton B1/DP-2510 MXC-31HP	Loom Woven Low Density Quartz	
C3	Silica/Phenolic (C-100-48/USP95 FM 5020	Loom Woven Low Density Quartz	

1. Ablative layer was fabricated from impregnated cloth, cut on a 45 degree bias and oriented at 20 degrees to the surface.
2. Insulative layer was fabricated from Q-24 quartz yarn impregnated with HT424 epoxy-phenolic resin and loom woven in a non-interlaced configuration, 22 yarn layers in each direction for samples C1 and C3 and 18 yarn layers for sample C2.
3. Structural layer was a chromic acid etched, 2024-T3 aluminum plate, 0.0625 inch thick.

TABLE II. DESCRIPTION OF TEST SPECIMENS

Sample Designation Parameter	R1	R2	R3	A1	A2	A3	A4	C1	C2	C3
Ablative Prepreg										
Fabric	Refrasil C100-48	Carbon CCA1-1641	Carbon Pluton B1	Carbon VCX	Refrasil C100-48	Refrasil C100-48	Carbon CCA1-1641	Carbon CCA1-1641	Carbon Pluton B1	Refrasil C100-48
Resin	Phenolic USP95	Phenolic USP95	Phenolic DP 2510	Phenolic DP 2510	Phenolic DP 2510	Polyimide Skybond 700	Polyimide Skybond 700	Phenolic USP95	Phenolic DP 2510	Phenolic USP95
Resin Content, %	36.8	35.0	48.5	46.2	34.0	28.4	37.4	36.1	33.0	32.8
Volatiles, %	4.0	4.1	6.4	5.8	5.0	8.2	11.6	4.0	12.6	3.8
Flow, %	17.0	16.1	11.1		11.0	9.8	22.4	12.2	17.3	16.5
Thickness, in.	0.600	0.500	0.475	0.500	0.475			0.402	0.473	0.345
Density, gm/cc	1.67	1.51	1.43	1.33	1.59			1.50	1.43	1.65
LDQ Prepreg Yarn										
Resin								Quartz Q-24	Quartz Q-24	Quartz Q-24
Resin Content, %								HT424 26.6	HT424 26.6	HT424 26.6
Volatiles, %								10.0	10.0	10.0
Thickness, in.								0.29	0.26	0.28
Density, gm/cc								0.54	0.34	0.55
Cured Composite										
Thickness, in.								0.754	0.800	0.703
Density, gm/cc								1.14	1.17	1.31

TABLE III. MATERIALS DATA

AFML-TR-70-95

Part I

ATJ-S-GRAPHITE			
	With Grain	Across Grain	
Density, g/cc	1.82	1.82	
UTS, Psi	4700	3800	
Flex Strength, Psi	6200	5100	
Compressive Strength, Psi	11800	12400	
Young's Modulus, Psi	1.04×10^6	0.65×10^6	
Thermal Conductivity, $\frac{\text{Btu-ft}}{\text{hr-ft}^2 \cdot ^\circ\text{F}}$	106	88	

PRE-PREG MATERIALS			
	MXC-31HP (Pluton B-1 HP Fabric)	FM5055A (CCAT-1641 Fabric)	FM5020 (C-100-43 Fabric)
Resin, %	45-50	34-38	27-33
*Volatile %	7-10	4-8	3-6
*Flow % at 150, Psi	12-20	10-18	10-18

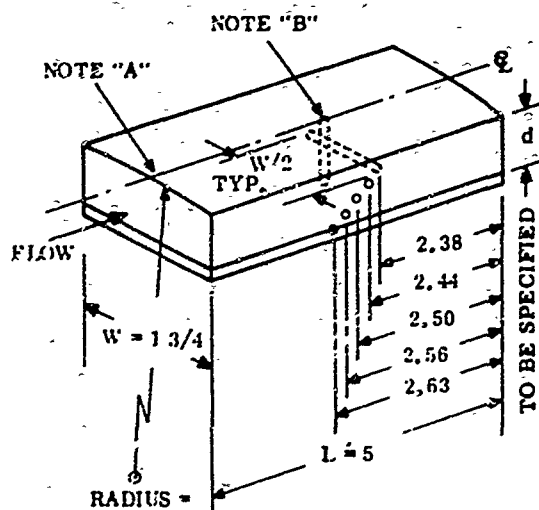
*Note that flow and volatile values are high
to permit autoclave processing.

Q24/HT424 IMPREGNATED QUARTZ THREAD	
Lot W-1108	
Resin 26.6%	
Volatile 10%	

TABLE IV. ABLATION PARAMETERS

Measurement	Instrument	Application	Frequency
OPERATIONAL TEST			
Current Voltage Air Mass Flow Cooling Water Mass Flow Cooling Water Temp. Change Plenum Pressure Test Chamber Static Pressure	Oscillograph Oscillograph Flow Meter Turbine Flowmeter Digital Counter Fe/const. T/C Pressure transducer Pressure Transducer	Heat balance for enthalpy Stagnation Properties Static Pressure	Every Run (Applicable to B and D tests noted below)
CALIBRATION TEST			
Calorimeter at Model Stations Static Pressure at Model Stations	Steady State Asymptotic Calorimeter Pressure Transducer	Heat Transfer	Each Calibration
PRE- AND POST TEST MODEL MEASUREMENTS			
Weight before Test Weight after Test Char Thickness Recession Pre- and Post Test Photographs	Analytical Balance Cathetometer Speedgraphic	Heat of Ablation Insulative Index Recession Rates	Every Test Model
MODEL MEASUREMENT DURING TEST			
Surface Temperature Local Model Station Pressure Subsurface Temperatures Motion Picture	2-color Pyrometer Pressure Transducer C/A T/C Photsonics	Ablation Mechanism Heat Transfer Thermal Properties Ablation Mechanism	Every Test Model

FABRICATION:



STATION 1 IS INDICATED. READ ALL
LOCATIONS ON MODEL PROFILE FROM
THIS STATION

INSERT TUNGSTEN WIRE VERTICALLY
THRU SPECIMEN ON CENTERLINE

OVERMARK DIMENSIONAL VARIATIONS

NO	NOMINAL	ACTUAL (INCHES)
1	$d/5$	
2	$2d/5$	
3	$3d/5$	
4	$4d/5$	
5	d	

NO	WIRE		CONFIRMED DEPTH, (INCHES)
	GA	TYPE	
1	36	C/A	.107
2	36	C/A	.242
3	36	C/A	.280
4	36	C/A	.366
5	36	C/A	.500

SPECIMEN CODE: R2-1

SPECIMEN MATERIAL: Carbon-phenolic (Ram 89)

PROFILE MEASUREMENTS

MEASURED BY A. C. Nedby

STATION	LOCATION INCHES	BEFORE		AFTER		CHAR
		(1)	(2)	(3)	(4)	
1	END	.605	.512	.487	.025	
2	.2		.512	.492	.020	.061
3	.4		.512	.488	.024	.110
4	.6		.512	.491	.021	.111
5	.8		.512	.491	.021	.157
6	1.0		.512	.491	.021	.158
7	1.2		.512	.488	.024	.158
8	1.4		.512	.491	.021	.163
9	1.6	.604	.511	.492	.019	.181
10	1.8		.511	.499	.012	.141
11	2.0		.511	.498	.013	.119
12	2.2		.511	.494	.017	.131
13	2.4	.604	.511	.492	.019	.119
14	2.6		.511	.487	.024	.117
15	2.8		.511	.487	.024	.120
16	3.0		.511	.485	.026	.121
17	3.2		.511	.483	.028	.108
18	3.4		.511	.498	.013	.117
19	3.6	.605	.512	.486	.026	.111
20	3.8		.512	.500	.012	.115
21	4.0		.512	.496	.016	.084
22	4.2		.512	.494	.018	.094
23	4.4		.512	.503	.009	.102
24	4.6	.606	.513	.503	.010	.088
25	4.8		.513	.502	.011	.074
26	END		.513	.506	.005	.049

REMARKS

- (1) Sample thickness including backing plate and bond
- (2) Sample thickness not including backing plate and bond
- (3) Sample thickness after recession not including backing plate and bond
- (4) Total recession

Backing plate: 2024-T3 aluminum 0.0625 in.

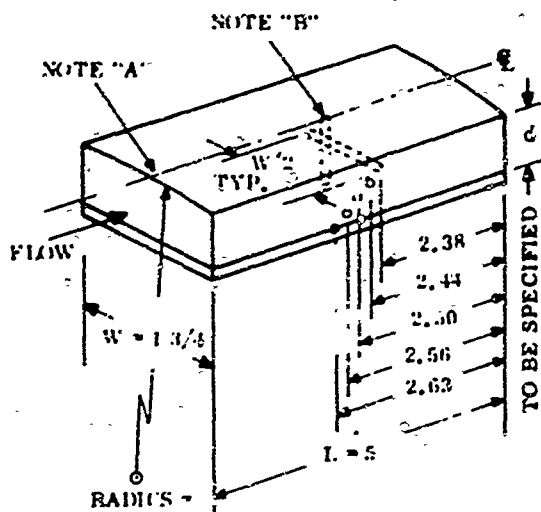
Bond: RTV-560

Weight before: 106.6195 gm

Weight after: 102.5098 gm

TABLE VI. SPECIMEN R1-1 MODEL MEASUREMENTS

FABRICATION:



NOTE "A"
STATION 1 IS INDICATED, READ ALL
LOCATIONS ON MODEL PROFILE FROM
THIS STATION

NOTE "B"
INSERT TUNGSTEN WIRE VERTICALLY
THRU SPECIMEN ON CENTERLINE

NOTE "C"
OVERMARK DIMENSIONAL VARIATIONS

HOLE LOCATIONS

NO	NOMINAL	ACTUAL (INCHES)
1	d/5	
2	2d/5	
3	3d/5	
4	4d/5	
5	d	

MODEL INSTRUMENTATION
INSTALLER A. C. Nedby

NO	WIRE		CONFIRMED DEPTH, (INCHES)
	GA	TYPE	
1	36	C/A	.155
2	36	C/A	.281
3	36	C/A	.382
4	36	C/A	.469
5	36	C/A	.600

Photographed

SPECIMEN CODE: R1-1

SPECIMEN MATERIAL: Phenolic-Refrasil (Run 95)

PROFILE MEASUREMENTS

MEASURED BY A. C. Nedby

STATION	LOCATION INCHES	BEFORE		AFTER		CHAR
		(1)	(2)	(3)	(4)	
1	END	705	.612	.587	.025	162
2	.2		.612	.578	.034	171
3	.4		.612	.566	.046	182
4	.6		.612	.555	.056	160
5	.8		.612	.544	.068	155
6	1.0		.612	.545	.067	156
7	1.2	704	.611	.546	.065	157
8	1.4		.611	.516	.095	142
9	1.6		.611	.518	.093	135
10	1.8		.611	.528	.083	141
11	2.0		.611	.528	.083	135
12	2.2		.611	.525	.096	142
13	2.4	704	.611	.524	.087	111
14	2.6		.611	.527	.084	143
15	2.8		.611	.526	.085	127
16	3.0		.611	.528	.083	122
17	3.2		.611	.551	.060	137
18	3.4		.611	.575	.036	158
19	3.6	703	.610	.577	.033	156
20	3.8		.610	.568	.044	152
21	4.0		.610	.567	.043	153
22	4.2		.610	.569	.044	149
23	4.4		.610	.574	.036	154
24	4.6		.610	.572	.038	140
25	4.8		.610	.591	.019	161
26	END	703	.610	.598	.012	163

REMARKS

- (1) Sample thickness including backing plate and bond
- (2) Sample thickness not including backing plate and bond
- (3) Sample thickness after recession not including backing plate and bond
- (4) Total recession

Backing plate: 2024-T3 aluminum 0.0625 in.

Bond: RTV-560

Weight before: 142.743 gm.

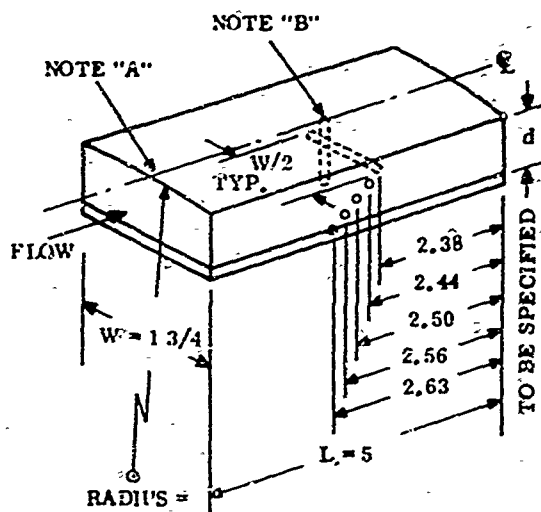
Weight after: 132.025 gm.

TABLE VII. SPECIMEN R2-2 MODEL MEASUREMENTS

AFML-TR-70-95

Part I

FABRICATION:



NOTE "A"

STATION 1 IS INDICATED. READ ALL LOCATIONS ON MODEL PROFILE FROM THIS STATION

NOTE "B"

INSERT TUNGSTEN WIRE VERTICALLY THRU SPECIMEN ON CENTERLINE

NOTE "C"

OVERMARK DIMENSIONAL VARIATIONS

HOLE LOCATIONS

NO	NOMINAL	ACTUAL (INCHES)
1	d/5	
2	2d/5	
3	3d/5	
4	4d/5	
5	d	

MODEL INSTRUMENTATION

INSTALLER A. C. Nedby

NO	WIRE		CONFIRMED DEPTH, (INCHES)
	GA	TYPE	
1	36	C/A	.071
2	36	C/A	.295
3	36	C/A	.321
4	36	C/A	.399
5	36	C/A	.500

Photographed

SPECIMEN CODE: R2-2

SPECIMEN MATERIAL: Carbon-Phenolic (Run 96)

PROFILE MEASUREMENTS

MEASURED BY A. C. Nedby

STATION	LOCATION INCHES	AFTER			
		BEFORE	RECESSION		CHAR
		(1)	(2)	(3)	(4)
1	END	.602	.499	.498	.001
2	.2		.499	.478	.021
3	.4		.499	.464	.035
4	.6	.603	.500	.471	.029
5	.8		.500	.473	.027
6	1.0	.604	.501	.476	.025
7	1.2		.501	.483	.018
8	1.4	.605	.502	.486	.016
9	1.6		.502	.491	.011
10	1.8	.606	.503	.492	.011
11	2.0		.503	.492	.011
12	2.2		.503	.496	.007
13	2.4	.607	.504	.494	.010
14	2.6		.504	.500	.004
15	2.8		.504	.499	.005
16	3.0		.504	.496	.008
17	3.2	.606	.503	.499	.004
18	3.4		.503	.501	.002
19	3.6		.503	.501	.002
20	3.8		.503	.497	.006
21	4.0	.605	.502	.502	.000
22	4.2		.502	.507	-.005
23	4.4		.502	.503	-.001
24	4.6	.604	.501	.503	+.002
25	4.8		.501	.503	-.002
26	END	.604	.501	.503	-.002

REMARKS

(1) Sample thickness including backing plate and bond

(2) Sample thickness not including backing plate and bond

(3) Sample thickness after recession not including backing plate and bond

(4) Total recession

Backing plate: 2024-T3 aluminum 0.0625 in.

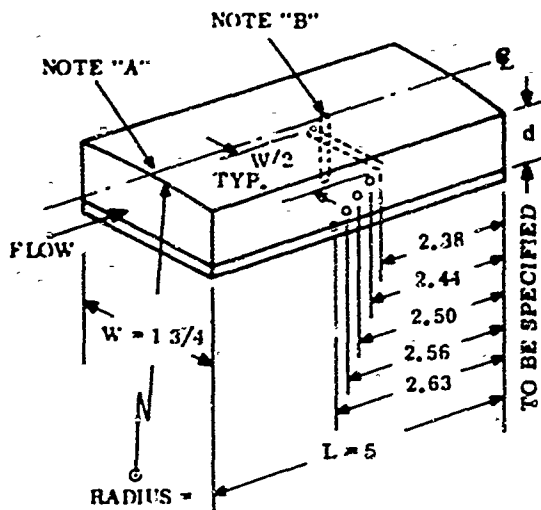
Bond: RTV-560

Weight before: 106.8967 gm.

Weight after: 102.5780 gm.

TABLE VIII. SPECIMEN RI-3 MODEL MEASUREMENTS

FABRICATION:



NOTE "A"
STATION 1 IS INDICATED. READ ALL
LOCATIONS ON MODEL PROFILE FROM
THIS STATION

NOTE "B"
INSERT TUNGSTEN WIRE VERTICALLY
THRU SPECIMEN ON CENTERLINE

NOTE "C"
OVERMARK DIMENSIONAL VARIATIONS

HOLE LOCATIONS

NO	NOMINAL	ACTUAL (INCHES)
1	d/5	
2	2d/5	
3	3d/5	
4	4d/5	
5	d	

MODEL INSTRUMENTATION

INSTALLER A. C. Nedby

NO	WIRE		CONFIRMED DEPTH, (INCHES)
	GA	TYPE	
1	36	C/A	.141
2	36	C/A	.205
3	36	C/A	.315
4	36	C/A	.444
5	36	C/A	.600

Photographed

SPECIMEN CODE: R1-3

SPECIMEN MATERIAL: Phenolic Refrasil (Run 97)

PROFILE MEASUREMENTS

MEASURED BY A. C. Nedby

STATION	LOCATION INCHES	BEFORE		AFTER		CHAR.
		(1)	(2)	RECESSION (3)	(4)	
1	END	.706	.613	.598	.015	177
2	.2		.613	.599	.014	256
3	.4		.613	.600	.013	265
4	.6		.613	.598	.015	309
5	.8		.613	.602	.011	269
6	1.0		.613	.599	.014	267
7	1.2	.707	.614	.601	.013	271
8	1.4		.614	.596	.014	262
9	1.6		.614	.581	.033	247
10	1.8	.708	.615	.571	.041	250
11	2.0		.615	.571	.041	247
12	2.2		.615	.571	.045	238
13	2.4	.709	.616	.587	.029	252
14	2.6		.616	.590	.026	250
15	2.8		.616	.595	.021	250
16	3.0	.710	.617	.594	.023	242
17	3.2		.617	.605	.012	241
18	3.4		.617	.608	.009	240
19	3.6		.617	.609	.008	237
20	3.8		.617	.610	.007	233
21	4.0	.710	.617	.605	.012	212
22	4.2		.617	.606	.011	205
23	4.4		.617	.604	.013	193
24	4.6		.617	.605	.012	185
25	4.8		.617	.602	.015	174
26	END	.711	.618	.600	.018	168

REMARKS

- (1) Sample thickness including backing plate and bond
- (2) Sample thickness not including backing plate and bond
- (3) Sample thickness after recession not including backing plate and bond
- (4) Total recession

Backing plate: 2024-T3 aluminum 0.0625 in

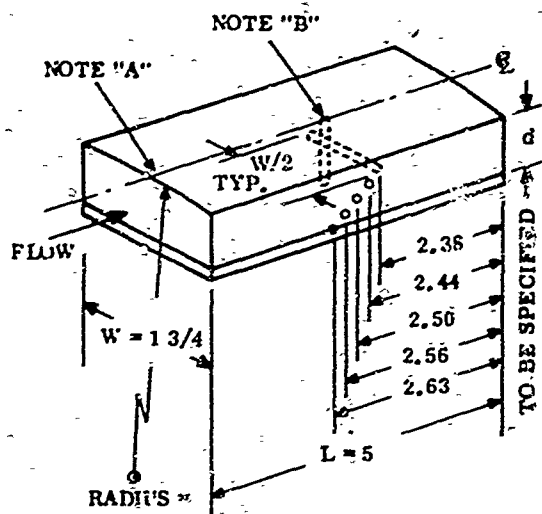
Bond: RTV-560

Weight before 142.7096 gms

Weight after: 128.6432 gms

TABLE IX. ATJ GRAPHITE SPECIMEN MODEL MEASUREMENTS

FABRICATION:



NOTE "A"
STATION 1 IS INDICATED. READ ALL
LOCATIONS ON MODEL PROFILE FROM
THIS STATION

NOTE "B"
INSERT TUNGSTEN WIRE VERTICALLY
THRU SPECIMEN ON CENTERLINE

NOTE "C"
OVERMARK DIMENSIONAL VARIATIONS

HOLE LOCATIONS

NO	NOMINAL	ACTUAL (INCHES)
1	d/5	
2	2d/5	
3	3d/5	
4	4d/5	
5	d	

MODEL INSTRUMENTATION
INSTALLER _____

NO	WIRE		CONFIRMED DEPTH, (INCHES)
	GA	TYPE	

Photographed

SPECIMEN CODE:

SPECIMEN MATERIAL: ATJ Graphite (Run 98)

PROFILE MEASUREMENTS
MEASURED BY A. C. Nedby

STATION	LOCATION INCHES	BEFORE		AFTER		CHAR
		(1)	(2)	(3)	(4)	
1	EDGE	.627		.614	.013	
2	.2			.610	.017	
3	.4			.605	.022	
4	.6			.608	.019	
5	.8			.602	.025	
6	1.0			.601	.026	
7	1.2			.601	.026	
8	1.4			.604	.023	
9	1.6			.600	.027	
10	1.8	.626		.594	.033	
11	2.0			.581	.045	
12	2.2			.583	.043	
13	2.4			.588	.038	
14	2.6			.593	.033	
15	2.8			.593	.033	
16	3.0			.593	.033	
17	3.2			.592	.034	
18	3.4			.599	.027	
19	3.6			.598	.028	
20	3.8			.604	.022	
21	4.0			.604	.022	
22	4.2			.607	.019	
23	4.4			.606	.020	
24	4.6			.607	.019	
25	4.8			.610	.016	
26	EDGE			.611	.015	

REMARKS

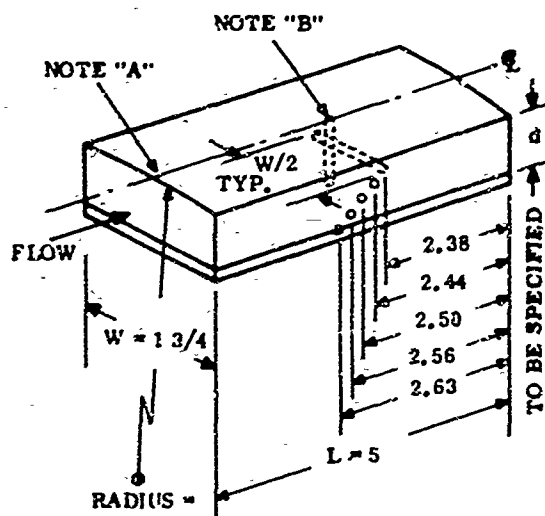
- (1) Sample thickness
- (3) Sample thickness after recession
- (4) Total recession

Bond: RTV-560

Density: 108 lb/ft³

TABLE X. SPECIMEN R2-3 MODEL MEASUREMENTS

FABRICATION:



NOTE "A"
STATION 1 IS INDICATED. READ ALL
LOCATIONS ON MODEL PROFILE FROM
THIS STATION

NOTE "B"
INSERT TUNGSTEN WIRE VERTICALLY
THRU SPECIMEN ON CENTERLINE

NOTE "C"
OVERMARK DIMENSIONAL VARIATIONS

HOLE LOCATIONS

NO	NOMINAL	ACTUAL (INCHES)
1	d/5	
2	2d/5	
3	3d/5	
4	4d/5	
5	d	

MODEL INSTRUMENTATION
INSTALLER A. C. Nedby

NO	WIRE		CONFIRMED DEPTH, (INCHES)
	GA	TYPE	
1	36	C/A	.148
2	36	C/A	.203
3	36	C/A	.295
4	36	C/A	.412
5	36	C/A	.500

Photographed

SPECIMEN CODE: R2-3

SPECIMEN MATERIAL: Carbon Phenolic (Run 102)

PROFILE MEASUREMENTS

MEASURED BY A. C. Nedby

STATION	LOCATION INCHES	AFTER			
		BEFORE (1)	(2)	RECESSION (3)	CHAR (4)
1	EDGE	.604	.511	.491	.020
2	.2		.511	.495	.016
3	.4		.511	.499	.012
4	.6		.511	.503	.008
5	.8	.605	.512	.502	.010
6	1.0		.512	.504	.008
7	1.2		.512	.504	.008
8	1.4	.606	.513	.509	.004
9	1.6		.513	.505	.008
10	1.8		.513	.504	.009
11	2.0		.513	.508	.005
12	2.2	.607	.514	.510	.004
13	2.4		.514	.513	.001
14	2.6		.514	.514	.000
15	2.8	.605	.513	.504	.009
16	3.0		.513	.509	.004
17	3.2		.513	.510	.003
18	3.4	.605	.512	.511	.001
19	3.6		.512	.508	.004
20	3.8	.604	.511	.508	.003
21	4.0		.511	.508	.003
22	4.2	.603	.510	.507	.003
23	4.4		.510	.503	.007
24	4.6	.602	.509	.506	.003
25	4.8		.509	.505	.004
26	EDGE	.601	.508	.508	.000

REMARKS

- (1) Sample thickness including backing plate and bond
- (2) Sample thickness not including backing plate and bond
- (3) Sample thickness after recession not including backing plate and bond
- (4) Total recession

Backing plate: 2024-T3 aluminum 0.0625 in.

Bond: RTV-560

Weight before: 106.830 gm.

Weight after: 104.2676 gm.

Run No.		69-69	70-69	71-69	73-69	74-69	75-69	76-69
Specimen		Calibration	Calibration	Calibration	Calibration	Calibration	Calibration	Calibration
Run Time (low q/high q)	(sec)	10.2	27.0	251.6	71.4	91.6	78.7(52/26.7)	78.7(56)
Current	Amps	2360	2260	2280	2250	2220	2185	2320
Voltage	Volts	774	777	767	774	775	777	848
Power	kw	1827	1756	1749	1742	1720	1698	1967
Air Flow - IN	lb/sec	0.0600	0.0600	0.0600	0.0600	0.0600	0.0600	0.0600
- Exh		0.0286	0.0283	0.0265	0.0268	0.0269	0.0290	0.0165
- Nozz.		0.0314	0.0317	0.0335	0.0332	0.0331	0.0310	0.0435
Cooling Water	gpm	446	449	448	447	446	444	447
Flow	lb/sec	62.2	62.59	62.32	62.31	62.03	61.9	62.31
Cooling Water ΔT	$^{\circ}F$	19.7	23.7	22.6	24.4	25.1	23.6	26.5
Arc Power	btu/sec	1732	1659	1658	1651	1631	1610	1865
Energy Los		1225	1486	1500	1520	1457	1498	1651
Energy to Air		507	182	158	131	174	112	214
Air Enthalpy	btu/lb	15146	5741	4700	3546	5250	4800	4920
Plenum Press.	lb/in ² abs	50.45	49.45	49.0	5395	50.7	51	79.0
Plenum (2) Press.					14.7	19.4	14.7/33.8	13.9/5
Wall Press., Stn. 1							14.9/13.0	14.7/9
3							14.9/14.5	14.7/1
4							14.7/14.5	14.7/1
Wall Heat Transfer, Stn. 2 (btu/sec ft ²)							14.2/27.8	

(c) preliminary

A

75-69	76-69	77-69	79-69	80-69	82-69	85-69	86-69	87-69	89-69
Calibration	Calibration	Calibration	Calibration	Calibration	Calibration	Calibration	Calibration	Calibration	R2-1
7(52/26.7)	78.7(56/22.7)	89.2(43.6/45.6)	37.9(30.0/7.9)	130.6(26.7/103.9)	22.7(4/4/18.3)	21.0(11.0/10.0)	31.2(3.4/27.8)	32.0(2.4/29.6)	289.6(234.7)
85	2320	2000	2080	2100	2060	1920	1860	2040	2080
7	848	915	936	910	905	960	951	927	910
88	1967	1830	1947	1911	1864	1842	1769	1891	1890
0600	0.0600	0.0650	0.0650	0.0650	0.0650	0.0650	0.0650	0.0650	0.0650
0290	0.0165	0.0197	0.0195	0.0182	0.0195	0.0195	0.0195	0.0195	0.0156
0310	0.0435	0.0453	0.0455	0.0468	0.0455	0.0455	0.0455	0.0455	0.0494
4	447	444	444	446	444	443	443	444	444
1.9	62.31	61.9	61.9	62.17	61.9	61.5	61.5	61.6	61.7
3.6	26.5	25.4	25.8	25.2	26.04	25.3	23.04	25.0	25.00
10	1865	1735	1846	1801	1767	1749	1677	1793	1792
498	1651	1572	1597	1566	1612	1547	1413	1540	1543
12	214	163	249	1235	155	193	264	253	259
800	4920	3598	5473	5030	3410	4240	5810	5550	5240
1	79.0	92.5	94.0	95.0	91.2	97.9	97.95	90.0	90.0
4.7/33.8	13.9/52.3	13.6/59.5	14.0/52.9	13.8/57.0	13.8/58.0	13.8/55.0	13.2/52.5	15.2/54.5	13.0/63.
4.9/13.0	14.7/3.3	14.7/9.2	14.7/11.5	14.7/11.0	14.7/11.47	14.7/12.5	15.0/22.5	15.2/19.0	14.7/22
4.9/14.5	14.7/12.8	14.7/12.6	14.7/13.5	14.7/13.4	14.7/13.42	14.7/9.9	14.7/14.7	14.3/14.7	14.0/24
4.7/14.5	14.7/14.3	14.7/13.6	14.7/14.2	14.7/14.2	14.7/14.34	14.7/6.9	14.7/14.7	14.3/15.6	14.0/17
4.2/27.8		-/280		-/225 -/660 (Variable)	-/220 /245*,175*	-/121 -/128*,109*	26/445		

B

TABLE XI. ABLATION TEST RESULTS (UNCORRECTED)

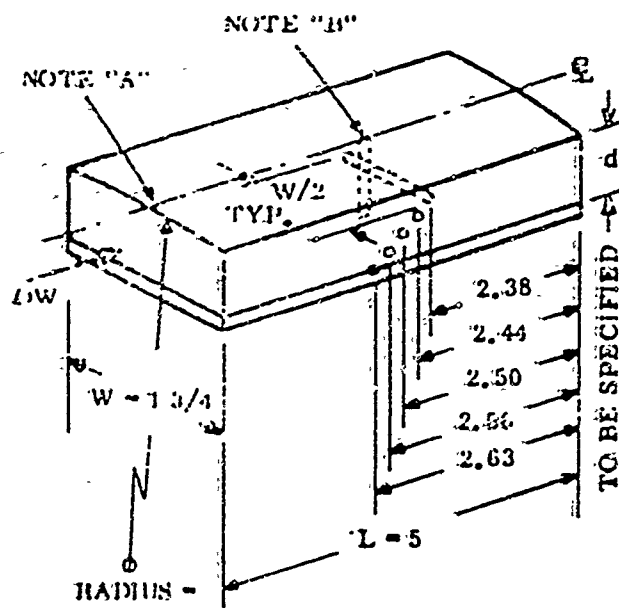
86-69	87-69	89-69	95-69	96-69	97-69	98-69	102-69	117-69
Calibration	Calibration	R2-1	R1-1	R2-2	R1-3	ATJ Graphite	R2-3	C2-1
31.2(3.4/27.8)	32.0(2.4/29.6)	289.6(234/55.6)	264.4(239/25.4)	175.6	288.7(239/50.7)	288.2(236.7/51.5)	254.5	249.3
1860	2040	2080	1940	1840	2140	2040	1740	2180
951	927	910	935	987	900	918	936	900
1769	1891	1890	1875	1816	1926	1873	1629	1962
0.0650	0.0650	0.0650	0.0650	0.0650	0.0650	0.0650	0.0650	0.0650
0.0195	0.0195	0.0156	0.0165	0.0195	0.0160	0.0160	0.0160	0.0155
0.0455	0.0455	0.0494	0.0485	0.0455	0.0490	0.0490	0.0490	0.0495
443	444	444	444	446	444	442	445	452
61.5	61.6	61.7	61.7	61.3	61.7	61.4	61.6	62.7
23.04	25.0	25.00	25.3	25.3	24.7	24.9	21.59	25.7
1677	1793	1792	1779	1723	1826	1776	1540	1860
1413	1540	1543	1560	1568	1524	1529	1330	1611
264	253	259	219	153	302	247	210	249
5810	5550	5240	4520	3420	6160	5082	4290	5040
97.95	90.0	90.0	101.2	103.0	96.5	105.7	102(p)	97.2(p)
13.2/52.5	15.2/54.5	13.0/63.0	13.5/64.0	13.7	13.6/50.6	13.6/52.8		
15.0/22.5	15.2/19.0	14.7/22.0	14.2/19.7	14.7	14.5/30.2	14.4/14.9		
14.7/14.7	14.3/14.7	14.0/24.5	14.3/35.0	14.5	14.5/14.5	14.4/15.9		
14.7/14.7	14.3/15.6	14.6/17.5	14.1/25.1	14.7	15.0/14.5	14.6/15.5		
26/445								

TABLE XII. SPECIMEN R1-4 MODEL MEASUREMENTS

AFML-TR-70-95

Part I

ABRICATION



NOTE "A"

STATION 1 IS INDICATED. READ ALL
LOCATIONS ON MODEL PROFILE FROM
THIS STATION

NOTE "B"

BERT TUNGSTEN WIRE VERTICALLY
THRU SPECIMEN ON CENTERLINE

NOTE "C"

OVERMARK DIMENSIONAL VARIATIONS

HOLE LOCATIONS

NO	NOMINAL	ACTUAL (INCHES)
1	1/5	
2	21/5	
3	31/5	
4	41/5	
5	5	

MODEL INSTRUMENTATION
INSTALLER

NO	WIRE		CONFIRMED DEPTH, (INCHES)
	GA	TYPE	
1	36	C/A	.103
2	36	C/A	.184
3	36	C/A	.271
4	36	C/A	.375
5	36	C/A	.500

SPECIMEN CODE: R1-4

SPECIMEN MATERIAL: Silica-Phenolic (Run 129)

PROFILE MEASUREMENTS

MEASURED BY Neddy

STATION	LOCATION INCHES	BEFORE (1)	AFTER	
			RECESSION	CHAR
1	0	570	557	.013
2			553	.017
3			540	.030
4		572	526	.056
5			508	.064
6		572	537	.067
7			494	.079
8		560	480	.070
9			482	.078
10			486	.077
11		560	484	.076
12			478	.082
13			458	.102
14		559	458	.101
15			457	.102
16		558	462	.096
17			468	.090
18		555	475	.080
19			478	.077
20			488	.063
21		553	473	.080
22			475	.078
23			487	.066
24		553	491	.062
25			503	.050
26	5	555	534	.021

Overall Refractory Layer Thickness .014

Remarks

(1) Sample thickness including backing plate
and bond

Pretest measurements every 0.50 inch
Post test measurements every 0.20 inch

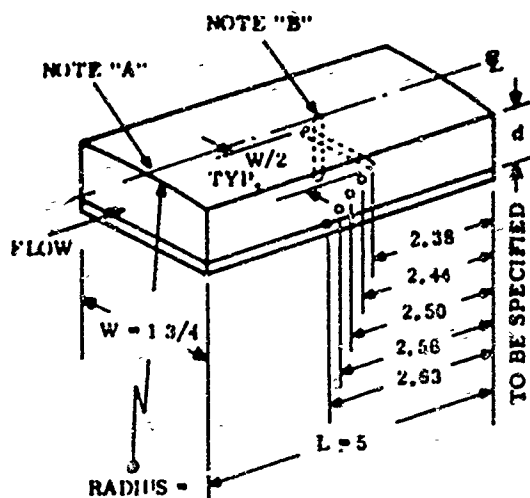
Backing Plate: 2024-T3 aluminum, 0.0625 in.

Weight Before: 146.967 gm

Weight After: 136.872 gm

TABLE XIII. SPECIMEN R2-3 MODEL MEASUREMENTS

FABRICATION:



NOTE "A"
STATION 1 IS INDICATED. READ ALL LOCATIONS ON MODEL PROFILE FROM THIS STATION

NOTE "B"
INSERT TUNGSTEN WIRE VERTICALLY THRU SPECIMEN ON CENTERLINE

NOTE "C"
OVERMARK DIMENSIONAL VARIATIONS

WIRE LOCATIONS

NO	NOMINAL	ACTUAL (INCHES)
1	d/5	
2	2d/5	
3	3d/5	
4	4d/5	
5	d	

MODEL INSTRUMENTATION
INSTALLER A. C. Nedby

NO	WIRE		CONFIRMED DEPTH (INCHES)
	GA	TYPE	
1	36	C/A	.148
2	36	C/A	.203
3	36	C/A	.295
4	36	C/A	.412
5	36	C/A	.500

Photographed

SPECIMEN CODE: R2-3

SPECIMEN MATERIAL: Carbon Phenolic (Run 102)

PROFILE MEASUREMENTS

MEASURED BY A. C. Nedby

STATION	LOCATION INCHES	AFTER			
		BEFORE (1)	(2)	RECESSION (3)	CHAR (4)
1	EDGE	.604	.511	.491	.020
2	.2		.511	.495	.016
3	.4		.511	.499	.012
4	.6		.511	.503	.008
5	.8	.605	.512	.502	.010
6	1.0		.512	.504	.008
7	1.2		.512	.504	.008
8	1.4	.606	.513	.509	.004
9	1.6		.513	.505	.008
10	1.8		.513	.504	.009
11	2.0		.513	.508	.005
12	2.2	.607	.514	.510	.004
13	2.4		.514	.513	.001
14	2.6		.514	.514	.000
15	2.8	.606	.513	.504	.009
16	3.0		.513	.509	.004
17	3.2		.513	.510	.003
18	3.4	.605	.512	.511	.001
19	3.6		.512	.508	.004
20	3.8	.604	.511	.508	.003
21	4.0		.511	.508	.003
22	4.2	.603	.510	.507	.003
23	4.4		.510	.503	.007
24	4.6	.602	.509	.506	.003
25	4.8		.509	.505	.004
26	EDGE	.601	.508	.508	.000

REMARKS

- (1) Sample thickness including backing plate and bond
- (2) Sample thickness not including backing plate and bond
- (3) Sample thickness after recession not including backing plate and bond
- (4) Total recession

Backing plate: 2024-T3 aluminum 0.0625 in.

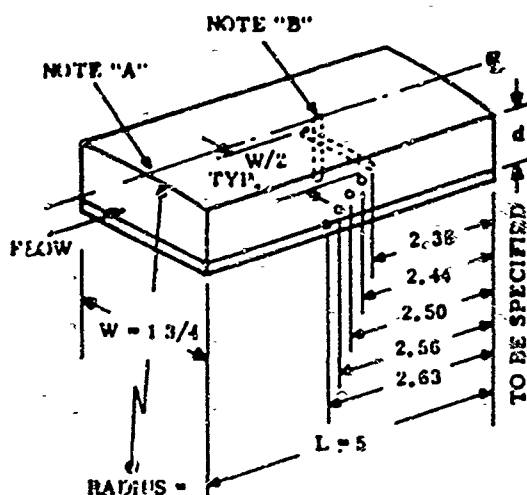
Bond: RTV-560

Weight before: 106.8830 gm.

Weight after: 104.2676 gm.

TABLE XIII. SPECIMEN R2-3 MODEL MEASUREMENTS

FABRICATION:



NOTE "A"

STATION 1 IS INDICATED. READ ALL LOCATIONS ON MODEL PROFILE FROM THIS STATION

NOTE "B"

INSERT TUNGSTEN WIRE VERTICALLY THRU SPECIMEN ON CENTERLINE

NOTE "C"

OVERMARK DIMENSIONAL VARIATIONS

HOLE LOCATIONS

NO	NOMINAL	ACTUAL (INCHES)
1	1/5	
2	21/5	
3	31/5	
4	41/5	
5	1	

MODEL INSTRUMENTATION

INSTALLER A. C. Nedby

NO	WIRE		CONFIRMED DEPTH (INCHES)
	GA	TYPE	
1	36	C/A	.148
2	36	C/A	.203
3	36	C/A	.295
4	36	C/A	.412
5	36	C/A	.500

Photographed

SPECIMEN CODE: R2-3

SPECIMEN MATERIAL: Carbon Phenolic (Run 102)

PROFILE MEASUREMENTS

MEASURED BY A. C. Nedby

STATION	LOCATION INCHES	BEFORE		AFTER		CHAR
		(1)	(2)	(3)	(4)	
1	EDGE	.604	.511	.491	.020	
2	.2		.511	.495	.016	.066
3	.4		.511	.499	.012	.079
4	.6		.511	.503	.008	.062
5	.8	.605	.512	.502	.010	.061
6	1.0		.512	.504	.008	.062
7	1.2		.512	.504	.008	.070
8	1.4	.606	.513	.509	.004	.073
9	1.6		.513	.505	.008	.075
10	1.8		.513	.504	.009	.069
11	2.0		.513	.508	.005	.079
12	2.2	.607	.514	.510	.004	.075
13	2.4		.514	.513	.001	.072
14	2.6		.514	.514	.000	.061
15	2.8	.608	.513	.504	.009	.057
16	3.0		.513	.509	.004	.068
17	3.2		.513	.510	.003	.059
18	3.4	.605	.512	.511	.001	.061
19	3.6		.512	.508	.004	.055
20	3.8	.604	.511	.508	.003	.051
21	4.0		.511	.508	.003	.060
22	4.2	.603	.510	.507	.003	.050
23	4.4		.510	.503	.007	.045
24	4.6	.602	.509	.506	.003	.040
25	4.8		.509	.505	.004	.038
26	EDGE	.601	.508	.508	.000	.012

REMARKS

- (1) Sample thickness including backing plate and bond
- (2) Sample thickness not including backing plate and bond
- (3) Sample thickness after recession not including backing plate and bond
- (4) Total recession

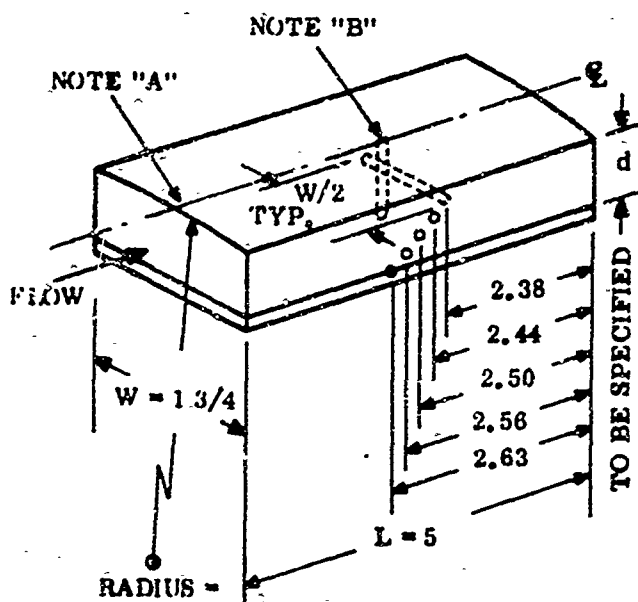
Backing plate: 2024-T3 aluminum 0.0625 in.

Bond: RTV-560

Weight before: 106.8830 gm.

Weight after: 104.2676 gm.

FABRICATION:



NOTE "A"
STATION 1 IS INDICATED. READ ALL
LOCATIONS ON MODEL PROFILE FROM
THIS STATION

NOTE "B"
INSERT TUNGSTEN WIRE VERTICALLY
THRU SPECIMEN ON CENTERLINE

NOTE "C"
OVERMARK DIMENSIONAL VARIATIONS

HOLE LOCATIONS

NO	NOMINAL	ACTUAL (INCHES)
1	$d/5$	
2	$2d/5$	
3	$3d/5$	
4	$4d/5$	
5	d	

MODEL INSTRUMENTATION INSTALLER

NO	WIRE		CONFIRMED DEPTH, (INCHES)
	GA	TYPE	
1	36	C/A	.110
2	36	C/A	.218
3	36	C/A	.316
4	36	C/A	.432
5	36	C/A	.510

SPECIMEN CODE: R2-4

SPECIMEN MATERIAL: CARBON-PHENOLIC (RUN 134)

PROFILE MEASUREMENTS
MEASURED BY NEDBY

STATION	LOCATION INCHES	BEFORE (1)	AFTER		
			RECESSION	CHAR	
1	0	.575	.571	.004	
2			.531	.044	.212
3			.521	.054	.214
4		.575	.514	.061	.237
5			.519	.056	.269
6		.577	.524	.053	.270
7			.524	.053	.275
8		.578	.524	.054	.268
9			.526	.052	.285
10			.521	.056	.275
11		.578	.534	.044	.292
12			.526	.052	.289
13			.521	.057	.285
14		.578	.523	.055	.286
15			.523	.055	.286
16		.577	.491	.086	.251
17			.490	.087	.249
18		.577	.509	.068	.264
19			.517	.060	.265
20			.516	.061	.241
21		.575	.517	.058	.244
22			.521	.054	.244
23			.520	.055	.208
24		.575	.523	.052	.195
25			.520	.055	.181
26	5	.574	.520	.054	.121

REMARKS

(1) **SAMPLE THICKNESS INCLUDING BACKING
PLATE AND BOND**

PRE-TEST MEASUREMENTS EVERY 0.50 INCH

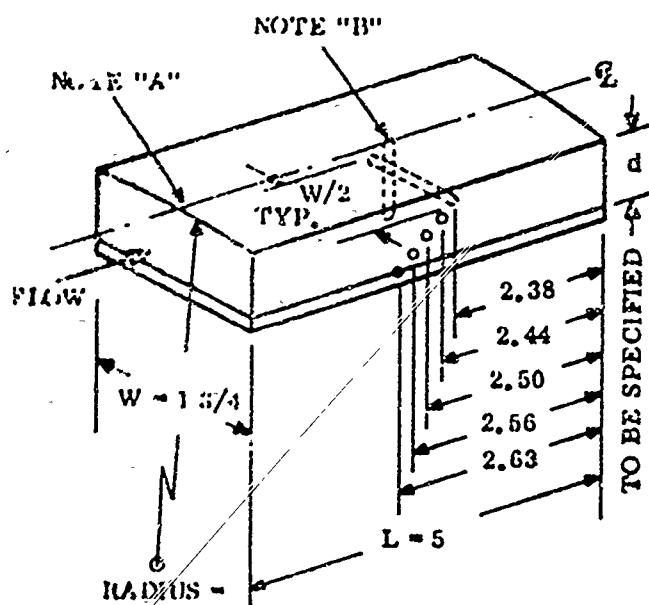
POST-TEST MEASUREMENTS EVERY 0.20 INCH

BACKING PLATE: 2024-T3 ALUMINUM, 0.0625 INCH

WEIGHT BEFORE: 133.5590 gm

WEIGHT AFTER: 118.0650

FABRICATION:



STATION 1 IS INDICATED. READ ALL
LOCATIONS ON MODEL PROFILE FROM
THIS STATION

INSERT TUNGSTEN WIRE VERTICALLY
THRU SPECIMEN ON CENTERLINE

OVERMARK DIMENSIONAL VARIATIONS

HOLE LOCATIONS

NO	NOMINAL	ACTUAL (INCHES)
1	d/5	
2	2d/3	
3	3d/5	
4	4d/5	
5	d	

MODEL INSTRUMENTATION INSTALLER

NO)	WIRE		CONFIRMED DEPTH, (INCHES)
	GA	TYPE	
1	36	C/A	.100
2	36	C/A	.198
3	36	C/A	.285
4	36	C/A	.405
	36	C/A	.475

SPECIMEN MATERIAL: Carbon-Phenolic

MEASURED BY Nearby

STATION	LOCATION INCHES	BEFORE (1)	AFTER		
			RECESSION	CHAR	
1	0	556	540	.016	
2			462	.094	.183
3			399	.157	.173
4		554	372	.182	.157
5			419	.135	.207
6		550	400	.150	.197
7			376	.174	.183
8		550	383	.167	.189
9			391	.159	.188
10			399	.151	.190
11		549	418	.131	.207
12			430	.119	.213
13			441	.108	.211
14		551	443	.108	.218
15			453	.098	.223
16		554	453	.101	.226
17			452	.102	.224
18		556	455	.103	.216
19			458	.088	.222
20			480	.076	.231
21		556	481	.075	.226
22			481	.075	.219
23			480	.076	.219
24		558	483	.075	.219
25			486	.072	.208
26	5	558	490	.068	.166

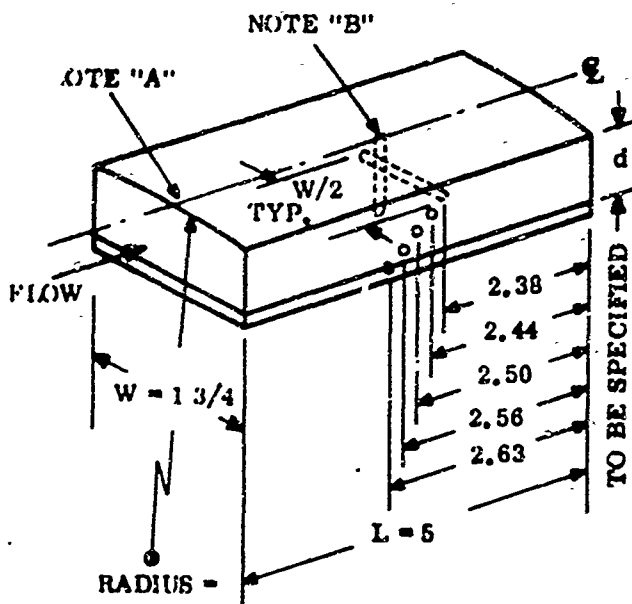
Remarks:

(1) Sample Thickness including backing plate and bond.

Pre test measurements every 0.50 inch
Post test measurements every 0.20 inch

Backing Plate: 2024-Tc Aluminum, 0.0625 inch
Weight Before: 124.97 gm
Weight After: 103.636 gm

FABRICATION:



STATION 1 IS INDICATED. READ ALL
LOCATIONS ON MODEL PROFILE FROM
THIS STATION

**INSERT TUNGSTEN WIRE VERTICALLY
THRU SPECIMEN ON CENTERLINE**

OVERMARK DIMENSIONAL VARIATIONS

HOLE LOCATIONS

NO	NOMINAL	ACTUAL (INCHES)
1	$d/5$	
2	$2d/5$	
3	$3d/5$	
4	$4d/5$	
5	d	

MODEL INSTRUMENTATION INSTALLER

NO	WIRE		CONFIRMED DEPTH, (INCHES)
	GA	TYPE	
1	36	C/A	.085
2	36	C/A	.200
3	36	C/A	.280
4	36	C/A	.400
5	36	C/A	.502

SPECIMEN MATERIAL: CARBON-PHENOLIC (RUN 133)

MEASURED BY NEDBY

STATION	LOCATION INCHES	BEFORE (1)	AFTER		
			RECESSION	CHAR	
1	0	571	.539	.032	.104
2			.479	.092	.253
3			.410	.161	.219
4		571	.381	.190	.190
5			.366	.205	.169
6		572	.453	.119	.241
7			.441	.131	.204
8		572	.427	.145	.262
9			.425	.147	.233
10		571	.445	.126	.244
11			.452	.119	.246
12			.394	.177	.249
13			.473	.098	.256
14		570	.472	.098	.252
15			.478	.092	.252
16		570	.483	.087	.236
17			.472	.098	.241
18		568	.462	.105	.229
19			.494	.074	.254
20			.499	.069	.256
21		568	.488	.080	.250
22			.487	.081	.251
23			.492	.076	.256
24		567	.496	.071	.229
25			.505	.062	.222
26	5	567	.531	.036	.174

REMARKS

(1) SAMPLE THICKNESS INCLUDING BACKING
PLATE AND BOND

PRE-TEST MEASUREMENTS EVERY 0.50 INCH

POST-TEST MEASUREMENTS EVERY 0.20 INCH

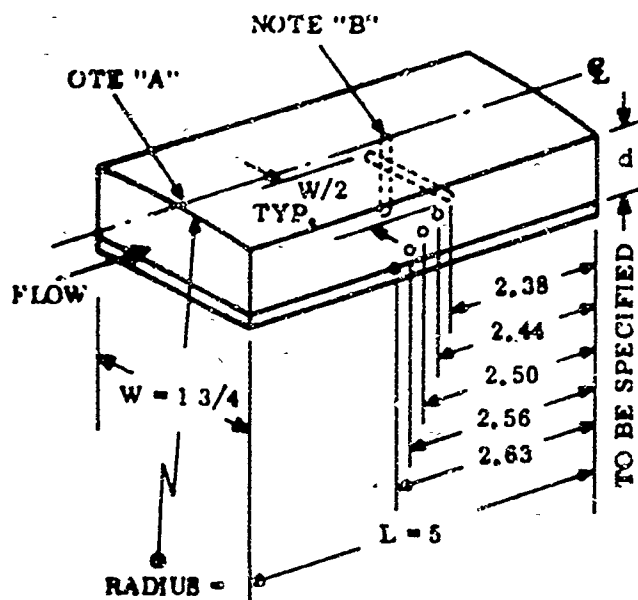
BACKING PLATE 2024-T3 ALUMINUM, 0.0625 INCH

WEIGHT BEFORE: 120.6395 gm

WEIGHT AFTER: 98.7125 gm

TABLE XVII. SPECIMEN A2-1 MODEL MEASUREMENTS

FABRICATION.



STATION 1 IS INDICATED. READ ALL
LOCATIONS ON MODEL PROFILE FROM
THIS STATION

INSERT TUNGSTEN WIRE VERTICALLY
THRU SPECIMEN ON CENTERLINE

OVERMARK DIMENSIONAL VARIATIONS

HOLE LOCATIONS

NO	NOMINAL	ACTUAL (INCHES)
1	d/5	096
2	2d/5	192
3	3d/5	288
4	4d/5	384
5	d	.475

MODEL INSTRUMENTATION INSTALLER

NO	WIRE		CONFIRMED DEPTH, (INCHES)
	GA	TYPE	
1	36	C/A	082
2	36	C/A	.208
3	36	C/A	.298
4	36	C/A	.392
5	36	C/A	458

SPECIMEN CODE: A2-1 (RUN 138)

SPECIMEN MATERIAL: SILICA-PHENOLIC.

PROFILE MEASUREMENTS

MEASURED BY NEDBY

STATION	LOCATION INCHES	BEFORE (1)	AFTER		
			RECESSION	CHAR	
1	0	562	535	.027	177
2	.2		559	.003	226
3	.4		550	.012	225
4	.6	556	533	.023	223
5	.8		525	.031	211
6	1.0	552	523	.029	200
7	1.7		496	.056	196
8	1.0	547	476	.071	181
9	1.6		459	.088	173
10	1.8		469	.078	172
11	2.0	544	483	.061	182
12	2.2		472	.072	180
13	2.4		448	.096	161
14	2.6	542	443	.099	149
15	2.8		445	.097	155
16	3.0	543	453	.090	158
17	3.2		457	.086	163
18	3.4	546	454	.092	146
19	3.6		461	.085	145
20	3.8		469	.077	157
21	4.0	550	479	.071	166
22	4.2		487	.063	172
23	4.4		490	.060	177
24	4.6	556	488	.068	177
25	4.8		498	.058	181
26	5.0	558	512	.046	181

REMARKS

(1) SAMPLE THICKNESS INCLUDING BACKING
PLATE AND BOND

PRE-TEST MEASUREMENTS EVERY 0.50 INCH

POST-TEST MEASUREMENTS EVERY 0.20 INCH

BACKING PLATE. 2024-T3 ALUMINUM. 0.0625 INCH

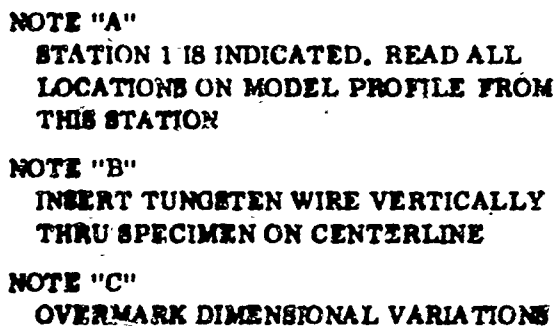
WEIGHT BEFORE: 140.8835 gm

WEIGHT AFTER: 132.1890 gm

AFML-TR-70-95
Part I

SPECIMEN CODE: A4-2A

PROFILE MEASUREMENTS
MEASURED BY _____



NO	NOMINAL	ACTUAL (INCHES)
1	d/5	.086
2	2d/5	.172
3	3d/5	.258
4	4d/5	.344
5	d	.428

NO	WIRE		CONFIRMED DEPTH, (INCHES)
	GA	TYPE	
1	36	C/A	.072
2	36	C/A	.186
3	36	C/A	.246
4	36	C/A	.336
5	36	C/A	.414

STATION	LOCATION INCHES	BEFORE		AFTER			
		(1)	(2)	RECESSION		CHAR	
1	0	.492	.491	.021	.470	-	
2				.070	.421	.231	
3				.090	.401	.274	
4		.493	.486	.092	.394	.298	
5				.092	.394	.331	
6		.493	.481	.087	.394	.331	
7				.086	.395	.332	
8		.492	.476	.096	.380	.314	
9				.116	.350	.293	
10		.492	.472	.118	.354	.286	
11				.128	.344	.273	
12				.139	.333	.262	
13				.147	.325	.251	
14		.491	.472	.154	.318	.244	
15				.157	.315	.243	
16		.497	.475	.169	.306	.239	
17				.229	.246	.246	
18		.491	.476	.204	.272	.207	
19				.202	.274	.206	
20				.132	.344	.281	
21		.490	.479	.122	.357	.289	
22				.121	.358	.292	
23				.128	.351	.285	
24		.490	.484	.126	.355	.278	
25				.119	.365	.256	
26	5	.490	.488	.124	.364	.215	

- (1) SAMPLE THICKNESS INCLUDING BACKING
PLATE AND BOND
- (2) THICKNESS DIMENSIONS AFTER MILLING OF
BOWED SAMPLE

PRE-TEST MEASUREMENTS EVERY 0.50 INCH

POST-TEST MEASUREMENTS EVERY 0.20 INCH

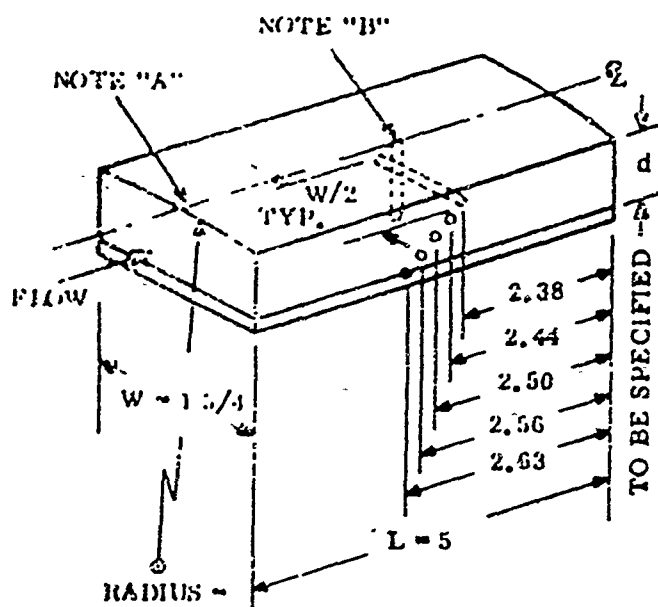
BACKING PLATE: 2024-T3 ALUMINUM, 0.0625 INCH

WEIGHT BEFORE: 126 6592 gm

WEIGHT AFTER: 106.3778 gm

TABLE XIX. SPECIMEN CI-1 MODEL MEASUREMENTS

REMARKS.



NOTE "A"
IF FROM 1 IS INDICATED, READ ALL
LOCATIONS ON MODEL PROFILE FROM
THIS STATION

NOTE "H"
INSERT TUNGSTEN WIRE VERTICALLY
THRU SPECIMEN ON CENTERLINE

NOTE "C"
OVERMARK DIMENSIONAL VARIATIONS

HOLE LOCATIONS

NO	NOMINAL	ACTUAL (INCHES)
1	d/5	
2	2d/5	
3	3d/5	
4	4d/5	
5	d	

MODEL INSTRUMENTATION INSTALLER

NO	WIRE		CONFIRMED DEPTH, (INCHES)
	GA	TYPE	
1	36	C/A	.128
2	36	C/A	.262
3	36	C/A	.481
	36	C/A	.506
6	36	C/A	.606

SPECIMEN CODE: CI-1

SPECIMEN MATERIAL: Carbon-Phenolic Composite
(Run 126)

PROFILE MEASUREMENTS
MEASURED BY Nedby

STATION	LOCATION INCHES	BEFORE (1)	AFTER	
			RECESSION	CHAR
1	0	753	741	.012
2			677	.076
3			624	.129
4		753	594	.159
5			589	.164
6		754	600	.154
7			608	.146
8		754	607	.147
9			619	.135
10			636	.118
11		754	648	.106
12			660	.094
13			673	.081
14		754	691	.063
15			700	.054
16		755	711	.044
17	W WIRE		691	.064
18		755	676	.079
19			672	.083
20			688	.071
21		755	691	.064
22			695	.060
23			707	.048
24		755	700	.055
25			704	.051
26	5	753	698	.055

Note - No char figures shown as model is approx. complete charred.

Remarks:

(1) Sample thickness including backing plate and bond.

Pretest measurements every 0.50 inch
Post test measurements every 0.20 inch

Backing Plate: 2024-T3 Aluminum, 0.0625 inch
Weight Before: 122.358 gm
Weight After: 101.277 gm

Part I

NOTE "A"

NOTE "B"

W/2

W = 1 1/4

FLOW

RADIUS

L = 5

2.38

2.44

2.50

2.56

2.63

TO BE SPECIFIED

NOTE: "C"
OVERMARK DIMENSIONAL VARIATIONS

NO	NOMINAL	ACTUAL (INCHES)
1	d/	
2	2d/	
3	3d/	
4	4d/	
5	d	

NO	WIRE		CONFIRMED DEPTH, (INCHES)
	GA	TYPE	
1	36	C/A	.160
2	36	C/A	.298
3	36	C/A	.438
4	36	C/A	.554
	36	C/A	.660

MEASURED BY Nedby

[illegible]

Backing Plate: 2024-T3 aluminum, 0.0625 inch
Weight Before: 133.901 gm
Weight After: 121.072 gm

Part I

SPECIMEN MATERIAL: Silica Phenolic Composite
(run 117)

MEASURED BY Mediv



NO	NOMINAL	ACTUAL (INCHES)
1	$d/5$	
2	$2d/5$	
3	$3d/5$	
4	$4d/5$	
5	d	

NO	WIRE		CONFIRMED DEPTH, (INCHES)
	GA	TYPE	
1	30	C/A	.137
2	36	C/A	.259
3	36	C/A	.439
4	36	C/A	.498
5	36	C/A	.556

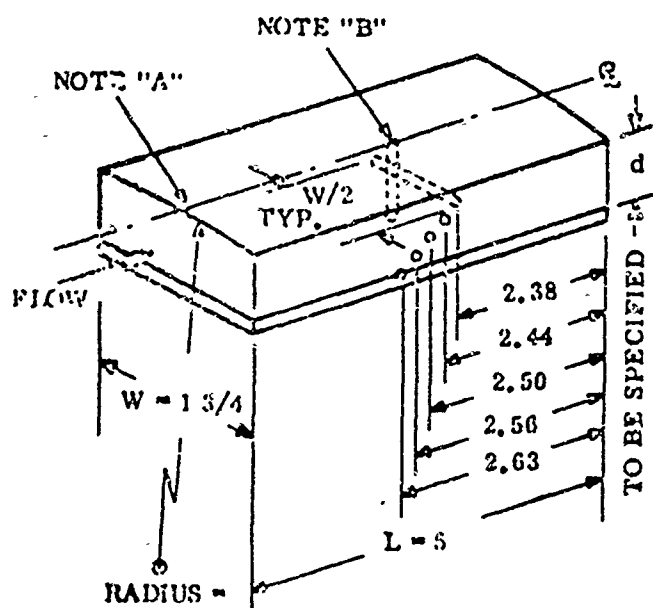
[illegible]

Overall refractory layer thickness .017"

(1) Sample thickness including backing, plate and bond

Pretest measurements every 0.50 inch
Post test measurements every 0.20 inch

Backing plate: 2024-Tc aluminum, 0.0025 in.
Weight Before: 130.588 gm
Weight After: 125.246 gm



STATION 1 IS INDICATED. READ ALL
LOCATIONS ON MODEL PROFILE FROM
THIS STATION

INSERT TUNGSTEN WIRE VERTICALLY
THRU SPECIMEN ON CENTERLINE

OVERMARK DIMENSIONAL VARIATIONS

HOLE LOCATIONS

NO	NOMINAL	ACTUAL (INCHES)
1	$d/5$	
2	$2d/5$	
3	$3d/5$	
4	$4d/5$	
5	d	

MODEL INSTRUMENTATION INSTALLER

NO	WIRE		CONFIRMED DEPTH, (INCHES)
	GA	TYPE	
1	36	C/A	.121
2	36	C/A	.237
3	36	C/A	.362
4	36	C/A	.481
5	36	C/A	.547

SPECIMEN MATERIAL: Silica Phenolic Composites

PROFILE MEASUREMENTS

MEASURED BY Nedby

STATION	LOCATION INCHES	BEFORE (1)	AFTER	
			RECESSION	CHAR
1	0	702	691	.011 698 013
2			701	.001 221 007
3			678	.024 222 009
4		701	669	.032 233 007
5			650	.051 218 003
6		701	657	.044 227 003
7			646	.055 209 004
8		702	647	.055 224 004
9			639	.063 208 005
10			646	.056 216 010
11		702	635	.067 204 005
12			636	.066 196 006
13			635	.069 195 00
14		204	642	.062 202 006
15			657	.047 195 010
16		707	679	.028 224 003
17			701	.006 227 008
18		708	709	.001 236 003
19			709	.001 231 005
20		709	709	.001 234 002
21		709	709	.000 228 005
22			722	.013 231 013
23			721	.012 222 007
24		707	726	.017 212 015
25			729	.020 187 007
26		708	721	.017 118 005

Remarks

(1) Sample thickness including backing, plate and bond

Pretest measurements every 0.50 inch

Post test measurements every 0.20 inch

Back ing plate: 2024-T3 Aluminum, 0.0625 inch

Weight before: 131.464 gm

Weight after: 124.808 gm

TABLE XXIV. ABLATION TEST RESULTS REFERENCE TEST SPECIMENS

MATERIAL ^①	S/P	S/P	S/P	C/P	C/P	C/P	C/P	C ₁ /P ₁
SAMPLE NO.	R1-1	R1-3	R1-4	R2-1	R2-2	R2-3	R2-4	R3-6
RUN NO.	95 ^②	97 ^③	129 ^④	89 ^⑤	96 ^⑥	102 ^⑦	134 ^⑧	130 ^④
RUN TIME (Low \dot{q} /High \dot{q}), sec	239/25	238/51	243/48	234/56	176/-	255/-	242/51	243/52
CURRENT, amp	1940	2140	2085	2080	1840	1800	2180	1940
VOLTAGE, volt	935	900	822	910	987	924	870	942
POWER, kw	1875	1926	1797	1890	1816	1663	1888	1827
AIR FLOW - in, lb/sec	.0650	.0650	.0650	.0650	.0650	.0650	.0650	.0650
AIR FLOW - exh, lb/sec	.0165	.0160	.0163	.0156	.0195	.0160	.0152	.0134
AIR FLOW - nozz., lb/sec	.0485	.0490	.0487	.0494	.0455	.0490	.0498	.0486
COOLING WATER, gal/min	444	444	449	444	446	445	452	449
FLOW, lb/sec	61.7	61.7	62.2	61.7	61.9	61.6	62.7	62.3
COOLING WATER ΔT , °F	25.3	24.7	23.7	25.0	25.3	21.6	24.7	24.3
ARC POWER, BTU/sec	1779	1826	1695	1792	1723	1573	1792	1732
ENERGY LOSS, BTU/sec	1560	1524	1475	1543	1568	1330	1548	1514
ENERGY TO AIR, BTU/sec	219	302	220	259	155	243	244	218
AIR ENTHALPY, BTU/lb	4520	6160	4540	5240	3420	4980	4900	4486
PLENUM PRESSURE, psia	101	96.5	98	90	193	98.4	82.5	100
PLENUM (2) PRESSURE, psia	13/64	14/51	15/61	13/63	14/-	14/-	15/59	14/59
WALL PRESSURE, St. 1, psia	14/20	15/30	15/38	15/22	15/-	12/-	15/13	15/17
WALL PRESSURE, Sp. 3, psia	14/35	15/15	15/29	14/25	15/-	15/-	14/11	14/16
WALL PRESSURE, Sp. 4, psia	14/25	15/15	15/-	14/18	15/-	15/-	15/9	14/14
HEAT FLUX (calc'd), BRU/ft ² -sec	21.2/ 390	27/ 470	21.4/ 276	③	16.5	23.3	23.0/ 255	21.0/ 312
Integrated Heat Flux BTU/ft ²								
Low \dot{q} Portion	5060	6430	5200		2810	5930	5560	5100
High \dot{q} Portion	9750	23950	13230				13010	16220
Total Heat	14810	30380	18430		2810	5930	18570	21320

- 1 - S/P = silica/phenolic, C100-48/USP 95
C/P = carbon/phenolic, CCA1-1641/USP 95
C₁/P₁ = carbon/phenolic, Pluton B1/DP2510
- 2 - Pressure hose failure
- 3 - Failure of insulator causing lateral leakage
- 4 - Good design data run
- 5 - Bypass tube rupture added water to mass flow
- 6 - Erosion of anode of arc heater and arc was extinguished by coolant water
- 7 - Bypass plug did not seat properly
- 8 - Mass addition to flow due to water makes \dot{q} evaluation uncertain

TABLE XXV. ABLATION TEST RESULTS LDQ COMPOSITE TEST SPECIMENS

MATERIAL ^①	C/P-LDQ	C ₁ /P ₁ -LDQ	C ₁ /P ₁ -LDQ	S/P-LDQ	S/P-LDQ
SAMPLE NO.	C1-1	C2-1	C2-2	C3-1	C3-2
RUN NO.	126 ^②	131 ^③	132 ^②	117 ^④	127 ^②
RUN TIME (Low q/High q), sec	244/54	244/50	244/50	244/16	245/50
CURRENT, amp	1940	2040	2080	2280	1880
VOLTAGE, volt	942	942	894	894	942
POWER, kw	1827	1922	1859	2038	1771
AIR FLOW - in, lb/sec	.0650	.0650	.0650	.0650	.0650
AIR FLOW - exh., lb/sec	.0157	.0154	.0154	.0155	.0164
AIR FLOW - nozz., lb/sec	.0493	.0496	.0496	.0495	.0486
COOLING WATER, gal/min	442	448	448	452	455
FLOW, lb/sec	61.3	62.1	62.3	62.7	63.1
COOLING WATER ΔT , °F	24.1	24.9	24.7	26.7	23.2
ARC POWER, BTU/sec	1732	1822	1762	1932	1679
ENERGY LOSS, BTU/sec	1478	1549	1539	1671	1462
ENERGY TO AIR, BTU/sec	254	273	223	261	217
AIR ENTHALPY, BTU/lb	5160	5500	4487	5273	4460
PLENUM PRESSURE, psia	100	110	90	94.7	102
PLENUM (2) PRESSURE, psia	15/58	14/63	14/62	14/57	15/62
WALL PRESSURE, St. 1, psia	15/30	15/34	15/18	15/31	15/36
WALL PRESSURE, Sp. 3, psia	15/22	14/26	14/18	15/21	15/30
WALL PRESSURE, Sp. 4, psia	15/17	15/18	15/15	15/16	15/22
HEAT FLUX (calc'd), BTU/ft ² -sec	25.1/442	⑤	21.1/260	24.8/383	21.7/396
Integrated Heat Flux BTU/ft ²					
Low q Portion	6120		5150	6300	5310
High q Portion	23900		13000	6130	19600
Total Heat	30020		18150	12430	24910

- 1 - C/P-LDQ = carbon/phenolic, CCA1-1641/USP 95-low density quartz
C₁/P₁-LDQ = carbon/phenolic, Pluton B1/DP-2510-low density quartz
S/P-LDQ = silica/phenolic, C100-48/USP95-low density quartz
- 2 - Good design data run
- 3 - Abortive run due to leak in bypass valve
- 4 - Aborted run due to insulator failure
- 5 - Mass addition to flow due to water makes q evaluation uncertain

TABLE XXVI. ABLATION TEST RESULTS EXPERIMENTAL TEST SPECIMENS

MATERIAL	C ₂ /P ₁	S/P ₁	C/I	Graphite
SAMPLE NO.	A1-2	A2-1	A4-2A	ATJ
RUN NO.	133	135	138	98
RUN TIME (Low \dot{q} /High \dot{q}), sec	248/52	241/49	240/52	238/52
CURRENT, amp	1980	2000	2160	2040
VOLTAGE, volt	915	900	888	918
POWER, kw	1822	1800	1918	1873
AIR FLOW - in, lb/sec	.0650	.0650	.0650	.0650
AIR FLOW - exh., lb/sec	.0153	.0151	.0170	.0160
AIR FLOW - nozz., lb/sec	.0497	.0499	.0480	.0490
COOLING WATER, gal/min	449	452	450	442
FLOW, lb/sec	62.2	62.7	62.4	61.4
COOLING WATER ΔT , °F	23.4	23.7	25.4	24.9
ARC POWER, BTU/sec	1728	1766	1818	1776
ENERGY LOSS, BTU/sec	1461	1485	1584	1529
ENERGY TO AIR, BTU/sec	267	281	232	247
AIR ENTHALPY, BTU/lb	5180	5630	4830	5082
PLENUM PRESSURE, psia	90.2	87.7	84.0	105.7
PLENUM (2) PRESSURE, psia	14/63	15/61	12/41	14/53
WALL PRESSURE, St. 1, psia	15/18	15/39	15/10	15/15
WALL PRESSURE, Sp. 3, psia	15/12	14/20	14/9	14/16
WALL PRESSURE, Sp. 4, psia	14/13	15/13	15/13	15/16
HEAT FLUX (calc'd), BTU/ft ² -sec	24.4/ 333	27.1/ 368	20.9/ 321	23.4/ 390
Integrated Heat Flux BTU/ft ²				
Low \dot{q} Portion	6050	6530	5020	5570
High \dot{q} Portion	17300	17920	16690	20380
Total Heat	23350	24450	21710	25950

C₂/P₁ = carbon/phenolic, VCX/DP-2510S/P₁ = silica/phenolic, C100-48/DP-2510

C/I = carbon/polyimide, CCA1-9641/Skybond 700

Model	R1-1	R2-2	R1-3	ATJ	R2-3	C3-1*	C1-1	C3-
Run No.	95	96	97	98	102	117	126	127
\dot{q}_1 (cw)	21.1	16.5	27.0	23.4	23.3	24.8	25.1	21.1
\dot{q}_2 (cw)	390	-	470	390	-	383	442	396
h_s	4520	3420	6160	5082	4980	5273	5160	446
$T_{s1}^{\circ R}$	2300	2250	2180	2650	2280	2600	2000	250
$T_{s2}^{\circ R}$	4000	-	5100	4300	-	4500	3800	435
h_{w1}	580	570	560	630	580	670	570	670
h_{w2}	1110	-	1540	1350	-	1290	1040	123
Δh_1	3940	2850	5600	4452	4400	4603	4590	379
Δh_2	3410	-	4620	3732	-	3983	4120	328
t (sec)	239/25	176	238/51	238/52	255	244/16	244/54	245
$\int sdt$ (mils)	90	13	41	37	9.5	7.0	106	68
q^*_1	9020	15300	26500 \neq	24700	22800	60600	20600	165
q^*_2	7820		21900	20750		52400	18600	139

* High q^* resulted from lateral blow-by

\neq Values Affected by Unusually High Enthalpy

NOTE: Runs 89, 131 Omitted-water added to mass flow; evaluation in progress

A

TABLE XXVII.
SUMMARY OF HEAT OF ABLATION DATA

C3-1*	C1-1	C3-2	R1-4	R3-6	C2-2	A1-2	R2-4	A2-1	A4-2A
117	126	127	129	130	132	133	134	135	138
24.8	25.1	21.7	21.4	21.0	21.2	24.4	23.0	27.1	20.9
383	442	396	276	312	260	332	255	368	321
5273	5160	4460	4540	4486	4487	5180	4900	5630	4830
2600	2000	2500	1980	1970	1970	1980	2090	2080	2040
4500	3800	4350	4020	4070	3950	3980	4040	4650	4100
670	570	670	510	510	510	510	540	530	520
1290	1040	1230	1120	1130	1090	1110	1120	1270	1130
4693	4590	3790	4030	3976	3977	4670	4360	5100	4310
3983	4120	3230	3420	3356	3397	4070	3780	4360	3700
244/16	244/54	245/50	243/48	243/52	244/50	248/52	242/51	241/49	240/52
7.0	106	68	77	108	110	105	56	90	128
60600	20600	16350	14800	11360	11440	18850	20600	12440	13020
52400	18600	13920	12550	9600	9790	16400	17800	10620	11180

progress

B

UNCLASSIFIED

Security Classification

DOCUMENT CONTROL DATA - R & D		
Security Classification of title, body of abstract and indexing annotation must be entered when the overall report is classified		
1. ORIGINATING ACTIVITY (Corporate author)		2a. REPORT SECURITY CLASSIFICATION
General Electric Company Re-Entry and Environmental Systems Division Philadelphia, Pennsylvania 19101		UNCLASSIFIED
		2b. GROUP
3. REPORT TITLE		
ABLATIVE MATERIALS FOR HIGH HEAT LOADS, PART I. ENVIRONMENTAL SIMULATION AND MATERIALS CHARACTERIZATION.		
4. DESCRIPTIVE NOTES (Type of report and inclusive dates)		
Interim Summary Report - March 1968 to March 1969		
5. AUTHOR(S) (First name, middle initial, last name)		
P. W. Juneau, Jr. F. P. Curtis J. Metzger L. Markowitz		
6. REPORT DATE	7a. TOTAL NO. OF PAGES	7b. NO. OF REFS
June 1970	175	None
8a. CONTRACT OR GRANT NO	9a. ORIGINATOR'S REPORT NUMBER(S)	
Contract No. F33615-69-C-1503	AFML-TR-70-95, Part I	
b. PROJECT NO.		
7340		
c. Task No.	9b. OTHER REPORT NO(S) (Any other numbers that may be assigned this report)	
734001		
d.		
10. DISTRIBUTION STATEMENT		
This document is subject to special export controls and each transmittal to foreign governments or foreign nationals may be made only with prior approval of the Air Force Materials Laboratory (MANC), Wright-Patterson AFB Ohio 45433.		
11. SUPPLEMENTARY NOTES		12. SPONSORING MILITARY ACTIVITY
		Air Force Materials Laboratory Air Force Systems Command (AFSC) Wright-Patterson Air Force Base Ohio 45433
13. ABSTRACT		
<p>Ablative plastic composite materials were investigated and developed for long time heating environments. The desirable materials performance goals were high erosive resistance, insulative ability, and low weight without asymmetrical ablation, char instability, spallation or other thermo-mechanical effects.</p> <p>Carbon cloth reinforced phenolic resin and silica cloth reinforced phenolic resin heat shield materials gave acceptable thermochemical ablative surface patterns, erosive rates, and internal temperatures, but these heat shield materials are relatively heavy. Consequently, the multilayer concept was examined with the objective of determining if such constructions could perform comparably with appropriate weight savings. Low density quartz (LDQ) was an effective insulative layer, when bonded between the heat shield and metallic substrates. The LDQ consisted of phenolic impregnated silica strands, which alternated at right angles to yield a square wall, non-laced construction.</p> <p>The environment to which the specimens were subjected was generated by a five megawatt arc heater which was operated stepwise for 300 seconds. Calibration of the heat transfer rates indicated nominal values of 25 and 440 Btu/ft²-sec, yielding an integrated heat transfer of 34500 Btu/ft². Other nominal conditions over the 230 and 70 second heating intervals were: 5000 and 5000 Btu/lb enthalpy, 25 and 400 Btu/ft² sec heat flux, 0.4 and 2.5 lb/ft² shear stress. Specimen dimensions were 5-inches long by 1.75-inch wide by a variable thickness. There was a bonded aluminum structure, five thermocouples, and a 20 degree fiber angle for the simulated tapewrap specimen.</p> <p>The ablative response to high heat loads was found to be dependent upon material composition and construction. Asymmetrical erosion, excessive erosion, or high internal temperatures was found for six of the candidate composites.</p> <p>This Abstract is subject to export controls and each transmittal to foreign governments or foreign nationals may be made only with prior approval of the Air Force Materials Laboratory (MANC), Wright-Patterson Air Force Base, Ohio 45433.</p>		

UNCLASSIFIED

Security Classification

14. KEY WORDS	LINK A		LINK B		LINK C	
	ROLE	WT	ROLE	WT	ROLE	WT
Ablation Ablative Materials Arc-Heater Characterization Hyperthermal Environment Insulation Reentry Environment Reinforced Plastics						

UNCLASSIFIED

Security Classification